THE UNIVERSITY OF QUEENSLAND

DIVISION OF CIVIL ENGINEERING

REPORT CH72/08

REEF-TOP CURRENTS IN VICINITY OF HERON ISLAND BOAT HARBOUR, GREAT BARRIER REEF, AUSTRALIA

1. OVERALL INFLUENCE OF TIDES, WINDS AND WAVES

AUTHORS: Michael R. GOURLAY & Jennifer L.F. HACKER

HYDRAULIC MODEL REPORTS

This report is published by the Division of Civil Engineering at the University of Queensland. Lists of recently-published titles of this series and of other publications are provided at the end of this report. Requests for copies of any of these documents should be addressed to the Civil Engineering Secretary.

Division of Civil Engineering
The University of Queensland
Brisbane QLD 4072
AUSTRALIA

Telephone: (61 7) 3365 3619
Fax: (61 7) 3365 4599

URL: http://www.eng.uq.edu.au/civil/

First published in 2008 by
Michael R. GOURLAY and Jennifer L.F. HACKER
Division of Civil Engineering
The University of Queensland, Brisbane QLD 4072, Australia

ISBN No. 9781864999 358

The University of Queensland, St Lucia QLD

REEF-TOP CURRENTS IN VICINITY OF HERON ISLAND BOAT HARBOUR, GREAT BARRIER REEF, AUSTRALIA

1. Overall influence of tides, winds and waves

Michael R. Gourlay

and

Jennifer L. F. Hacker

Division of Civil Engineering
School of Engineering
The University of Queensland
Brisbane, Qld 4072
Australia

Email: j.hacker@uq.edu.au

REPORT No. CH72/08

ISBN 9781864999 358

Division of Civil Engineering

The University of Queensland

October 2008

ABSTRACT

Heron Island is a small coral cay on the western end of a large platform reef in the southern Great Barrier Reef, Australia. In 1967 a boat access channel and a small mooring basin were dredged between the western reef-rim and the island. Since then reef-top currents have flowed out through this channel, removing sediment from the reef-flat and the island's beaches. The mooring basin and access channel were enlarged in 1987. Offreef waves (hourly) and reef-top currents (at 10 minute intervals) were measured on either side of the island during a twelve month period (17 March 1996 – 18 March 1997). An initial analysis of the experimental data gathered during this period is presented in this report. Under mild (tidally dominated) conditions, maximum reef-top currents of about 0.3 m/s occurred during ebb spring tides when flow on the reef-flat was controlled by weir action at the harbour bund walls. There were four current reversals per tidal cycle on the northern reef-flat and two on the southern reef-flat. As offreef wave heights increased, waves breaking on the reef-rims generated wave-generated flows towards the boat harbour and these became sufficiently strong to reverse and eventually suppress the tidal flow on the reef-top around the island. The wave height required to reverse the tidal flow increased with increasing tidal range. When offreef wave heights reached 3 m there were unidirectional flows from the reef-rims into the boat harbor throughout the tidal cycle. When tidal ranges were small, the magnitudes of the wave-generated currents increased approximately linearly with increasing wave heights. A second report provides a more detailed analysis of this data set.

Keywords: coral reefs, Great Barrier Reef, Heron Island, current measurements, wave measurements, tidal currents, wave-generated currents.

ACKNOWLEDGEMENTS

The data used in this report was collected and supplied by the former Queensland Department of the Environment (now Queensland Environmental Protection Agency) as an in-kind contribution to a field measurement and monitoring program undertaken by the authors for the Great Barrier Reef Marine Park Authority between September 1993 and December 1997. That monitoring program was supported by funds and in-kind contributions from P&O Australian Resorts Pty Ltd and by in-kind contributions from The University of Queensland (Department of Civil Engineering and the Heron Island Research Station), Queensland Department of Environment and volunteer research assistants, including post graduate students, academic and technical staff and university visitors.

Field work from 1998 to June 2000 was funded by the Cooperative Research Centre for Sustainable Tourism Pty Ltd and CRC Reef Research Centre with continuing in-kind support from P&O Australian Resorts Pty Ltd, Heron Island Research Station, The University of Queensland academic staff and volunteer research assistants.

The subsequent analysis of the data and preparation of this report have been funded by the Cooperative Research Centre for Sustainable Tourism Pty Ltd, the National Committee for Coastal and Ocean Engineering (Engineers Australia) and consultancy work through Uniquest by the senior author.

The authors wish to express their thanks to Professor Ray Volker, Professor Peter Dux and Associate Professor Peter Nielsen for the use of facilities within the Division of Civil Engineering at The University of Queensland and to Tom Baldock and David Robinson and his colleagues for reviewing this report.

TABLE OF CONTENTS

LIST OF TABLES

LIST OF FIGURES

1. INTRODUCTION

Heron Island is located in the Southern Great Barrier Reef, approximately 80 km eastnortheast of Gladstone (Figure 1). The island, at the western end of a large lagoonal platform reef, is a vegetated coral cay, *ca* 800 m long, formed from calcareous sand and rubble derived from marine organisms living on the surrounding reef. The island is divided between a National Park, a tourist resort and a marine research station. The reef and surrounding seas lie within the Great Barrier Reef Marine Park.

During the last 60 years, various works have been constructed; both to provide facilities for access (boats and helicopters) and to protect buildings located near the changing shoreline. These facilities, particularly the boat harbour and its entrance channel (Figure 2) which have been dredged through the reef-flat at the western end of the island, have had adverse effects upon both the island's beaches and the ecology of the reef-flat (Gourlay 1995).

In essence, the boat harbour and entrance channel were acting as a drain for water from the adjacent reef during the falling tide, particularly spring tides. Sand and other sediments were being removed from both beaches and reef-flat, thus causing both shoreline recession on the island and sedimentation in the boat harbour.

Lowered reef-flat water levels resulted in death and stunting of the growth of corals and other undesirable changes to reef-flat ecology near the harbour. Between October 1993 and March 1994, two low bund walls, formed of interlocking concrete blocks, were constructed, one on either side of the harbour (Gourlay 1995). The horizontal crests of these walls facilitate a uniform distribution of flow from the reef-flat into the boat harbour. The crest height was selected with the objective of restoring reef-flat water levels at low spring tides to those existing before harbour construction.

A field monitoring and measurement programme was initiated by the Great Barrier Reef Marine Park Authority (GBRMPA) in September 1993, prior to bund wall construction. It continued as a GBRMPA project until October 1997 and subsequently as a CRC Sustainable Tourism project. Initially, the performance of the walls was studied (Gourlay 1995, Hacker and Gourlay 1997). The principal aspects of concern were: -

(i) the hydraulic behaviour of the walls and their effects upon reef-top water levels;

(ii) the magnitude and frequency of any continuing inflow of sediment into the boat harbour;

(iii) The response of the reef-top ecology to the changed hydraulic conditions.

The construction of the bund walls has resulted in improved conditions on the reef-top. Reef-top water levels at low spring tides have been restored and reef-top organisms have benefited (Berkelmans *et al.* 1997, Hacker and Gourlay 1997). Nevertheless, the reef-top current system is still continuing to move sediment into the boat harbour. Two preliminary summaries of this complex three-dimensional current system influenced by waves, winds and tides have already been published (Gourlay and Hacker 1997, 1999).

This report presents the first part of the results of a more comprehensive analysis of the extensive wave and current data set collected during 1996 and 1997, together with a detailed description of the current system at the western end of Heron Reef. A second report (Gourlay and Hacker 2008b) presents the results of a more specific analysis of reef-top currents at the western end of the reef, both under mild (*i.e.* tidally dominated) conditions and under the influence of waves.

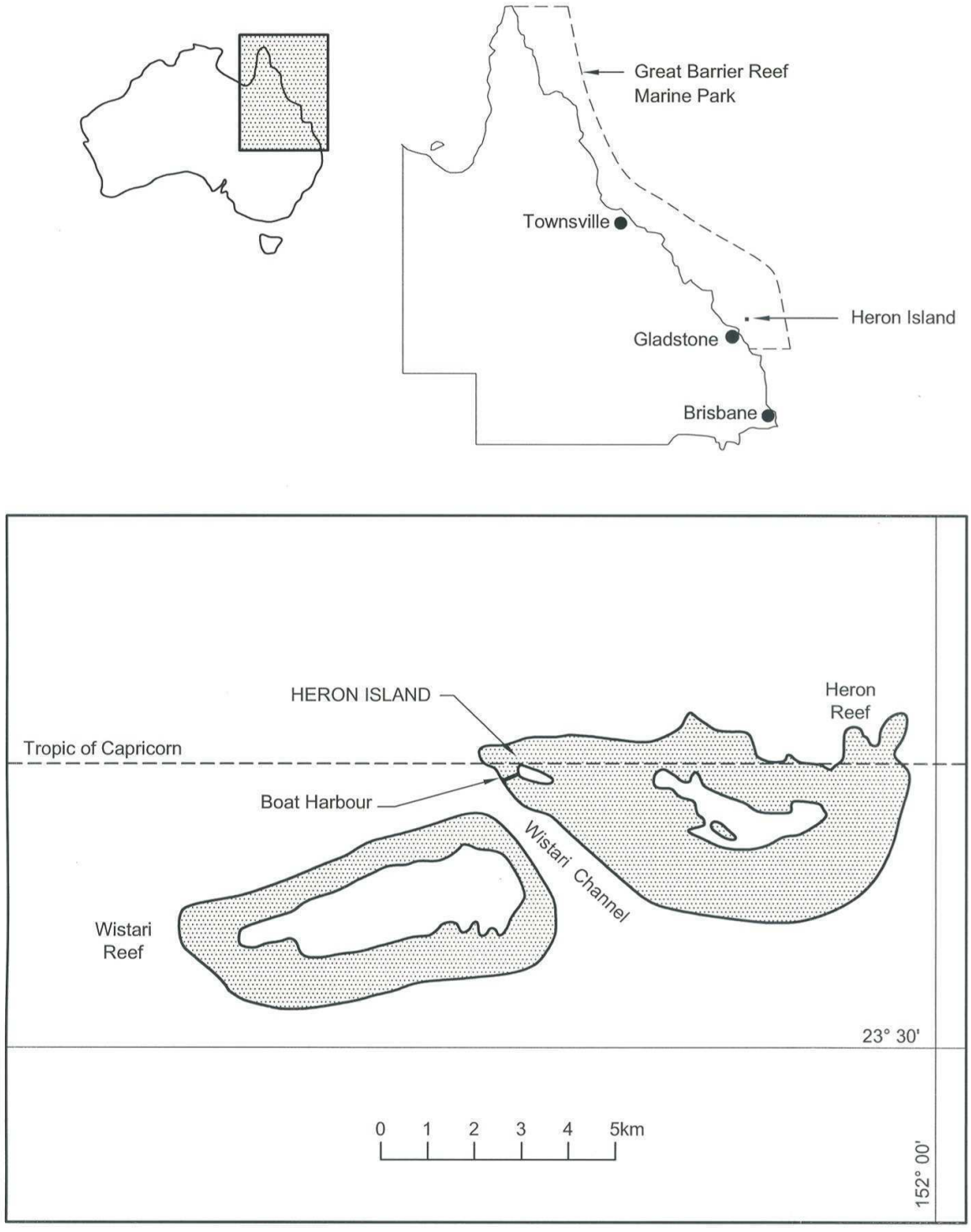

Figure 1. Location of Heron Island

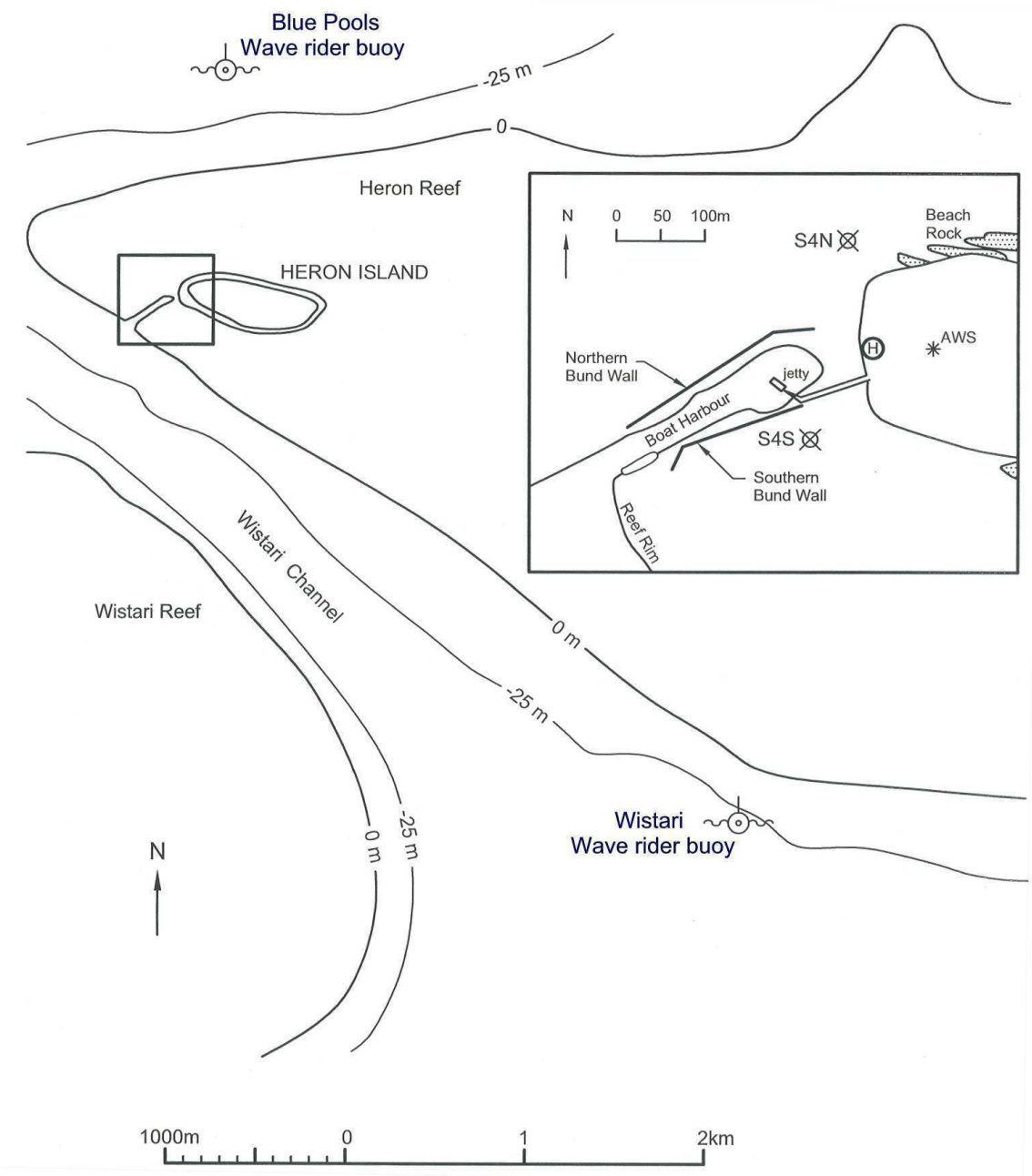

Figure 2. Heron Island and western end of Heron Reef

S4N - Northern S4 current meter
S4S - Southern S4 current meter
AWS - Automatic weather station

2. FIELD MEASUREMENTS OF REEF-TOP CURRENTS

The current system on the reef-top is driven by the astronomical tide and by meteorological variations in winds and wind-generated waves. The system is sensitive to small changes in both tidal range and offreef wave-height. The current system is also controlled by the size and shape of the reef and by variations in reef-top topography. Even though the reef-top may appear to be horizontal, small differences in elevation or zones with different roughness, *i.e*. coral zones, sandy zones, algal rim, are likely to exert significant influence upon the reef-top currents. Hence, it is not sufficient just to measure winds, waves and tides; it is essential also to measure the topographic characteristics of the reef-top.

Between 16 March 1996 and 13 May 1997, simultaneous wave, current, wind and tidal data were obtained at Heron Island. Wave and current measuring instruments were supplied and deployed by the former Queensland Department of Environment (DoE), now the Queensland Environmental Protection Agency (EPA)

- Offreef waves were measured by two Datawell wave rider buoys deployed in the deeper water surrounding the reef. One buoy was located north of the reef, near "Blue Pools", and the other south of the reef, at the southeastern entrance to Wistari Channel (Figure 2). The wave rider buoys measured wave conditions for 25 minutes every hour and transmitted the data onshore.
- Reef-top currents were measured using two InterOcean Systems S4 current meters, one located north and the other south of the boat harbour (Figures 1 and 2). Their sites were chosen so that they were located in coral-free sandy areas where significant currents could be expected to occur, but not where they might conflict with normal boating activities. Current speed and direction and water depth were measured every 10 minutes. At low tide, the water level often fell below the sensors. Data stored in binary format within the instruments had to be downloaded at approximately six-weekly intervals. The northern current meter did not operate after 19 March 1997.
- Local winds at Heron Island were measured by the Bureau of Meteorology's automatic weather station (AWS) on the island. Hourly 10 minute average data for wind speed and direction are available.
- Ocean tide levels were not measured, but predicted tide levels at 10 minute intervals were supplied by Queensland Transport.

The western end of Heron Reef was surveyed by John Reader and Associates Pty Ltd in 1993 prior to construction of the bund walls. During the GBRMPA monitoring programme, additional surveys were made of the northern reef-face, beach changes and sediment deposits in the boat harbour. During this project, surveys of beach changes and sediment deposits in the boat harbour have been continued. Additional surveys have been made along the reef-face and reef-rim south from the entrance of the boat harbour. All elevations are relative to Heron Island low water datum (LWD), which is 0.085 m below lowest astronomical tide level (LAT) (See Appendix A – Tidal Planes at Heron Island). The mean tide level at Heron Island for the period of observations was 1.52 m (LWD) or 1.44 m (LAT). (Queensland Department of Transport 1997, p222).

3. DATA ANALYSIS 1 – Events

3.1 Objective and Methods

The objectives of the data analysis program were to examine

(i) the relationships between the forcing functions, the wind, waves and tide, and the resultant currents that developed on the reef-top; and

(ii) the variations in these relationships in response to different tidal and meteorological conditions during an extended period, *i.e.* over twelve months.

In order to achieve these objectives, it was necessary to combine the data in a format that could be manipulated easily. Microsoft Excel was used, as it is readily available. The strengths of Excel were further enhanced with the use of Visual Basic, an object-based programming language.

3.2 Data processing

3.2.1 Current meter data

Both S4 current meters recorded the current velocity components, v_E, v_N, and water level. The northern instrument, which had a larger data storage capacity, also recorded water conductivity and water temperature. The original data sets for the northern meter were recorded at 0.5 s intervals for one minute every 10 minutes and for the southern meter as 5 s averages for 2 minutes every 10 minutes.

The data, which was stored in the instruments, was downloaded by DoE staff onto a laptop computer every 4 to 8 weeks as a binary file (filesize up to 9 Mb). These files were then transferred to The University of Queensland by direct computer link.

The InterOcean's software supplied with the current meters for processing the binary format data could only be used to produce ASCII data files and graphical results in a standardised format. None of these files or graphs was compatible with the other data to be used. Consequently the following procedures were used for the initial data processing: -

- The binary data was converted, one day's data *per* file, into ASCII format using InterOcean's software.
- The daily ASCII data then was processed using QuickBasic to give a one minute average value every 10 minutes, *i.e.* 144 readings *per* day at each instrument. The two component velocities, v_E, and v_N, were converted into speed and direction with the latter corrected for magnetic variation. Standard deviations were calculated for the current speeds and directions

and maximum and minimum values extracted. The water levels were converted to Heron Island Low Water Datum (LWD) using the zero water level offset readings measured at the beginning and end of each deployment and the measured elevation of each instrument.

3.2.2 Tide data

The tide data, at ten-minute intervals, was supplied by Queensland Transport in ASCII format for predicted tide levels at Heron Island relative to LWD.

3.2.3 Wave rider buoy data

The wave rider data was transmitted to the shore station at Heron Island at hourly intervals. The wave rider buoys (WRB) each recorded for 25 minutes. The WRB at Blue Pools transmitted on the hour and the one in the Wistari Channel at half past the hour. This data was then downloaded by modem to DoE, Brisbane.

Standard wave statistics, such as significant wave height, H_s, root mean square wave height, H_{rms}, significant period, T_{Hs}, and spectral peak period, T_p, were computed by DoE and supplied on disk in ASCII format.

3.2.4 Meteorological data

Hourly and three hourly meteorological data were supplied by the Bureau of Meteorology, Brisbane. Both sets of data were supplied in ASCII format on disk.

The hourly meteorological data was supplied in a very "user unfriendly" format. It was transcribed into a consistent useable format using Excel Visual Basic macros. If data was missing from the hourly data, data was taken from the three-hourly set, when available, and inserted manually.

3.3 Preparation of data plots

Data was collected from the source files, for currents, predicted tide, wave height and winds, for each day. This also was done using Excel Visual Basic macros. The use of Visual Basic was essential; otherwise it would not have been possible to align the graphs accurately. Furthermore, the use of Visual Basic shortened the preparation time by a factor of at least 30.

Selected data was plotted for each day, five plots for each day, all to the same time scale (Figures 3 to 5). These plots enable the current speeds and directions at each meter to be compared with

predicted and recorded tide levels as well as with offreef wave heights and local wind speed and direction. In agreement with meteorological and oceanographical conventions, **wind directions** are directions **from which the wind blows**, whereas **current directions** are directions **towards which the current flows**. The data plots include the following: -

Northern current meter	current speed
	current direction
	standard deviation of current speed
Tide levels	predicted tide level
	tide level from northern current meter
	tide level from southern current meter
	conductivity
	water temperature
Southern current meter	current speed
	current direction
	standard deviation of current speed
Wave height, H_s,	Blue Pools WRB
	Wistari WRB
Wind speed and direction	wind speed
	wind direction

Originally each day's data for all 423 days (16 March 1996 to 13 May 1997) was plotted on a single page. In those plots, current directions were plotted as zero when the current speed fell below 0.08 m/s. Subsequently, it was found necessary to replot many of these figures so as to include all current directions and the wave period T_p at both sites. All daily data figures presented in this report are in the latter format (see Figures 3, 4 and 5).

The water levels measured by the S4 meters are not totally reliable. Both meters gave values that drifted. The southern meter values are much more consistent than were those from the northern meter. The same meter was used consistently for the southern deployment. For the northern deployment, two meters were used, the first from 16 March 1996 to 27 August 1996 and the second for the remainder of the deployment. For the first two months of the northern current meter's deployment, it did not register depths at lower tide levels. Initially, it did not record depths below 1.9 m LWD. Fortunately, the drift on the instrument drifted in a useful direction and after the end of May 1996, the instrument recorded levels when the water level was low. The conductivity readings from the northern meter were helpful in that they provided a check on the water level. When the water level dropped below the top conductivity sensor on the instrument, the conductivity dropped abruptly to almost zero. As the elevation, to LWD, of the sensor is known, this enabled the conductivity readings to be used to correct the water level for the northern

current meter. This correction has been carried out for all readings after 26 May 1996. Before that date, the levels of the northern and southern meters were compared between tide levels of 1.5 and 2.2 m and the northern meter adjusted on the average difference. The value of any adjustment to the northern current meter water level is given as the value for 'Nadj' on the tide level graphs (Figures 3, 4 and 5). No adjustment was made for the southern meter. Sometimes it is evident that an adjustment is required.

3.4 Calibration changes at southern current meter

During the latter part of the data analysis involving the second and third periods of analysis, i.e. 1 July to 31 October 1996 and 1 November 1996 to 18 March 1997, some inconsistencies in the current measurements at the southern current meter became apparent. These included bivalued currents during the final stages of the ebb tide when weir control occurred at the southern bund wall. A partial explanation of this "crab's claw" effect observed in Figures 72 to 77 has been identified as being associated with different wind and wave conditions (section 7.3.2, pp 48-53).

Subsequently, after this report was completed, an analysis of velocity measurements at the beginning and end of each instrument deployment period revealed that the calibration of the southern current meter tended to change with time. Velocities measured at the end of a deployment were usually lower than those measured at the beginning of that deployment. In some cases the difference was negligible or less than 10% but in others it was as much as 25 to 33%. The smaller differences generally occurred during the first six months of deployment and the larger ones during the latter six months. Fortunately, most of the analyses described in this report are based on the period from 17 March to 30 June 1996 when the reductions in velocities between beginning and end of deployment measurement periods only varied between 4 and 10%. When compared with the scatter arising from other causes, these reductions probably do not affect the general conclusions of these analyses. In the case of the latter two periods of analysis (Chapter 7) some recorded velocities at the southern current meter will be significantly lower (25 to 33%) than they actually were. These records may be the reason for some of the still unexplained inconsistencies in Figures 79 to 84. This matter is discussed further in the second report on the analysis of reef-top currents in the vicinity of Heron Island (Gourlay and Hacker 2008b, section 2.4.1).

4. REEF-TOP CURRENTS 1 – Events

4.1 Overview

An initial appraisal of the data showed that current conditions during "events" with strong winds and waves are very different from those occurring during "mild" conditions when the currents are dominated by tidal flows.

At Heron Island meteorological events, involving winds between 10 and 15 m/s (20 and 30 kn) and causing wave heights H_s up to 3 m, occur fairly frequently. Three such events were recorded during the 14 month instrumentation period – on 1 May 1996, 27-28 July 1996 and 7 to 11 March 1997.

In the following sections examples of three conditions are given:

(i) mild meteorological conditions and average tide (Figure 3);

(ii) easterly to northeasterly event (Figure 4);

(iii) southeasterly event (Figure 5).

These examples, together with several others, are discussed in more detail in Chapter 3 of Gourlay and Hacker (2008b).

4.2 Mild meteorological conditions and average spring tide – 11 October 1996 (Figure 3)

Calm conditions occur very seldom at Heron Island, so it has not been possible to obtain information about tidal currents in the absence of winds and waves. Here, wind speeds $W < 5$ m/s (10 kn) and waves $H_s < 0.5$ m are taken to represent mild conditions. Under these conditions, with an average spring tide (range 2.1 to 2.2 m), the maximum average current velocities measured at the current meters were about 0.3 m/s and occurred generally on the late ebb tide.

Commencing at low water, the tide rises, flowing into the boat harbour, over the bund walls and eastward around both sides of the island. On the southern reef-flat, the flow generally continues in an eastsoutheastward direction past the peak of the high tide and does not change direction until the tide has fallen to about mean tide level. It then reverses and flows northwestward over the bund wall into the boat harbour. There are only two current reversals each tidal cycle. Low tide level on the reef-flat is higher than in the harbour and offreef because of ponding caused by the bund walls and reef topography (see Figure 6b).

North of the boat harbour, the current initially flows in from the boat harbour and over the reef-flat in a northeastward direction until the tide level reaches about mean tide level, when this flow changes to southwestward. When the tide starts to fall, the flow again changes direction and flows northeastwards until about mean tide level and then, reversing again, flows southwestward over the bund walls and into the boat harbour at low tide. Hence, there are four current reversals *per* tidal cycle on the northern reef-flat.

This apparently anomalous behaviour is a consequence of both the reef-top topography and the phasing of the tide as it flows around the reefs. The western end of the reef is lower than most of the reef, so the rising tide flows over it first and then progressively over increasingly elevated portions of the reef-rim. The northern rim is slightly lower than that on the southern side and radial inflow over the northern rim quickly dominates and reverses the flow direction on the northern side of the harbour. The higher southern rim inhibits radial inflow and the inflow from the north sets up an anti-clockwise flow around the island. When the tide commences to fall, it flows out radially over the reef-rim on both sides of the reef before changing to westward flow around the island and out through the boat harbour.

The characteristics of reef-top currents under mild conditions are considered in more detail in Chapter 2 of Gourlay and Hacker (2008b)

4.3 Easterly to northerly winds – 27 July 1996 (Figure 4)

On 27 July 1996 there was a fairly rapid increase in wind speed from <10 m/s to 15 m/s, associated with a consequent increase in wave height H_s on the northern side of the reef from 1 m to 3 m during a period of three hours. Waves on the southern side were approximately 1 m. The tidal range varied from 1.4 m to 2.4 m.

Current conditions on the northern reef-flat changed dramatically. The combined effect of wind and waves dominated over both tidal and topographical influences to produce a unidirectional flow in a generally southwestward direction from the northern reef edge towards the boat harbour. As the tide rose, currents on the southern side of the boat harbour were also affected by the wind and wave-generated flow and tended to flow more to the south. Current velocities on the northern side increased significantly, up to 0.6 m/s, as the tide began to fall. Flood tide velocities on the southern side of the island, normally about 0.1 m/s, increased to 0.3 to 0.4 m/s.

The recorded reef-top tide levels clearly show the development of significant wave set-up after 3 m waves began to break on the reef-edge at about 12:00 h during low tide. The waves pumped water onto the reef-flat and the water level at the northern current meter rose about 0.2 m above the low tide level of 0.95 m before the incoming tide started to affect it. The set-up at high tide was about 0.15 m (*ca* 18:30 h).

4.4 Southeasterly wind – 9 March 1997 (Figure 5)

On 9 March 1997, when Tropical Cyclone "*Justin*" was in the northern Coral Sea, 15 m/s (30 kn) winds were recorded at Heron Island. Waves with H_s over 2 m and approaching 3 m were recorded in Wistari Channel on the southern side of the reef. Tides were high spring tides with ranges approaching 3 m. On this occasion, unidirectional flow developed on the southern side of the island with currents consistently flowing northwestward into the boat harbour. Velocities were generally 0.3 m/s or more and exceeded 0.4 m/s during the ebb tide before ponding on the reef-flat commenced. Wave set-up was probably at least 0.2 m.

4.5 Summary

During mild conditions currents on the reef-top are dominated by tidal flows. Events with strong winds and waves significantly change the reef-top current patterns.

Under mild conditions ($W < 5$ m/s, $H_s < 0.5$ m) and average spring tides, tidal flows are dominant around Heron Island and on the western end of Heron Reef. Variations in reef-top topography and tidal phasing influence the magnitude and direction of the tidal currents during a tidal cycle. The presence of the boat harbour channel and a low reef-rim level at the western end of the reef influence both the initial inflow onto the reef-flat and also the final outflow off the reef-flat. When tide levels are above mean sea level flow on the reef-flat is generally radial over the reef-rim on either side of the island.

On the northwestern side of the island, the reef-top tidal currents experience four reversals of flow during a tidal cycle. Initially, on the rising tide, northeastward inflow occurs over the western end of the reef and through the boat harbour. This inflow is later opposed and reversed by radial inflow over the northern reef-rim. Then, after high tide, outflow is initially radially out over the reef-rim, before finally flowing southwestward out through the boat harbour at low tide. On the southern side of the island, anticlockwise flow occurs around the island during the rising tide with the radial inflow over the southern reef-rim reinforcing the initial eastward flow along the island's southern shore. The tidal current only reverses during the ebb tide when the water level falls

below mean sea level. Hence on the southern side of the island, only two current reversals occur during a tidal cycle. Maximum velocities on both sides of the island occur during the ebb tide and are *ca* 0.3 m/s.

Meteorological events with wind speeds W = 10 to 15 m/s and wave heights H_s approaching 3 m occurred three times during the fourteen month period of observations. During these events, wave-generated currents caused by waves breaking on the reef-rim were sufficiently strong to suppress the tidal currents of average tides and cause continuous unidirectional flow from the northern reef-rim into the boat harbour when the waves came from the northeastern sector. At the current meter sites wave set-up was probably 0.15 to 0.2 m and current velocities were up to 0.6 m/s. When southeasterly waves broke on the southern reef-rim, the unidirectional flow was from the southern reef-flat westward into the boat harbour. With high spring tides, the wave-generated unidirectional flow fluctuated over a tidal cycle, producing maximum velocities of about 0.4 m/s.

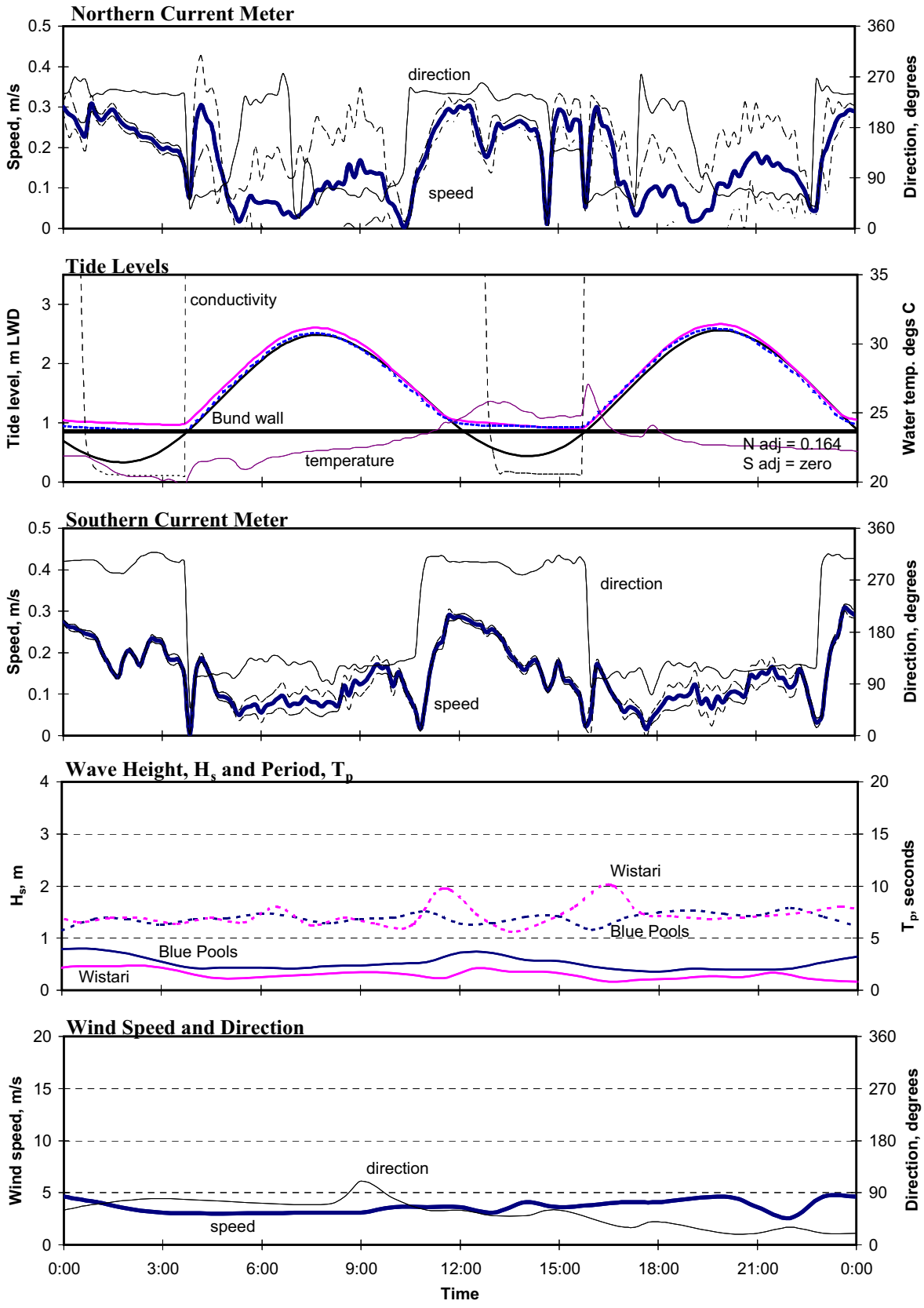

Figure 3. Waves and currents at Heron Island under mild meteorological conditions and average spring tide - 11 October 1996

Predicted tide level - solid line; Measured tide levels - broken lines
Wave heights - solid lines; Wave periods - broken lines

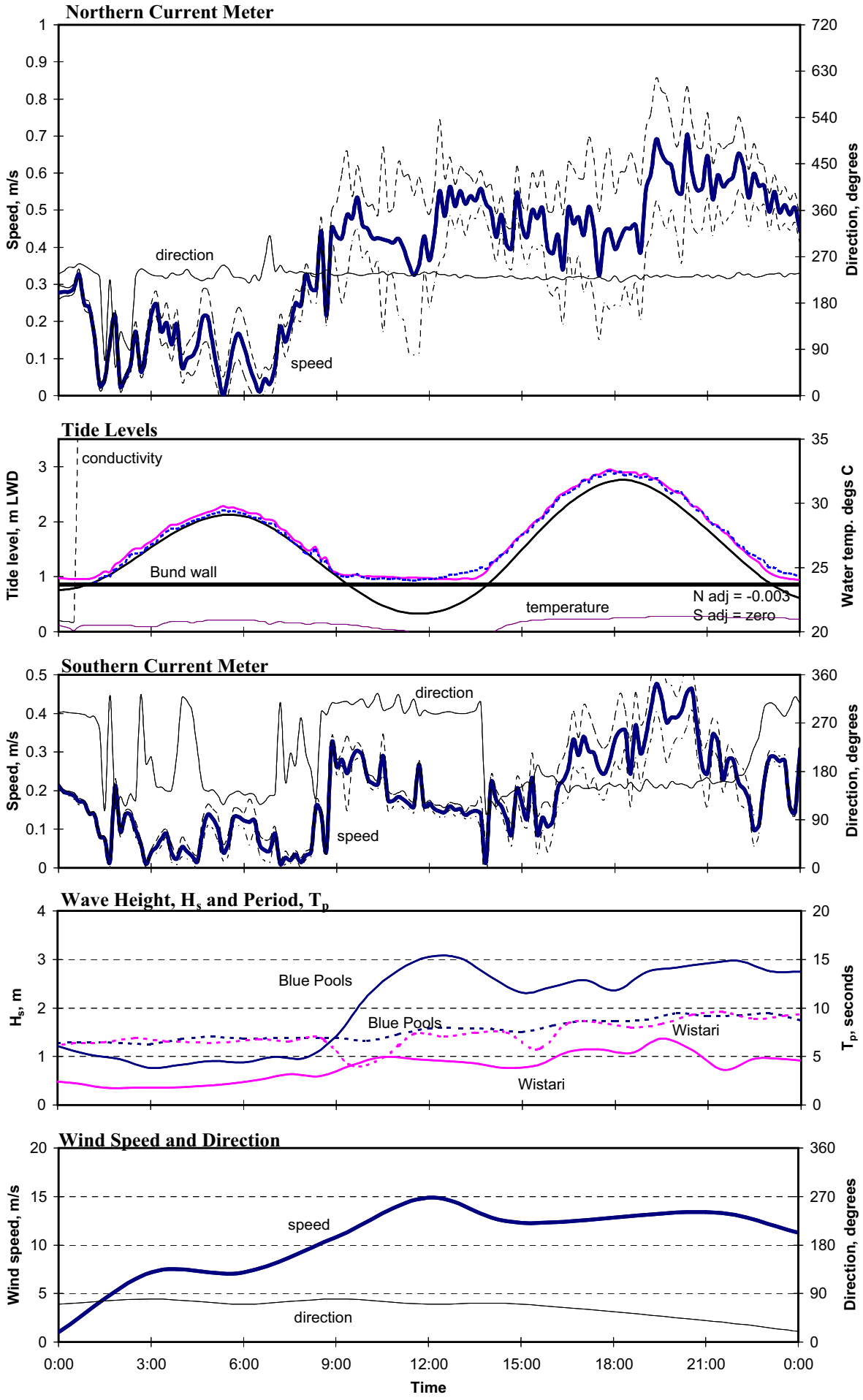

Figure 4. Waves and currents at Heron Island under easterly to northerly winds - 27 July 1996

Predicted tide level - solid line; Measured tide levels - broken lines
Wave heights - solid lines; Wave periods - broken lines

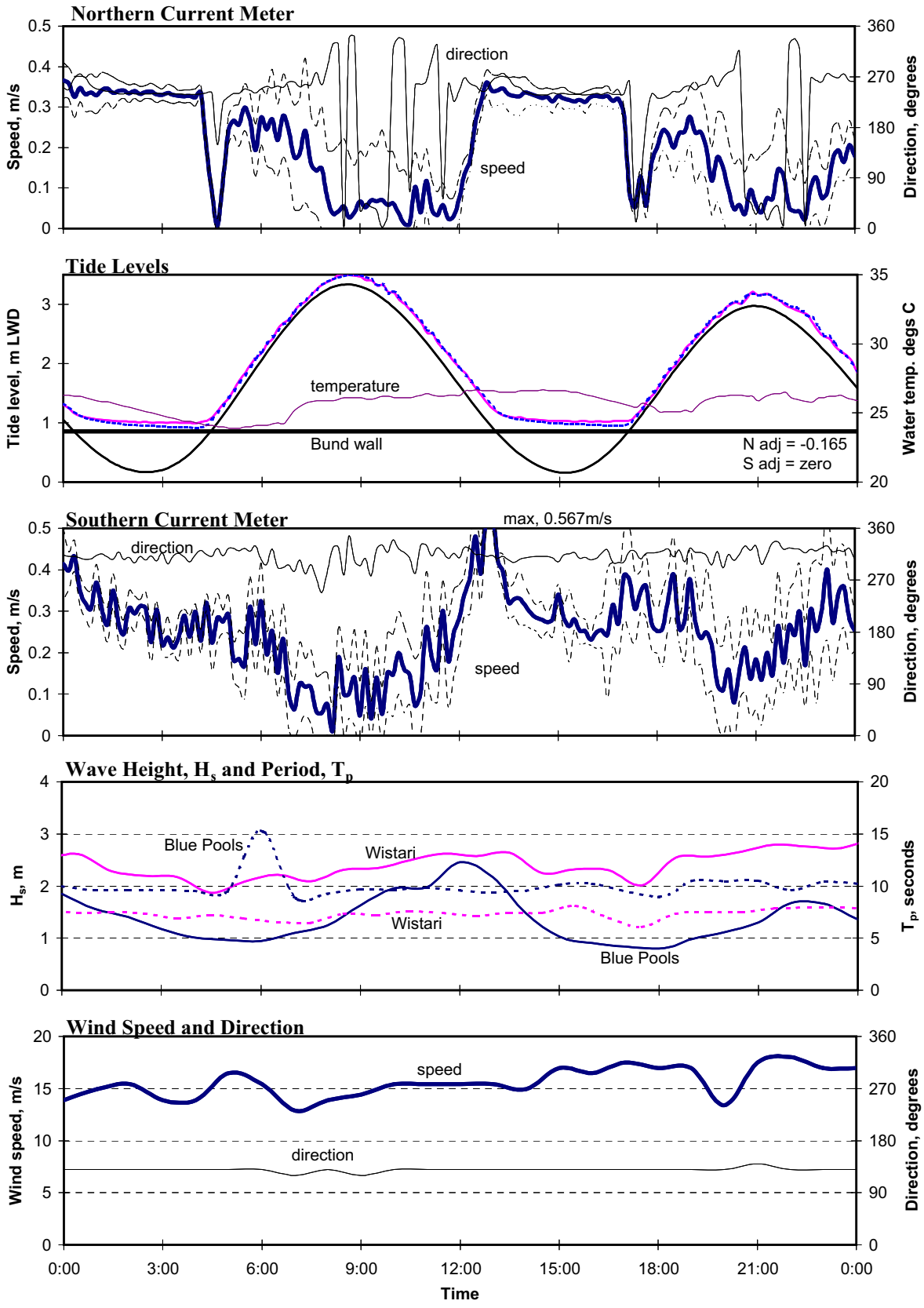

Figure 5. Waves and currents at Heron Island under southeasterly winds - 9 March 1997

Predicted tide level - solid line; Measured tide levels - broken lines
Wave heights - solid lines; Wave periods - broken lines

5. DATA ANALYSIS 2 – 17 March to 30 June 1996

5.1 Need for further analysis

The complex interdependency of the various parameters involved in determining the strengths and directions of the reef-top currents at Heron Island requires further analysis in order to determine the thresholds at which changes occur. For instance, it is desirable to determine the conditions that result in the current flowing into the boat harbour for the full tidal cycle. In order to examine the relevance of the different parameters involved the data was subjected to filtering.

5.2 Procedure for filtering data

Initially, the first four months of data were considered. Selected data was combined into files for each month, again using Visual Basic macros. The selected data comprises: -

- Date and time (every 10 minutes)
- Current speed, v, and direction, θ_c, for both northern and southern current meters
- Wind speed, W, and direction, θ_w
- Wave height measured by Blue Pools WRB, H_{BP}, and Wistari WRB, H_{Wis}
- Predicted tide level, z_o, and whether the tide is rising or falling

As the wind data and wave data were only recorded every hour, values for the intermediate time slots were interpolated using Visual Basic macros. Values for the tidal range, R, and the half-tidal period, T, were calculated (See Figure 6a and Appendix B for explanation of symbols).

Initially, filters of wind speed less than 5 m/s and then greater than 5 m/s, tide rising and tide falling, were applied to the data files for each of the first four months. After preliminary analysis and assessing the relative importance of the parameters involved, it was concluded that the first filter should be on tidal range, not wind speed. So the data was filtered on three tidal range groups, $R < 1.4$ m, $1.4 \text{ m} \leq R < 2.0$ m and $R \geq 2.0$ m. Rising tide data and falling tide data were separated. This filtered data was collected into three files for the three tidal range groups, each file covering the first 106 days in the first four months, 17 March to 30 June 1996. Further filters could then be applied as required.

Three similar files were compiled for each of the two following four month periods, 1 July 1996 to 31 October 1996 and 1 November 1996 to 18 March 1997. However, because of the large

number of individual data points, it was not possible to combine the data for each tidal range group for the whole twelve month period. The results given in Chapter 6 refer only to the initial period 17 March 1996 to 30 June 1996 but all three periods have been analysed and a comparison of their results is presented in Chapter 7.

Data obtained when the meters' sensors were partially or totally out of water was removed (Table 1). For the northern meter, all data obtained when the conductivity readings were less than the maximum value was removed. The decision as to which data should be removed from the southern meter data set was more difficult. The southern meter was deployed 20 mm lower in elevation than the northern meter. Often the southern meter continued to give "reasonably sensible" readings even when the sensors must have been largely out of the water. Generally, it was considered that the southern meter's sensors were exposed approximately one hour after the conductivity dropped on the northern meter. Southern current meter data was removed on this basis, unless there was strong contradictory evidence, for example, pronounced wave set-up. On the rising tide, both current meters would have been submerged at the same time; therefore a sharp rise in the conductivity at the northern meter indicates the time of submergence.

Table 1 Details of data utilised for period 17 March 1996 to 30 June 1996

Beginning of deployment	1996 March 17; 15:36
End of deployment	1996 June 30; 23:50
Total possible number of measurement sets (144 *per* day)	15,170
% measurements lost due to malfunction or deployment change	1.7
Number of measurements after removal of out-of-water data Northern meter	12,239
Number of measurements after removal of out-of-water data Southern meter	13,437
% time northern meter produced useable data	**80.7**
% time southern meter produced useable data	**88.6**

As already mentioned, the water level data recorded by the current meters was found to be unreliable as it was subject to drift, particularly the data from the northern meter. Consequently, it was considered preferable to use the predicted tide level data instead of water level data measured on the reef-top by the current meters. Furthermore, use of the predicted tide data gives the full tidal range not the restricted range experienced on the reef-top (Figure 6b). The difference in height between high and low water offreef (*i.e.* the predicted tidal range) contributes to the forcing function that drives the tidal currents. Unfortunately, using the predicted tide level data means that storm surge and wave set-up effects are not taken into account. The influence of actual recorded tide levels upon current velocities during some events is considered in Gourlay and Hacker (2008b, section 4.5).

5.3 Relationship between reef-top currents and predicted tide level

Measurements of current speed, v, and direction, θ_c, were plotted against predicted tide level, z_o, using various wind and wave filters on the data in order to determine the relative influence of the various parameters. The filters were selected so as to isolate conditions that could be expected to have a clear and direct influence on the currents. For both current meters, this entailed considering, initially mild conditions when tidal effects are likely to predominate; then conditions with stronger winds and larger waves. It was found that wind direction is important; therefore, at this stage, only stronger winds from limited direction sectors have been considered.

For the **southern current meter**, the relationships between current speed, v, and direction, θ_c, for the three groups of tidal ranges:

$$R < 1.4 \text{ m}; \qquad 1.4 \text{ m} \le R < 2.0 \text{ m}; \qquad 2.0 \text{ m} \le R$$

have been explored under the following conditions:

Mild conditions 1 – unrestricted wind direction

(i) $W < 5$ m/s; $H_{BP \text{ and } Wis} < 0.35$ m

(ii) $W < 5$ m/s; $H_{BP \text{ and } Wis} < 0.5$ m

(iii) $W < 5$ m/s; $0.35 \le H_{BP \text{ and } Wis} < 0.5$ m

Mild conditions 2 – restricted wind direction

(i) $W < 5$ m/s; $105^o \le \theta_w < 165^o$; $H_{BP \text{ and } Wis} < 0.35$ m

(ii) $W < 5$ m/s; $105^o \le \theta_w < 165^o$; $H_{BP \text{ and } Wis} < 0.5$ m

(iii) $W < 5$ m/s; $105^o \le \theta_w < 165^o$; $0.35 \le H_{BP \text{ and } Wis} < 0.5$ m

(iv) $W < 5$ m/s; $105^o \le \theta_w < 165^o$; $H_{BP} < 0.5$ m; $0.5 \le H_{Wis} < 0.75$ m

Wave/wind influenced conditions

(i) $W \geq 5$ m/s; $105^o \leq \theta_w < 165^o$; $H_{BP \text{ and } Wis} < 0.5$ m

(ii) $W \geq 5$ m/s; $105^o \leq \theta_w < 165^o$; $H_{BP} < 0.5$ m; $0.5 \leq H_{Wis} < 0.75$ m

(iii) $W \geq 5$ m/s; $105^o \leq \theta_w < 165^o$; $H_{BP} < 0.5$ m; $0.75 \leq H_{Wis} < 1.0$ m

(iv) $W \geq 5$ m/s; $105^o \leq \theta_w < 165^o$; $H_{BP} < 0.5$ m; $1.0 \leq H_{Wis} < 1.25$ m

(v) $W \geq 5$ m/s; $105^o \leq \theta_w < 165^o$; $H_{BP} < 0.5$ m; $1.25 \leq H_{Wis} < 1.5$ m

(vi) $W \geq 5$ m/s; $105^o \leq \theta_w < 165^o$; $H_{BP} < 0.5$ m; $1.5 \text{ m} \leq H_{Wis}$

Similar filters were applied to the **northern current meter** data with appropriate changes to the wind directions and to the selected wave height ranges. In some situations there was insufficient data available to establish the relationships between current speed and direction and given wind/wave conditions for a specified tidal range group. The data presented in Chapters 6 and 7 has been selected from these various analyses.

The relationship between current speed at each current meter, and the offreef wave height as measured at the wave rider buoys, was also examined. The results are presented in section 7.4.

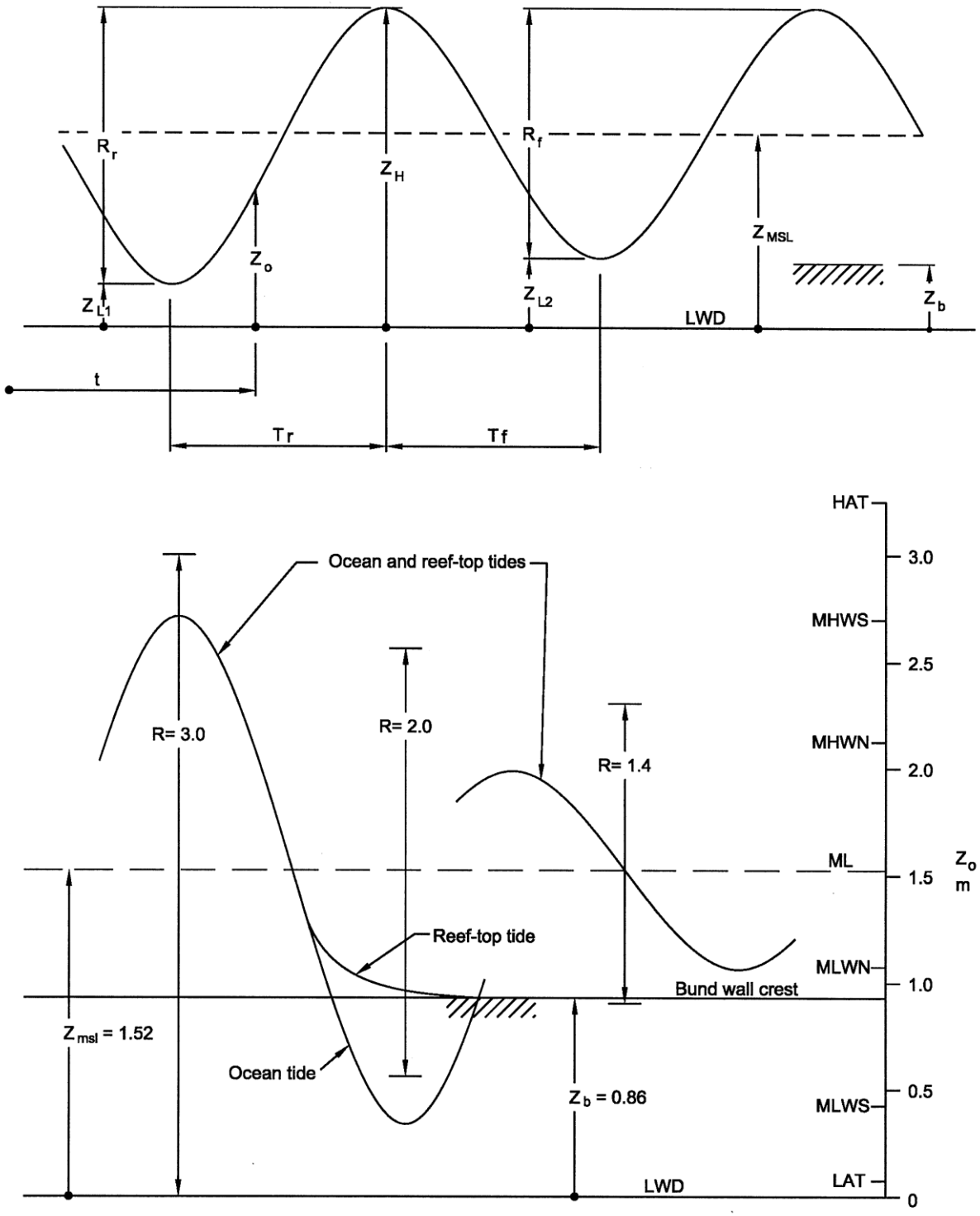

Figure 6. (a) Definition of symbols
(b) Reef-top tide levels

6. REEF-TOP CURRENTS 2 – 17 March to 30 June 1996

6.1 Introduction – tides, winds and waves

The current conditions occurring during the three different tidal range groups differ markedly. The effect of the tidally generated flows is modified substantially by both the reef-top topography and the control exerted by the bund walls as water levels approach low tide. Consequently, the relationship between the reef-top currents and the water level relative to the bund wall crest cannot be ignored. Moreover, the tides are often asymmetric with the range of the falling tide differing from that of the rising tide. For these reasons, the dimensionless parameter $Z = (z_o-z_b)/(z_H-z_b)$ [z_b = elevation of the crest of the bund wall; z_H = high tide level for each tide (Figure 6 a and b)] was selected for representing the water level variation during a tidal cycle.

As is to be expected, the larger tidal ranges produced larger currents under conditions of low wind and wave action. It also was found that differences in wind direction, even at low wind strengths, less than 5 m/s, cause marked differences in current patterns. Frequently, even for quite restricted conditions, there was a marked scatter in the data, but closer examination was able to provide a reason for that scatter, *e.g.* it may have been a difference in wind direction, or lag from earlier conditions. As there is such a large amount of data, it is not practical to examine all possibilities.

As found in Chapter 4, the presence of strong winds and large waves substantially changes the current patterns that occur during "mild" conditions.

The analysis of the data is considered in four sections: -

- Southern current meter, rising tide (Section 6.2)
- Southern current meter, falling tide (Section 6.3)
- Northern current meter, rising tide (Section 6.4)
- Northern current meter, falling tide (Section 6.5)

6.2 Southern current meter, rising tide

6.2.1 Tidal range greater than 2.0 m

All data (Figure 7). When the tidal range is greater than 2 m, the currents flow predominantly eastsoutheastward (105°), parallel to the island, for 80% of the time. For the remainder of the time they flow generally northwestward (315°) towards the boat harbour. Currents flowing in the eastsoutheastward direction are considered to be positive whilst those in the northwestward direction are negative; the division is taken at 225°. It must be remembered that, for the most part,

the data does not cover the part of some tidal cycles when the ocean tide level was below that of the bund wall crests because the instrument was out of the water. During this time flow would have been negative, *i.e*. into the boat harbour. Occasionally, during very mild conditions, this flow at low tide into the boat harbour would have been negligible.

Low waves, H_{BP} and H_{Wis} < 0.35 m and low winds, W < 5m/s (Figure 8). When winds and waves are low, currents are controlled by the tide. The general pattern is that, as the tide rises, the tide flows into the boat harbour, then over the southern bund wall and along the southern side of the island initially towards 105° (ESE), gradually turning towards 135° (SE) between mid and high tide. The trendline for current speed rises rapidly to a maximum of *ca* 0.2 m/s when the ocean tide level is *ca* 1.2 m. The speed then gradually falls to *ca* 0.08 m/s when the tide level is 2 m before rising again as the tide level approaches its maximum level at high tide. Actual velocities can vary between ± 0.06 to ± 0.13 m/s from the trendline.

Wave/wind influenced conditions (Figure 9). With increasing offshore wave height, H_{Wis}, (waves between 0.5 and 1.0 m high, curves C and D), the magnitude of the flow reduces after the initial velocity maximum. Initially the flow is eastsoutheastwards. After mid-tide, the direction of the low flow velocity swings, in a clockwise direction, towards the south, then towards the southwest and eventually to the west. At these wave heights, the current then turns back towards 135° as high tide is approached.

When waves, H_{Wis}, are between 1.0 and 1.25 m high (curve E), the current flow reverses at about mid-tide level, *ca* 1.5 m, and the current flows into the boat harbour for the remainder of the rising tide. The initial tide-induced velocity is only *ca* 0.05 to 0.08 m/s, whereas the maximum wave-generated velocity is *ca* 0.15 m/s after mid-tide. Higher waves, $H_{Wis} \geq 1.25$m (curve F), virtually eliminate tidal inflow through the boat harbour onto the southern reef-flat. These higher waves generate a continuous northwestward flow (*ca* 315°) into the boat harbour at all states of the tide with a maximum velocity on the rising tide of at least 0.2 m/s occurring just above mean tide level.

Winds also influence the tide-wave current system. The influence appears to be greatest when waves, H_{Wis}, are less than 1 m, since with larger waves, the wind and wave effects are generally similar in direction. Wind effects are more evident as the tide level increases above mean level and when tidal and wave current velocities are relatively low. Stronger winds increase the possibilities of flow reversal occurring at lower wave heights than would otherwise occur. Wind

direction also influences the system, particularly when current velocities are low. There is a greater likelihood that wave-induced current reversal will be maintained with eastsoutheasterly winds than with southsoutheasterly winds.

For example, at different wind speeds there are differences in current speeds for similar wave conditions and wind direction ($105^o \leq \theta_w < 165^o$). Firstly, with H_{BP} and $H_{Wis} < 0.5$ m, when the wind speed is < 5 m/s (curve M), current directions are consistent with generally mild conditions. However when wind speeds are greater than 5 m/s (curve N), there is a shift in current direction at mid to high tide levels similar to that which occurs with wave heights of the order of 0.75 m (curves C and D). Secondly, when $0.5 \text{ m} \leq H_{Wis} < 0.75$ m (curves P and C), current speeds are higher when wind speeds are lower (curve P) and *vice versa, i.e.* current speeds are lower when southeasterly wind speeds are higher (curve C).

6.2.2 Tidal range between 1.4 and 2.0 m

All data (Figure 10). At the intermediate tidal range, on the rising tide, the currents flow for about half the time in the positive direction, 105^o to 150^o, and for about half the time in the negative direction, *ca* 315^o (51% and 49% respectively). This does not include the time when the instrument was out of the water. The negative currents reach maximum speeds of *ca* 0.3 m/s, which are greater than those for tidal ranges ≥ 2 m, whereas the positive current's maxima of *ca* 0.25 m/s are less than the maxima for tidal ranges ≥ 2 m.

Low waves, H_{BP} and H_{Wis} < 0.35 m and low winds, W < 5 m/s (Figure 11). During mild conditions, initially, as the tide comes in over the bund wall, the flow is eastsoutheastward, with the mean trend speeds reaching *ca* 0.15 m/s when the tide level is around 1.0 to 1.2 m. As the tide rises to between 1.5 and 2.0 m, the current speed drops to less than 0.1 m/s and the direction tends more to the south. At the top of the tide, the speed increases slightly to around 0.1 m/s and the direction becomes southeastwards again.

Wave/wind influenced conditions (Figure 12). As wind and wave, H_{Wis}, conditions increase, the flow tends first more southerly (curves Bd and B2d). Then, as H_{Wis} increases further (curves C and D), the flow tends southwestwards and finally northwestwards into the boat harbour. When H_{Wis} is greater than 1 m (curve Ed), flow is completely reversed and flows into the boat harbour for the whole of the rising tide. Once the current has been reversed (curves D, Es and Fs), speeds increase with increasing wave height, H_{Wis}, reaching a speed of around 0.2 m/s (maximum 0. 32 m/s), at the largest wave heights ($H_{Wis} \approx 1.8$ to 1.9 m), when tide levels are between 1.5 and 2 m.

6.2.3 Tidal range less than 1.4 m

All data (Figure 13). At the lower tidal ranges, less than 1.4 m, the tidally generated currents are much weaker and flow into the boat harbour predominates (61%). Flow in the positive direction, *ca* 105°, only occurs for 39% of the time, excluding the time when the instrument is exposed. Positive currents achieve a maximum of around 0.25 m/s at a fairly high tide level, around 2 m. These stronger positive currents only occurred under quite strong northwesterly wind conditions, wind speed 8 to 10 m/s (16 to 20 kn). Considering only winds from the sector 105° to 165°, the maximum positive current again occurs early on the rising tide at a level of around 1.1 m and has a value of about 0.2 m/s. The maximum negative currents for winds both in this sector and other directions are about 0.35 m/s and occur at tide levels between 1 and 2 m.

Low waves, H_{BP} and H_{Wis} < 0.35 m and low winds, w < 5m/s (Figure 14). During mild conditions, flow on the rising tide is in the eastsoutheastward to southward direction. The eastsoutheastward flow is maintained only during periods of westerly winds (165° to 345°). When the wind is from the 105° to 165° sector, the currents initially flow in the eastsoutheastward direction with a magnitude of up to 0.2 m/s and then fall to almost zero and turn southwards.

Wave/wind influenced conditions (Figure 15). As the winds and waves increase, the weak tidal currents are not able to persist and the current reversal, *i.e.* flow into the boat harbour, occurs when waves, H_{Wis}, exceed 0.5 m (curves C and Dd). As high tide is approached and H_{Wis} is less than 0.75 m the flow may just return to the positive, eastsoutheastward direction (curve C). Current speeds increase in the negative direction as wave height, H_{Wis}, increases and reach speeds of around 0.3 m/s (curve Fs), with maximum values approaching 0.4 m/s.

6.2.4 Effect of tidal range

For easier comparison of the effects of different tidal ranges, the current data have been plotted as a function of the dimensionless tide level parameter $(z_o-z_b)/(z_H-z_b)$ (≡ Z) (Figure 16). When the tide is at the same level as the bund wall crest, Z = 0 and, when the tide is at high tide level, Z = 1.0 for all tidal ranges.

For the calmest conditions, particularly at the larger tidal ranges, the currents flow in an eastsoutheastward direction parallel to the island (Figure 16a, curve A). As wind strengths and wave heights increase, the flows become more southward during the latter stages of the tide (curves B and C) and with increasing wave height swing round to the northwest (curve D). When offshore wave height, H_{Wis}, is greater than 0.75 m and the tidal range is less than 1.4 m (curve E),

current reversal occurs at all tide levels. This complete current reversal then occurs at progressively higher values of H_{Wis} as the tidal range increases (curve E).

The threshold conditions at which the current reverses (*i.e.* flows towards the northwest into the boat harbour) change with increasing tidal range (Table 2). At small tidal ranges (R < 1.4 m) current reversal occurs at relatively low values of H_{Wis} (≈ 0.75 m), whereas at medium tidal ranges (1.4 m ≤ R < 2.0 m), reversal occurs when H_{Wis} ≈ 1.0 m. At large tidal ranges (R ≥ 2.0 m), H_{Wis} must exceed 1.25 m to cause complete reversal of current flow on the southern side of the island during the rising tide.

Table 2 Current directions at southern current meter during rising tide under different wind and wave conditions for three tidal range groups

Wave and wind conditions Wave height, m; wind speed, m/s	**R < 1.4 m**	**1.4 m ≤ R < 2.0 m**	**R ≥ 2.0 m**
H < 0.35, W < 5	ESE	ESE	ESE
H < 0.5, W < 5	ESE	ESE – S – ESE	ESE – S – ESE
0.5 ≤ H_{Wis} < 0.75, W ≥ 5	NW – SW	ESE – W	ESE – W – ESE
0.75 ≤ H_{Wis} < 1.0, W ≥ 5	NW	ESE – NW	ESE – W
1.0 ≤ H_{Wis} < 1.25, W ≥ 5	NW	NW	ESE – NW
H_{Wis} ≥ 1.25, W ≥ 5	NW	NW	(ESE) - NW

The speed of the eastsoutheastward currents on the rising tide under mild conditions is greater for large tidal ranges than it is for small tidal ranges, as would be expected (Figure 16b, curves A, B and C). Maximum speeds occur during the early stages of the rising tide (Z ≈ 0.2) with some observations reaching 0.3 m/s. Current speeds fall to a general mean minimum of about 0.06 m/s just about mean tide level (Z ≈ 0.6) and then rise again as high tide is approached (curves A, B and C). When the current direction has been reversed by wave-generated flows, the magnitude of the current speed for similar wave conditions increases with decreasing tidal range (curves D, E and F). Under these conditions, currents are generally greatest at about or above mean tide level (0.5 < Z < 0.7) and decrease towards both high and low tide levels. For wave heights greater than 1.5 m and tidal ranges less than 1.4 m (curve F), maximum currents are between 0.3 and 0.4 m/s. On the other hand, tides with large tidal ranges (R ≥ 2 m) produce currents that are sufficiently strong to counteract or significantly reduce the wave-generated flow into the boat harbour during

the early and late stages of the rising tide ($Z < 0.2; > 0.8$) when wave heights are between 1.35 and 1.5 m (curve D).

For mild conditions, when waves are small and tidal flow conditions dominate on the reef-top, the current speeds v (Figure 16b) can be represented by the dimensionless parameter vT/R, where T is the half tidal period. In Figure 17, vT/R is plotted as a function of Z for mild conditions, (a) wave heights < 0.35 m, (b) wave heights < 0.5 m. For tidal ranges $R \geq 1.4$ m, vT/R and Z represent the trend of the data well (curves A and B) but this is not so for $R < 1.4$ m, although the discrepancy is less for the lower wave heights (< 0.35 m). There is insufficient data to examine these relationships for even lower wave heights (< 0.25 m) but it could be expected that curve C ($R < 1.4$ m) would coincide with curves A and B as calm conditions are approached. However, most of these tides with small ranges do not expose the bund wall and so there may be some residual differences between curve C and curves A and B for values of Z approaching zero.

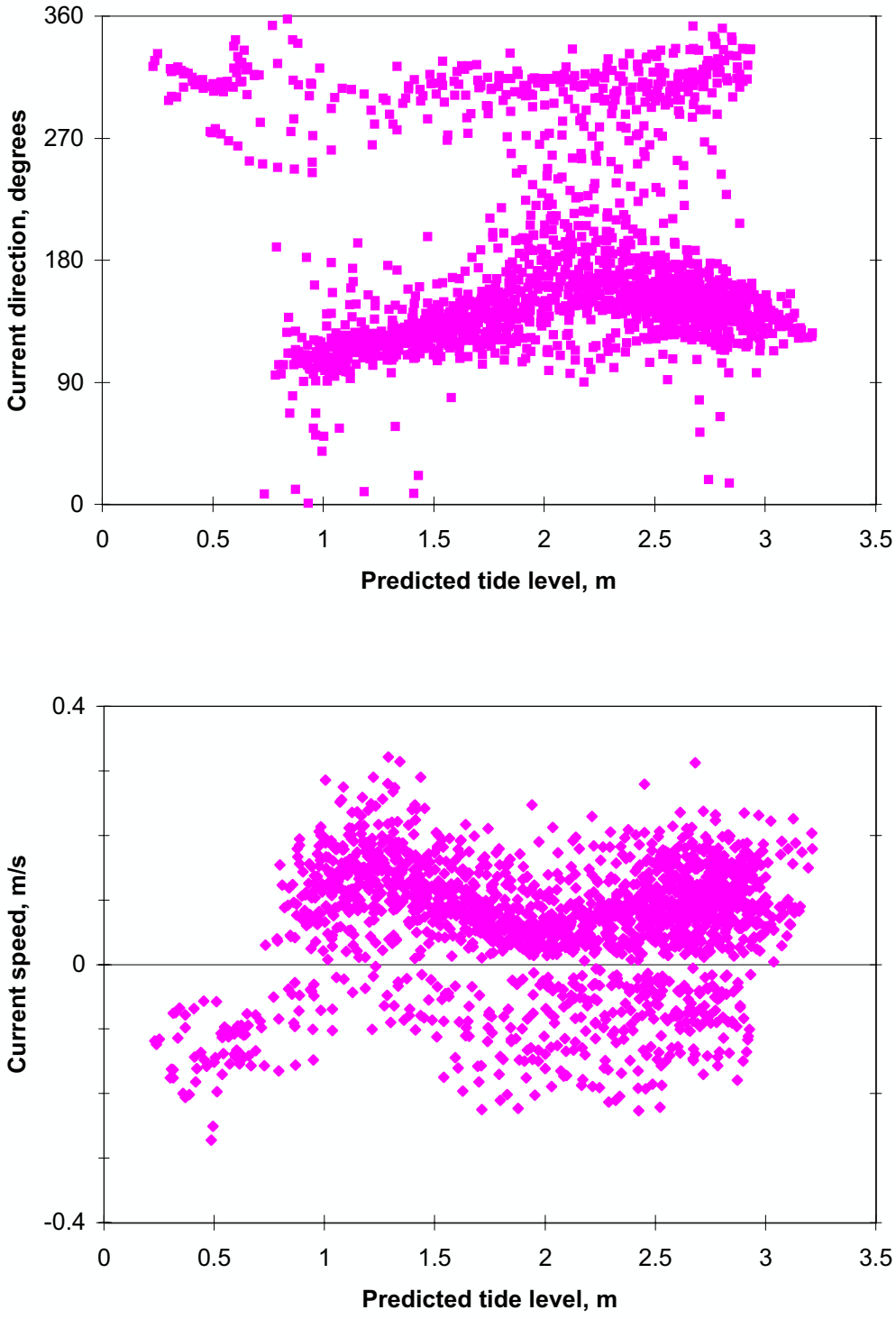

Figure 7. Southern current meter, rising tide, R >= 2.0 m
17 March 1996 to 30 June 1996

Above: Current direction *vs* predicted tide level; all data

Below: Current speed *vs* predicted tide level; all data

θ_c < 225°, positive θ_c >= 225°, negative

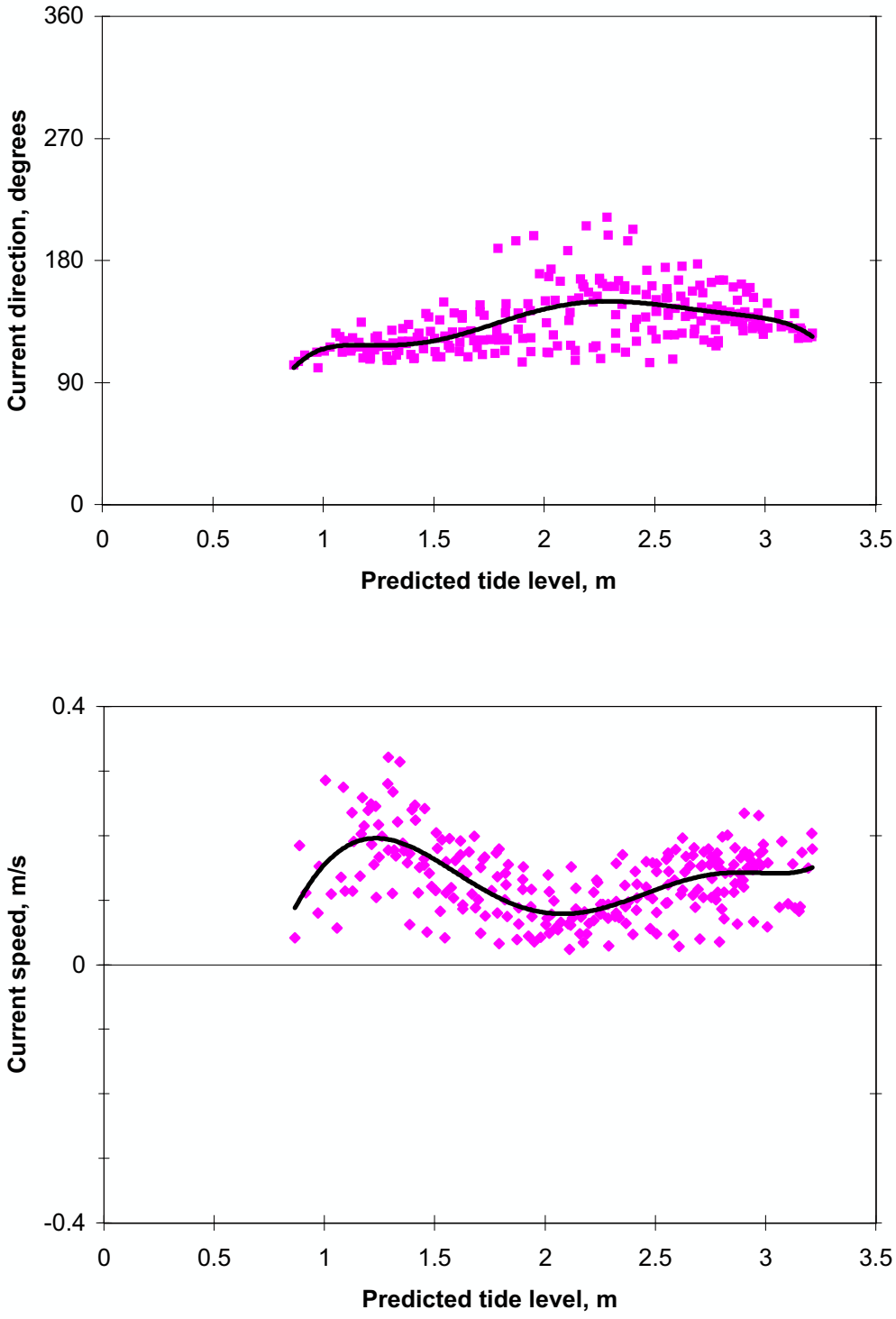

Figure 8. Southern current meter, rising tide, R >= 2.0 m
17 March 1996 to 30 June 1996

Above: Current direction *vs* predicted tide level

Below: Current speed *vs* predicted tide level

Only including data with W < 5m/s

H_{BP} and H_{Wis} < 0.35 m

θ_c < 225°, positive θ_c >= 225°, negative

Trendlines 6th order polynomials

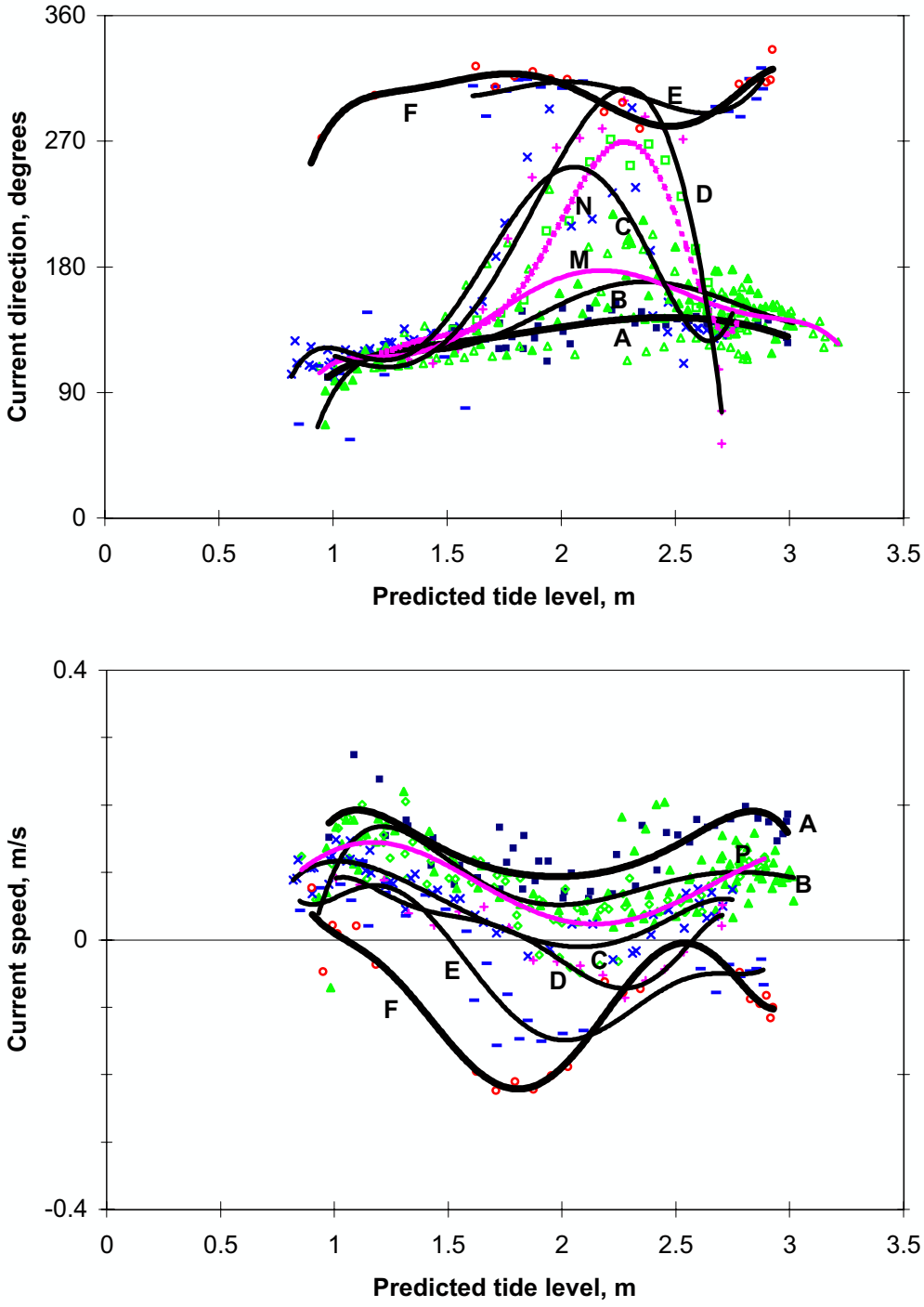

Figure 9. Southern current meter, rising tide, R >= 2.0 m
17 March 1996 to 30 June 1996

Above: Current direction variation with increasing wave height

Below: Current speed variation with increasing wave height

A	W < 5 m/s	All directions	H_{BP} and H_{Wis} < 0.25 m
B	W < 5 m/s	All directions	0.35 m <= H_{BP} and H_{Wis} < 0.5 m
C	W >= 5 m/s	$105^{o} <= \theta_w < 165^{o}$	H_{BP} < 0.5 m; 0.5 m <= H_{Wis} < 0.75 m
D	W >= 5 m/s	$105^{o} <= \theta_w < 165^{o}$	H_{BP} < 0.5 m; 0.75 m <= H_{Wis} < 1.0 m
E	W >= 5 m/s	$105^{o} <= \theta_w < 165^{o}$	H_{BP} < 0.5 m; 1.0 m <= H_{Wis} < 1.25 m
F	W >= 5 m/s	$105^{o} <= \theta_w < 165^{o}$	H_{BP} < 0.5 m; 1.35 m <= H_{Wis} < 1.5 m
M	W < 5 m/s	$105^{o} <= \theta_w < 165^{o}$	H_{BP} and H_{Wis} < 0.5 m
N	W >= 5 m/s	$105^{o} <= \theta_w < 165^{o}$	H_{BP} and H_{Wis} < 0.5 m
P	W < 5 m/s	$105^{o} <= \theta_w < 165^{o}$	H_{BP} < 0.5 m; 0.5 m <= H_{Wis} < 0.75 m
	$\theta_c < 225^{o}$, positive	$\theta_c >= 225^{o}$, negative	Trendlines 4th or 6th order polynomials

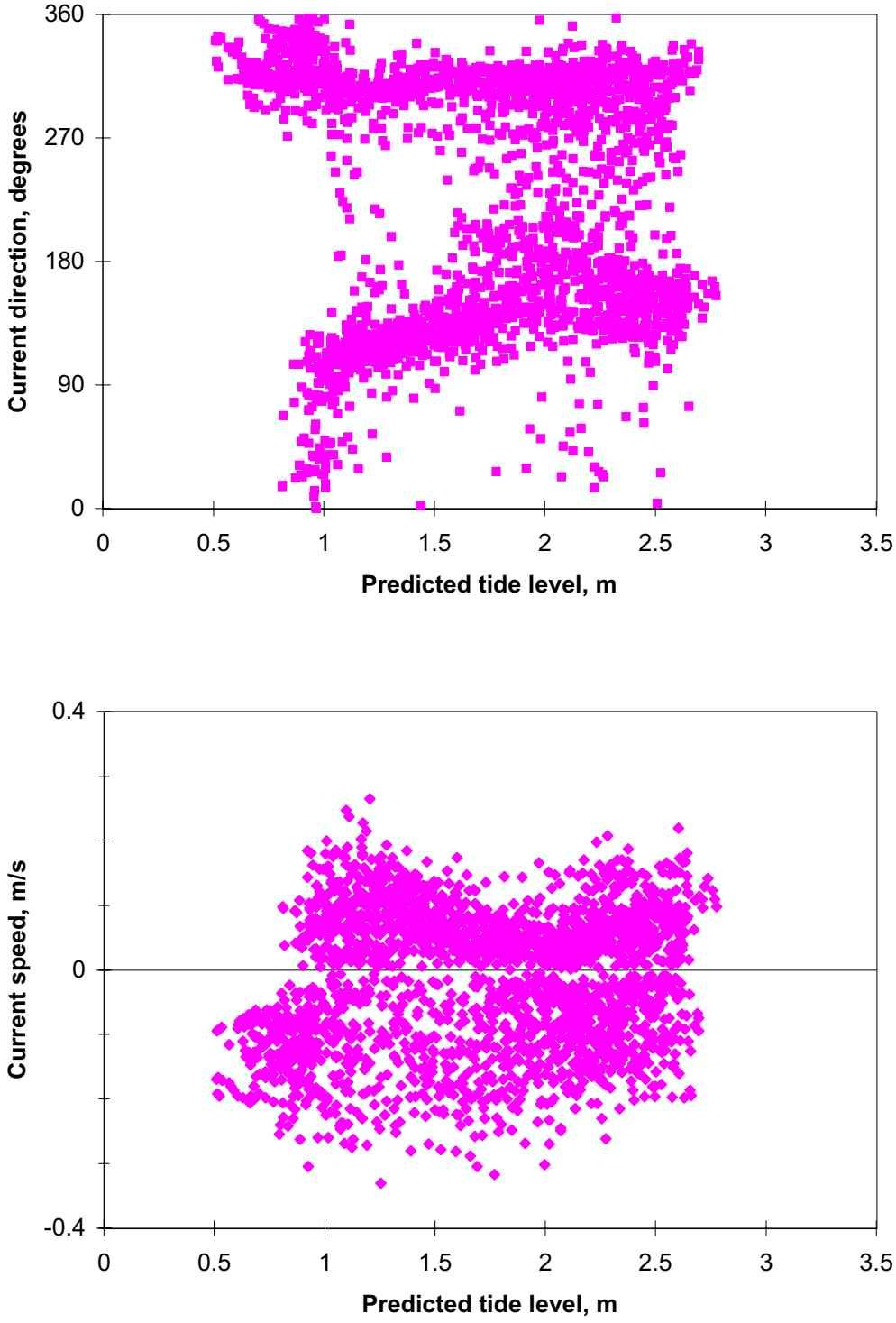

Figure 10. Southern current meter, rising tide, 1.4 m <= R < 2.0 m
17 March 1996 to 30 June 1996

Above: Current direction *vs* predicted tide level; all data

Below: Current speed *vs* predicted tide level; all data

θ_c < 225°, positive θ_c >= 225°, negative

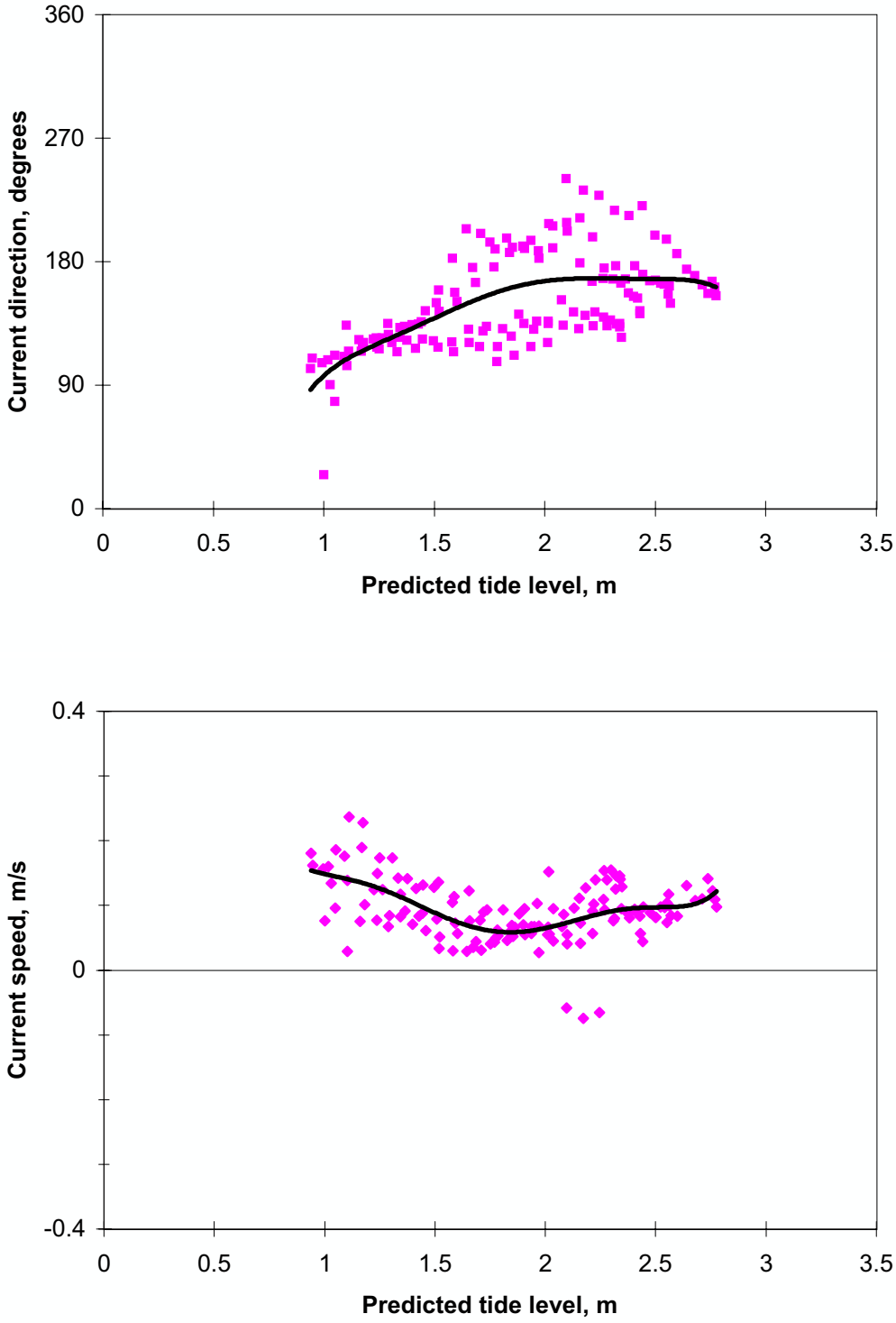

Figure 11. Southern current meter, rising tide, 1.4 m <= R < 2.0 m 17 March 1996 to 30 June 1996

Above: Current direction *vs* predicted tide level

Below: Current speed *vs* predicted tide level

Only including data with W < 5m/s

H_{BP} and H_{Wis} < 0.35 m

θ_c < 225°, positive θ_c >= 225°, negative

Trendlines 6th order polynomials

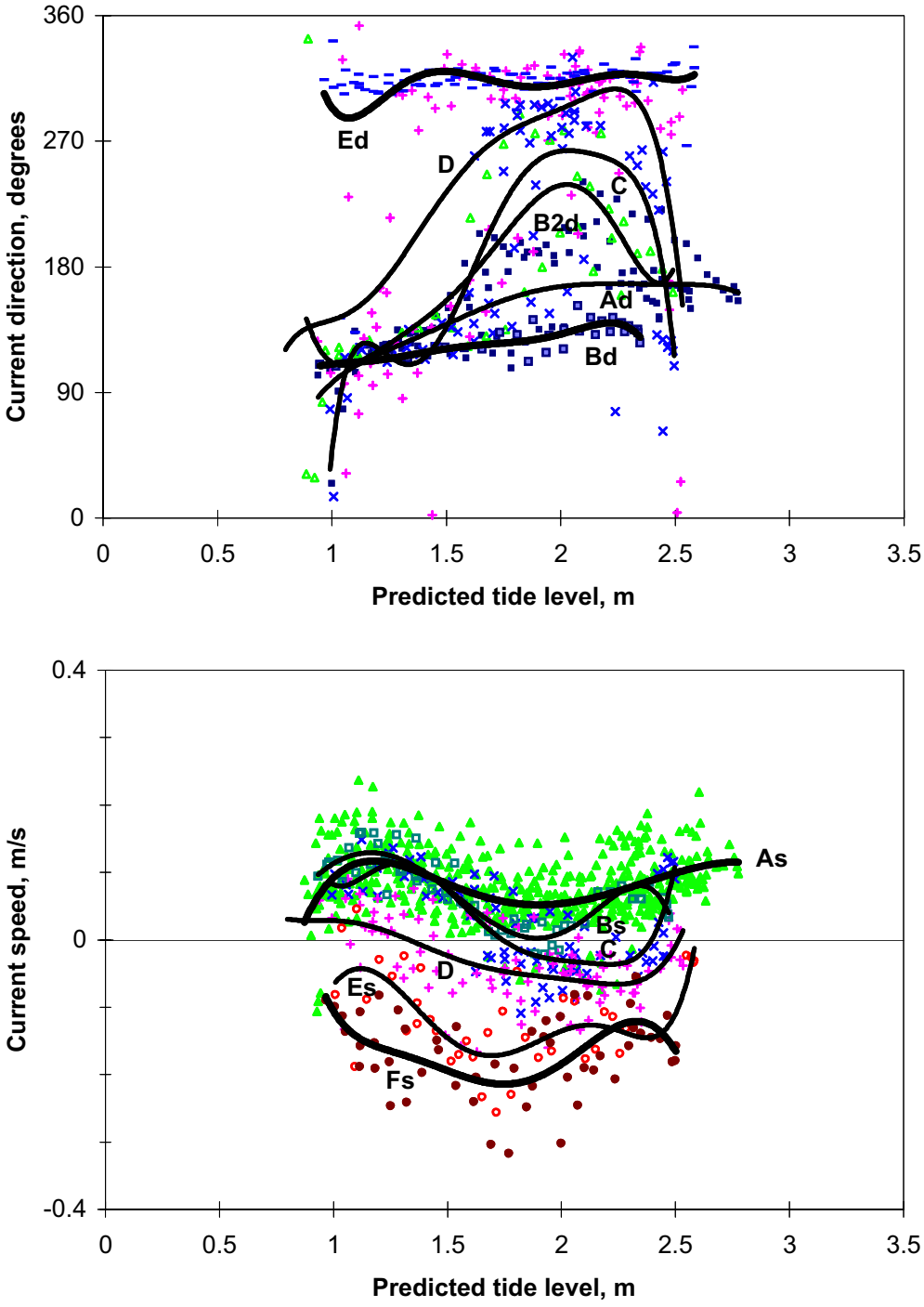

Figure 12. Southern current meter, rising tide, 1.4 m <= R < 2.0 m
17 March 1996 to 30 June 1996
Above: Current direction variation with increasing wave height
Below: Current speed variation with increasing wave height

Ad	W < 5 m/s	All wind directions	H_{BP} and H_{Wis} < 0.35 m
As	W < 5 m/s	All wind directions	H_{BP} and H_{Wis} < 0.5 m
Bd	W < 5 m/s	$105^o <= \theta_w < 165^o$	H_{BP} and H_{Wis} < 0.35 m
B2d	W < 5 m/s	$105^o <= \theta_w < 165^o$	0.35 m <= H_{BP} and H_{Wis} < 0.5 m
Bs	W >= 5 m/s	$105^o <= \theta_w < 165^o$	H_{BP} and H_{Wis} < 0.5 m
C	W >= 5 m/s	$105^o <= \theta_w < 165^o$	H_{BP} < 0.5 m; 0.5 m <= H_{Wis} < 0.75 m
D	W >= 5 m/s	$105^o <= \theta_w < 165^o$	H_{BP} < 0.5 m; 0.75 m <= H_{Wis} < 1.0 m
Ed	W >= 5 m/s	$105^o <= \theta_w < 165^o$	H_{BP} < 0.5 m; H_{Wis} >= 1.0 m
Es	W >= 5 m/s	$105^o <= \theta_w < 165^o$	H_{BP} < 0.5 m; 1.0 m <= H_{Wis} < 1.5 m
Fs	W >= 5 m/s	$105^o <= \theta_w < 165^o$	H_{BP} < 0.5 m; H_{Wis} >= 1.5 m
	$\theta_c < 225^o$, positive	$\theta_c >= 225^o$, negative	Trendlines 6th order polynomials

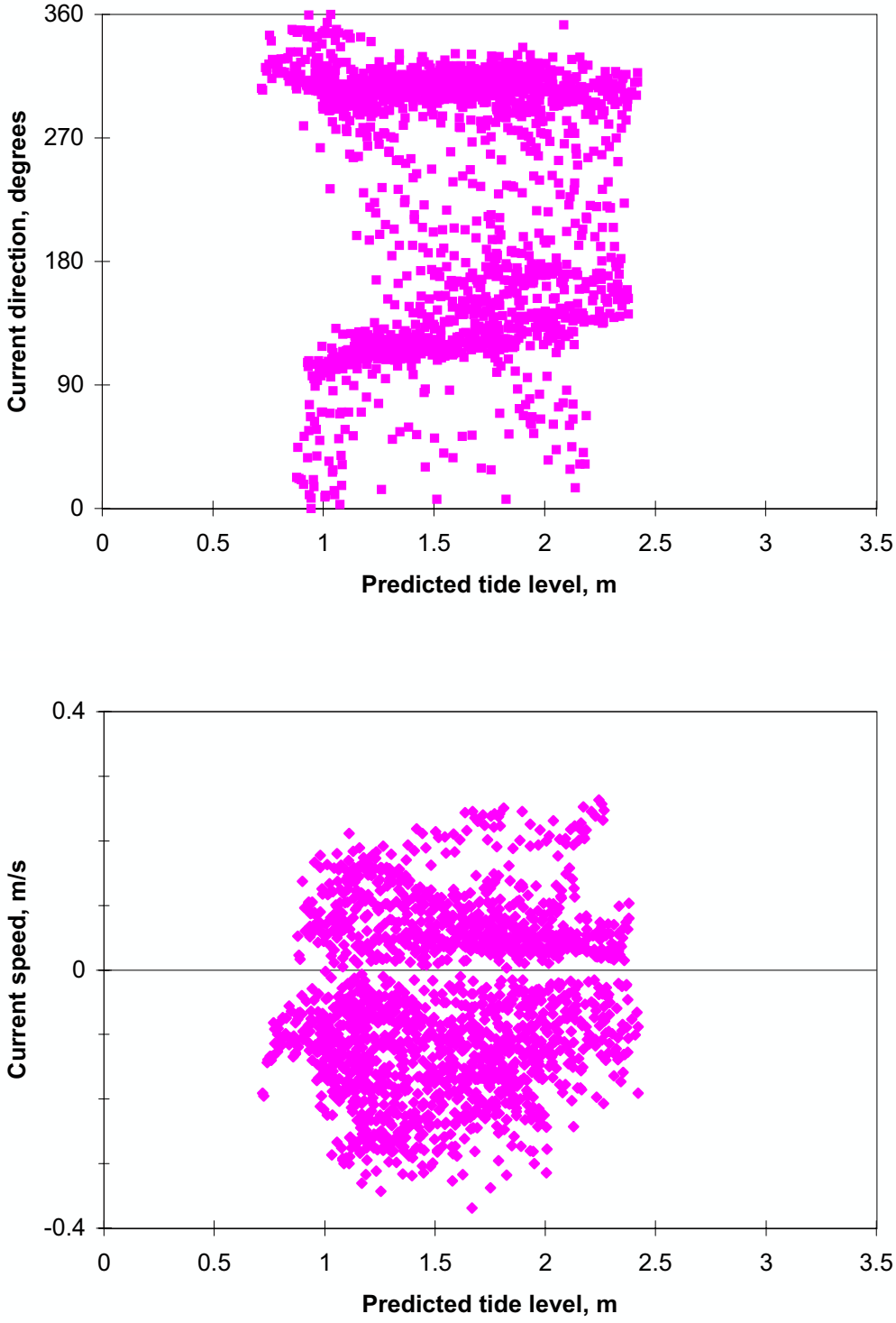

Figure 13. Southern current meter, rising tide, R < 1.4 m
17 March 1996 to 30 June 1996

Above: Current direction *vs* predicted tide level; all data

Below: Current speed *vs* predicted tide level; all data

θ_c < 225°, positive θ_c >= 225°, negative

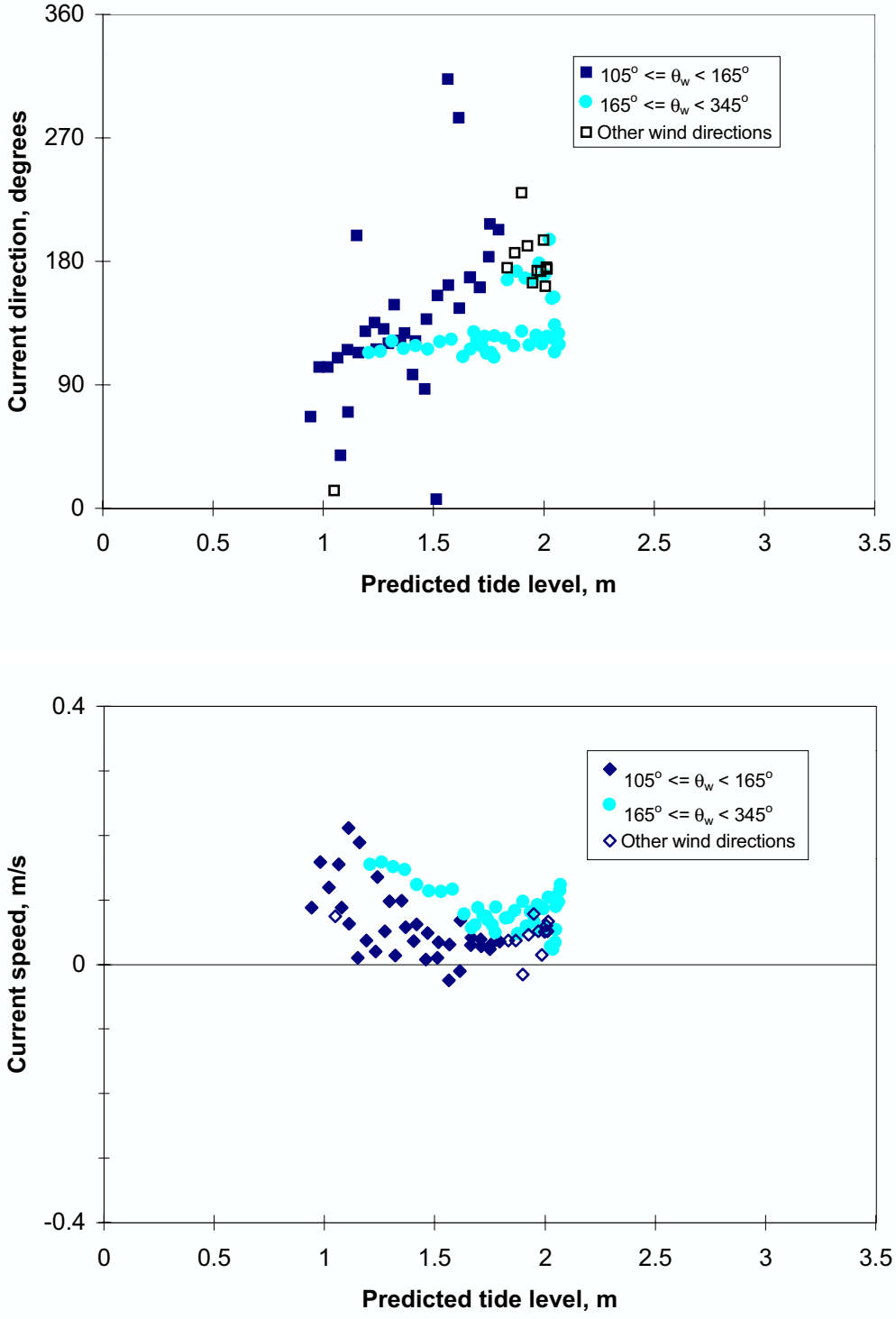

Figure 14. Southern current meter, rising tide, R < 1.4 m
17 March 1996 to 30 June 1996

Above: Current direction *vs* predicted tide level

Below: Current speed *vs* predicted tide level

Only including data with W < 5m/s
H_{BP} and H_{Wis} < 0.35 m

θ_c < 225°, positive θ_c >= 225°, negative

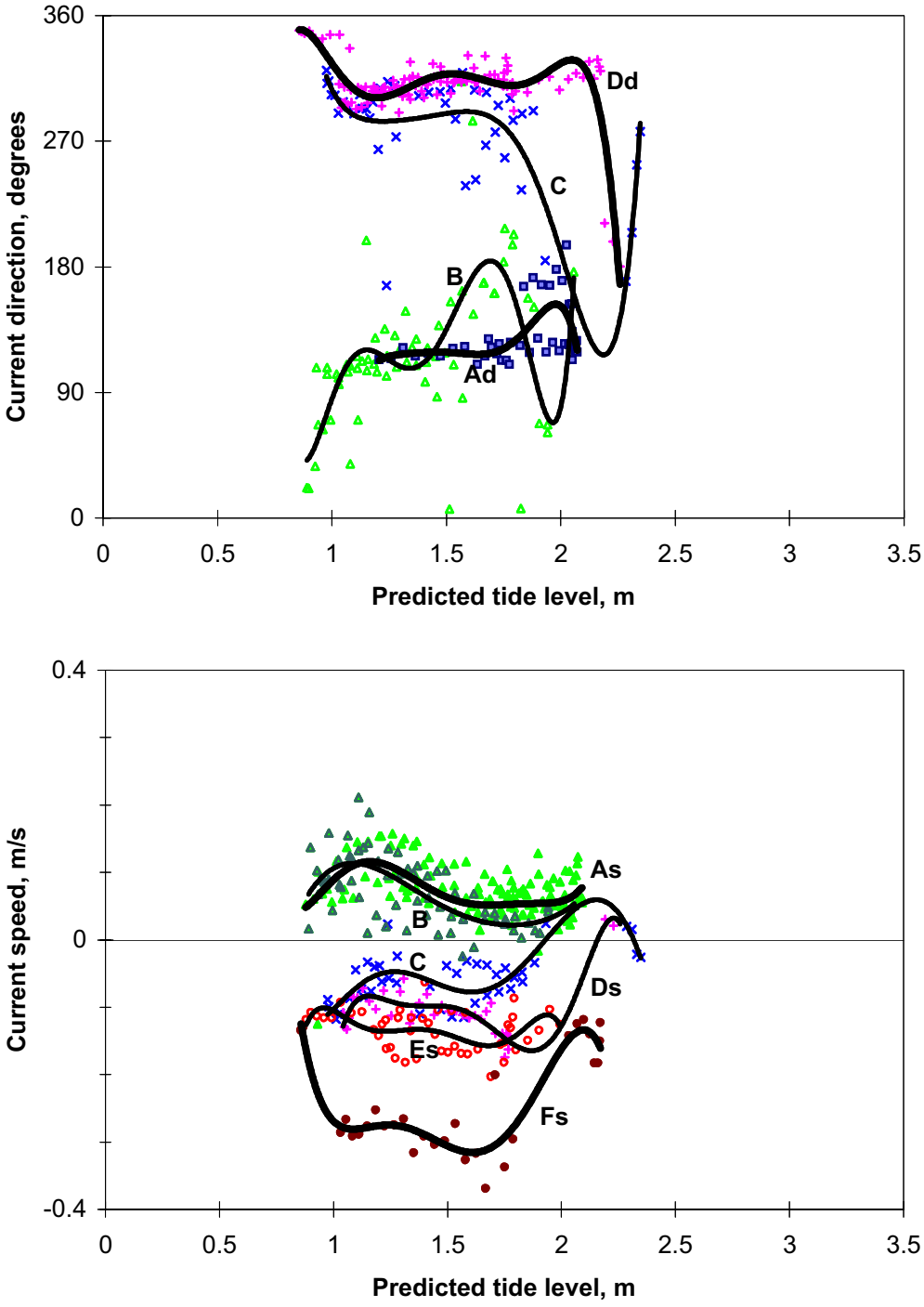

Figure 15. Southern current meter, rising tide, R < 1.4 m
17 March 1996 to 30 June 1996
Above: Current direction variation with increasing wave height
Below: Current speed variation with increasing wave height

Ad	W < 5 m/s	$165^o <= \theta_w < 345^o$	H_{BP} and H_{Wis} < 0.35 m
As	W < 5 m/s	All wind directions	H_{BP} and H_{Wis} < 0.5 m
B	W < 5 m/s	$105^o <= \theta_w < 165^o$	H_{BP} and H_{Wis} < 0.5 m
C	W >= 5 m/s	$105^o <= \theta_w < 165^o$	H_{BP} < 0.5 m; 0.5 m <= H_{Wis} < 0.75 m
Dd	W >= 5 m/s	$105^o <= \theta_w < 165^o$	H_{BP} < 0.5 m; H_{Wis} >= 0.75 m
Ds	W >= 5 m/s	$105^o <= \theta_w < 165^o$	H_{BP} < 0.5 m; 0.75 m <= H_{Wis} < 1.0 m
Es	W >= 5 m/s	$105^o <= \theta_w < 165^o$	H_{BP} < 0.5 m; 1.0 m <= H_{Wis} < 1.5 m
Fs	W >= 5 m/s	$105^o <= \theta_w < 165^o$	H_{BP} < 0.5 m; H_{Wis} >= 1.5 m
	$\theta_c < 225^o$, positive	$\theta_c >= 225^o$, negative	Trendlines 6th order polynomials

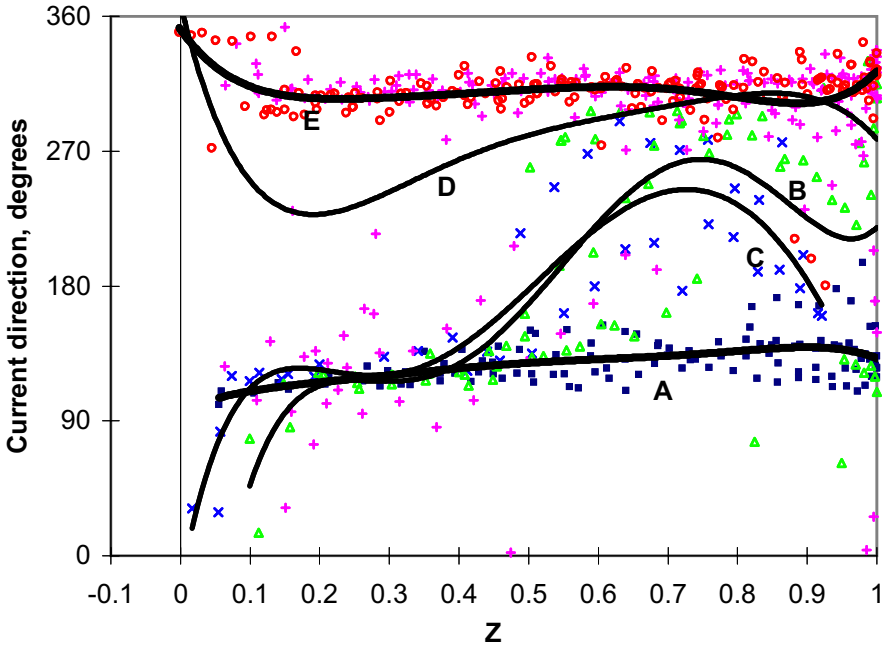

Current direction vs Dimensionless water level, $Z = (z - z_b)/(z_H - z_b)$

A	W < 5 m/s	All wind directions	R >= 2.0 m,	H_{BP} and H_{Wis} < 0.25 m
		$105^o <= \theta_w < 165^o$	1.4 m <= R < 2.0 m,	H_{BP} and H_{Wis} < 0.35 m
		$165^o <= \theta_w < 345^o$	R <= 1.4 m,	H_{BP} and H_{Wis} < 0.35 m
B	W < 5 m/s	$105^o <= \theta_w < 165^o$	1.4 m <= R < 2.0 m,	0.35 m <= H_{BP} and H_{Ws} < 0.5 m
C	W >= 5 m/s	$105^o <= \theta_w < 165^o$	1.4 m <= R < 2.0 m,	H_{BP} < 0.5 m, 0.5 m <= H_{Wis} < 0.75 m
D	W >= 5 m/s	$105^o <= \theta_w < 165^o$	1.4 m <= R < 2.0 m,	H_{BP} < 0.5 m, 0.75 m <= H_{Wis} < 1.0 m
E	W >= 5 m/s	$105^o <= \theta_w < 165^o$	R <= 1.4 m,	H_{BP} < 0.5, H_{Wis} >= 0.75 m
			1.4 m <= R < 2.0 m,	H_{BP} < 0.5 m, H_{Wis} >= 1.0 m
			R >= 2.0 m,	H_{BP} < 0.5 m, H_{Wis} >= 1.25 m

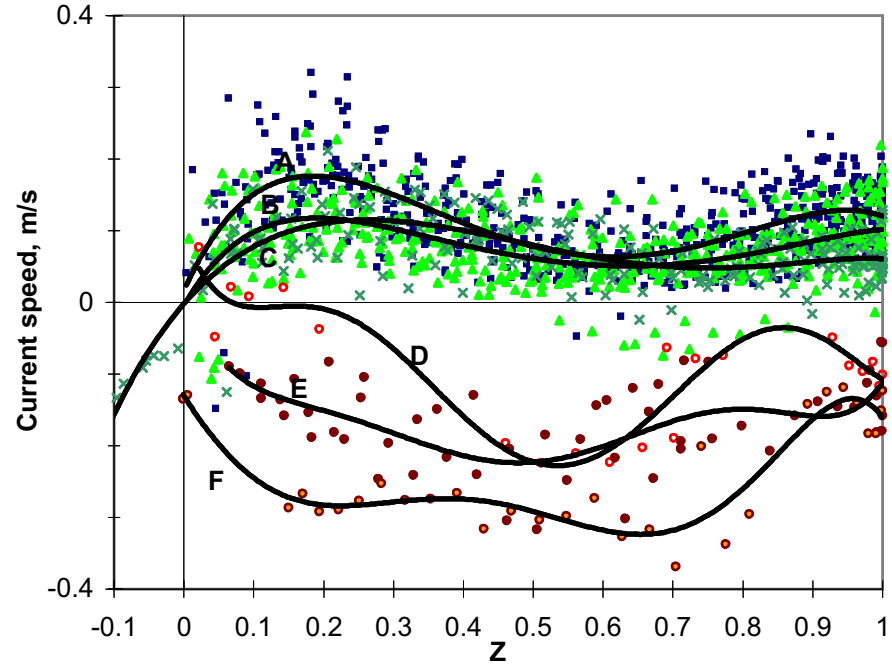

Current speed vs Dimensionless water level, $Z = (z - z_b)/(z_H - z_b)$, ($<225^o$ +'ve, $>= 225^o$ -'ve)

A	W < 5 m/s	All wind directions	R >= 2.0 m,	H_{BP} and H_{Wis} < 0.5 m
B	W < 5 m/s	All wind directions	1.4 m <= R < 2.0 m,	H_{BP} and H_{Wis} < 0.5 m
C	W < 5 m/s	All wind directions	R <= 1.4 m,	H_{BP} and H_{Wis} < 0.5 m
D	W >= 5 m/s	$105^o <= \theta_w < 165^o$	R >= 2.0 m,	H_{BP} < 0.5 m, 1.35 m <= H_{Wis} < 1.5 m
E	W >= 5 m/s	$105^o <= \theta_w < 165^o$	1.4 m <= R < 2.0 m,	H_{BP} < 0.5 m, H_{Wis} >= 1.5 m
F	W >= 5 m/s	$105^o <= \theta_w < 165^o$	R <= 1.4 m,	H_{BP} < 0.5 m, H_{Wis} >= 1.5 m

Figure 16. Southern Current meter, rising tide, all tidal ranges 17 March 1996 to 30 June 1996

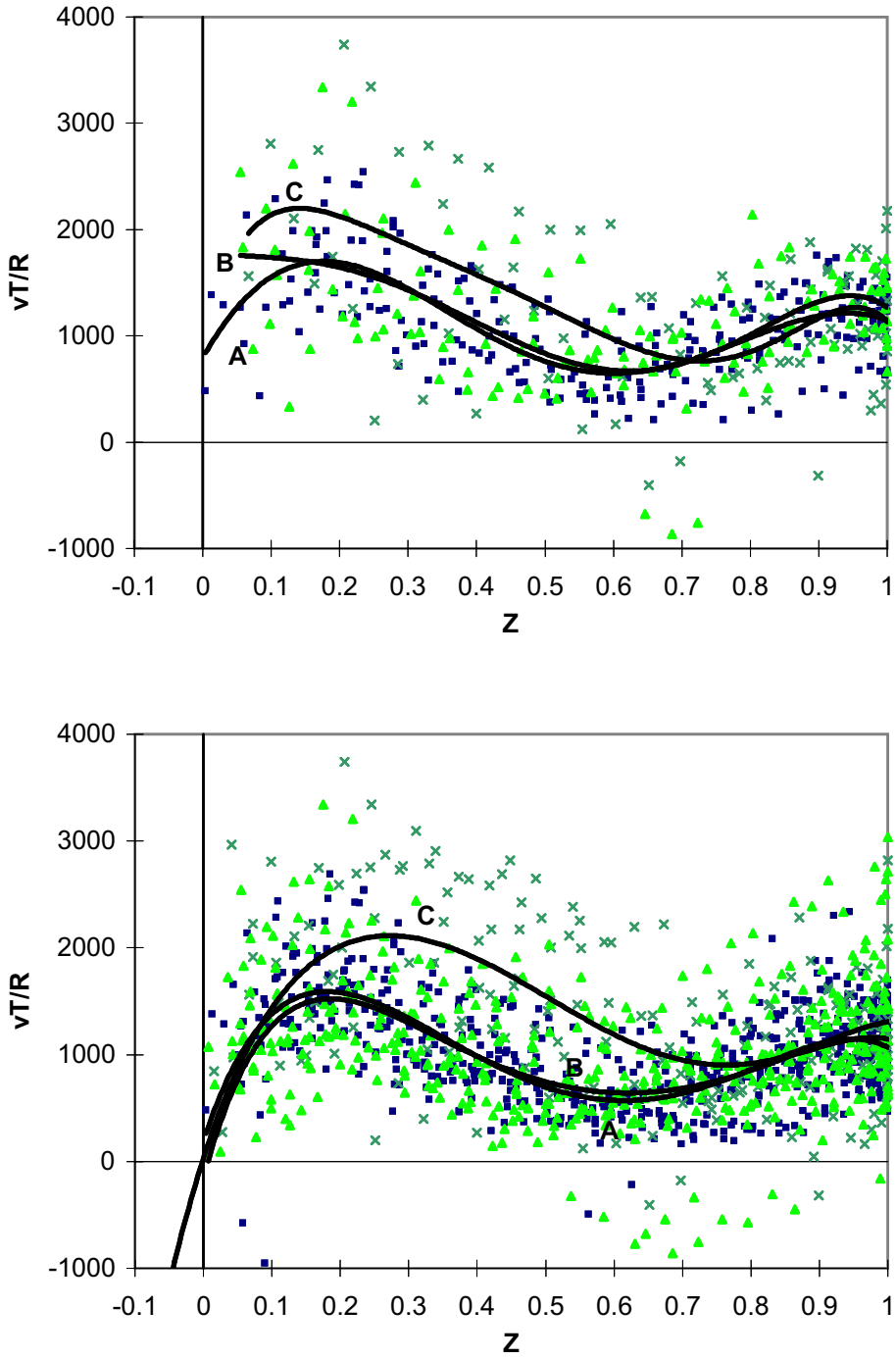

Figure 17. Southern Current meter, rising tide, W < 5 m/s
Dimensionless velocity, vT/R vs Dimensionless water level Z
$Z = (z_o - z_b)(z_H - z_b)$
17 March 1996 to 30 June 1996

Above	**H_{BP} and H_{Wis} < 0.35 m**
Below	**H_{BP} and H_{Wis} < 0.5 m**
A	R >= 2.0 m
B	1.4 m <= R < 2.0 m
C	R < 1.4 m

6.3 Southern current meter, falling tide

6.3.1 Tidal range greater than 2.0 m

All data (Figure 18). On the falling tide, initially the flow at the southern current meter is predominantly to the southeast (140^o) until the tide level drops to about 1.5 m (close to the mean tide value of 1.52 m LWD). When the tide level is below mean tide level, the current reverses and flows in a northwestward direction (around 320^o) out through the boat harbour (Figure 18a). Overall, the flow was out through the boat harbour for 52% of the time for which data is available. The presence of the reef begins to affect the water level on the reef-top as the ocean tide level falls below 1.3 m LWD (Figure 6b). Current speeds in the positive direction reach maxima of *ca* 0.3 m/s when the tide level has fallen to *ca* 2.3 m (Figure 18b). The maximum southeastward falling tidal velocities are generally greater than the rising tidal velocities in that direction. After the current has reversed, flow into the boat harbour reaches maximum speed of *ca* 0.4 m/s when the tide level has fallen to 1.1 m. The speed then diminishes until the bund wall crest level of 0.86 m is reached after which it continues to drop but at a more gradual rate. In contrast with the rising tide, current data is available for the falling tide at predicted tide levels below the bund wall crest level since the actual water level on the reef-top was still above the current meter sensors for much of the time.

Low waves, H_{BP} and H_{Wis} < 0.35 m and low winds, W < 5m/s (Figure 19). As is the case for the rising tide, when winds and waves are low, currents are controlled by the tide. As the tide falls, initially the current continues to flow out towards the southeast with speeds of up to 0.3 m/s. Shortly after the water level falls below 1.5 m the flow reverses quite quickly towards the northwest and then northnorthwest (330^o) as the tide flows into the boat harbour. Current speed is at a maximum of *ca* - 0.2 m/s when z_o is 1.1 m.

Wave/wind influenced conditions (Figure 20). As the offshore wave height, H_{Wis}, increases, the magnitude of the initial velocity in the southeastward direction decreases until H_{Wis} reaches 1.15 m, when the current is reversed towards the boat harbour for the whole of the falling tide (Figure 20a, curve C_d). Conversely, at water levels below 1.5 m, current velocity in the negative direction increases with increasing H_{Wis}, reaching a maximum of around 0.3 m/s when H_{Wis} is greater than 1.5 m (Figure 20b, curve C_s).

6.3.2 Tidal range between 1.4 and 2.0 m

All data (Figure 21). At the intermediate tidal range, when the tide is falling, the amount of time that the currents flow in the positive direction (*i.e*. away from the boat harbour) is reduced

considerably when compared with the higher tidal ranges (from 48% to 28% of the time for which data is available). The positive currents reach maximum speeds of *ca* 0.25 m/s when the tide level has fallen to *ca* 2.3 m and the negative currents a maximum of *ca* 0.4 m/s when the tide level falls to between 1.3 m and 1.1 m.

Low waves, H_{BP} and H_{Wis} < 0.35 m and low winds, w < 5m/s (Figure 22). During mild conditions, initially, flow on the falling tide is in a southeast to southsoutheastward direction (150°); then, as with the higher tidal ranges, at a tide level of 1.5 m, the current reverses and flows out through the boat harbour (340°). Both the southeast to southsoutheastward flows and the northnorthwestward flows are not as strong as they were at the higher tidal ranges, 0.2 m/s as compared with 0.3 m/s for the southeast to southsoutheastward flows and 0.15 m/s compared with 0.2 m/s for the northnorthwestward flows.

Wave/wind influenced conditions (Figure 23). As with the higher tidal ranges, current speeds during the early stage of the ebb tide decrease with increasing H_{Wis} until the current has reversed, z_o = 1.5 m. Then the current speeds increase slightly with H_{Wis} during the later stages of the falling tide. At higher values of H_{Wis}, the reversal to northnorthwestward flow occurs earlier on the falling tide than at higher tidal ranges, *i.e*. it occurs at higher values of z_o. The reversal may go in either a clockwise or anticlockwise direction. For values of the offshore wave height, H_{Wis}, greater than 1 m (curves D and E), the current is reversed into the boat harbour all the time.

6.3.3 Tidal range less than 1.4 m

All data (Figure 24). At the lower tidal ranges, less than 1.4 m, the tidally generated currents are weaker than those at higher tidal ranges and flow into the boat harbour predominates. Flow in the positive direction, *ca* 150°, only occurs for 24% of the time, excluding the time when the instrument is exposed. Positive currents achieve a maximum of around 0.3 m/s at tide levels between 2 and 1.5 m, but again, as with the rising tide, these stronger positive currents occurred only during northwesterly wind conditions. If only current speeds when winds were from the sector 105° to 165° are considered, the maximum positive current only reached a value of 0.18 m/s. The maximum negative currents are between 0.4 and 0.5 m/s and occur when the tide falls to a level of *ca* 1.2 m.

Low waves, H_{BP} and H_{Wis} < 0.35 m and low winds, W < 5m/s (Figure 25). During mild conditions with small tides, the flow on the falling tide is generally somewhat confused until the tide level falls below about 1.4 m. Then flow is towards the northnorthwest, out through the boat harbour and attains speeds of up to 0.2 m/s. Southeastward flows, ≥ 0.1 m/s, at higher tide levels, almost all

occurred when winds were westerly. (*N.B.* This data set for tidal range < 1.4 m is somewhat anomalous as it contains no data for the wind direction sector 105^o – 165^o)

Wave/wind influenced conditions (Figure 26). As the winds and waves increase, the weak tidal currents are not able to persist and the current reversal, *i.e*. flow into the boat harbour, occurs for the whole of the falling tide when offshore waves, H_{Wis}, exceed 0.75 m (curves D, E and F). Positive (southeastward) current speeds rapidly decrease with increasing wave height during the first part of the falling tide until full reversal occurs at wave heights greater than 0.75 m. The reversed currents then increase with increasing wave height. The maximum current speeds in the northnorthwestward direction occur at tide levels close to 1.2 m and reach values between 0.4 and 0.5 m/s when $H_{Wis} \geq 1.25$ m. Paradoxically, the threshold wave height at which full current reversal occurs is greater for the falling tide ($H_{Wis} = 0.75$ m) than for the rising tide ($H_{Wis} = 0.5$ m). The reason for this is that the speeds of the initial southeastward currents during the early stages of the falling tide are greater than those that occurred during any stage of the rising tide (Figures 26 and 15).

6.3.4 Effect of tidal range

The same method of comparing the effects of different tidal ranges is used again, *i.e*. the current data have been plotted as a function of the dimensionless tide level parameter $Z = (z_o-z_b)/(z_H-z_b)$ together with trendlines (Figure 27).

During the falling tide, the current flows out through the boat harbour when the tide level is below 1.5 m (Z = 0.25 to 0.35) under all conditions. Therefore, when considering the effect of tidal range on current direction, an effect is only observed at tide levels greater than mean tide, 1.5 m, (Z = 0.25).

For the calmest conditions, particularly at the larger tidal ranges, the currents flow in a southeastward direction until mean tide level, 1.5 m, is reached, *i.e.* $Z \approx 0.25$. As wind strengths and wave heights increase, the reversal takes place at successively higher values of Z, until at offshore wave height, H_{Wis}, greater than 0.75 m, tidal range less than 1.4 m, current reversal occurs for the whole of the falling tide. This current reversal then occurs at progressively higher values of H_{Wis} as the tidal range increases (Table 3).

The threshold, at which the current reverses, *i.e*. to northwestward flow, changes with the tidal range (Table 3). For larger tidal ranges, higher values of H_{Wis} and stronger winds are required to reverse the southeastward tidal flow.

The highest current speeds measured on the falling tide at the southern current meter during the March – June 1996 period were in the negative direction, *i.e.* towards the boat harbour. These occurred when the tidal range was less than 1.4 m and the wave height greater than 1.25 m (Figure 27b, curve E). They occurred at around the half tide level, when $Z \approx 0.35$. The strongest positive currents occurred during the highest tidal ranges and the lower wave heights (Figure 27b, curve A). As on the rising tide, lower negative currents occurred when tidal ranges were large (Figure 27b, curve D). So again, the stronger southeastward flowing tidal current counteracts any wave- or wind-generated current towards the boat harbour.

Table 3 Current directions at southern current meter during falling tide under different wind and wave conditions for three tidal range groups
(tide levels ≥ 1.5 m; generalisations made for simplification)

Wave and wind conditions Wave height, m; wind speed, m/s Wave ht, m	**R < 1.4 m**	**1.4 m ≤ R < 2.0 m**	**R ≥ 2.0 m**
$H < 0.35$, $W < 5$	SE	SE	SE
$H < 0.5$, $W < 5$	SE - NW	SE	SE
$0.5 \le H_{Wis} < 0.75$, $W \ge 5$	(SE) - NW	SE – NW	SE
$0.75 \le H_{Wis} < 1.0$, $W \ge 5$	NW	(SE) – NW	SE - NW
$1.0 \le H_{Wis} < 1.25$, $W \ge 5$	NW	NW	SE – NW
$H_{Wis} \ge 1.25$, $W \ge 5$	NW	NW	NW

Again it is difficult to assess the validity of the dimensionless parameter vT/R in representing the velocity of tidal currents because of the lack of data with very small wave heights (Figure 28a). This difficulty is increased in this situation where the change in current direction occurs at a more or less constant water level z_o, *i.e.* 1.5 m, since this value does not correspond with a constant value of Z for different tidal ranges (Figure 28b).

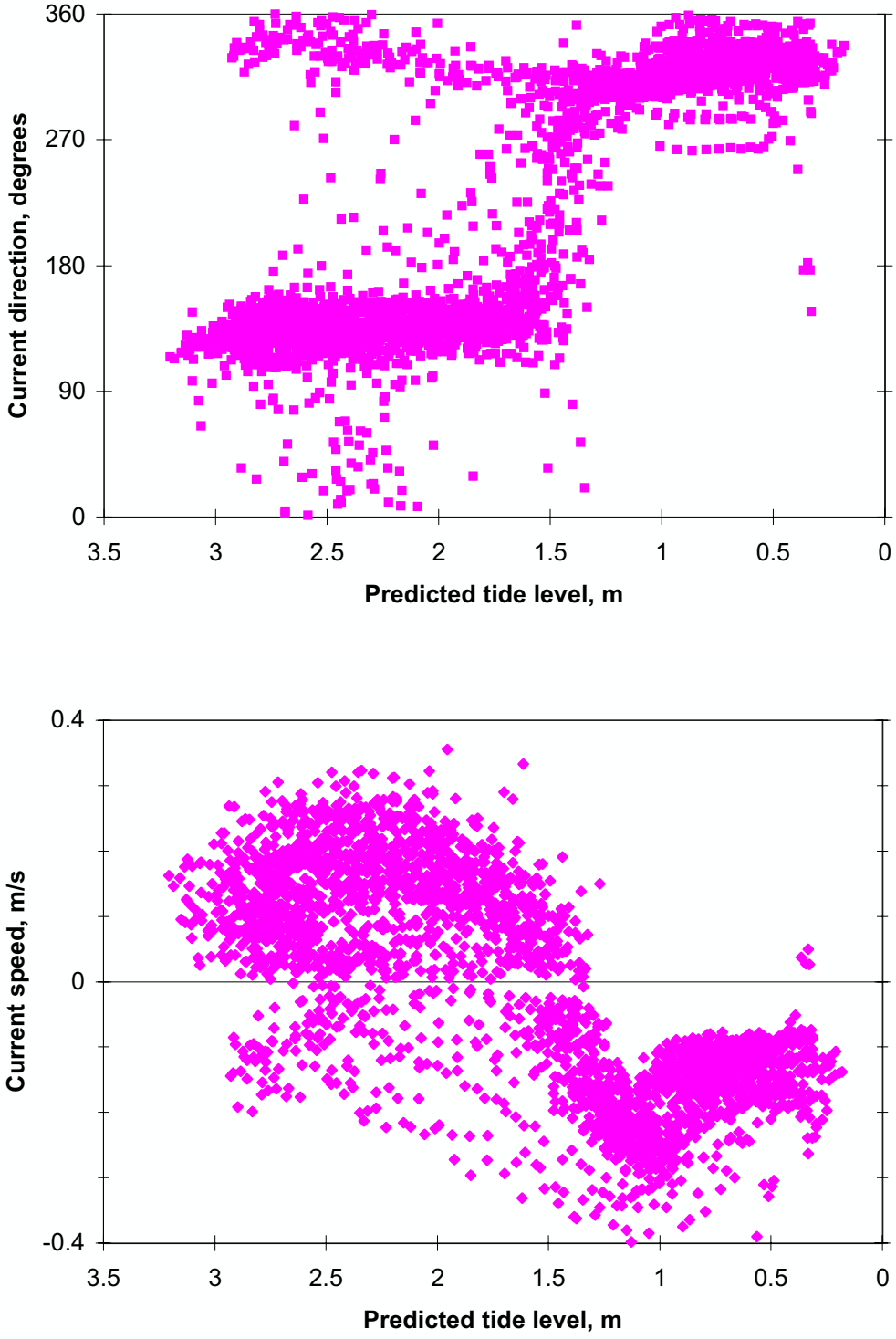

Figure 18. Southern current meter, falling tide, R >= 2.0 m
17 March 1996 to 30 June 1996

Above: Current direction *vs* predicted tide level; all data

Below: Current speed *vs* predicted tide level; all data

θ_c < 225°, positive θ_c >= 225°, negative

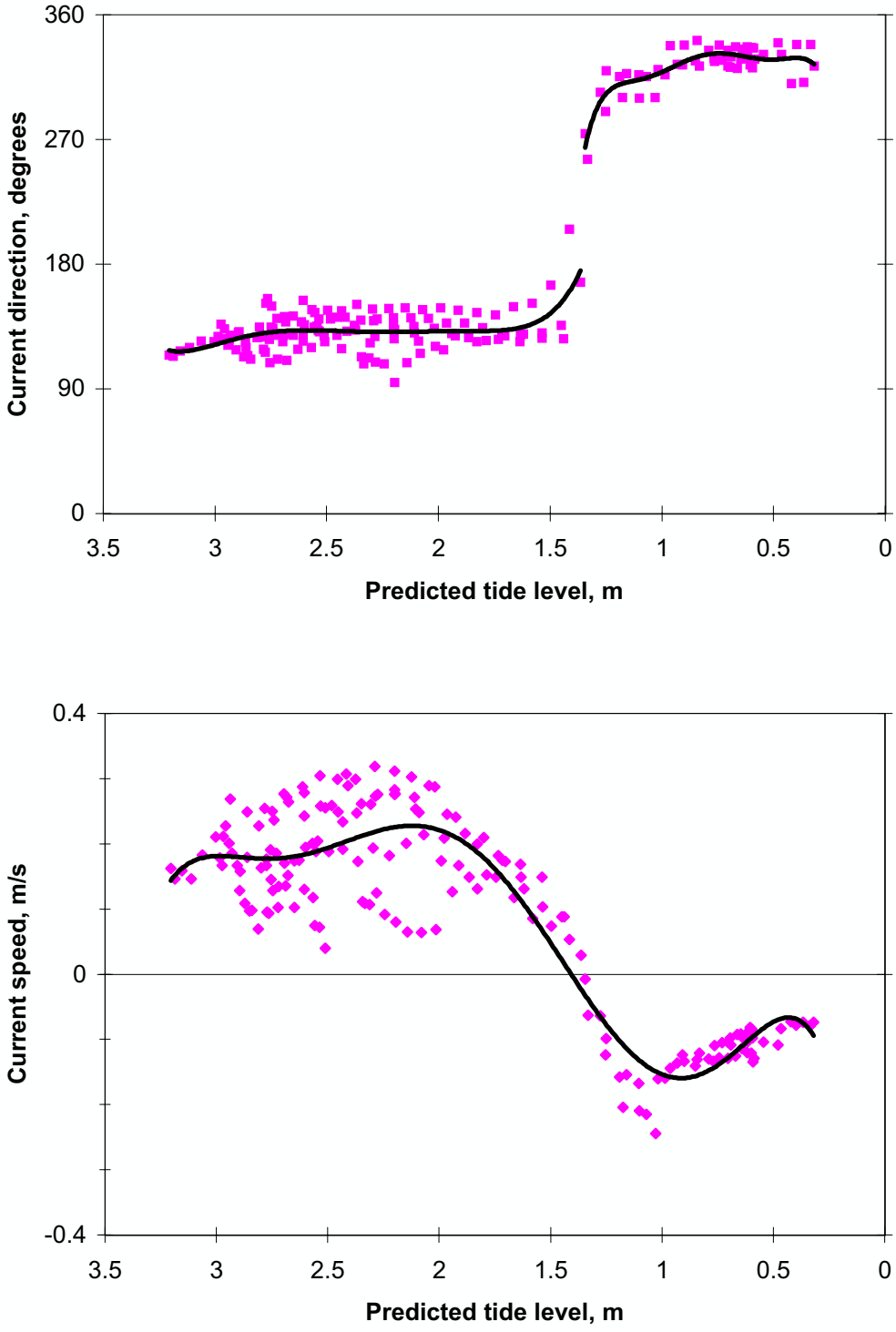

Figure 19. Southern current meter, falling tide, R >= 2.0 m
17 March 1996 to 30 June 1996

Above: Current direction *vs* predicted tide level

Below: Current speed *vs* predicted tide level

Only including data with W < 5m/s
H_{BP} and H_{Wis} < 0.35 m

θ_c < 225°, positive θ_c >= 225°, negative

Trendlines 6th order polynomials

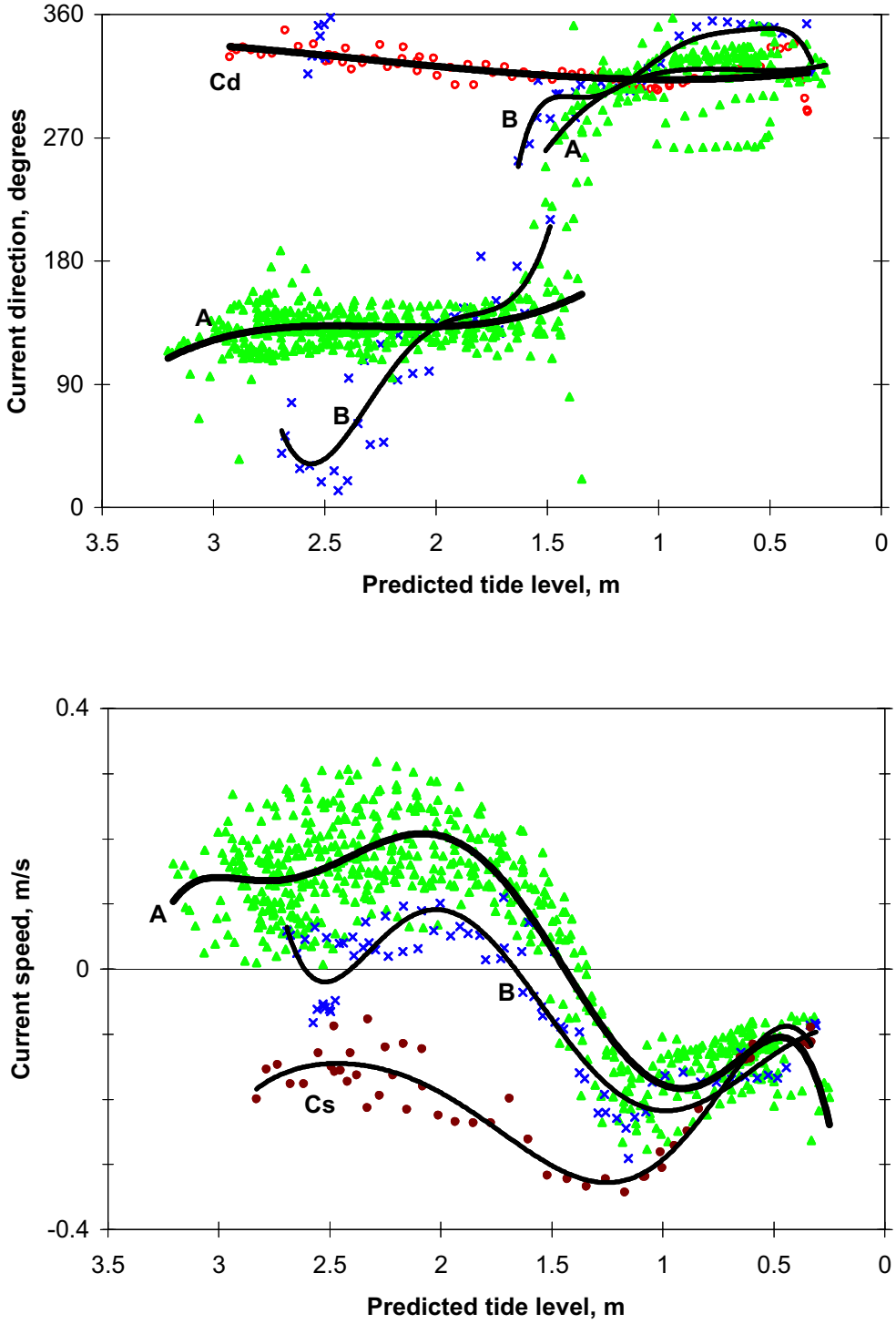

Figure 20. Southern current meter, falling tide, R >= 2.0 m
17 March 1996 to 30 June 1996
Above: Current direction variation with increasing wave height
Below: Current speed variation with increasing wave height

A	W < 5 m/s	All wind directions	H_{BP} and H_{Wis} < 0.5 m
B	W >= 5 m/s	$105^{o} <= \theta_w < 165^{o}$	H_{BP} < 0.5 m, 0.5 m <= H_{Wis} < 1.15 m
Cd	W >= 5 m/s	$105^{o} <= \theta_w < 165^{o}$	H_{BP} < 0.5 m, H_{Wis} >= 1.15 m
Cs	W >= 5 m/s	$105^{o} <= \theta_w < 165^{o}$	H_{BP} < 0.5 m, H_{Wis} >= 1.5 m
	$\theta_c < 225^{o}$, positive	$\theta_c >= 225^{o}$, negative	Trendlines various order polynomials

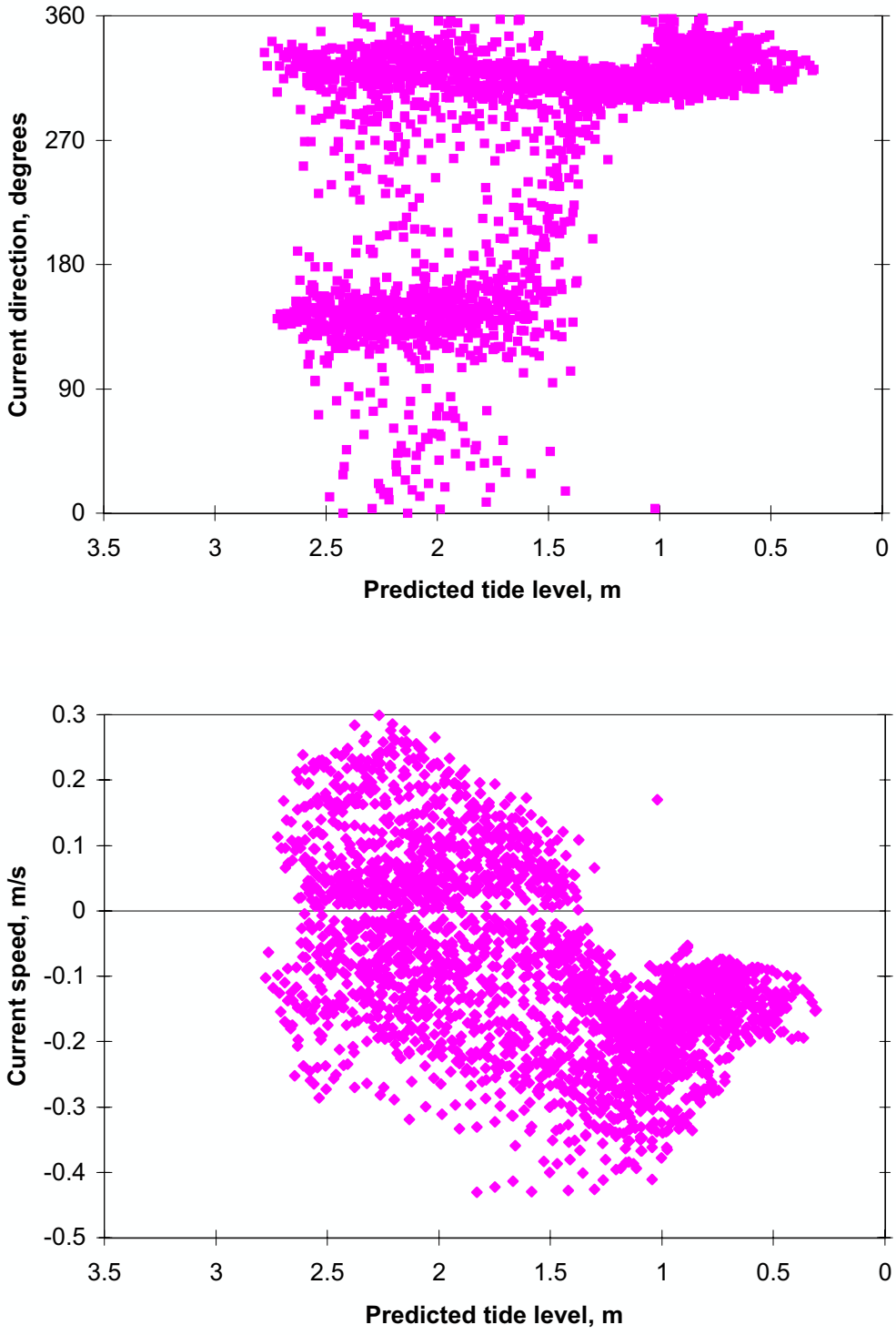

Figure 21. Southern current meter, falling tide, 1.4 m <= R < 2.0 m 17 March 1996 to 30 June 1996

Above: **Current direction *vs* predicted tide level; all data**

Below: **Current speed *vs* predicted tide level; all data**

$\theta_c < 225^o$, positive $\theta_c >= 225^o$, negative

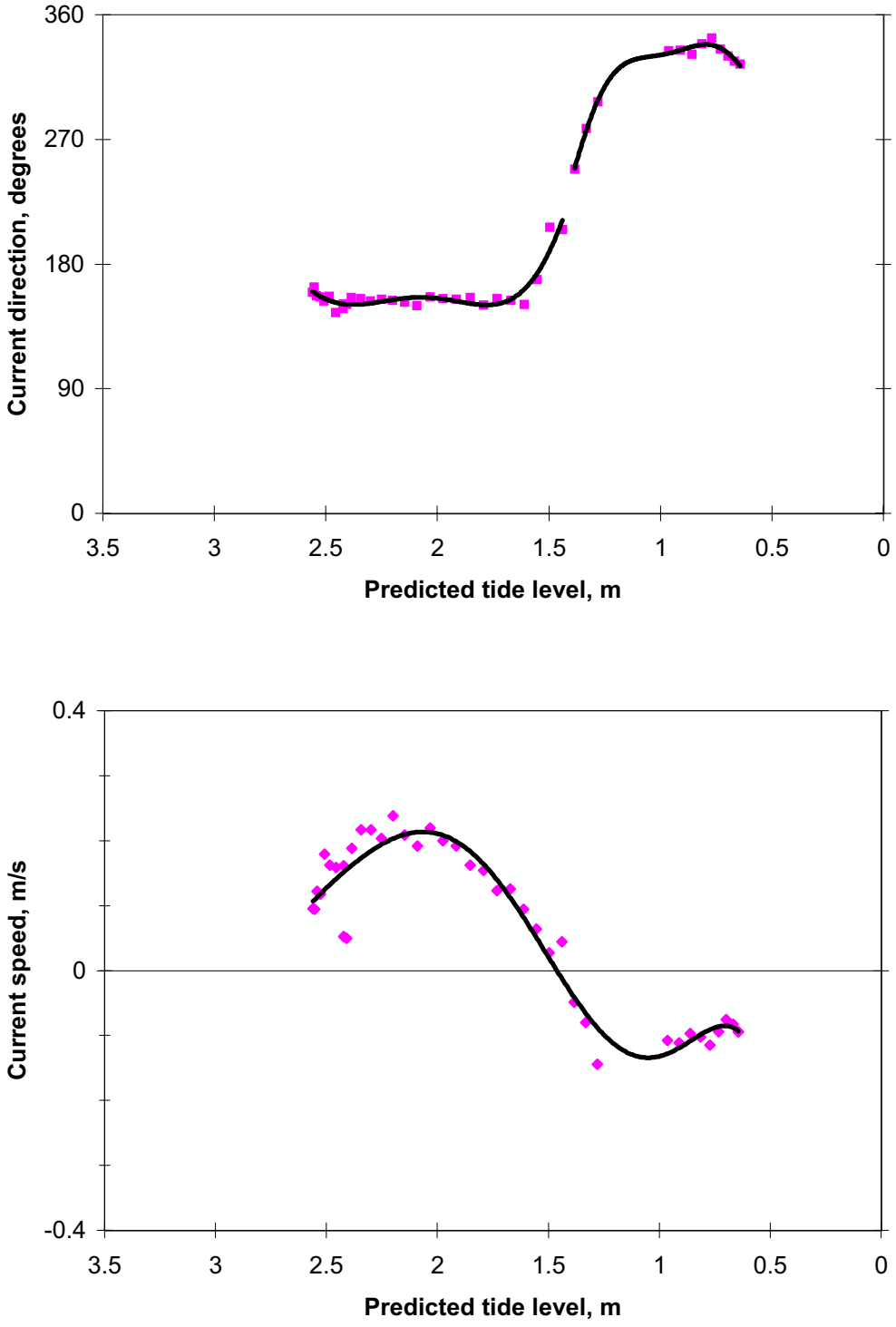

Figure 22. Southern current meter, falling tide, 1.4 m <= R < 2.0 m 17 March 1996 to 30 June 1996

Above: Current direction *vs* predicted tide level

Below: Current speed *vs* predicted tide level

Only including data with W < 5m/s
H_{BP} and H_{Wis} < 0.35 m

θ_c < 225°, positive θ_c >= 225°, negative

Trendlines 6th order polynomials

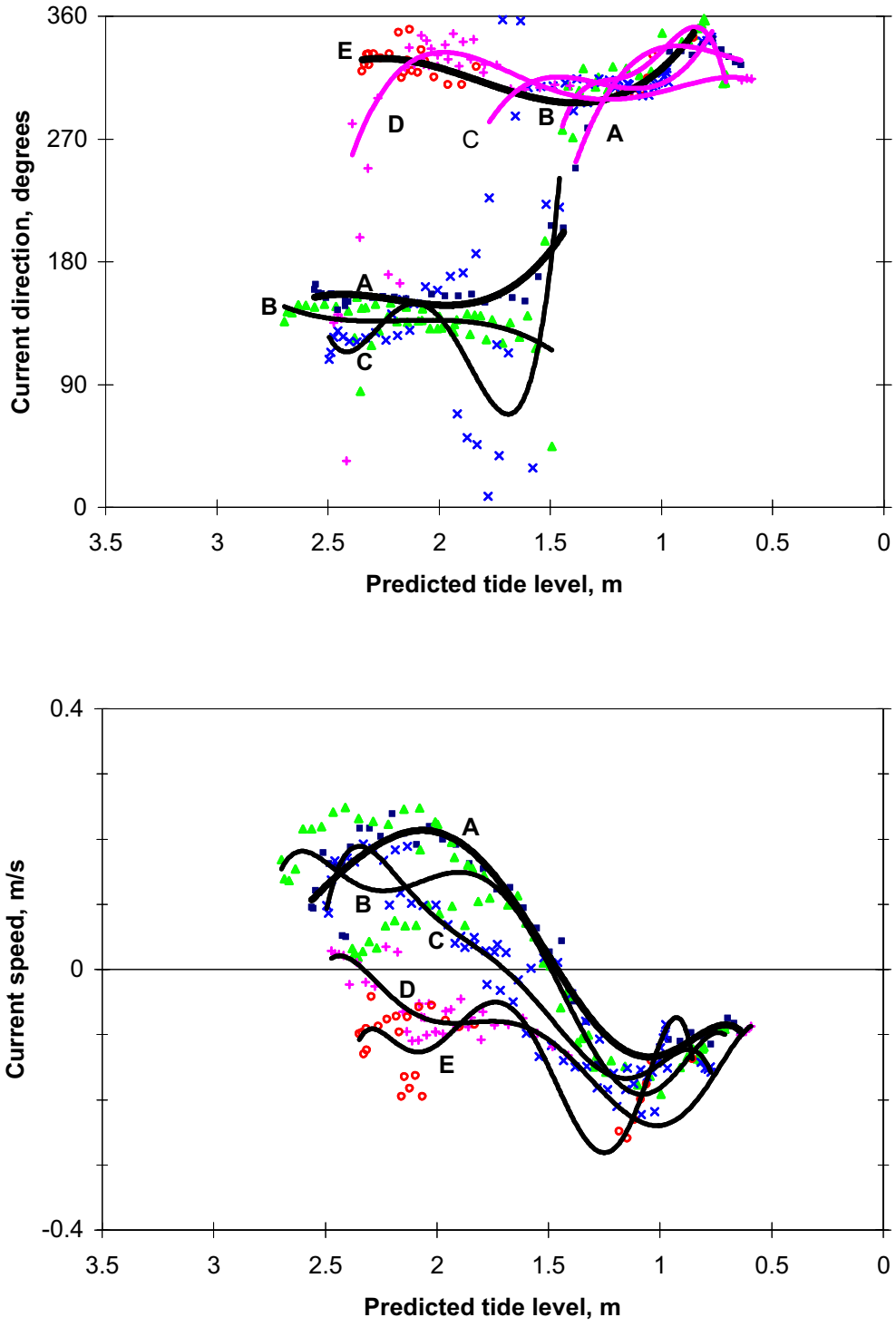

Figure 23. Southern current meter, falling tide, 1.4 m <= R < 2.0 m
17 March 1996 to 30 June 1996

Above: Current direction variation with increasing wave height

Below: Current speed variation with increasing wave height

A	W < 5 m/s	All wind directions	H_{BP} and H_{Wis} < 0.35 m
B	W < 5 m/s	All wind directions	0.35 m <= H_{BP} and H_{Wis} < 0.5 m
C	W >= 5 m/s	105^{o} <= θ_w < 165^{o}	H_{BP} < 0.5 m, 0.5 m <= H_{Wis} < 0.75 m
D	W >= 5 m/s	105^{o} <= θ_w < 165^{o}	H_{BP} < 0.5 m, 0.75 m <= H_{Wis} >= 1.0 m
E	W >= 5 m/s	105^{o} <= θ_w < 165^{o}	H_{BP} < 0.5 m, H_{Wis} >= 1.0 m
	θ_c < 225^{o}, positive	θ_c >= 225^{o}, negative	Trendlines various order polynomials

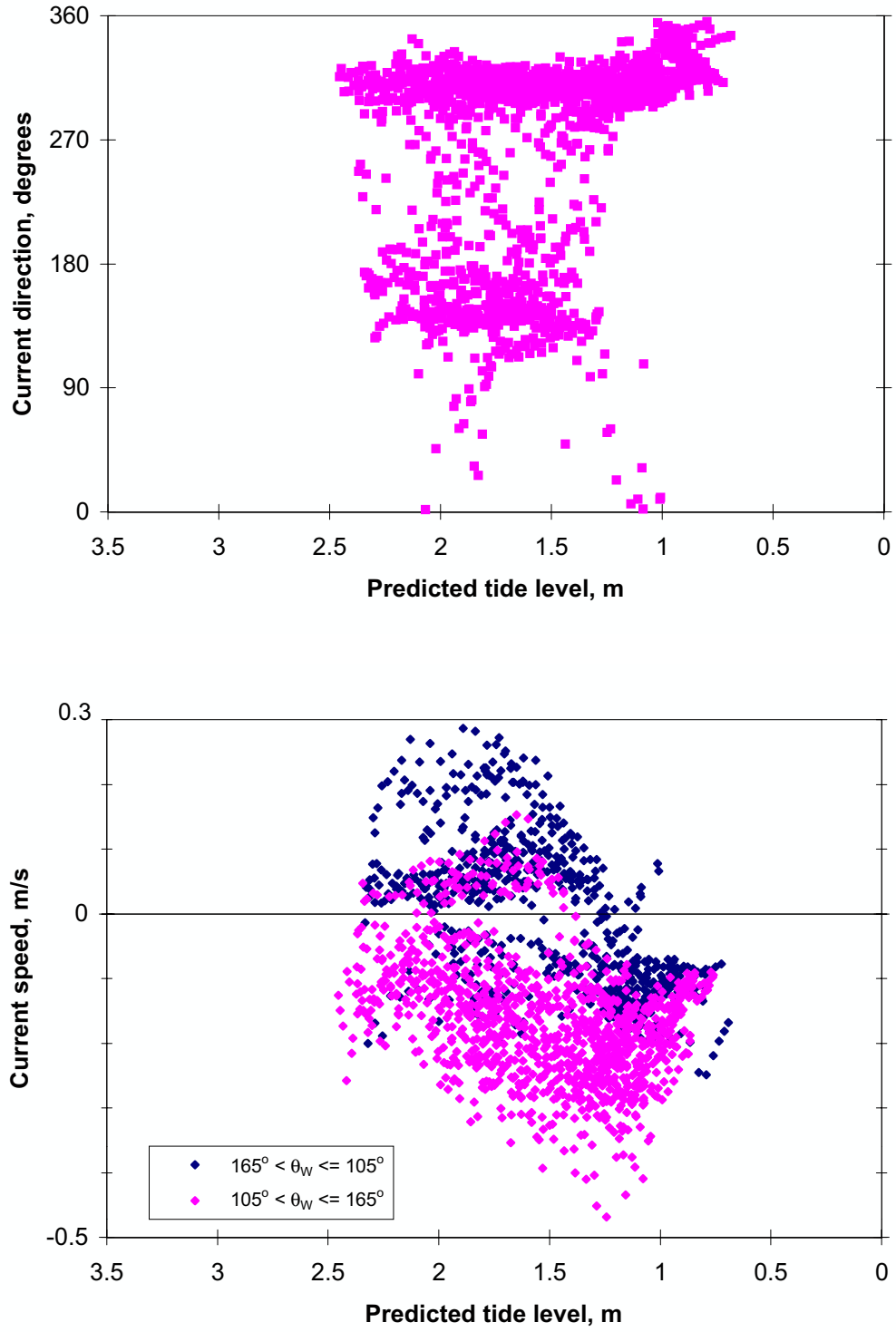

Figure 24. Southern current meter, falling tide, R < 1.4 m
17 March 1996 to 30 June 1996

Above: Current direction *vs* predicted tide level; all data

Below: Current speed *vs* predicted tide level; all data

$\theta_c < 225^o$, positive $\theta_c >= 225^o$, negative

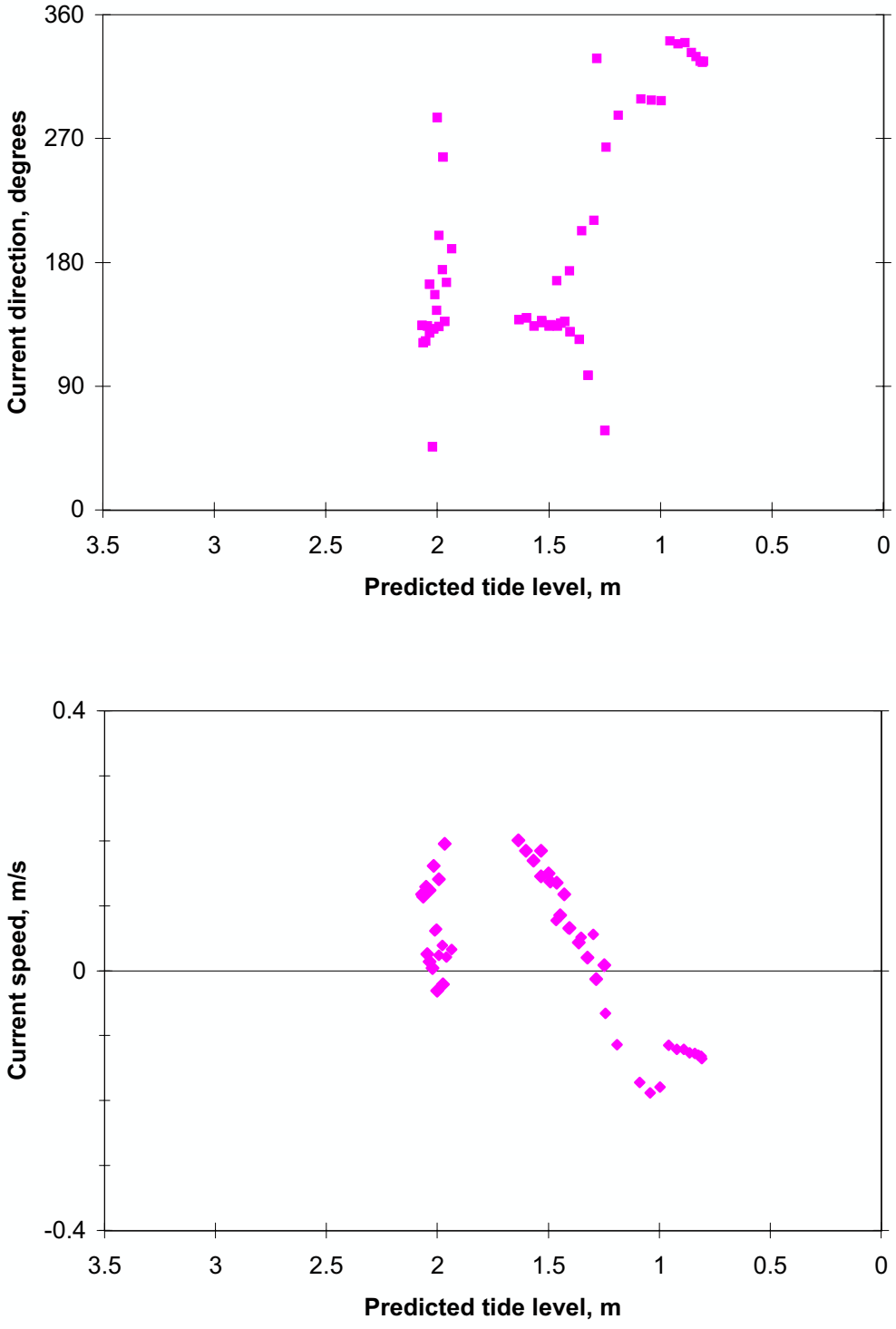

Figure 25. Southern current meter, falling tide, R < 1.4 m
17 March 1996 to 30 June 1996

Above: Current direction *vs* predicted tide level

Below: Current speed *vs* predicted tide level

Only including data with W < 5m/s
H_{BP} and H_{Wis} < 0.35 m

θ_c < 225°, positive θ_c >= 225°, negative

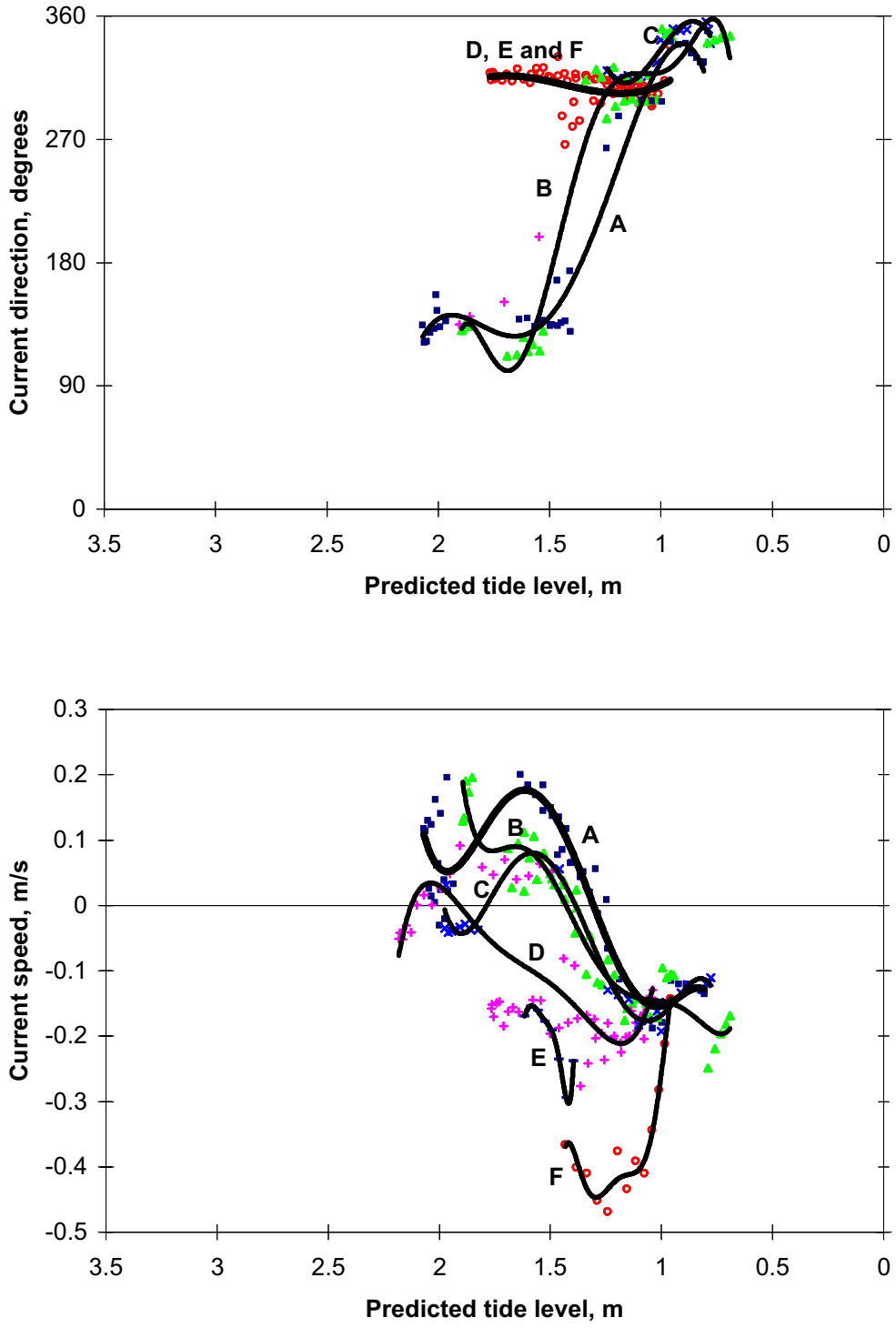

Figure 26. Southern current meter, falling tide, R < 1.4 m
17 March 1996 to 30 June 1996

Above: Current direction variation with increasing wave height
(speed >= 0.06 m/s)

Below: Current speed variation with increasing wave height

A	W < 5 m/s	All wind directions	H_{BP} and H_{Wis} < 0.35 m
B	W < 5 m/s	All wind directions	0.35 <= H_{BP} and H_{Wis} < 0.5 m
C	W < 5 m/s	105° <= θ_w < 165°	H_{BP} < 0.5 m; 0.5 m <= H_{Wis} < 0.75 m
D	W >= 5 m/s	105° <= θ_w < 165°	H_{BP} < 0.5 m; 0.75 m <= H_{Wis} < 1.0 m
E	W >= 5 m/s	105° <= θ_w < 165°	H_{BP} < 0.5 m; 1.0 m <= H_{Wis} < 1.25 m
F	W >= 5 m/s	105° <= θ_w < 165°	H_{BP} < 0.5 m; H_{Wis} >= 1.25 m
	θ_c < 225°, positive	θ_c >= 225°, negative	Trendlines various order polynomials

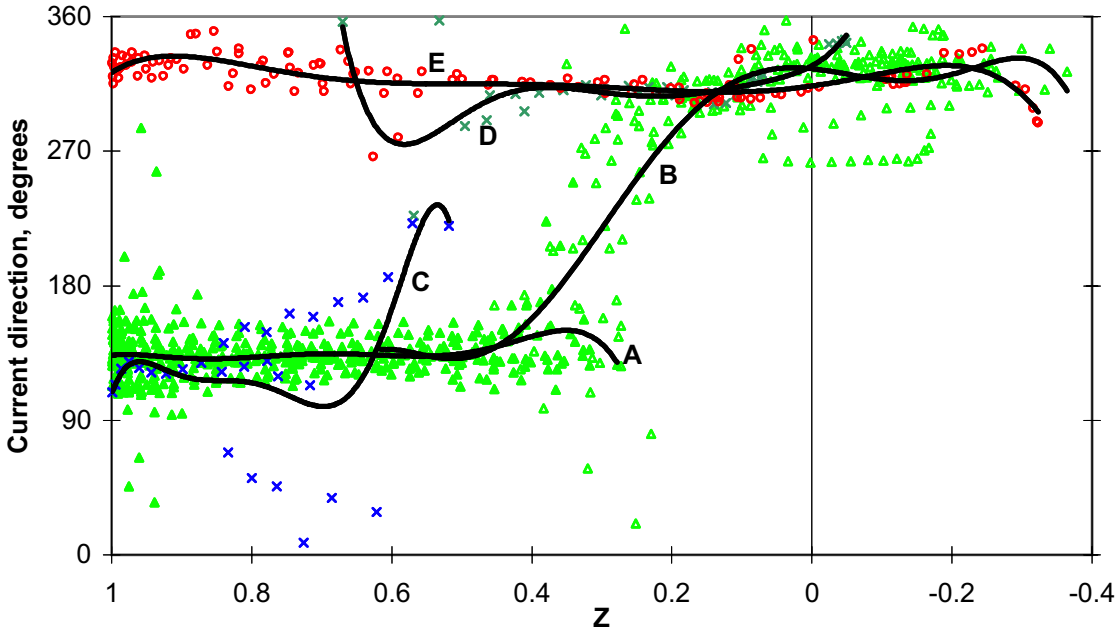

Current direction vs Dimensionless water level, $Z = (z - z_b)/(z_H - z_b)$

A & B	W < 5 m/s	All wind directions	R >= 2.0 m,	H_{BP} and H_{Wis} < 0.5 m
	(A, Z_o >= 1.5 m; B, Z_o < 1.5 m)		1.4 m <= R < 2.0 m,	H_{BP} and H_{Wis} < 0.35 m
			R <= 1.4 m,	H_{BP} and H_{Wis} < 0.35 m
C & D	W >= 5 m/s	105^o <= θ_w < 165^o	1.4 m <= R < 2.0 m,	H_{BP} < 0.5 m, 0.5 m <= H_{Wis} < 0.75 m
	C, current direction < 225 ; D, current direction >= 225^o			
E	W >= 5 m/s	105^o <= θ_w < 165^o	R <= 1.4 m,	H_{BP} < 0.5, H_{Wis} >= 1.0 m
			1.4 m <= R < 2.0 m,	H_{BP} < 0.5 m, H_{Wis} >= 1.0 m
			R >= 2.0 m,	H_{BP} < 0.5 m, H_{Wis} >= 1.15 m

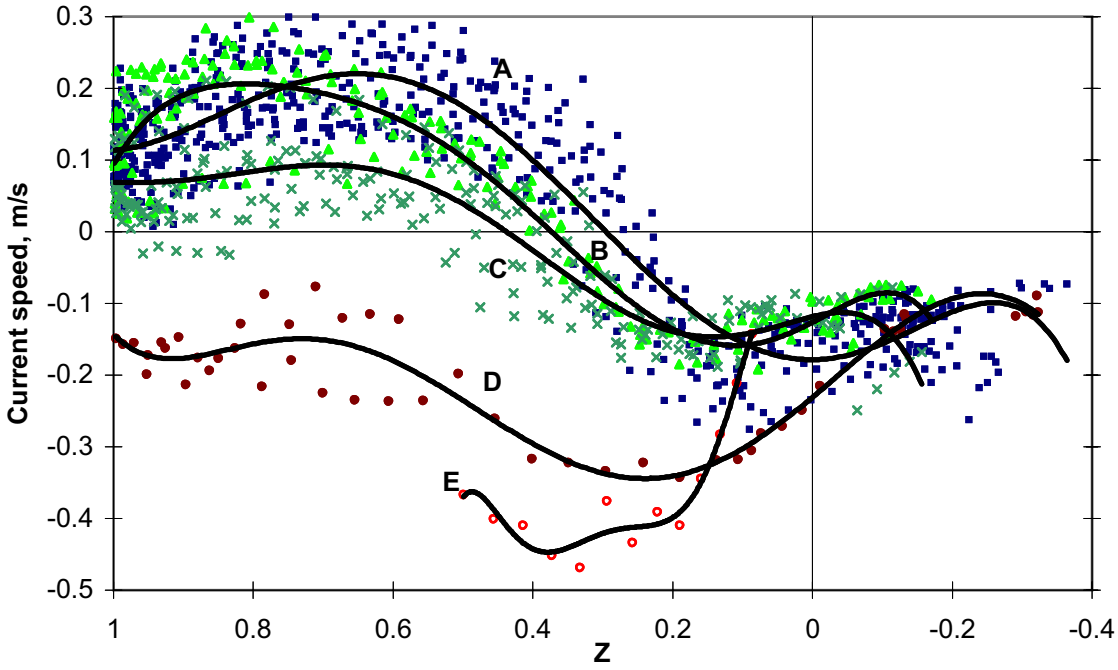

Current speed vs Dimensionless water level, $Z = (z - z_b)/(z_H - z_b)$, ($<225^o$ +'ve, $>= 225^o$ -'ve)

A	W < 5 m/s	All wind directions	R >= 2.0 m,	H_{BP} and H_{Wis} < 0.5 m
B	W < 5 m/s	All wind directions	1.4 m <= R < 2.0 m,	H_{BP} and H_{Wis} < 0.5 m
C	W < 5 m/s	All wind directions	R <= 1.4 m,	H_{BP} and H_{Wis} < 0.5 m
D	W >= 5 m/s	105^o <= θ_w < 165^o	R >= 2.0 m,	H_{BP} < 0.5 m, H_{Wis} >= 1.5 m
E	W >= 5 m/s	105^o <= θ_w < 165^o	R <= 1.4 m,	H_{BP} < 0.5, H_{Wis} >= 1.25 m

Figure 27. Southern Current meter, falling tide, all tidal ranges 17 March 1996 to 30 June 1996

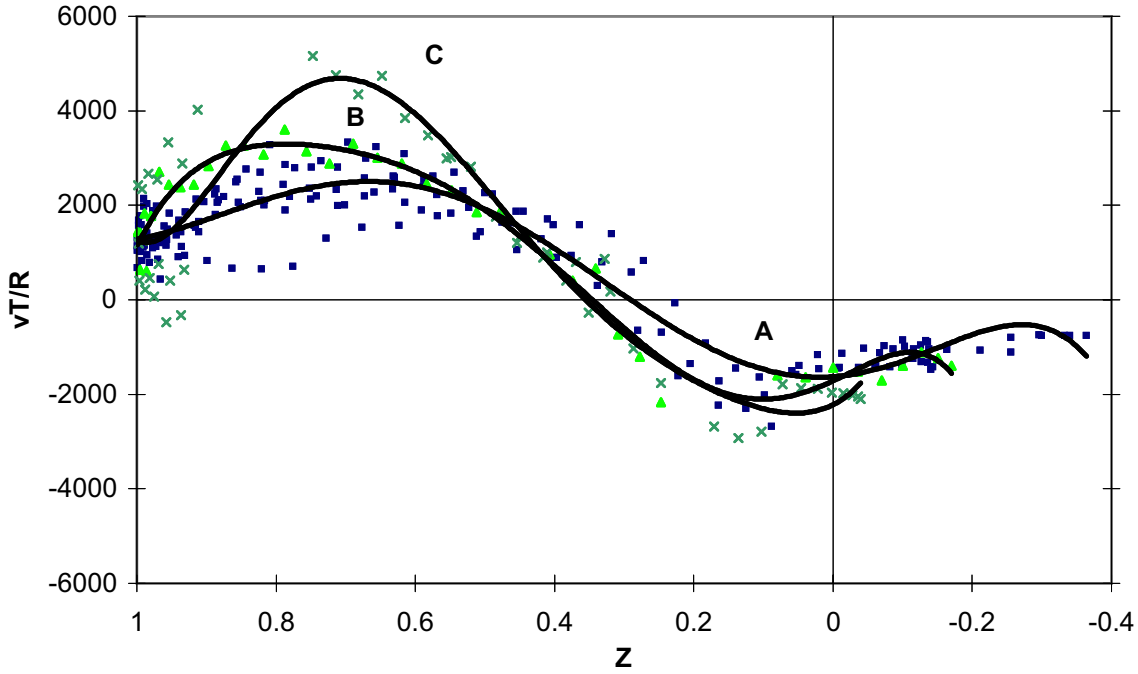

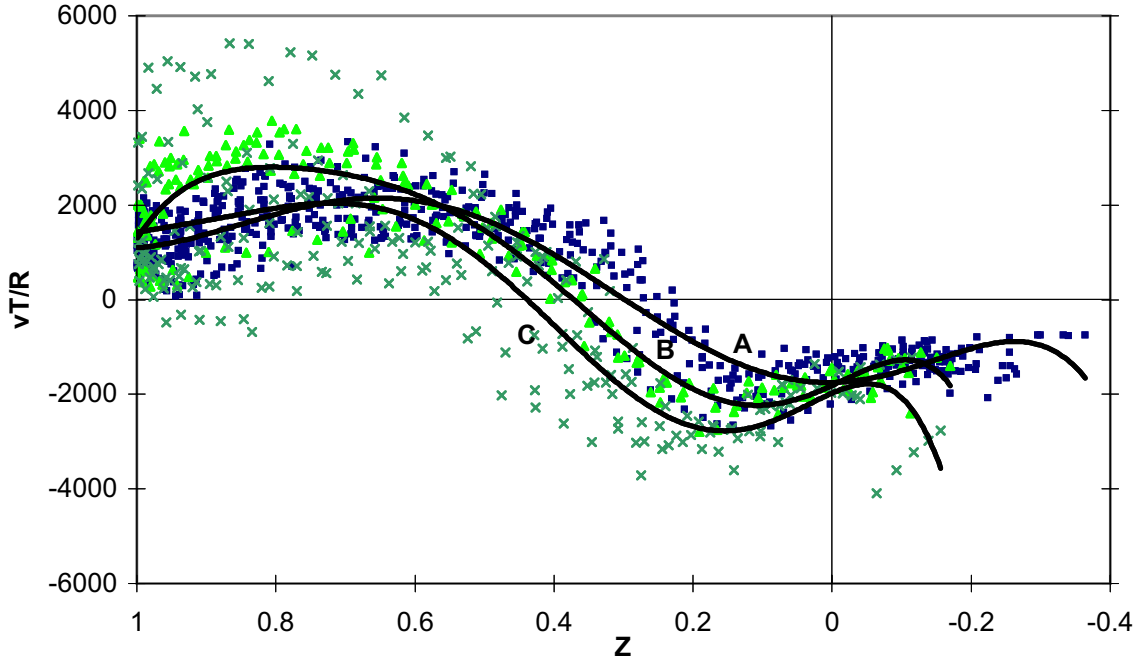

Figure 28. Southern Current meter, falling tide

Dimensionless velocity, vT/R vs Dimensionless water level Z

$Z = (z_o - z_b)(z_H - z_b)$

17 March 1996 to 30 June 1996

Above	**H_{BP} and H_{Wis} < 0.35 m**
Below	**H_{BP} and H_{Wis} < 0.5 m**
A	R >= 2.0 m
B	1.4 m <= R < 2.0 m
C	R < 1.4 m

6.4 Northern current meter, rising tide

6.4.1 Tidal range greater than 2.0 m

All data (Figure 29). The situation at the northern current meter during the rising tide differs from that at the southern meter and the tidal flow patterns are more complicated. Initially, as the tide flows in through the boat harbour entrance channel and over the northern bund wall the flow is to the northeast. This continues until the tide level is between 1.5 and 2 m when the flow reverses to a southwestwards direction. As high tide is approached, tide levels ≥ 2.5 m, the direction of the currents tends to change again as the tide turns and flows out in a northeastwards direction over the northern edge of the reef.

As at the southern meter, the eastward flowing current is taken as positive and the westward current negative. The division in this case is taken at 125°, which is the direction approximately normal to the island from the current meter (Figure 2, insert). At the larger tidal ranges (≥ 2.0 m), flow in the negative direction occurred for 65% of the time, whereas it only occurred for 20% of the time at the southern meter. During the portion of the time for which no measurements were obtained because the instrument was out of the water at low tide, the flow also would have been in the negative direction. As with the southern meter, on those occasions when conditions were very mild, there also would have been negligible flow into the boat harbour at that time.

There was one storm event during this period of observations which produced strong wave-generated currents at the northern current meter but not at the southern current meter.

Low waves, H_{BP} and H_{Wis} < 0.35 m and low winds, W < 5 m/s (Figure 30). As at the southern meter, when winds and waves are low, currents are controlled by the tide. The current flows in through the boat harbour entrance channel and over the northern bund wall in a northeastwards direction. Slightly above the mean tide level of 1.5 m, at about 1.75 m, the tidal current reverses, in either a clockwise or anticlockwise direction, and flows in a southwestwards direction. A possible explanation for this behaviour is that initially the tide flows in through the boat harbour entrance channel since the water levels there are below the reef-rim. As the tide rises, the currents then flow from the harbour onto the reef-flat, northeastwards north of the harbour and eastsoutheastwards south of the harbour. Then, when the tide has risen sufficiently to flow over the reef-rim without interference, the tidal flow reverses on the northern side of the harbour, since the incoming offreef tide is coming from the Coral Sea east of the reef. At the top of the tide, as the offreef tidal current reverses, the flow on the reef-top also reverses and flows towards the northeast again. The current speed reaches a maximum value of *ca* 0.25 m/s at a tide level of *ca*

1.25 m in the northeastwards flow and second slightly lower maximum of *ca* 0.18 m/s, but in the opposite direction, at a tide level of about 2.4 m.

Wave/wind influenced conditions (Figures 31 and 32). As the magnitude of the offshore wave height, H_{BP}, increases to 1 m (curves A, B, and C), the tide level at which the current direction changes from northeastwards to southwestwards reduces. Furthermore, the maximum speeds reached in the northeastward direction also reduce and occur earlier, at lower tide levels. When H_{BP} is greater than 1 m, the initial northeastward tidal current is almost completely over-ridden by the wave-generated current (curve D), although the initial magnitude is close to zero at a tide level of around 1.1 m.

During the measurement period, 17 March to 30 June 1996, there was a notable event at the beginning of May with strong winds, easterly at first, with speeds up to 16.5 m/s (33kn), then backing westerly. This event was similar to the one that occurred in July 1996 (Figure 4). These strong winds produced offshore waves, H_{BP}, greater than 3 m. Data recorded during this event (curve E) shows the substantial effect of the wave-generated currents. Reef-top currents attained speeds of around 0.6 m/s in the westsouthwestwards direction.

At all wave heights, the maximum speed in the southwestward direction was reached at tide levels between 1.5 and 2.5 m. This maximum speed occurred earlier, at lower tide levels, at progressively higher wave heights (curves A to D). The current speeds at wave heights above 2.5 m (curve E) do not continue this pattern, probably because the highest wind speeds were reached at the higher tide levels, $z_o > 2$ m. Furthermore, these highest winds were from the northeasterly directions, thus further enhancing the negative current flow.

All the above situations involve only conditions when the winds were in the sector 315^o to 180^o, with the exception of winds below 5 m/s (curve A). That is when the winds were not opposing the southwestward current. When considering currents on the reef-top during southwesterly wind conditions and opposing offshore waves ($H_{BP} > 1$m), the presence of the southwesterly wind assists the initial northeastward current and reduces the magnitude of the southwestward current (Figure 32, curves D and M).

6.4.2 Tidal range between 2.0 and 1.4 m

All data (Figures 33). With intermediate tidal ranges, the current pattern is not as well defined as it is for the larger tidal ranges. The currents flow in the negative direction for almost the same

amount of the time, 64%, as they did for the larger tidal ranges, 65% (not including the times when the current meter was out of the water). There is a greater proportion of observations at tide levels below 1 m because the current meter was not always exposed at low tide when the tidal range was smaller, *i.e*. because the low tide level was not so low. The initial positive, northeastward, velocity maximums are lower, less than 0.3 m/s (with one exception), than for the larger tidal ranges.

Low waves, H_{BP} and H_{Wis} < 0.35 m and low winds, W < 5 m/s (Figure 34). As at the higher tidal ranges, the tide initially comes in through the boat harbour entrance channel and over the northern bund wall onto the reef-flat. This flow is in a northeastwards direction and reaches maximum speeds of around 0.2 m/s. It does not persist for long and at about half tide level, 1.5 m, the current gradually reverses to the westsouthwestwards direction. When the tide level rises above 2 m, the flows, under these mild conditions, are towards the westsouthwest. The reversal takes place in both clockwise and anticlockwise directions. After the flow has reversed, it reaches maximum speeds of about 0.1 m/s in the westsouthwestward direction. Then, shortly before the tide turns, it tends to reverse again to the northeastward direction at low speeds.

Wave/wind influenced conditions (Figures 35 and 36). When wave heights are small (curves A and B) the current from the previous ebb tide sometimes continues to flow out over the bund wall and does not reverse until the ocean tide level rises above ca 1 m. The magnitude of the subsequent initial northeastward current drops as wind and wave conditions increase. When H_{BP} is greater than 0.75 m, the current is usually reversed (curve C). At wave heights greater than 1 m (curves D and E), there is no northeastward current and the flow maintains a constant westsouthwestward direction throughout the tidal cycle.

Maximum westsouthwestward flows usually occur at tide levels around 1.8 to 2 m, but this maximum is less well-defined at the larger wave heights. At the lower wave heights, the current decreases as the tide turns.

For the intermediate tidal range, 1.4 to 2.0 m, flows are only described for wind conditions other than southwesterly. There is insufficient data to examine the situation with southwesterly winds.

6.4.3 Tidal range less than 1.4 m

All data (Figure 37). At the smallest tidal ranges, less than 1.4 m, there does not appear to be a particular tide level at which the flow reverses. Nonetheless, there are clearly two preferred

directions, northeastward and westsouthwestward. Negative, westsouthwestward flow, predominates (72%) to a greater extent than at the higher tidal ranges.

Low waves, H_{BP} and H_{Wis} < 0.35 m and low winds, W < 5 m/s (Figure 38). Under mild conditions, there initially is a low flow, with maximum velocity of about 0.2 m/s, from the boat harbour northeastwards across the reef-top. It does not persist, and when the tide level reaches half tide (1.5 m), the current reverses briefly, only to return again to the northeastward direction as the tide turns. The flows in the negative, westsouthwestward direction, do not exceed 0.1 m/s.

Wave/wind influenced conditions (Figure 39). The feeble tidally induced currents at the low tidal ranges are easily overwhelmed by wind- and wave-generated currents. Even when offshore wave heights are in the range 0.5 to 0.75 m (curve B), the initial northeastward current is almost suppressed, provided that the wind is not southwesterly. When offshore wave heights are greater than 0.75 m, almost all flow is westsouthwestward (curves C and D). The exception occurs during southwesterly winds (curve M). With the assistance of southwesterly winds, the initial northeastward tidal current is able to persist until the tide level reaches about 1.4 m. When offshore waves are greater than 1 m (< 1.5 m), some westsouthwestward currents attained speeds approaching 0.4 m/s (curve D).

6.4.3 Effect of tidal range

For mild conditions and all tidal ranges the rising tide initially flows in through the boat harbour and onto the reef flat on the northwestern side of the island in a northeastward direction (Figure 40). For R > 1.4 m (curves A and B) the tide changes direction to southwestward when $Z \approx 0.5$, whereas for smaller tides (curve C) this change does not occur until $Z \approx 0.7$ and is only completed when $Z \approx 0.9$. When $H_{BP} \geq 1.0$ m (curve E) the flow is almost always from the northern reef-rim southwestwards towards the boat harbour regardless of the tide level or the tidal range.

The actual threshold conditions at which the current reverses, *i.e.* flows continuously towards the southwest into the boat harbour, change with increasing tidal range (Table 4). As on the southern side of the island, the current reversal on the northwestern side for small tidal ranges (R < 1.4 m) occurred at offreef wave heights (H_{BP}) *ca* 0.75 m and for medium range tides when $H_{BP} \approx 1.0$ m. For large tidal ranges (R ≥ 2.0 m), H_{BP} must exceed 1.25 m to cause complete reversal of the flow on the northern side of the island during the rising tide.

The strength of the current varies with the relative tidal level Z, tidal range and offreef wave height (Figure 41). Under mild conditions and large tidal ranges current velocities reach a

maximum of 0.3 m/s in the positive direction and *ca* 0.2 m/s in the negative direction (curve A). With small tides under these conditions the corresponding maximum current velocities are 0.2 and 0.1 m/s (curve C).

Table 4 Current directions at northern current meter during rising tide under different wind and wave conditions for three tidal range groups
(only tide levels at lower stage of rising tide as indicated for different tidal ranges)

Wave and wind conditions Wave height, m; wind speed, m/s	**R < 1.4 m** **z_o < 1.6 m**	**1.4 m ≤ R < 2.0 m** **z_o < 1.68 m**	**R ≥ 2.0 m** **z_o < 1.75 m**
H < 0.35, W < 5	NE	NE	NE
H < 0.5, W < 5	NE – E	NE – E	NE – E
0.5 ≤ H_{BP} < 0.75, no SW wind	SW – SE – SW	NE – N/SE	NE – E
0.75 ≤ H_{BP} < 1.0, no SW wind	SW	SW – NE – SW	NE – SE - SW
H_{BP} ≥ 1.25, no SW wind	SW	SW	SW
0.5 ≤ H_{BP} < 1.0, SW wind	NE – E	-	-
1.0 ≤ H_{BP} < 1.5, SW wind	-	-	NE – SE - SW

As wave heights increase above 1.0 m, the unidirectional flow both increases in magnitude and becomes increasingly less variable during the rising tide phase of the tidal cycle (Figure 41, curves D to H). With large tides, the significant variability of the tidal current is maintained until wave heights exceed 1.5 m, even when the flow is entirely in the negative direction (curve D); in other words tidal curve A becomes displaced downward by 0.2 to 0.3 m/s. With large waves (H_{BP} ≥ 2.5 m) (curve H) negative velocities range from 0.5 to > 0.6 m/s and the effect of the large tidal range becomes relatively minor. Unfortunately, this data set does not include any data for large waves (H_{BP} ≥ 2.5 m) and small tides (R ≤ 1.4 m). Under the latter circumstances it could be expected that there would be even less variation in current speed with Z.

When current velocities for mild conditions are nondimensionalised in terms of vT/R (Figure 42), the result is similar to that obtained for the southern current meter data (Figure 17). Large and medium tides (curves A and B) show an identical relationship between vT/R and Z, but small tides (curve C) give both relatively high maximum positive velocities and a change from positive to negative velocities at higher values of Z than for larger tides. This discrepancy relates clearly to the fact that many small tides are not significantly affected by the bund wall and so Z, which is based upon z_b, is not a satisfactory dimensionless parameter to represent their behaviour.

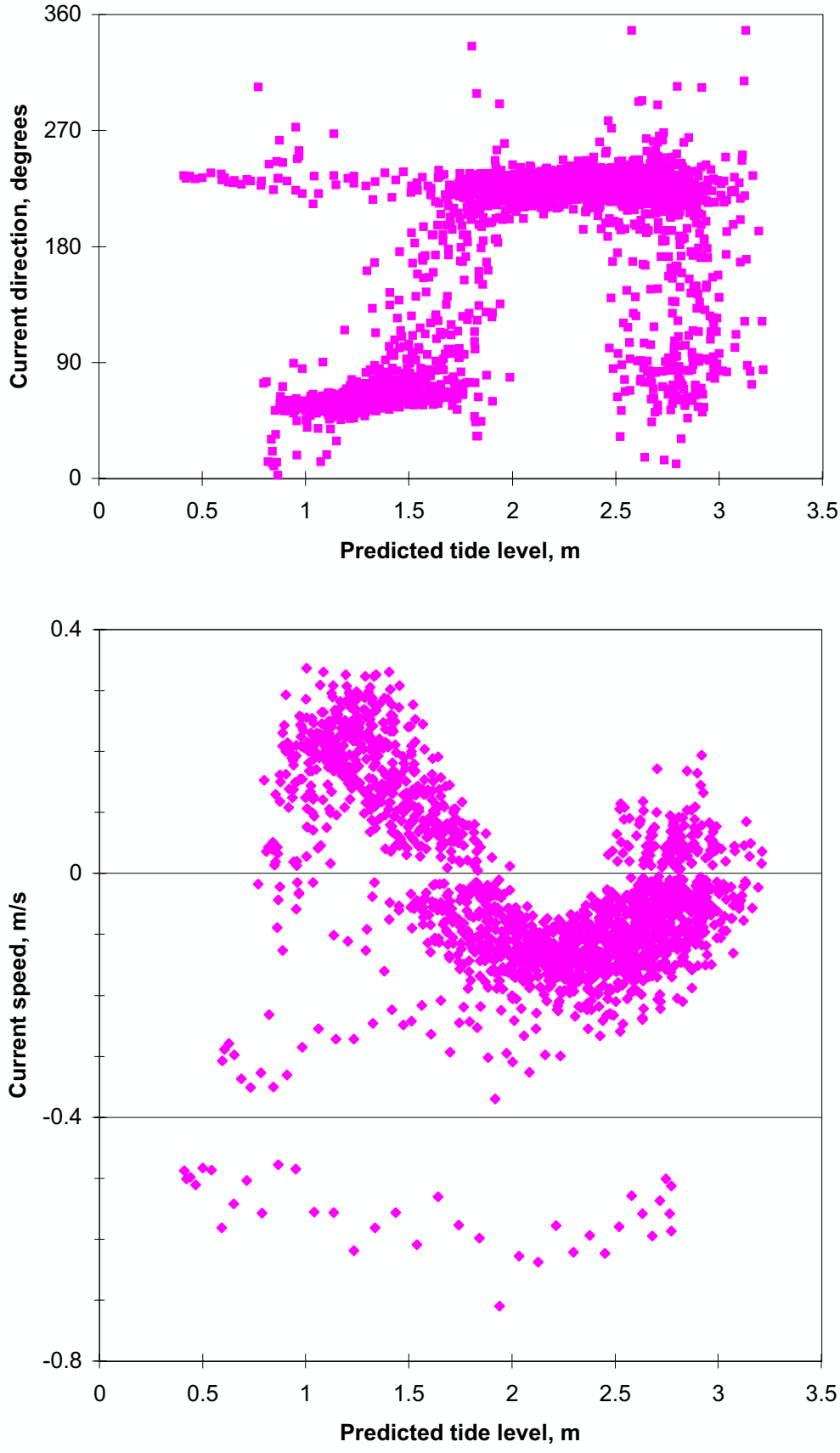

Figure 29. Northern current meter, rising tide, R >= 2.0 m
17 March 1996 to 30 June 1996

Above: **Current direction *vs* predicted tide level; all data**

Below: **Current speed *vs* predicted tide level; all data**

θ_c < 125°, positive θ_c >= 125°, negative

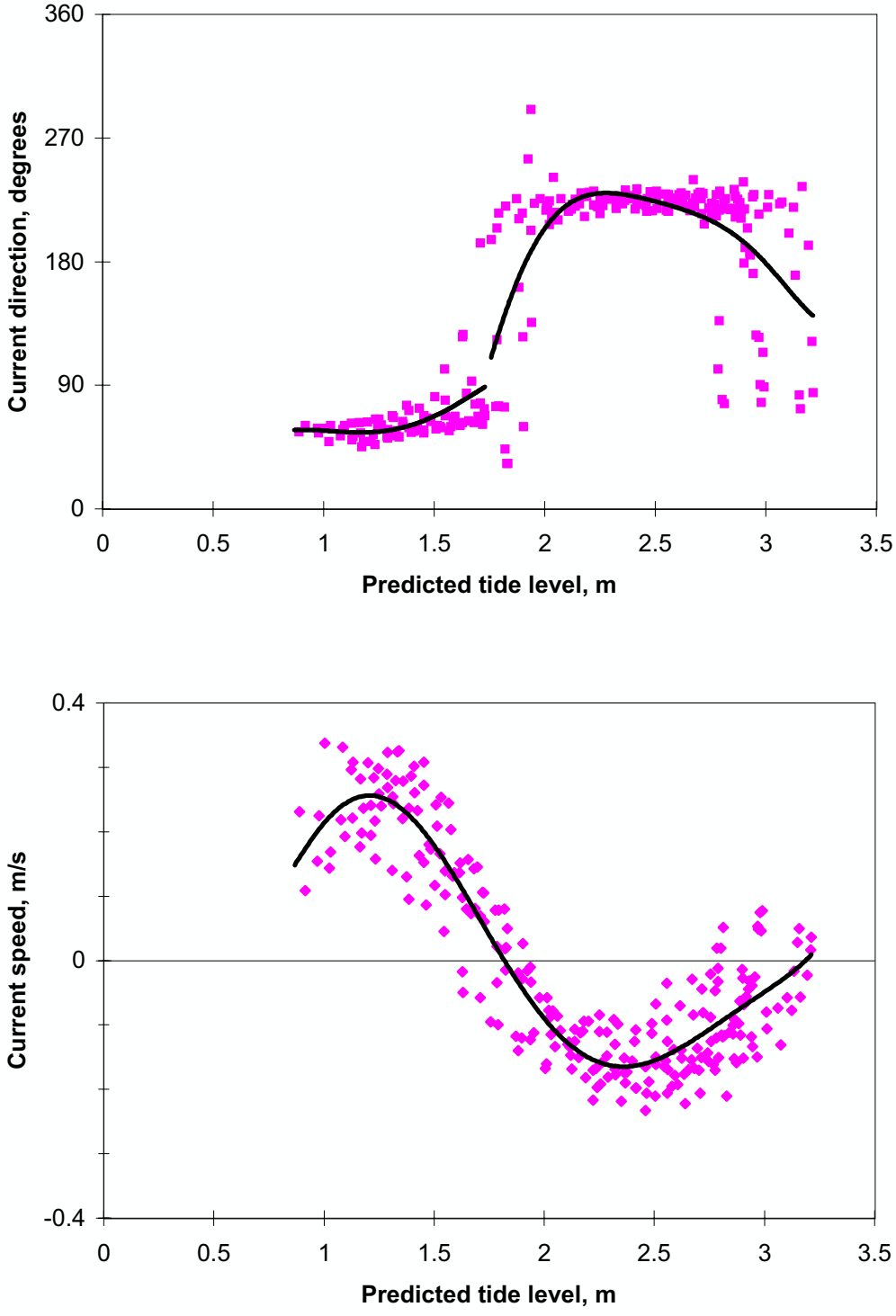

Figure 30. Northern current meter, rising tide, R >= 2.0 m
17 March 1996 to 30 June 1996

Above: Current direction *vs* predicted tide level
Below: Current speed *vs* predicted tide level

Only including data with W < 5m/s
H_{BP} and H_{Wis} < 0.35 m

θ_c < 125°, positive θ_c >= 125°, negative

Trendlines, various order polynomials

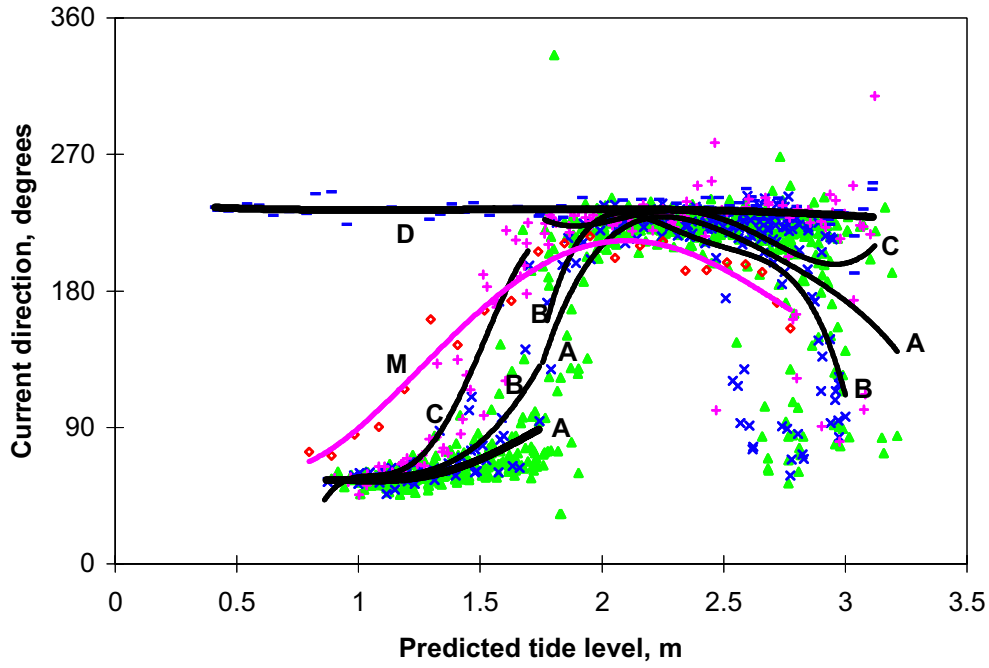

Figure 31. Northern current meter, rising tide, R >= 2.0 m
17 March 1996 to 30 June 1996
Current direction variation with increasing wave height

A	W < 5 m/s	All wind directions	H_{BP} and H_{Wis} < 0.5 m
B	All W	$315^o <= \theta_W < 180^o$	0.5 <= H_{BP} < 0.75 m; H_{Wis} < 0.75 m
C	All W	$315^o <= \theta_W < 180^o$	0.75 <= H_{BP} < 1.0 m; H_{Wis} < 1.0 m
D	All W	$315^o <= \theta_W < 180^o$	H_{BP} >= 1.0 m; All H_{Wis}
M	All W	$180^o <= \theta_W < 315^o$	1.0 <= H_{BP} < 1.5 m; All H_{Wis}

Only including data with V >= 0.02 m/s
Trendlines 4th order polynomials

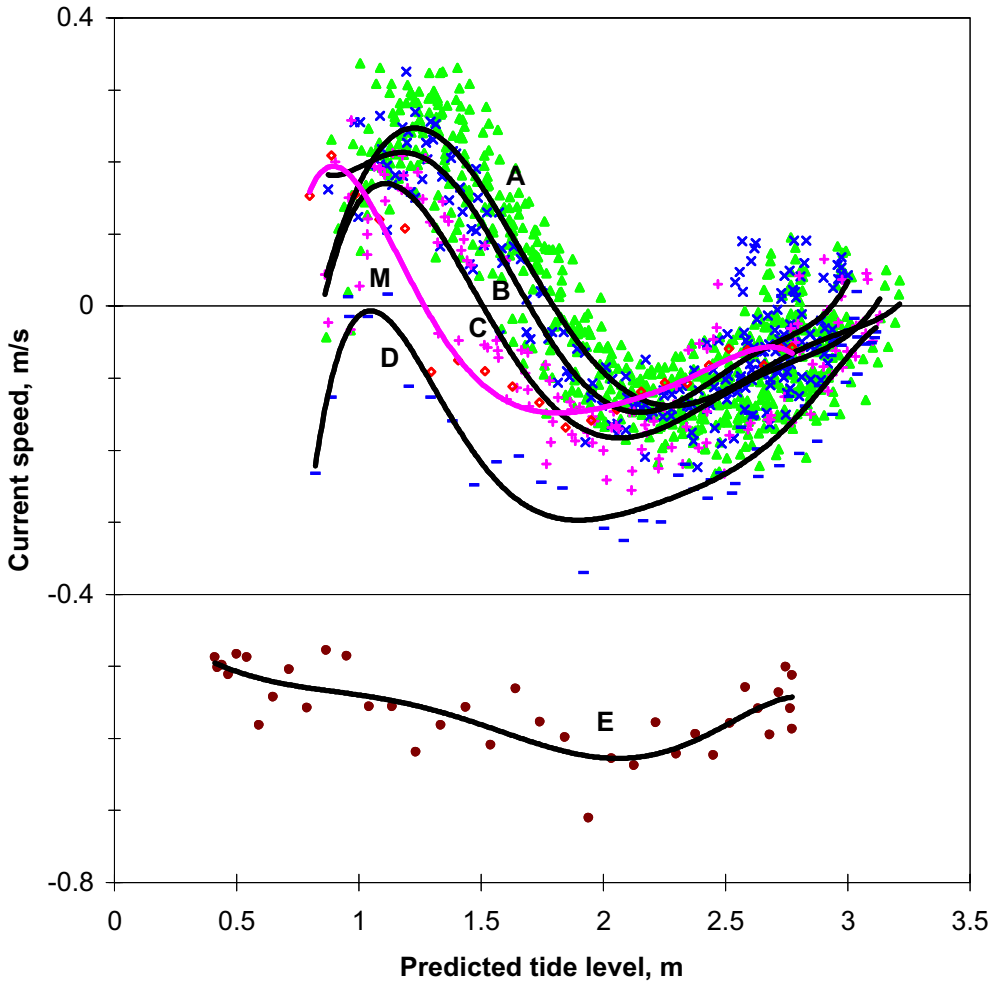

Figure 32. Northern current meter, rising tide, R >= 2.0 m
17 March 1996 to 30 June 1996
Current speed variation with increasing wave height

A	W < 5 m/s	All wind directions	H_{BP} and H_{Wis} < 0.5 m
B	All W	315° <= θ_W < 180°	0.5 m <= H_{BP} < 0.75 m; H_{Wis} < 0.75 m
C	All W	315° <= θ_W < 180°	0.75 m <= H_{BP} < 1.0 m; H_{Wis} < 1.0 m
D	All W	315° <= θ_W < 180°	1.0 m <= H_{BP} < 1.5 m; H_{Wis} < 1.5 m
E	All W	315° <= θ_W < 180°	H_{BP} >= 2.5 m; All H_{Wis}
M	All W	180° <= θ_W < 315°	1.0 m <= H_{BP} < 1.5 m; All H_{Wis}
	θ_c < 125°, positive	θ_c >= 125°, negative	Trendlines 6th order polynomials

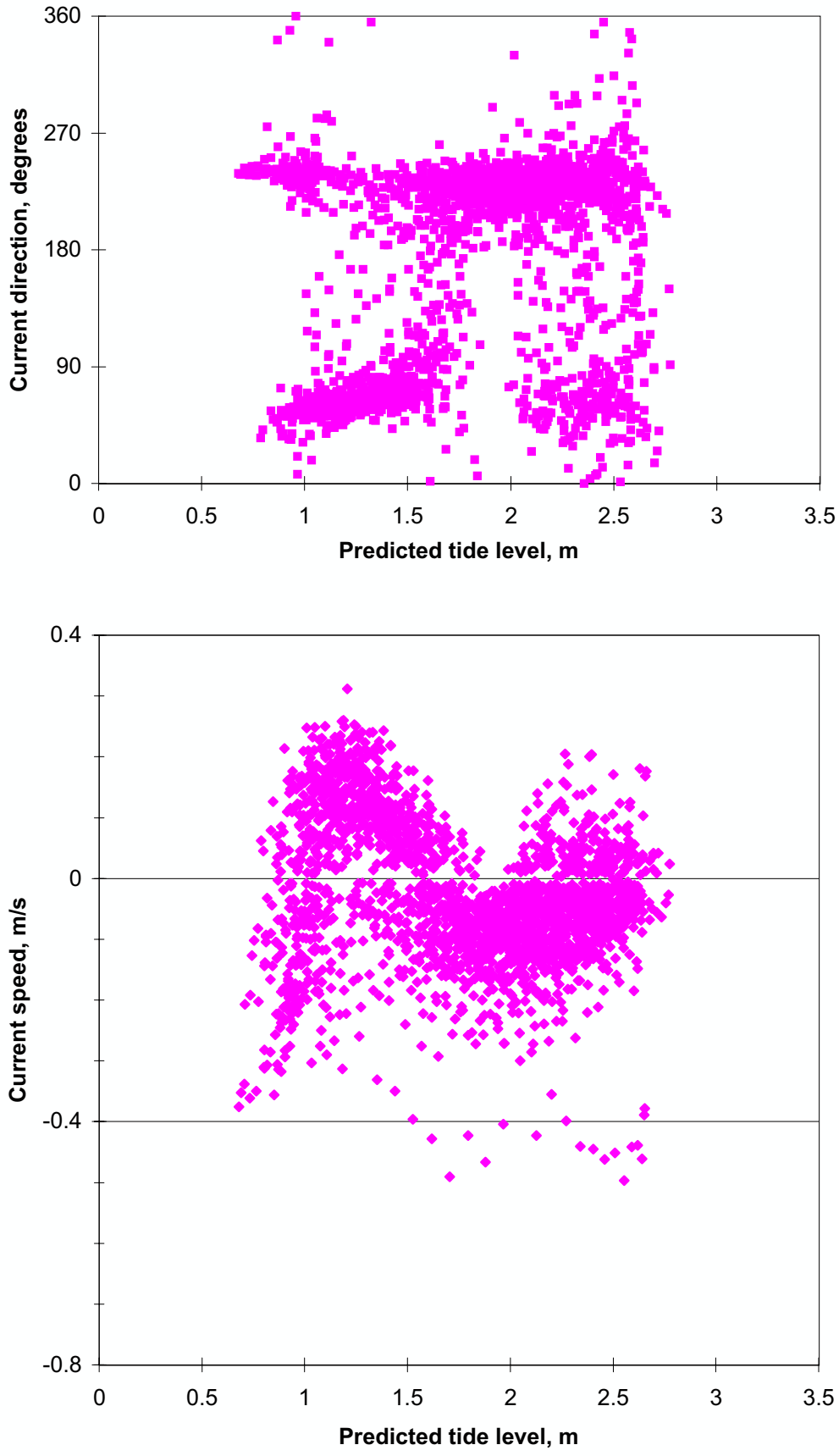

Figure 33. Northern current meter, rising tide, 1.4 m <= R < 2.0 m 17 March 1996 to 30 June 1996

Above: **Current direction *vs* predicted tide level; all data**

Below: **Current speed *vs* predicted tide level; all data**

θ_c < 125°, positive θ_c >= 125°, negative

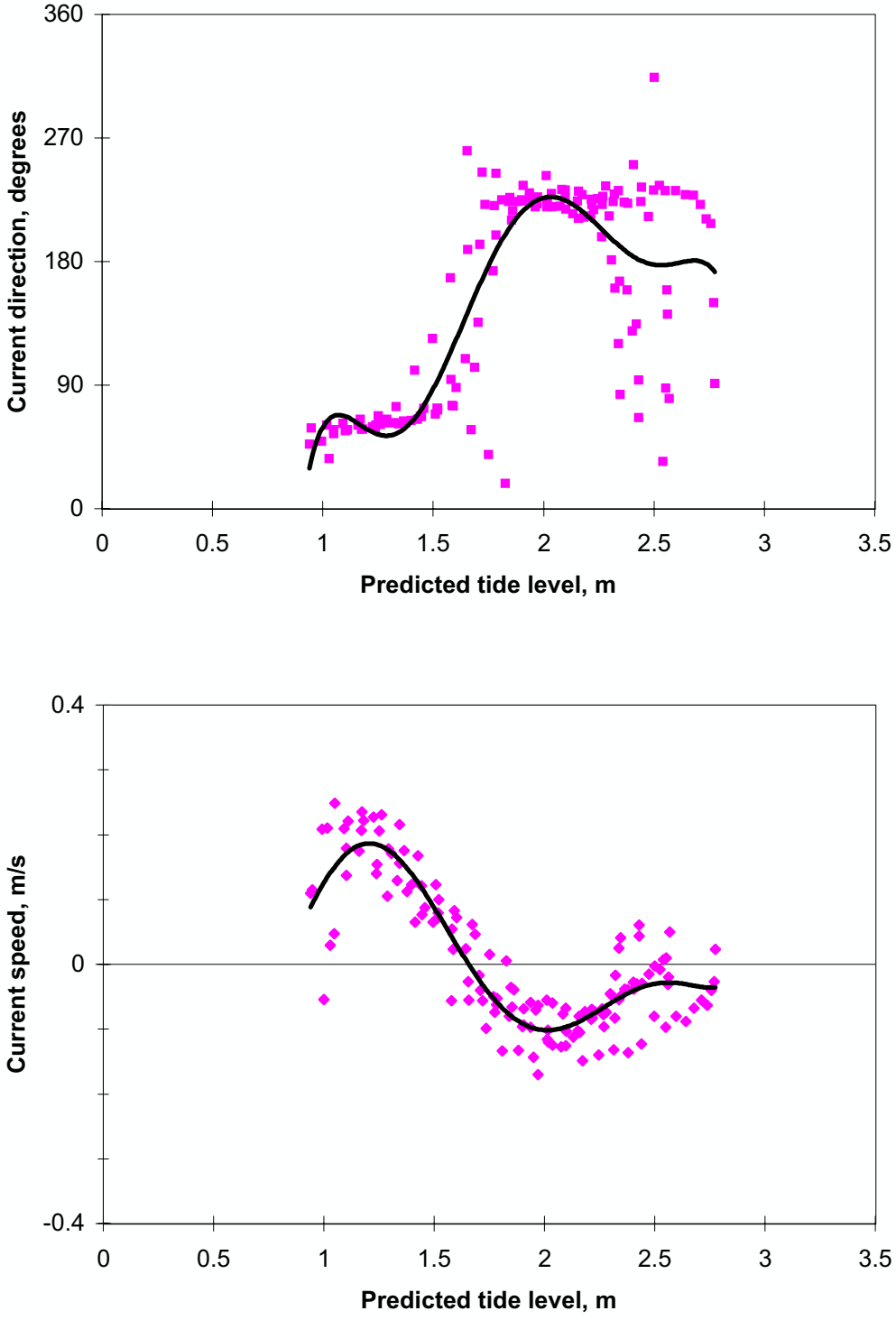

Figure 34. Northern current meter, rising tide, 1.4 m <= R < 2.0 m 17 March 1996 to 30 June 1996

Above: Current direction *vs* predicted tide level

Below: Current speed *vs* predicted tide level

Only including data with W < 5m/s

H_{BP} and H_{Wis} < 0.35 m

θ_c < 125°, positive θ_c >= 125°, negative

Trendlines, 6th order polynomials

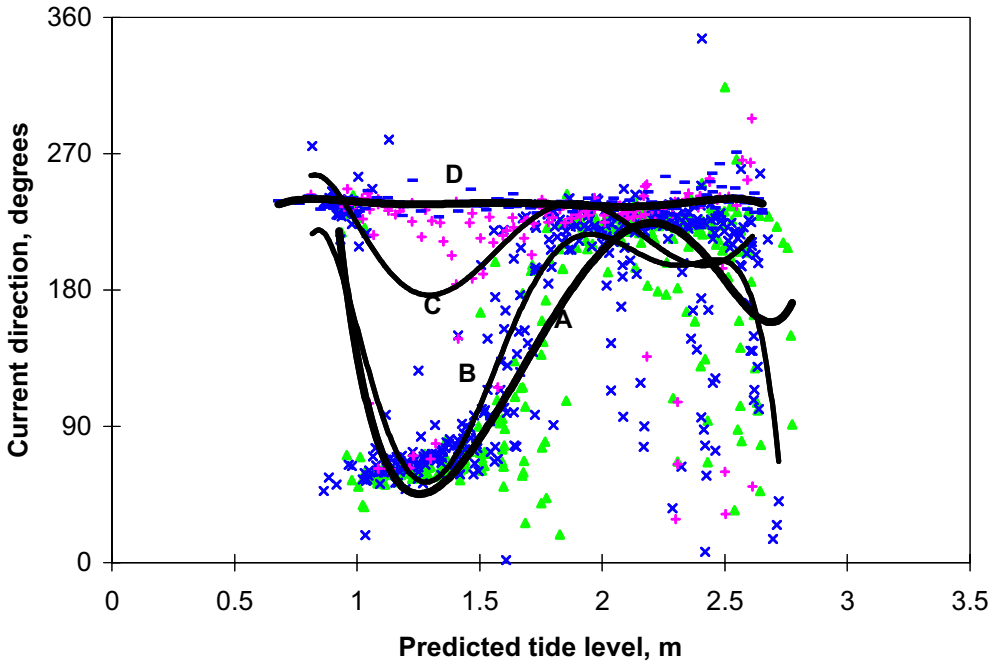

Figure 35. Northern current meter, rising tide, 1.4 <= R < 2.0 m
17 March 1996 to 30 June 1996
Current direction variation with increasing wave height

A	W < 5 m/s	All wind directions	H_{BP} and H_{Wis} < 0.5 m
B	All W	$315^o <= \theta_W < 180^o$	0.5 <= H_{BP} < 0.75 m; H_{Wis} < 0.75 m
C	All W	$315^o <= \theta_W < 180^o$	0.75 <= H_{BP} < 1.0 m; H_{Wis} < 1.0 m
D	All W	$315^o <= \theta_W < 180^o$	H_{BP} >= 1.0 m; All H_{Wis}

Trendlines 6th order polynomials

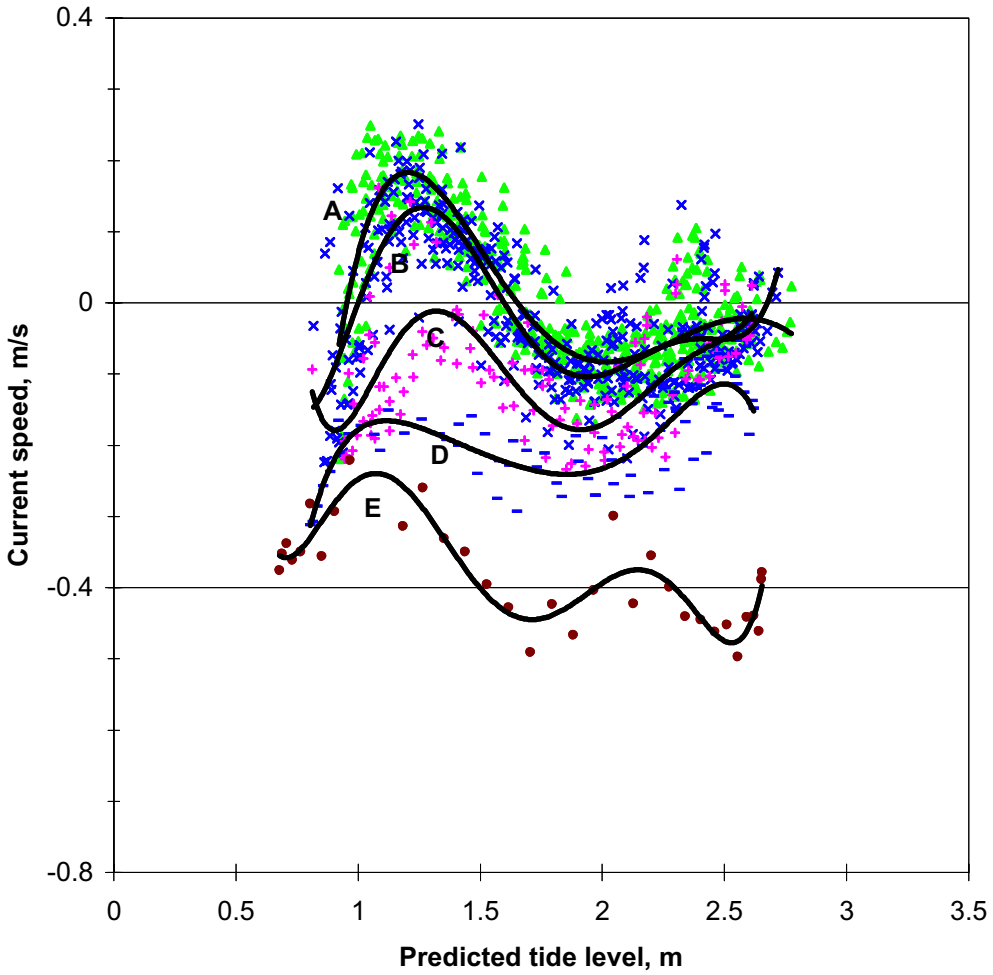

Figure 36. Northern current meter, rising tide, 1.4 <= R < 2.0 m
17 March 1996 to 30 June 1996
Current speed variation with increasing wave height

A	W < 5 m/s	All wind directions	H_{BP} and H_{Wis} < 0.5 m
B	All W	315° <= θ_W < 180°	0.5 m <= H_{BP} < 0.75 m; H_{Wis} < 0.75 m
C	All W	315° <= θ_W < 180°	0.75 m <= H_{BP} < 1.0 m; H_{Wis} < 1.0 m
D	All W	315° <= θ_W < 180°	1.0 m <= H_{BP} < 1.5 m; H_{Wis} < 1.5 m
E	All W	315° <= θ_W < 180°	H_{BP} >= 1.5 m; All H_{Wis}
	θ_c < 125°, positive	θ_c >= 125°, negative	Trendlines 6th order polynomials

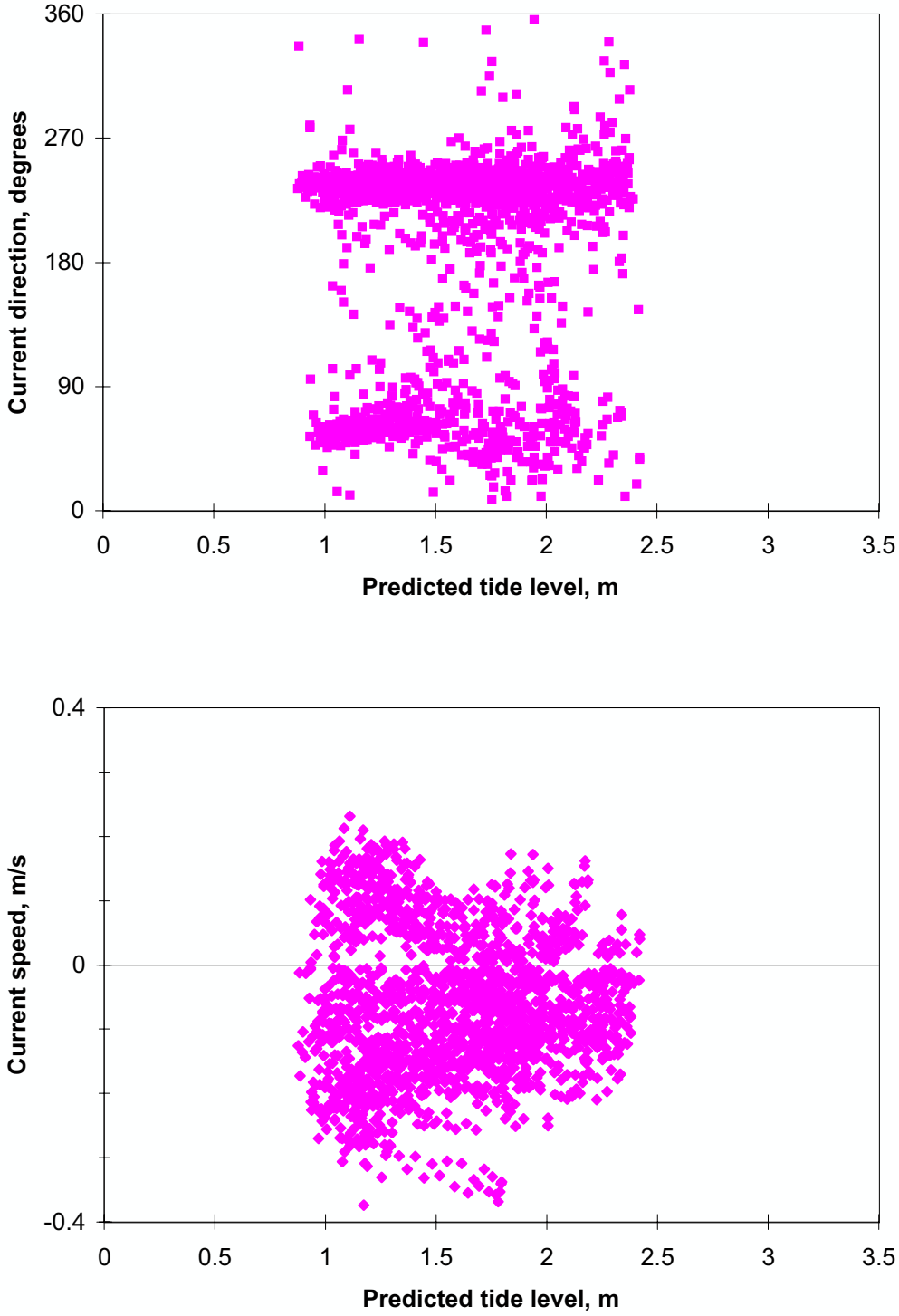

Figure 37. Northern current meter, rising tide, R < 1.4 m
17 March 1996 to 30 June 1996

Above: Current direction *vs* predicted tide level; all data

Below: Current speed *vs* predicted tide level; all data

θ_c < 125°, positive θ_c >= 125°, negative

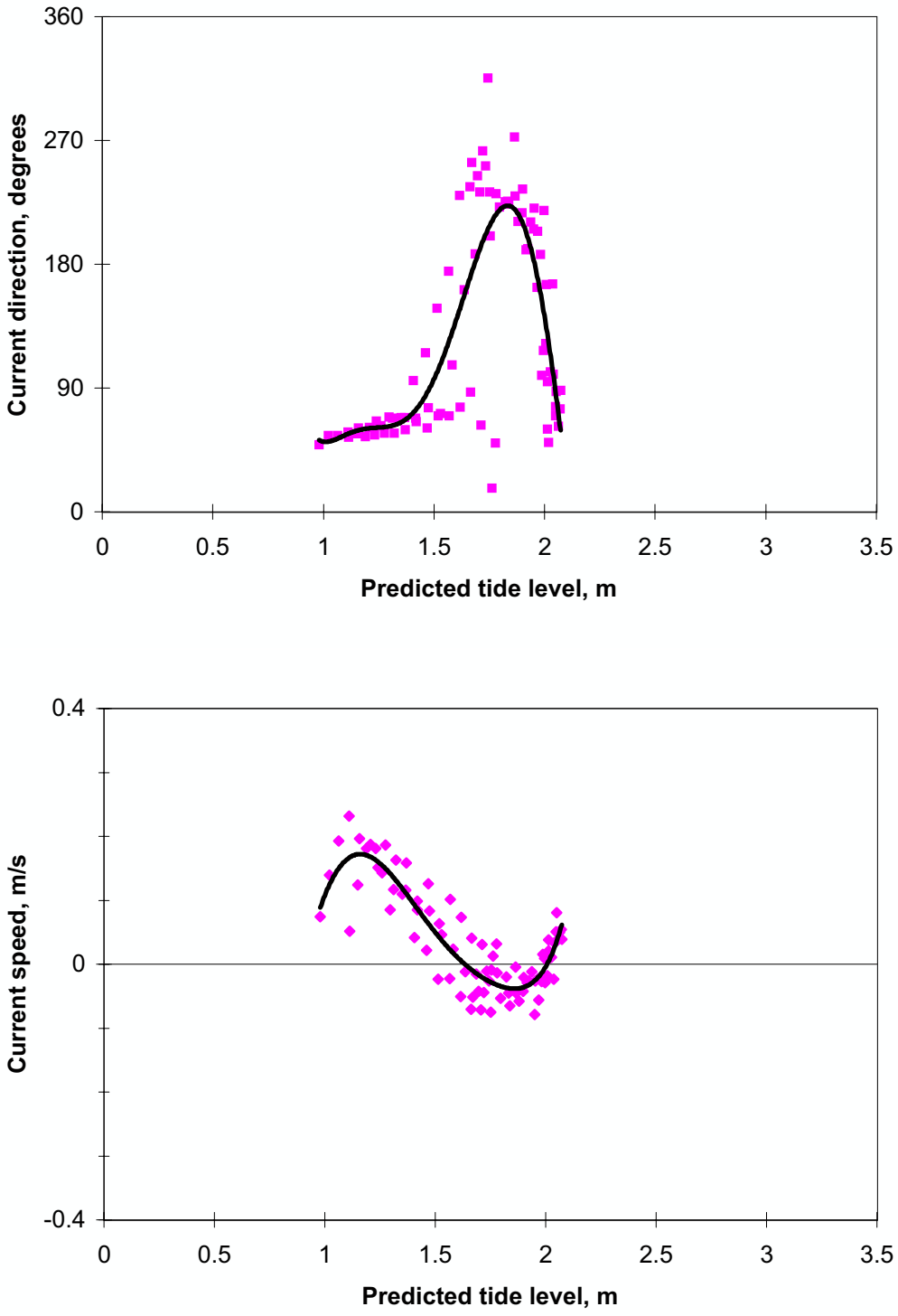

Figure 38. Northern current meter, rising tide, R < 1.4 m
17 March 1996 to 30 June 1996

Above: Current direction *vs* predicted tide level

Below: Current speed *vs* predicted tide level

Only including data with W < 5m/s

H_{BP} and H_{Wis} < 0.35 m

θ_c < 125°, positive θ_c >= 125°, negative

Trendlines, 6th order polynomials

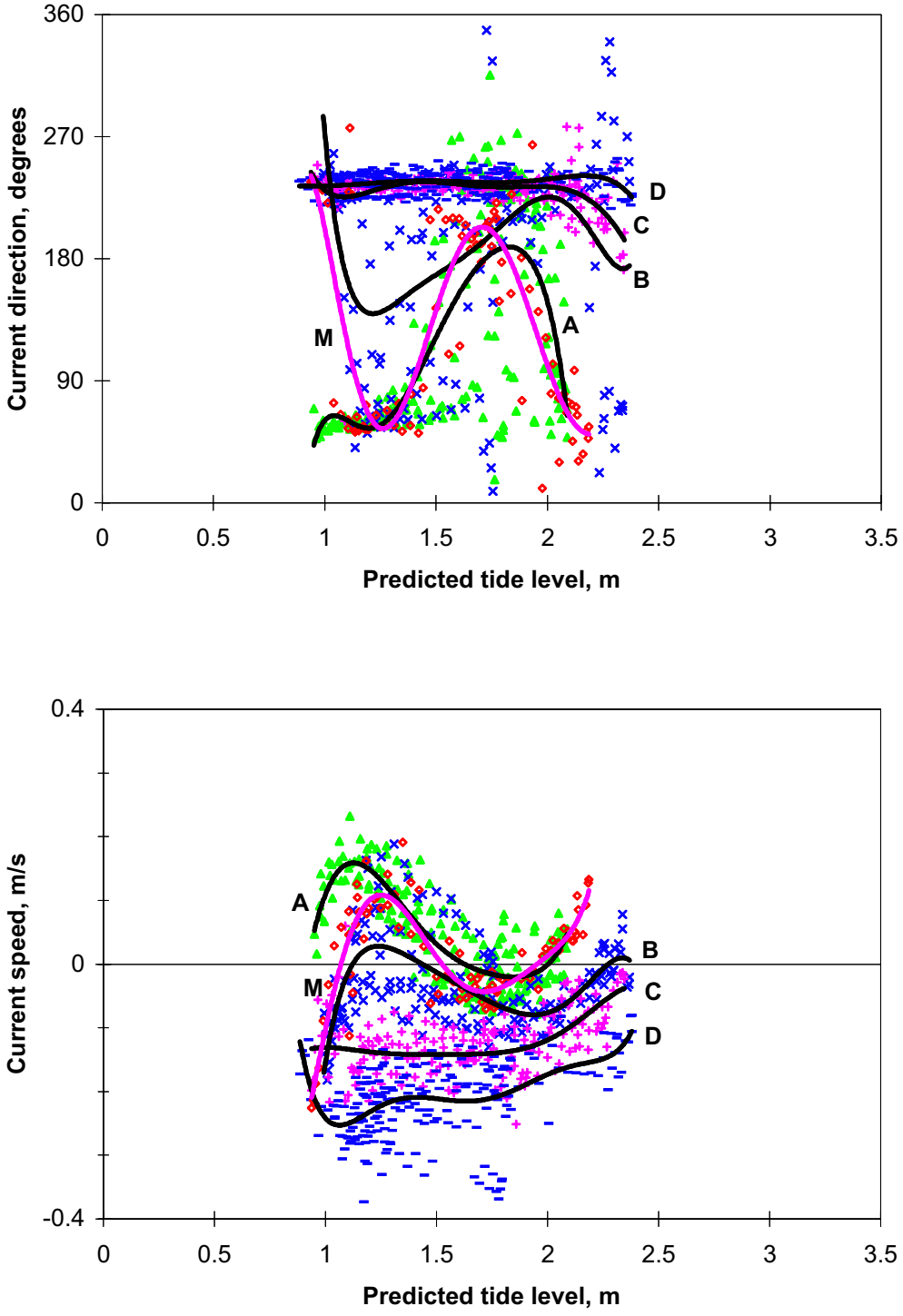

Figure 39. Northern current meter, rising tide, R < 1.4 m
17 March 1996 to 30 June 1996

Above Current direction variation with increasing wave height
Below Current speed variation with increasing wave height

A	W < 5 m/s	All wind directions	H_{BP} and H_{Wis} < 0.5 m
B	All W	$315^o <= \theta_W < 180^o$	0.5 m <= H_{BP} < 0.75 m; H_{Wis} < 0.75 m
C	All W	$315^o <= \theta_W < 180^o$	0.75 m <= H_{BP} < 1.0 m; H_{Wis} < 1.0 m
D	All W	$315^o <= \theta_W < 180^o$	H_{BP} >= 1.0 m; All H_{Wis}
M	All W	$180^o <= \theta_W < 315^o$	0.5 m <= H_{BP} < 1.0 m; All H_{Wis}
	$\theta_c < 125^o$, positive	$\theta_c >= 125^o$, negative	Trendlines 6th order polynomials

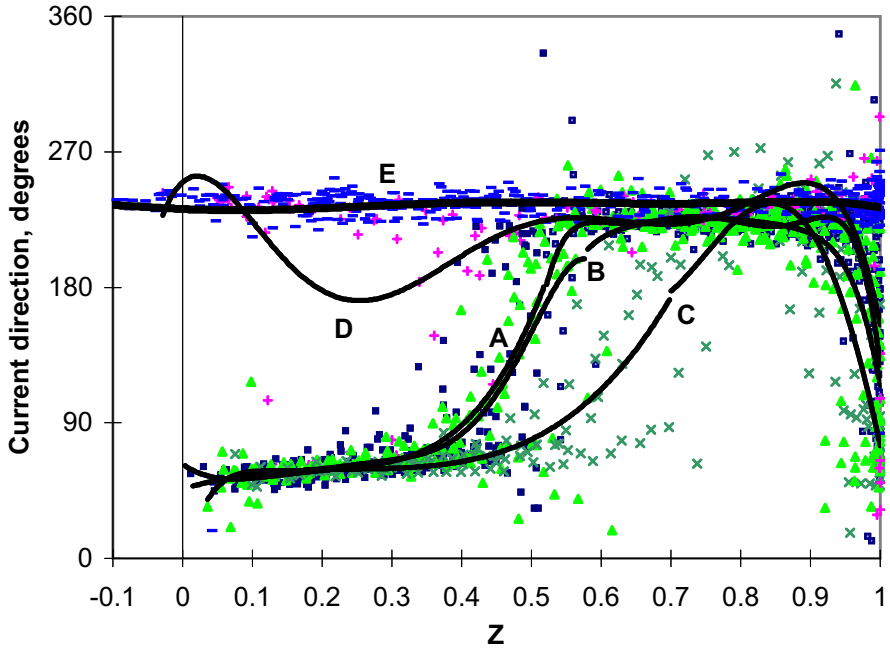

Figure 40. Northern current meter, rising tide, all tidal ranges 17 March 1996 to 30 June 1996

Current direction vs Dimensionless water level, $Z = (z - z_b)/(z_H - z_b)$

A	W < 5 m/s	All wind directions	R >= 2.0 m,	H_{BP} and H_{Wis} < 0.5 m
B	W < 5 m/s	All wind directions	1.4 m <= R < 2.0 m,	H_{BP} and H_{Wis} < 0.5 m
C	W < 5 m/s	All wind directions	R <= 1.4 m,	H_{BP} and H_{Wis} < 0.5 m
D	All W	$315^o <= \theta_W < 180^o$	1.4 m <= R < 2.0 m,	0.75 m <= H_{BP} < 1.0 m; H_{Wis} < 1.0 m
E	All W	$315^o <= \theta_W < 180^o$	R >= 2.0 m,	H_{BP} >= 1.0 m, All H_{Wis}
			1.4 m <= R < 2.0 m,	H_{BP} >= 1.0 m, All H_{Wis}
			R <= 1.4 m,	H_{BP} >= 1.0 m, All H_{Wis}

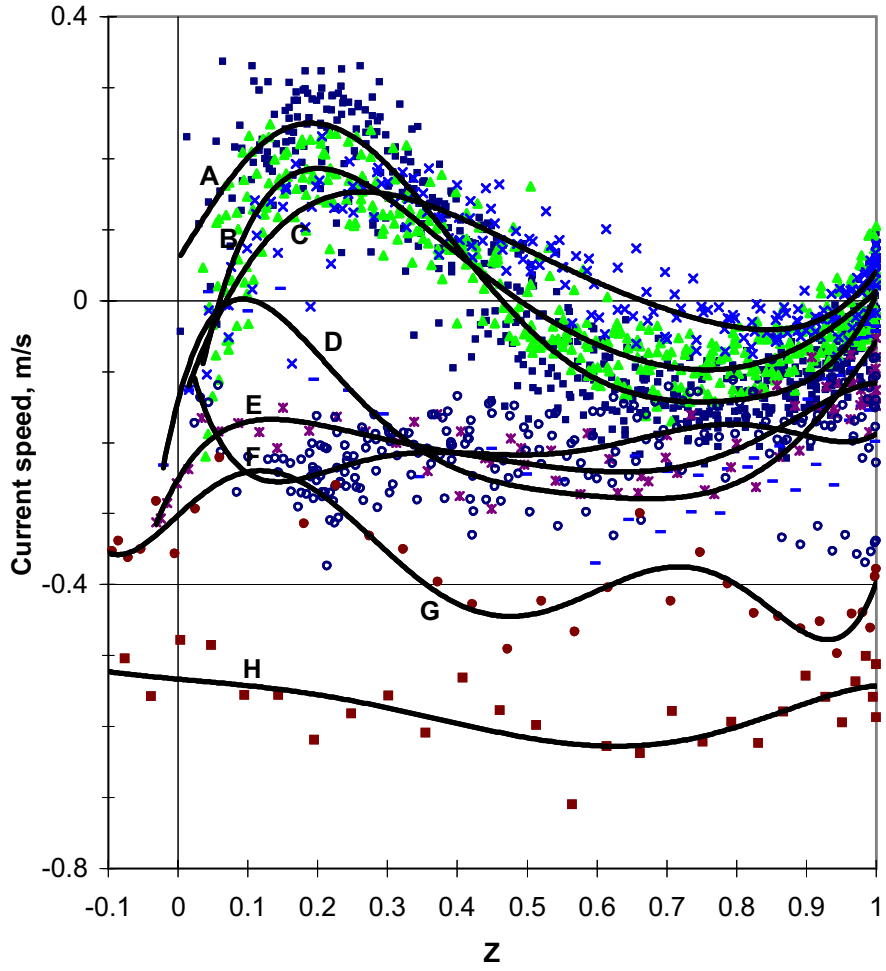

Figure 41. Northern Current meter, rising tide, all tidal ranges 17 March 1996 to 30 June 1996

Current speed vs Dimensionless water level, $Z = (z - z_b)/(z_H - z_b)$

A	W < 5 m/s	All wind directions	R >= 2.0 m,	H_{BP} and H_{Wis} < 0.5 m
B	W < 5 m/s	All wind directions	1.4 m <= R < 2.0 m,	H_{BP} and H_{Wis} < 0.5 m
C	W < 5 m/s	All wind directions	R <= 1.4 m,	H_{BP} and H_{Wis} < 0.5 m
D	All W	$315^o <= \theta_w < 180^o$	R >= 2.0 m,	1.0 m <= H_{BP} < 1.5 m; H_{Wis} < 1.5 m
E	All W	$315^o <= \theta_w < 180^o$	1.4 m <= R < 2.0 m,	1.0 m <= H_{BP} < 1.5 m; H_{Wis} >= 1.5 m
F	All W	$315^o <= \theta_w < 180^o$	R <= 1.4 m,	H_{BP} >= 1.0 m, All H_{Wis}
G	All W	$315^o <= \theta_w < 180^o$	1.4 m <= R < 2.0 m,	H_{BP} >= 1.5 m, All H_{Wis}
H	All W	$315^o <= \theta_w < 180^o$	R >= 2.0 m,	H_{BP} >= 2.5 m, All H_{Wis}

$\theta_c < 125^o$, positive $\theta_c >= 125^o$, negative Trendlines, 6th order polynomials

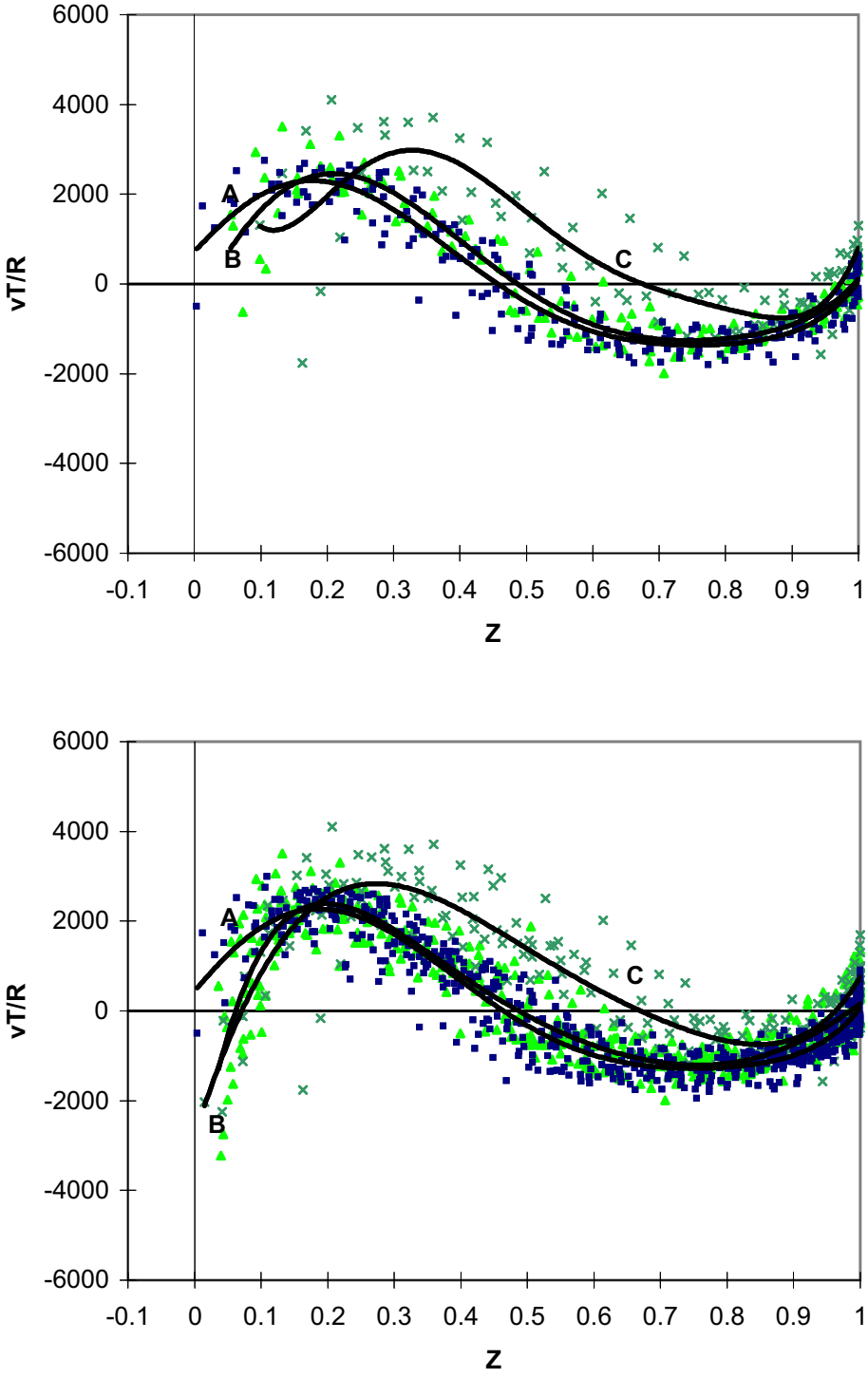

Figure 42. Northern Current meter, rising tide, W < 5 m/s
Dimensionless velocity, vT/R vs Dimensionless water level Z
$Z = (z_o - z_b)(z_H - z_b)$
17 March 1996 to 30 June 1996

Above	**H_{BP} and H_{Wis} < 0.35 m**
Below	**H_{BP} and H_{Wis} < 0.5 m**
A	R >= 2.0 m
B	1.4 m <= R < 2.0 m
C	R < 1.4 m

6.5 Northern current meter, falling tide

6.5.1 Tidal range greater than 2.0 m

All data (Figure 43). On the falling tide, initially flow is generally towards the eastnortheast. As the tide falls, the flow direction tends northwards and then reverses to the westsouthwestward direction. By the time the tide level has fallen to 1.4 m, the flow has almost completely reversed.

At tide levels above 1.4 m there are many observations with directions intermediate between the two main groups. Those observations with directions between 90^{o} and 200^{o} tend to be at the higher tide levels, greater than 1.75 m, whereas those with directions greater than 270^{o} are mostly at tide levels between 2 and 1.3 m. This indicates that current reversals that take place at the higher tide levels do so in the clockwise direction, whereas those that occur at the lower tide levels change direction in the anticlockwise direction.

Current speeds in the northeastward, positive, direction have a mean value of 0.12 m/s and a maximum value of 0.33 m/s. They occurred for 53% of the time in the period 17 March to 30 June 1996 (omitting the time when the instrument was exposed at low tide). After the current has reversed, when tide levels are between 1.3 and 0.7 m, most of the recorded current speeds are *ca* -0.3 m/s. There also are some observations of much higher current speeds in the negative direction, maximum – 0.74 m/s.

Low waves, H_{BP} and H_{Wis} < 0.35 m and low winds, W < 5m/s (Figure 44). When conditions are mild at the northern current meter on the falling tide, the current flows towards the eastnortheast, 60^{o} to 70^{0}, until the tide level drops to *ca* 1.5 m. The flow then reverses at tide levels between 1.5 and 1.4 m, usually in the anticlockwise direction, to flow towards the southwest, 230^{o} to 240^{o}, for the remainder of the falling tide.

There is some deviation in the direction of observations taken during the first part of the falling tide, while it is flowing towards the eastnortheast. The current speeds for almost all these observations are low, < 0.08 m/s, and most of the directions are between 70^{o} and 180^{o}. The standard deviations for the speeds of these observations are high. It is postulated that these readings represent wave action from the north and northeast causing flow towards the island. At least some of these observations were recorded when the offshore wave period was quite large, 10 to 11s; under these conditions, with low wave height and at higher tide levels, the waves would be able to pass over the reef-rim without breaking and therefore could influence the measured velocities.

The current speeds, apart from those with low speeds and directions between 70^{o} and 180^{o} discussed above, are generally between 0.05 and 0.2 m/s in the positive (northeastward) direction. There are a few readings with speeds greater than 0.2 m/s. After the current has reversed to the southwestward direction, the speed increases rapidly to almost - 0.3 m/s as the tide level falls to *ca* 1.0 m. This speed is then maintained until the water level drops to that of the instrument's sensors. During the low tide period, it has been observed that the current continues to flow out towards the boat harbour. After the tide level falls below the level of the bund walls (0.86 m), the flow direction is diverted by the wall to a direction parallel to the wall and then offreef out through the gaps in the coral.

Wave/wind influenced conditions (Figures 45 and 46). As offshore wave heights, H_{BP}, increase up to 1 m, the current reversal occurs slightly earlier, *i.e.* at a slightly higher tide level (Figure 45, curves A, B and C). Once H_{BP} exceeds 1 m, reversal is almost complete (curves D and E) and when H_{BP} exceeds 1.5 m (curve F), the currents are completely reversed for the whole falling tide.

The current speeds in the positive, northeastward, direction, decrease as H_{BP} increases (Figure 46, curves A, B, and C) but there is little change in the speed in the negative, southwestward, direction. When H_{BP} exceeds 1 m, current speeds are generally negative, but of low magnitude at the higher tide levels (Figure 46, curve D). As H_{BP} increases further, the negative current speeds increase, including the speed in the later part of the cycle (curves E and F). These latter speeds reach magnitudes of *ca* – 0.4 m/s.

As mentioned in the discussion about conditions during the rising tide at the northern meter, there was a significant event at the beginning of May 1996. During this event, offshore waves, H_{BP}, were large, up to 3.2 m (Figure 46, curves G and H). Southwestward currents during this event reached magnitudes of – 0.4 to - 0.74 m/s. The highest speeds were when the tide levels were between 2.5 and 1 m. When the tide level dropped below 1 m, the currents decreased.

All the above discussion has been for wind conditions other than southwesterly. As with the rising tide at the northern current meter, southwesterly winds cause the currents to flow more strongly towards the northeast and inhibit current reversal at the higher stages of the falling tide (curve M).

6.5.2 Tidal range between 2.0 and 1.4 m

All data (Figure 47). The current directions observed with intermediate tidal ranges during the falling tide still show two preferred directions, northeastward and westsouthwestward. At the higher tide levels, above *ca* 1.5 m, the current generally flows towards the northeast with velocities of up to 0.27 m/s. 42% of the observed currents are in the positive direction, towards the northeast, and 58% in the negative direction, towards the westsouthwest. (This does not include the period when the instrument was exposed at low tide). As with the larger tides current reversals are generally clockwise at higher tide levels and anticlockwise at lower tide levels.
At tide levels below *ca* 1.3 m, all flow is in the negative direction, towards the southwest. The maximum speed attained is – 0.48 m/s at a tide level just below 1 m.

Low waves, H_{BP} and H_{Wis} < 0.35 m and low winds, W < 5 m/s (Figure 48). During mild conditions when the tides are in the intermediate tidal range, currents are initially generally fairly weak. As the tide starts to fall, the current flows initially towards the east with speeds up to 0.12 m/s. However some flow is towards the island, towards 90^o to 180^o. This again probably reflects the effect of wave action on the flow; current speeds are very low, less than 0.1 m/s. At the later stages of the falling tide, when tide levels fall below 1.5 m, the currents are towards the southwest, approaching – 0.25 m/s when the tide level is 1 m. The current reversal at *ca* 1.5 m occurs in an anticlockwise direction.

Wave/wind influenced conditions (Figures 49 and 50). The situation for the lower values of offshore wave height, H_{BP}, is somewhat confused. For low values of H_{BP}, less than 0.5 m, current flow for the first part of the falling tide is weak and of indeterminate direction (curve A). As H_{BP} increases, the current flow in the positive direction, towards the northeast, becomes stronger (curve B) and then with increasing H_{BP} weaker again (curve C). When H_{BP} is greater than 1 m all flow is in the negative direction, towards the boat harbour, to the southwest (curves D, E and F). The current speed in the negative direction increases with increasing H_{BP} and reaches speeds between 0.4 and 0.5 m/s when H_{Bp} is greater than 1.5 m. *N.B.* there were no waves greater than 2 m during this measurement period, 17 March to 30 June 1996.

The explanation for the higher current speeds towards the northeast when 0.5 m ≤ H_{BP} <0.75 m (curve B) may be related to the wind direction. The wind directions for these observations are generally from the southeast whereas those for the observations with the lower offshore wave heights (curve A) include a high proportion of northerly and northwesterly winds which tend to suppress the northeastward tidal flow. Clearly, wind from the southwesterly direction, (curve M)

has a noticeable effect. During southwesterly wind conditions, greater positive current speeds (0.15 m/s) are attained during the earlier stage of the falling tide and the reversal to southwestward flowing currents occurs later, at tide levels below 1.4 m.

The occurrence of larger waves to the southeast of the reef also changes the pattern observed at the northern current meter. When H_{Wis} is greater than H_{BP}, flow in the positive direction is maintained for longer than otherwise would be the case (curves N and D).

6.5.3 Tidal range less than 1.4 m

All data (Figure 51). At the smallest tidal ranges, R < 1.4 m, the current directions at the northern current meter on the falling tide still maintain two preferred directions, *ca* 55^0 and *ca* 235^o. The flow is predominantly (82% of the time for which observations are available) in the negative, *ca* 235^o, direction. Flow is only in the positive direction at tide levels above 1.4 m. Below this level, flow is always in the negative direction towards the boat harbour. Flow reversals, from positive to negative, may occur at all tide levels above 1.4 m and may be in either the clockwise or the anticlockwise direction.

Maximum current speeds in the positive direction are always small, the maximum reached is just under 0.2 m/s when the tide level is about 2 m. The negative speeds are greater and reach magnitudes of up to – 0.42 m/s. The greatest negative speeds are attained at lower tide levels, between 1.8m and 1.0 m.

Low waves, H_{BP} and H_{Wis} < 0.35 m and low winds, W < 5 m/s (Figure 52). When conditions are mild, there is an initial brief period, during which the tide flows out towards the northeast, but it quickly reverses, in at least one case in a clockwise direction, and flows out towards the southwest for the remainder of the falling tide. Current speeds are generally low, the maximum obtained was 0.25 m/s in the negative direction when the tide level was below 1 m.

Wave/wind influenced conditions (Figure 53). As wind and offshore wave conditions increase, the weak northeastward flowing tidally induced current is progressively suppressed by wind- and wave-generated currents from the north. This causes current reversals to take place at higher tide levels. When the offshore wave height, H_{BP}, exceeds 0.75 m, the flow is towards the southwest for almost the whole of the falling tide (curve C). As there were no observations with the offshore wave height, H_{BP}, greater than 1.6 m during the measurement period, the wave-generated currents were never particularly large, the greatest speed attained was *ca* – 0.42 m/s.

As with the intermediate tidal range, the effect of larger waves southeast of the reef, H_{Wis}, may impede the wave-generated currents from the northeast (curve N). There were insufficient observations when winds were from the southwesterly direction to allow examination of the flow under those conditions.

6.5.4 Effect of tidal range

From the previous sections it is apparent that the reversal of the falling tide at the northern current meter is affected by the tide level. At higher tide levels the reversal is clockwise and at lower levels it is anticlockwise. Figure 54 shows that for mild conditions (H_{BP} and $H_{Wis} < 0.5$ m, $W < 5$ m/s) clockwise reversal occurs when $z_0 > 1.75$ m and anticlockwise reversal occurs when $z_0 < 1.75$ m. This critical value of z_0 is independent of tidal range. All falling tidal currents have reversed and are flowing towards the boat harbour when $z_0 < 1.35$ m.

The mild conditions data is plotted against the dimensionless water level Z in Figure 55 (curves A, B and C). Data for $v \leq 0.08$ m/s has been excluded and it is found that there are no significant differences for the three tidal range groups. Northeastward flow towards the northern reef-rim never occurs when $Z < 0.25$ but southwestward flow towards the boat harbour can occur at all values of Z and always occurs when wave heights (H_{BP}) are greater then 1.0 to 1.25 m. Considering Table 5, it is seen that for small tides currents are southwestward when H_{BP} is greater than 0.75 m; for average tides when $H_{BP} > 1.0$ m; and for large tides when $H_{BP} > 1.25$ m, provided winds are not southwesterly or the waves H_{Wis} on the southern side of the reef are not large.

During northeasterly flow on the falling tide, current speeds of up to *ca* 0.23 m/s occur for large tides when $Z > 0.35$ (Figure 56, curve A). However, as the tidal range reduces both the magnitude and duration of this flow decrease so that for small tides northeasterly flow only occurs when $Z > 0.8$ (curve C). Maximum ebb current velocities as $Z \rightarrow 0$ are *ca* 0.3 m/s for all tidal ranges. Once wave heights become large enough to completely reverse the flow (curves D, E, F and G), negative current velocities increase with increasing H_{BP} and become more or less independent of Z.

Table 5 Current directions at northern current meter during falling tide under different wind and wave conditions for three tidal range groups
(only early stage of falling tide, $z_0 \geq 1.5$ m)

Wave and wind conditions Wave height, m; wind speed, m/s	**R < 1.4m**	**1.4 m ≤ R < 2.0 m**	**R ≥ 2.0 m**
H < 0.35, W < 5	NE ($z_0 \geq 1.75$ m)	E (SE) – N	ENE (SE)
H < 0.5, W < 5	NE - N	ENE (SE) – N	ENE – N
$0.5 \leq H_{BP} < 0.75$, no SW wind	NE – SW	ENE – N	ENE – N (SE)
$0.75 \leq H_{BP} < 1.0$, no SW wind	(NE) SW	ENE - SE/N – SW	ENE – N (SE)
$1.0 \leq H_{BP} < 1.25$, no SW wind	SW*	SW*	ENE – SE – SW
$1.25 \leq H_{BP} < 1.5$, no SW wind	SW	SW*	(ENE) SW
$H_{BP} \geq 1.5$, no SW wind	SW	SW	SW
$0.5 \leq H_{BP} < 1.0$, SW wind	-	NE	-
$1.0 \leq H_{BP} < 1.6$, SW wind	-	-	ENE (SE)

*High values of H_{Wis} may counteract flow to SW

When the dimensionless velocity vT/R is plotted as a function of Z for mild conditions (Figure 57), the data for the different tidal range groups do not come together as is the case for the rising tide and for the southern current meter. In particular the average range tides (curve B) generally show negative vT/R values for Z > 0.6, although it could be expected that positive values should occur. It is probable that the high proportion of northeasterly winds for these tides during the period of this analysis influenced the tidal currents.

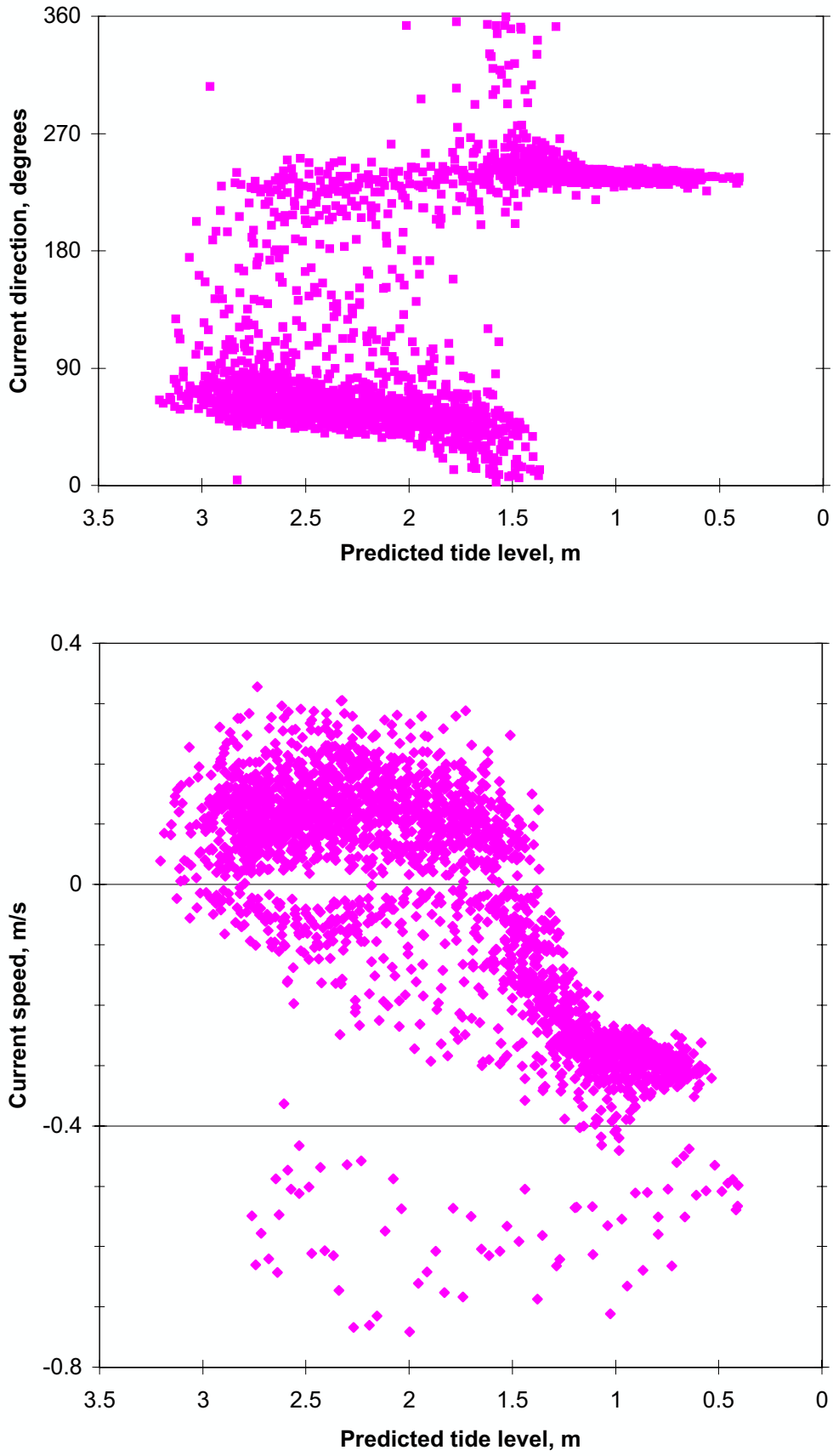

Figure 43. Northern current meter, falling tide, R >= 2.0 m
17 March 1996 to 30 June 1996

Above: **Current direction *vs* predicted tide level; all data**

Below: **Current speed *vs* predicted tide level; all data**

θ_c < 125°, positive θ_c >= 125°, negative

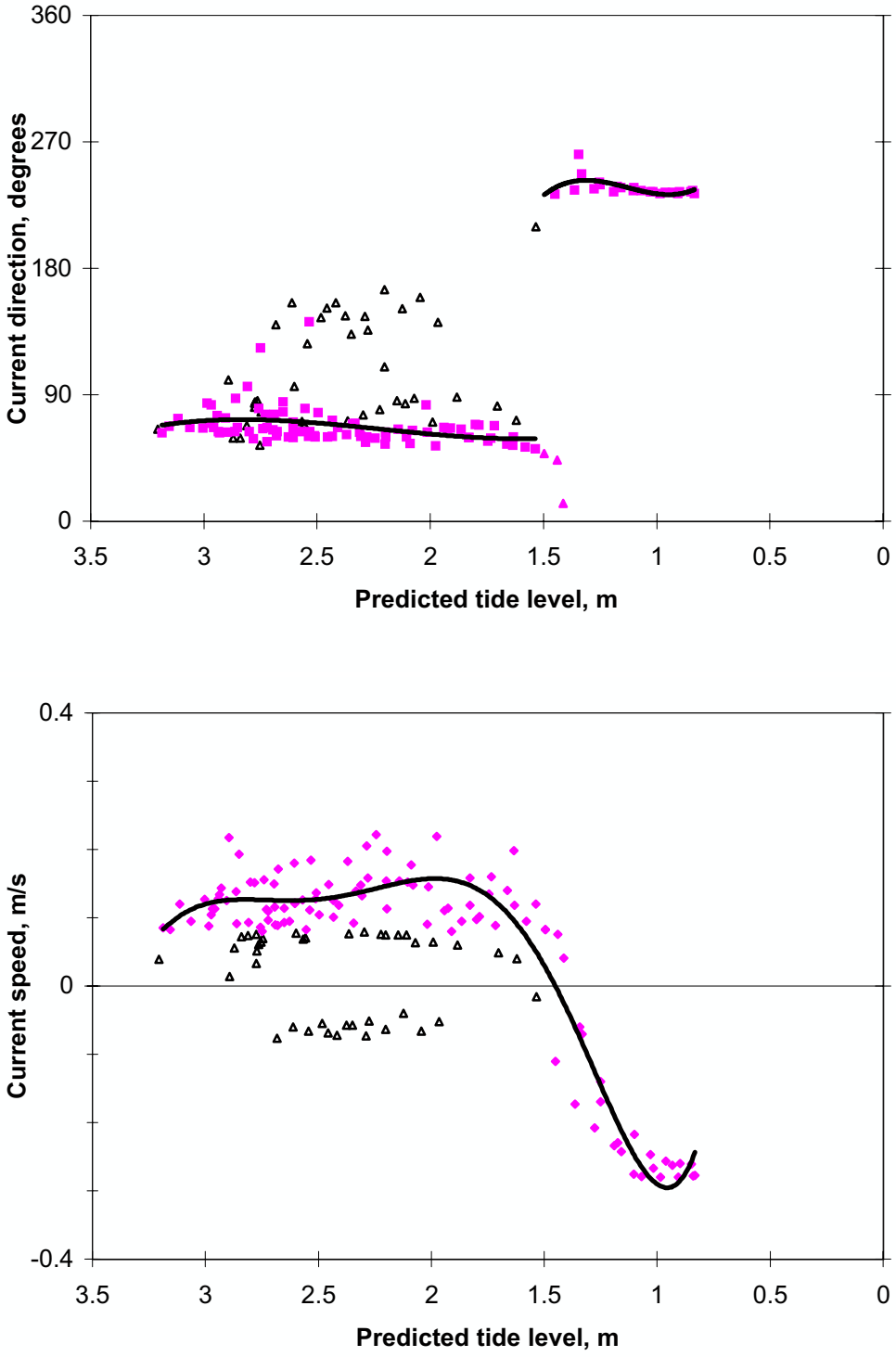

Figure 44. Northern current meter, falling tide, R >= 2.0 m
17 March 1996 to 30 June 1996

Above: Current direction *vs* predicted tide level

Below: Current speed *vs* predicted tide level

Only including data with W < 5m/s

H_{BP} and H_{Wis} < 0.35 m

θ_c < 125°, positive θ_c >= 125°, negative

△ = points where z_o >= 1.5 m and current speed < |0.08| m/s

Trendlines, various order polynomials

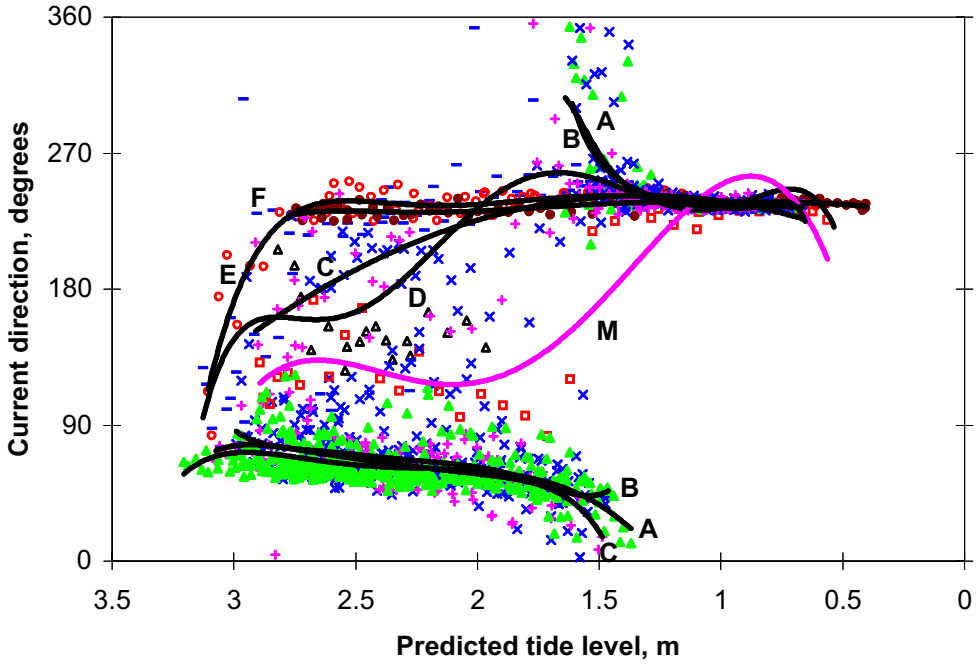

Figure 45. Northern current meter, falling tide, R >= 2.0 m
17 March 1996 to 30 June 1996
Current direction variation with increasing wave height

A	W < 5 m/s	All wind directions	H_{BP} and H_{Wis} < 0.5 m
	△ = points where	θ_c >= 125° and z_o >= 1.5 m	
B	All W	315° <= θ_W < 180°	0.5 m <= H_{BP} < 0.75 m; H_{Wis} < 0.75 m
C	All W	315° <= θ_W < 180°	0.75 m <= H_{BP} < 1.0 m; H_{Wis} < 1.0 m
D	All W	315° <= θ_W < 180°	1.0 m <= H_{BP} < 1.25 m; H_{Wis} < 1.25 m
E	All W	315° <= θ_W < 180°	1.25 m <= H_{BP} < 1.5 m; H_{Wis} < 1.5 m
F	All W	315° <= θ_W < 180°	H_{BP} >= 1.5 m; All H_{Wis}
M	All W	180° <= θ_W < 315°	1.0 m <= H_{BP} < 1.6 m, All H_{Wis}

Trendlines various order polynomials

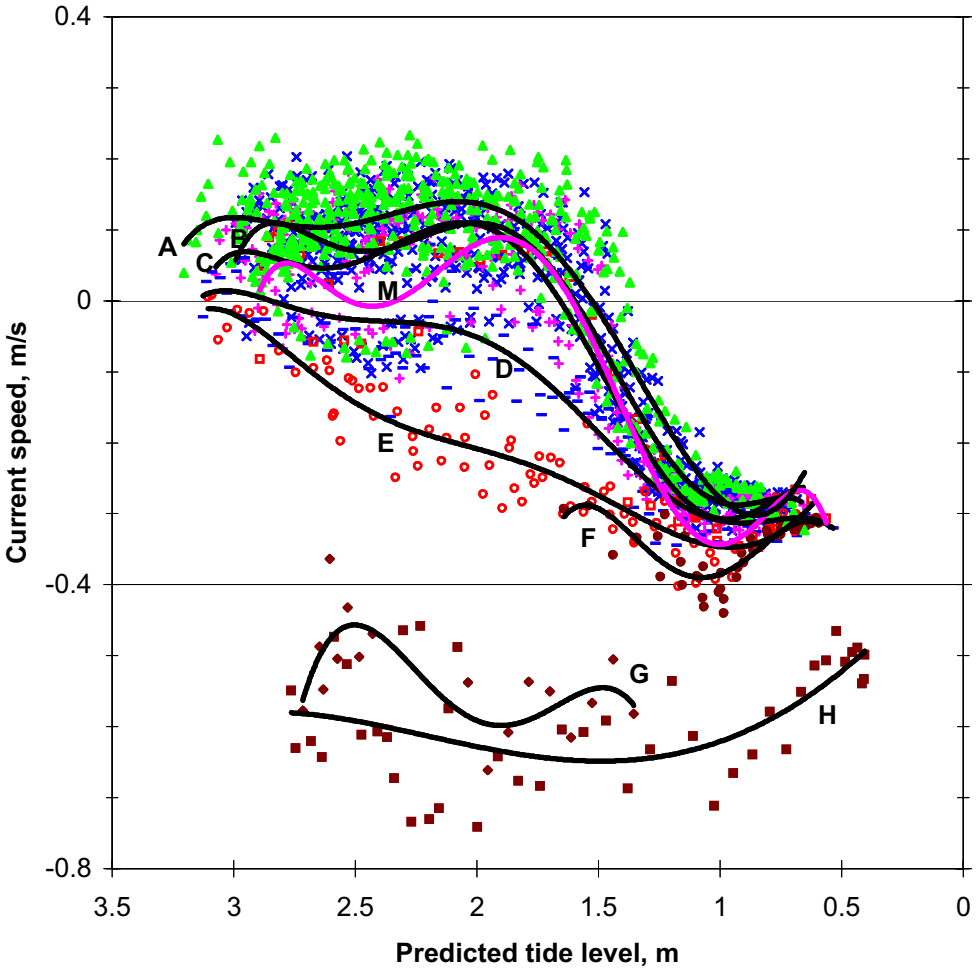

Figure 46. Northern current meter, falling tide, R >= 2.0 m
17 March 1996 to 30 June 1996
Current speed variation with increasing wave height

A	W < 5 m/s	All wind directions	H_{BP} and H_{Wis} < 0.5 m
B	All W	315° <= θ_W < 180°	0.5 m <= H_{BP} < 0.75 m; H_{Wis} < 0.75 m
C	All W	315° <= θ_W < 180°	0.75 m <= H_{BP} < 1.0 m; H_{Wis} < 1.0 m
D	All W	315° <= θ_W < 180°	1.0 m <= H_{BP} < 1.25 m; H_{Wis} < 1.25 m
E	All W	315° <= θ_W < 180°	1.25 m <= H_{BP} < 1.5 m; H_{Wis} < 1.5 m
F	All W	315° <= θ_W < 180°	1.5 m <= H_{BP} < 2.0 m; H_{Wis} < 2.0 m (all)
G	All W	315° <= θ_W < 180°	2.0 m <= H_{BP} < 2.75 m; All H_{Wis}
H	All W	315° <= θ_W < 180°	H_{BP} >= 2.75 m; All H_{Wis}
M	All W	180° <= θ_W < 315°	1.0 m <= H_{BP} < 1.6 m; All H_{Wis}
	θ_c < 125°, positive	θ_c >= 125°, negative	Trendlines 6th order polynomials

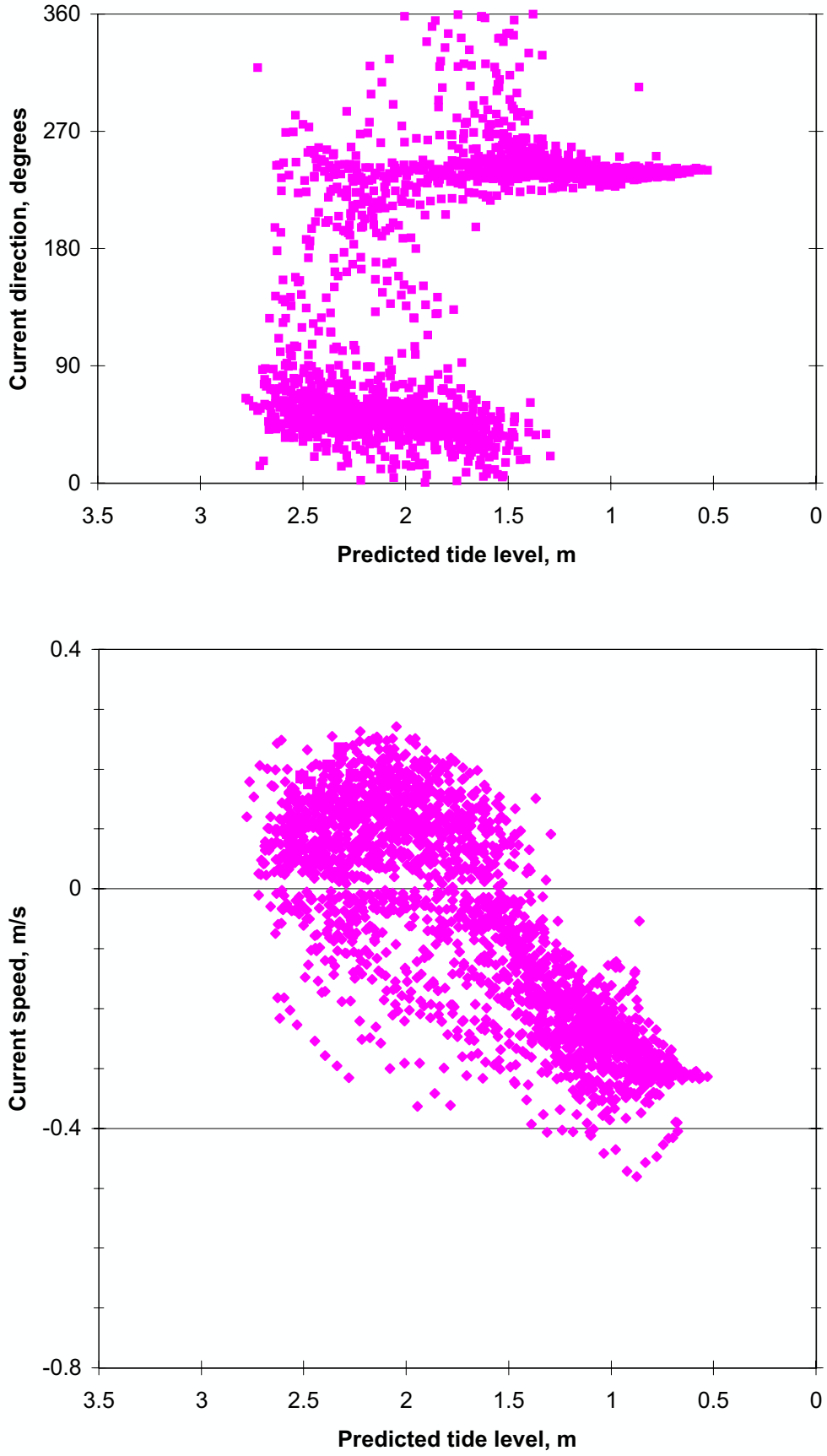

Figure 47. Northern current meter, falling tide, 1.4 m <= R < 2.0 m 17 March 1996 to 30 June 1996

Above: **Current direction *vs* predicted tide level; all data**

Below: **Current speed *vs* predicted tide level; all data**

θ_c < 125°, positive θ_c >= 125°, negative

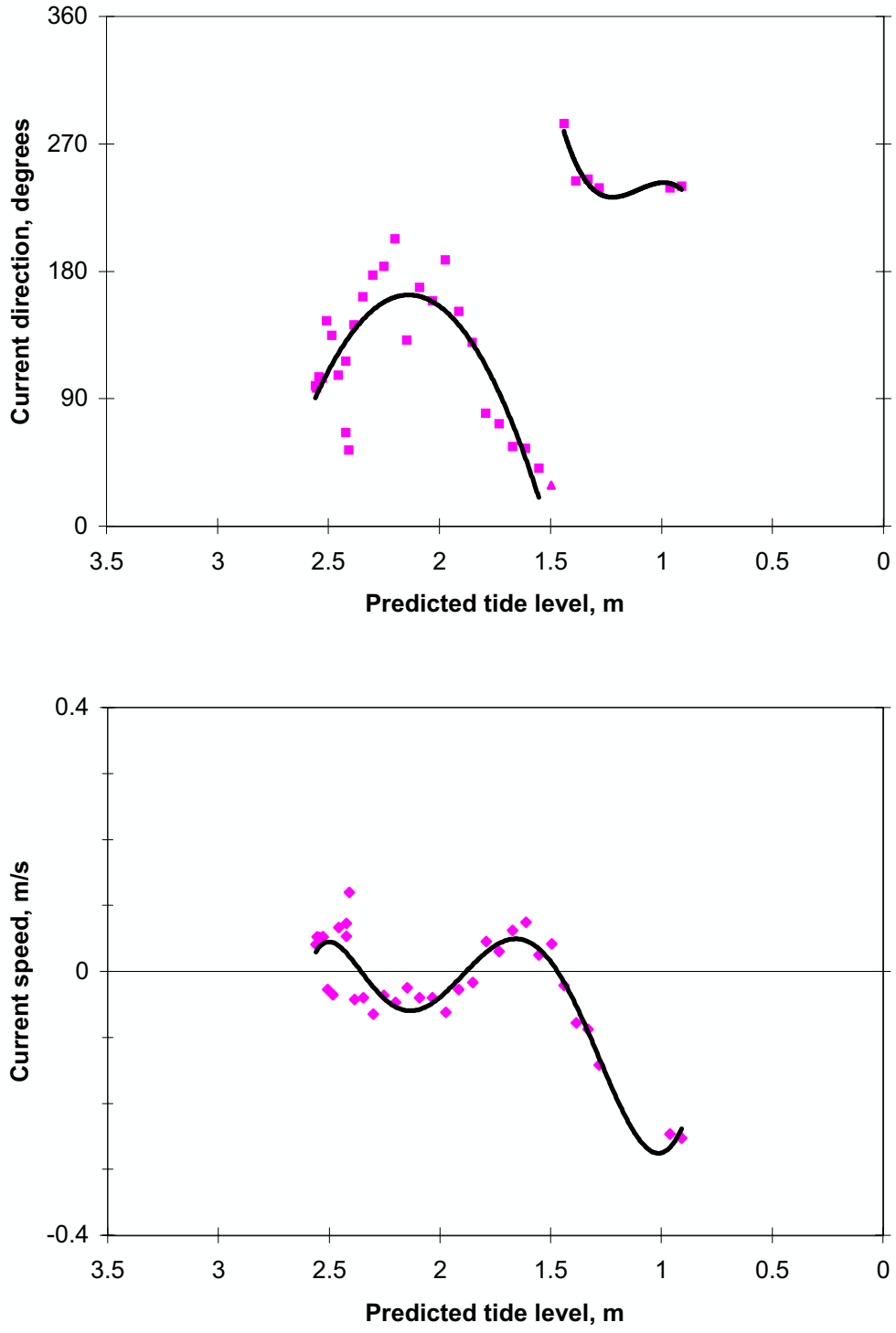

Figure 48. Northern current meter, falling tide, 1.4 m <= R < 2.0 m
17 March 1996 to 30 June 1996

Above: Current direction *vs* predicted tide level

Below: Current speed *vs* predicted tide level

Only including data with W < 5m/s

H_{BP} and H_{Wis} < 0.35 m

θ_c < 125°, positive θ_c >= 125°, negative

Trendlines, various order polynomials

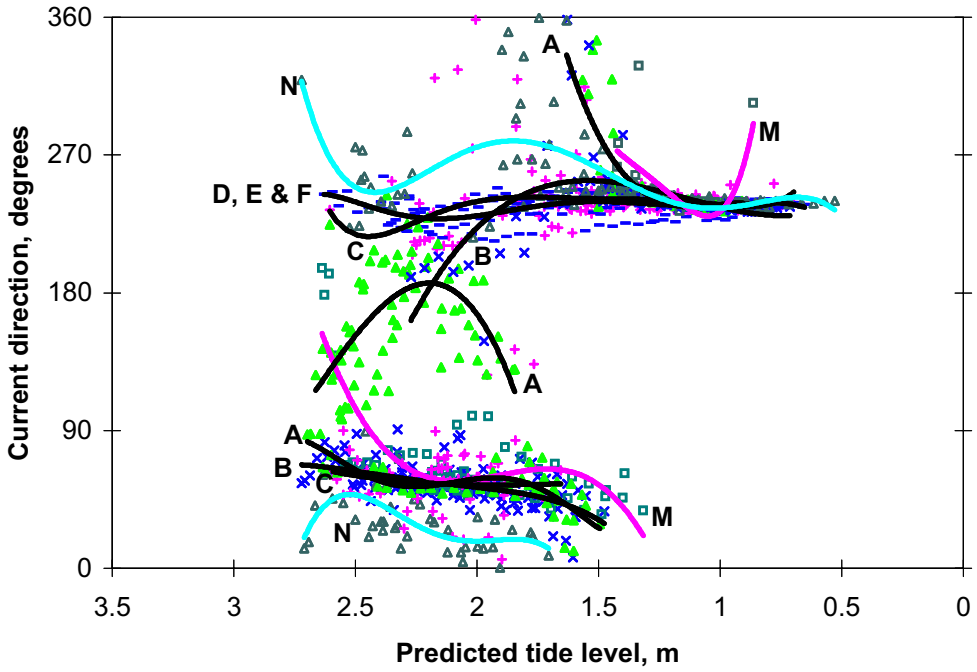

Figure 49. Northern current meter, falling tide, 1.4 m <= R < 2.0 m 17 March 1996 to 30 June 1996

Current direction variation with increasing wave height

A	W < 5 m/s	All wind directions	H_{BP} and H_{wis} < 0.5 m
B	All W	$315^o <= \theta_W < 180^o$	0.5 m <= H_{BP} < 0.75 m; H_{Wis} < 0.75 m
C	All W	$315^o <= \theta_W < 180^o$	0.75 m <= H_{BP} < 1.0 m; H_{Wis} < 1.0 m
D	All W	$315^o <= \theta_W < 180^o$	1.0 m <= H_{BP} < 1.25 m; H_{Wis} < 1.25 m
E	All W	$315^o <= \theta_W < 180^o$	1.25 m <= H_{BP} < 1.5 m; H_{Wis} < 1.5 m
F	All W	$315^o <= \theta_W < 180^o$	H_{BP} >= 1.5 m; All H_{Wis}
M	All W	$180^o <= \theta_W < 315^o$	0.5 m <= H_{BP} < 1.0; All H_{Wis}
N	All W	$315^o <= \theta_W < 180^o$	1.0 <= H_{BP} < 1.25 m; H_{Wis} >= 1.5 m

Trendlines various order polynomials

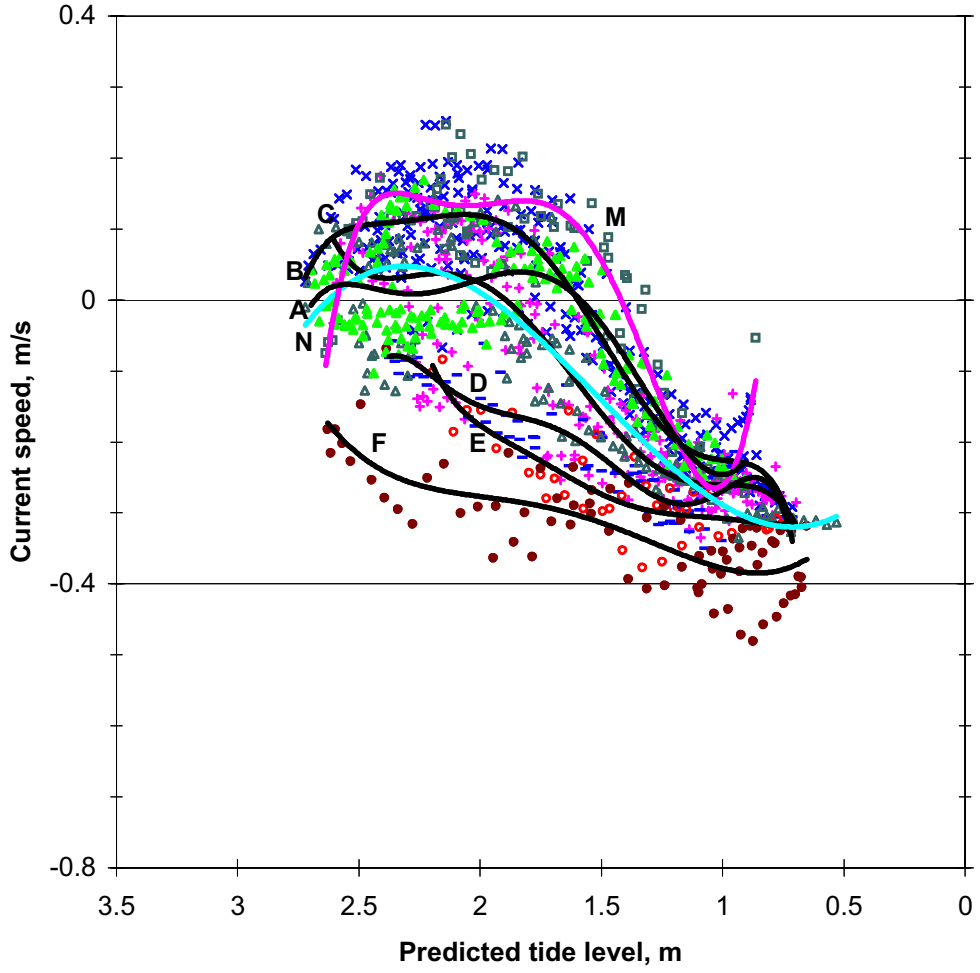

Figure 50. Northern current meter, falling tide, 1.4 m <= R < 2.0 m
17 March 1996 to 30 June 1996
Current speed variation with increasing wave height

A	W < 5 m/s	All wind directions	H_{BP} and H_{Wis} < 0.5 m
B	All W	$315^o <= \theta_W < 180^o$	0.5 m <= H_{BP} < 0.75 m; H_{Wis} < 0.75 m
C	All W	$315^o <= \theta_W < 180^o$	0.75 m <= H_{BP} < 1.0 m; H_{Wis} < 1.0 m
D	All W	$315^o <= \theta_W < 180^o$	1.0 m <= H_{BP} < 1.25 m; H_{Wis} < 1.25 m
E	All W	$315^o <= \theta_W < 180^o$	1.25 m <= H_{BP} < 1.5 m; H_{Wis} < 1.5 m
F	All W	$315^o <= \theta_W < 180^o$	H_{BP} >= 1.5 m; All H_{Wis}
M	All W	$180^o <= \theta_W < 315^o$	0.5 m <= H_{BP} < 1.0 m; All H_{Wis}
N	All W	$315^o <= \theta_W < 180^o$	1.0 m <= H_{BP} < 1.25 m; H_{Wis} >= 1.5 m
	$\theta_c < 125^o$, positive	$\theta_c >= 125^o$, negative	Trendlines various order polynomials

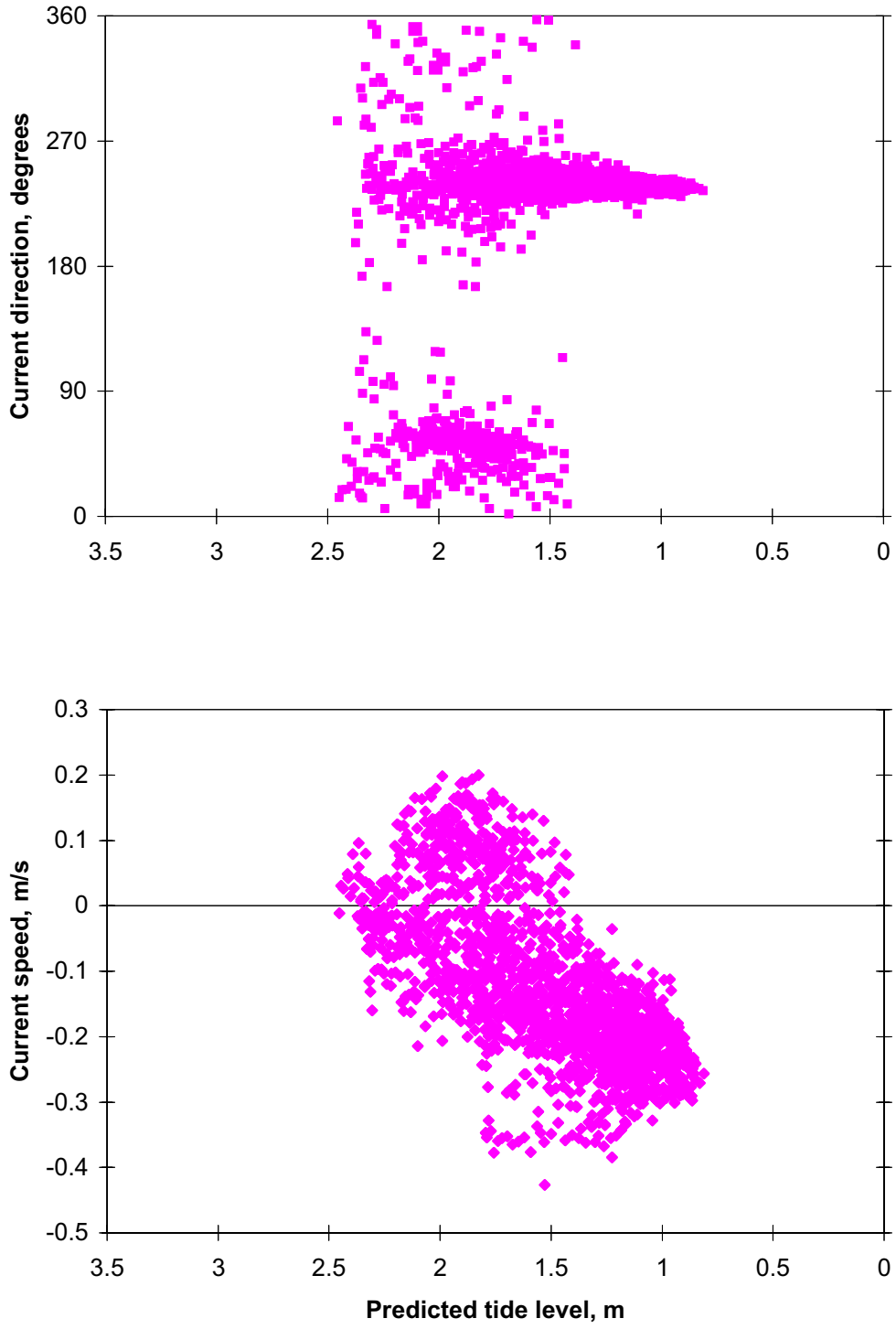

Figure 51. Northern current meter, falling tide, R < 1.4 m
17 March 1996 to 30 June 1996

Above: **Current direction *vs* predicted tide level; all data**

Below: **Current speed *vs* predicted tide level; all data**

θ_c < 125°, positive θ_c >= 125°, negative

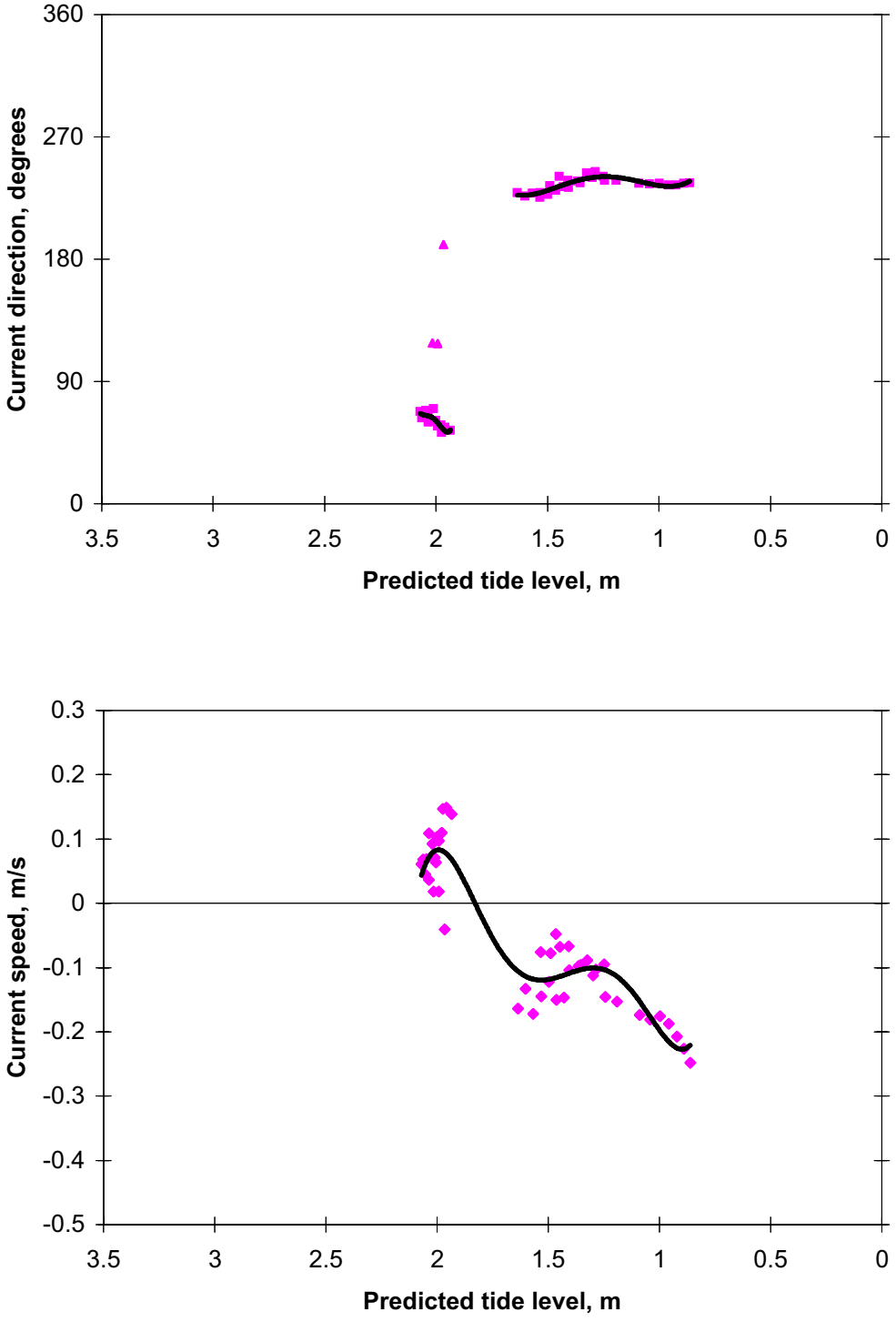

Figure 52. Northern current meter, falling tide, R < 1.4 m
17 March 1996 to 30 June 1996

Above: Current direction *vs* predicted tide level

Below: Current speed *vs* predicted tide level

Only including data with W < 5m/s

H_{BP} and H_{Wis} < 0.35 m

θ_c < 125°, positive θ_c >= 125°, negative

Trendlines, various order polynomials

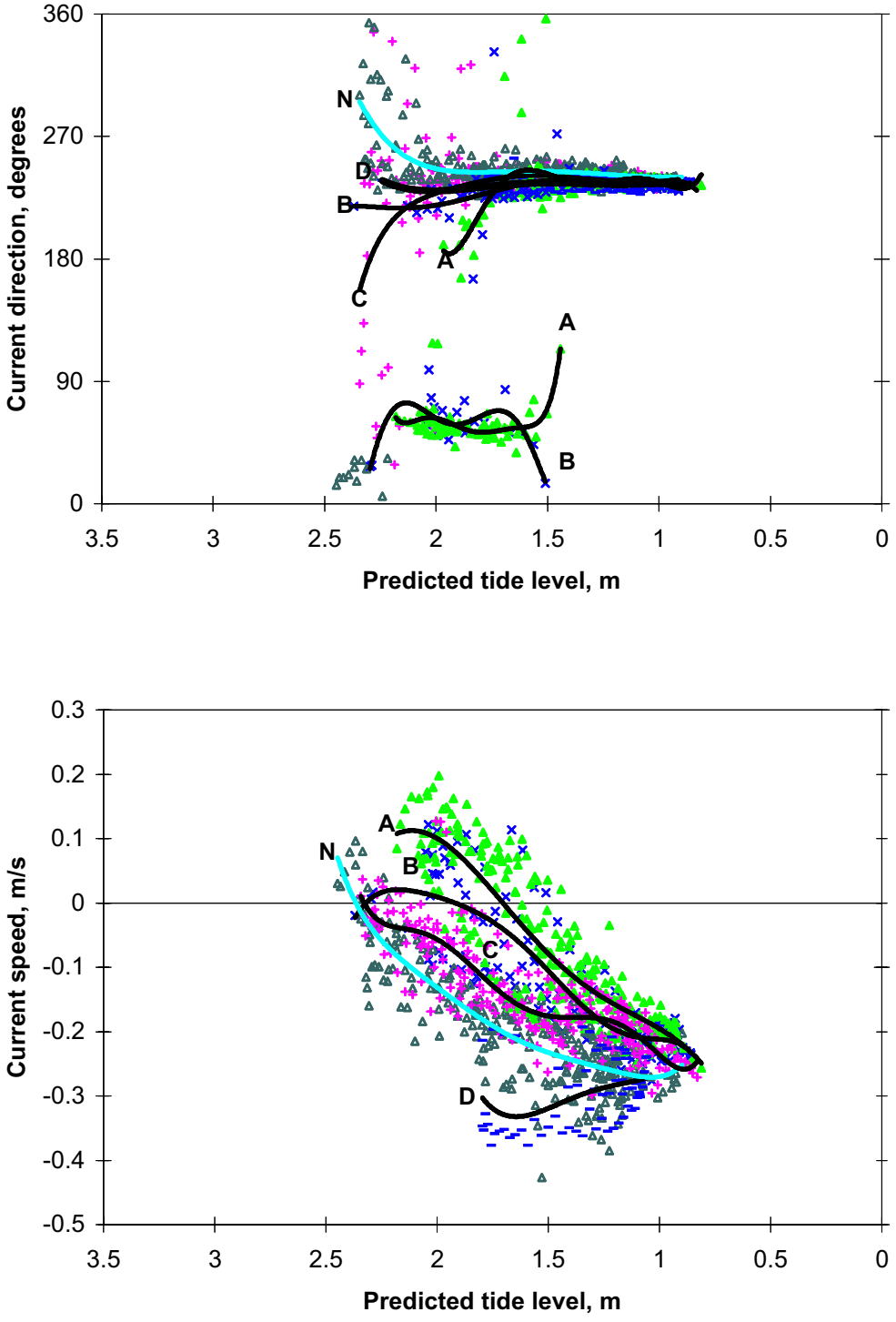

Figure 53. Northern current meter, falling tide, R < 1.4 m
17 March 1996 to 30 June 1996
Current speed variation with increasing wave height

A	W < 5 m/s	All wind directions	H_{BP} and H_{Wis} < 0.5 m
B	All W	$315^o <= \theta_W < 180^o$	0.5 m <= H_{BP} < 0.75 m; H_{Wis} < 0.75 m
C	All W	$315^o <= \theta_W < 180^o$	0.75 m <= H_{BP} < 1.0 m; H_{Wis} < 1.0 m
D	All W	$315^o <= \theta_W < 180^o$	H_{BP} >= 1.0 m
			Dir'n, H_{Wis} < 1.35 m; Speed, H_{Wis} < 1.0 m
N	All W	$315^o <= \theta_W < 180^o$	H_{BP} >= 1.0 m; H_{Wis} >= 1.35 m
	$\theta_c < 125^o$, positive	$\theta_c >= 125^o$, negative	Trendlines various order polynomials

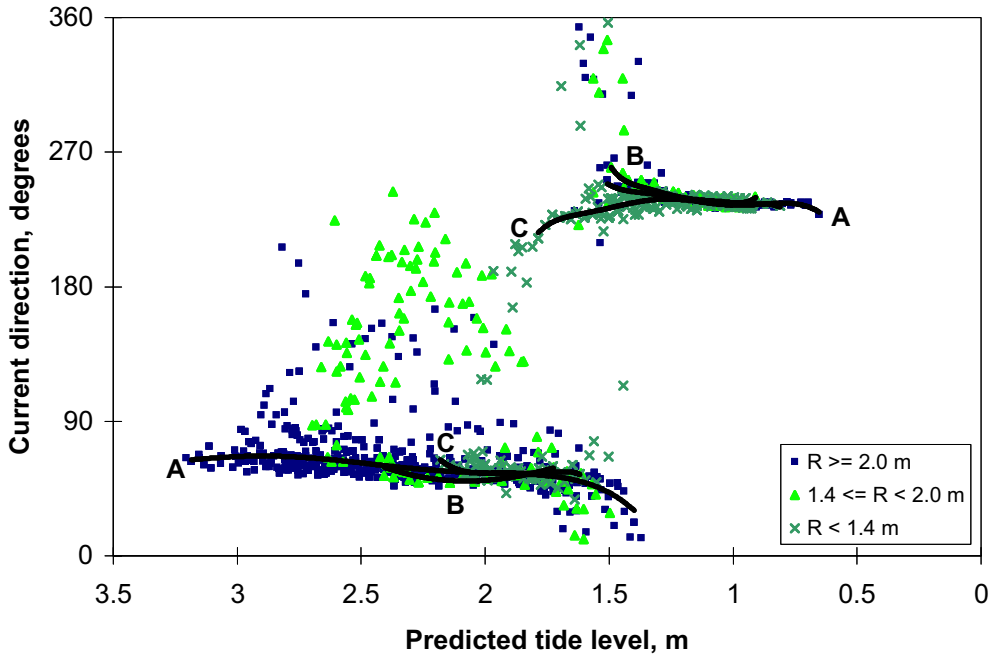

Figure 54. **Northern current meter, falling tide, all tidal ranges 17 March 1996 to 30 June 1996**

Current direction vs predicted tide level

W < 5 m/s All wind directions H_{BP} and H_{Wis} < 0.5 m

A R >= 2.0 m, 2 trendlines, division taken at z = 1.5 m

B 1.4 m <= R < 2.0 m, 2 trendlines, division taken at z= 1.5 m

C R < 1.4 m, 2 trendlines, division taken between θ_c >= 125° and θ_c < 125°

Trendlines are only for data where current speed >= |0.08| m/s

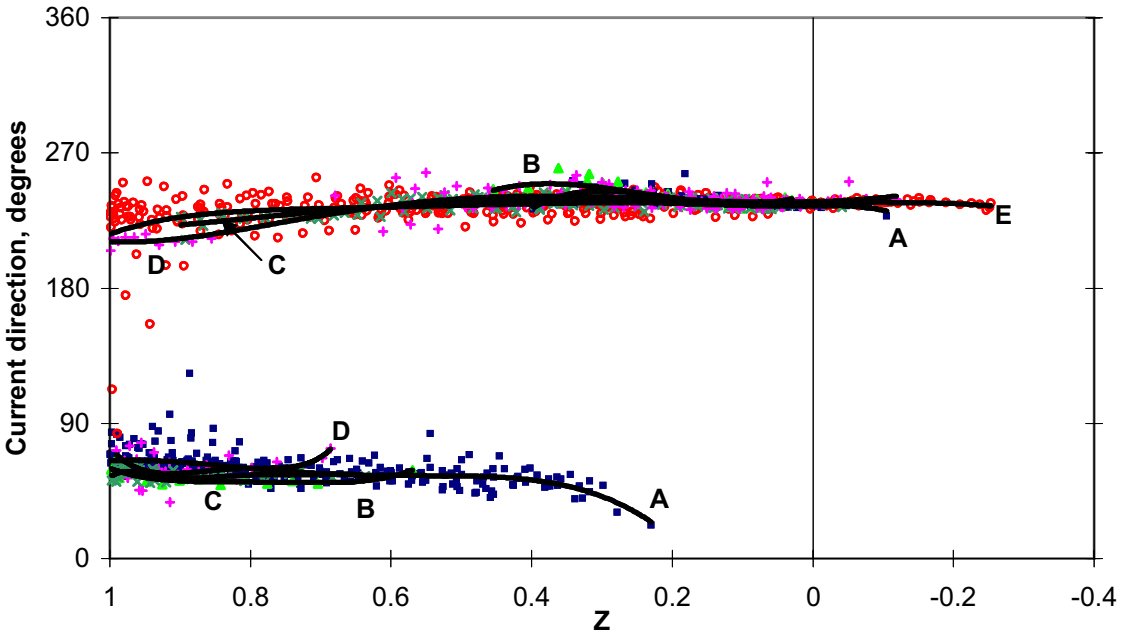

Figure 55. Northern current meter, falling tide, all tidal ranges 17 March 1996 to 30 June 1996

Current direction vs Dimensionless water level, $Z = (z - z_b)/(z_H - z_b)$

A	W < 5 m/s	All wind directions	R >= 2.0 m;	H_{BP} and H_{Wis} < 0.5 m
		2 trendlines, division taken at Z = 0.32		
B	W < 5 m/s	All wind directions	1.4 m <= R < 2.0 m;	H_{BP} and H_{Wis} < 0.5 m
		2 trendlines, division taken at Z = 0.7		
C	W < 5 m/s	All wind directions	R < 1.4 m;	H_{BP} and H_{Wis} < 0.5 m
		2 trendlines, division taken between $_c$ >= 125° and θ_c < 125°		
D	All W	315° <= θ_W < 180°	1.4 m <= R < 2.0 m;	0.75 m <= H_{BP} < 1.0 m; H_{Wis} < 1.0 m
		2 trendlines, division taken between $_c$ >= 125° and θ_c < 125°		
E	All W	315° <= θ_W < 180°	R >= 2.0 m;	H_{BP} >= 1.25 m; All H_{Wis}
			1.4 m <= R < 2.0 m;	H_{BP} >= 1.0 m; H_{Wis} < 1.25 m
			R < 1.4 m;	H_{BP} >= 1.0 m; H_{Wis} < 1.35 m

A, B, C and D only include data where current speed >= |0.08| m/s

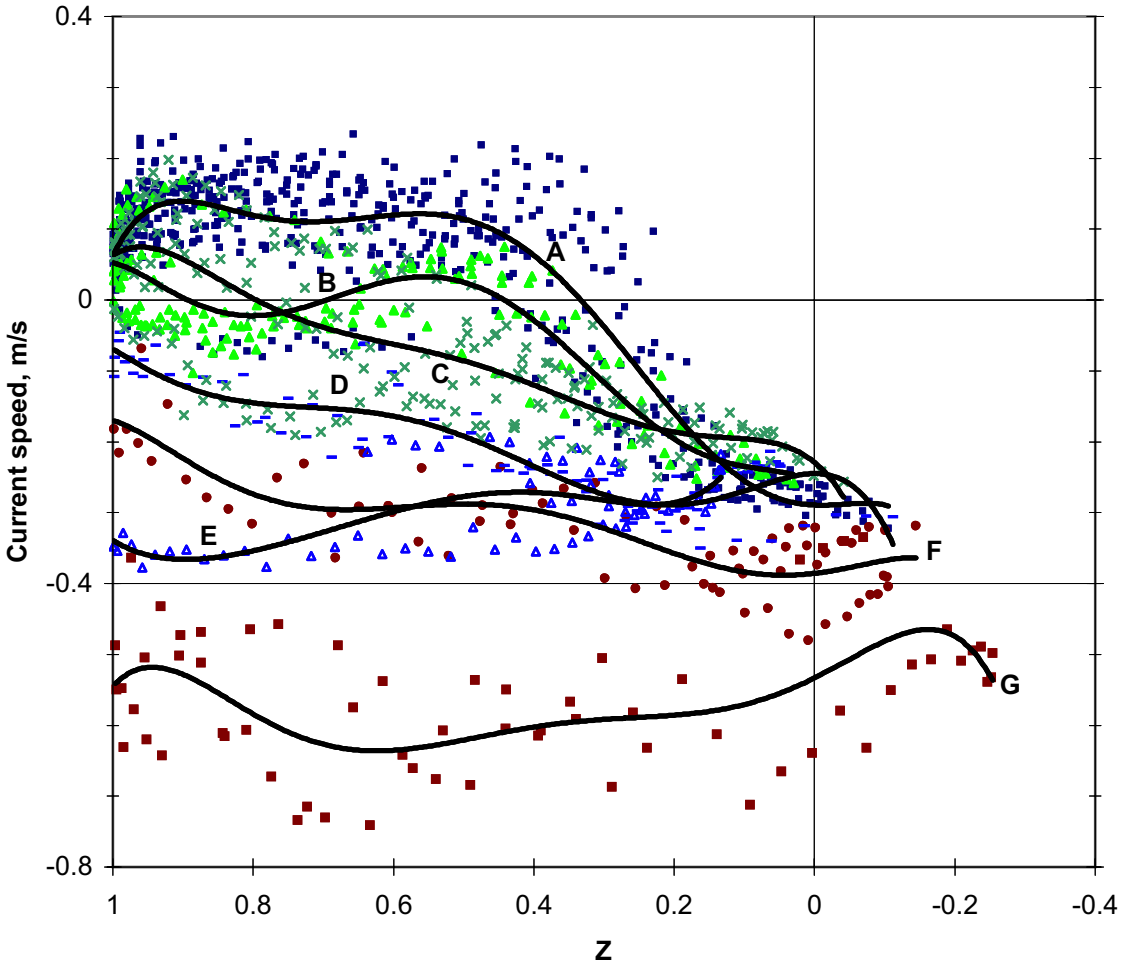

Figure 56. Northern Current meter, falling tide, all tidal ranges 17 March 1996 to 30 June 1996

Current speed vs Dimensionless water level, $Z = (z - z_b)/(z_H - z_b)$

A	W < 5 m/s	All wind directions	R >= 2.0 m;	H_{BP} and H_{Wis} < 0.5 m
B	W < 5 m/s	All wind directions	1.4 m <= R < 2.0 m;	H_{BP} and H_{Wis} < 0.5 m
C	W < 5 m/s	All wind directions	R < 1.4 m;	H_{BP} and H_{Wis} < 0.5 m
D	All W	$315^o <= \theta_W < 180^o$	1.4 m <= R < 2.0 m;	1.0 <= H_{BP} < 1.25 m; H_{Wis} < 1.25 m
E	All W	$315^o <= \theta_W < 180^o$	R < 1.4 m;	H_{BP} >= 1.0 m; H_{Wis} < 1.0 m
F	All W	$315^o <= \theta_W < 180^o$	1.4 m <= R < 2.0 m;	H_{BP} >= 1.5 m; all H_{Wis}
G	All W	$315^o <= \theta_W < 180^o$	R >= 2.0 m;	H_{BP} >= 2.0 m; all H_{Wis}

$\theta_c < 125^o$, positive $\theta_c >= 125^o$, negative Trendlines, 6^{th} order polynomials

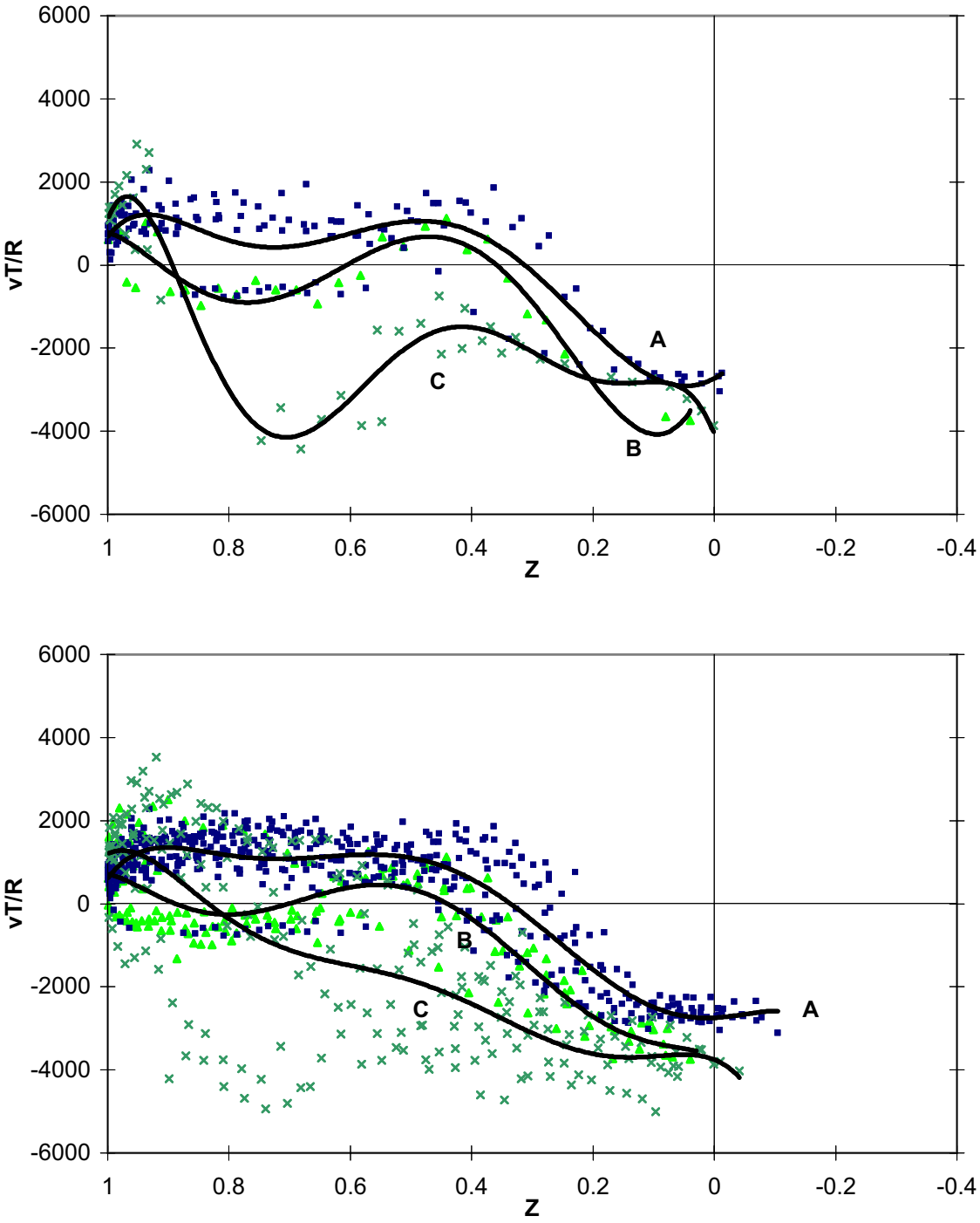

Figure 57. Northern Current meter, falling tide, W < 5 m/s
Dimensionless velocity, vT/R vs Dimensionless water level Z
$Z = (z_o - z_b)(z_H - z_b)$
17 March 1996 to 30 June 1996

Above	**H_{BP} and H_{Wis} < 0.35 m**
Below	**H_{BP} and H_{Wis} < 0.5 m**
A	R >= 2.0 m
B	1.4 m <= R < 2.0 m
C	R < 1.4 m

6.6 Summary

The current patterns that develop on the reef-top at Heron Island are the response to the complicated interaction of varying tides, winds and waves, modified by the reef-top topography.

Under mild conditions, when tidal flows dominate, the rising tide flows into the boat harbour, over the bund walls and onto the reef-flat. On the southern side of the island it flows in an eastsoutheastward direction. The speed of this eastsoutheastward current increases with increasing tidal range, attaining a maximum of 0.3 m/s when $Z \approx 0.2$, falling to *ca* 0.06 m/s when $Z \approx 0.6$ and rising again as $Z \rightarrow 1$. When the tide commences to fall, the current at the southern current meter site continues to flow in an eastsoutheastward direction until the tide level falls to 1.5 m, *i.e.* mean sea level, when it reverses and commences to flow northwestward over the bund wall into the boat harbour with increasing speed, attaining a maximum velocity as the ocean tide level z_0 approaches the bund wall level z_b.

On the northwestern side of the island, when tides are large ($R \geq 2.0$ m), the rising tide flows from the boat harbour over the northern bund wall onto the reef flat in a northeastward direction until z_o = 1.8 m or $Z \approx 0.5$. At this stage inflow from over the northern reef-rim reverses the current direction at the northern current meter site and flow there becomes southwestward towards the boat harbour. As the tidal range decreases this current reversal during the rising tide occurs at lower tide levels but higher values of Z, so that when $R < 1.4$ m, the current reverses when $z_0 = 1.55$ m or $Z = 0.7$ to 0.9. Maximum current speeds during the rising tide are *ca* 0.3 m/s for large tides and ≤ 0.2 m/s for small tides.

As high tide level is approached, the westsouthwestward current diminishes as the ocean tide begins to fall towards the east. Flow at the northern current meter reverses again to flow outwards, over the reef rim, in a northeastward direction, obtaining a maximum velocity of *ca.* 0.2 m/s for large R, this reversal at high tide generally occurs in an anticlockwise direction, although it may, particularly in the smaller tidal ranges, take place in a clockwise direction.

As the tide begins to fall some medium to large tides show a temporary reversal in flow southwestward towards the boat harbour before again flowing seawards over the northern reef-rim. Then as mean tide level, *ca.* 1.52 m, is approached, the tidal flow again reverses to southwestward direction as flow out through the boat harbour becomes dominant. The current reversal on the falling tide depends upon the tide level z_o. If $z_0 > 1.75$ m reversal occurs in a clockwise direction, whereas if $z_0 < 1.75$ m it is in an anticlockwise direction irrespective of tidal

range. All tides are flowing towards the boat harbour when $z_0 < 1.35$ m. The maximum velocity on this final phase of the falling tide as z_0 approaches z_b is 0.3 m/s

During mild conditions, current velocities over the tidal cycle can be represented nondimensionally by the parameter vT/R plotted against the nondimensional elevation Z referred to the bund wall crest. This representation is reasonable for rising tides with ranges $R \geq 1.4$ m but is not satisfactory for small tides ($R < 1.4$ m), many of which do not fall below the bund wall crest (Figures 17, 25, 42, 57). For the falling tide at both current meters the current direction changes at an approximately constant tide level, $z_o = 1.5$ m, and, since this value does not correspond with a constant value of Z for different tidal ranges, the representation by vT/R versus Z is poor. Furthermore, the presence of an extra current reversal, when $Z > 0.5$ in some medium to large falling tides at the northern current meter, is not accommodated by vT/R versus Z.

The tidal flow pattern on the reef-flat around Heron Island changes as wind speeds and/or wave heights increase. On the southern side of the island during the prevailing southeasterly weather and during the latter stages of the rising tide, the flow becomes more southward and, with increasing offshore wave height H_{Wis}, swings around clockwise to the northwestward direction, *i.e.* the currents generated by waves breaking on the reef-rim reverse the tidal currents. For small tides ($R < 1.4$ m) flow is reversed at all stages of the tide when $H_{Wis} > 0.75$ m; for medium tides ($1.4 \text{ m} \leq R < 2.0$ m), reversal occurs when $H_{Wis} > 1.0$ m; whereas for large tides ($R \geq 2.0$ m), H_{Wis} must be 1.25 m or larger to reverse the flow. During the rising tide on the southern side of the island wave-generated currents are a maximum when $0.5 < Z < 0.7$. For small tides ($R < 1.4$ m) and larger waves ($H_{Wis} > 1.5$ m) a maximum velocity of 0.3 to 0.4 m/s was recorded during the period under consideration. Large tides ($R \geq 2.0$ m) significantly reduce the northwestward wave-generated flow into the boat harbour, particularly when $Z < 0.2$ or > 0.8, even when offreef waves are between 1.35 and 1.5 m in height. During the falling tide, the tidal current at the southern current meter site is reversed by similar combinations of wave height and tidal range as during the rising tide. The strongest currents flowing into the boat harbour during falling tides with small ranges occur at about mid tide level, *i.e.* $z_0 = 1.5$ m, with slightly lower H_{Wis} than on the rising tide, *i.e.* $H_{Wis} > 1.25$ m, instead of $H_{Wis} > 1.5$ m.

When northeasterly wind/wave conditions occur, wave-generated flows modify the tidal flows on the northern reef-flat. Generally, continuous flow into the boat harbour occurs under the same threshold combinations of wave height and tidal range as on the southern reef-flat, *i.e.*

$R < 1.4$ m	and	$H_{BP} > 0.75$ m
$1.4 \leq R < 2.0$ m	and	$H_{BP} > 1.0$ m
2.0 m $\leq R$	and	$H_{BP} > 1.25$ m

On large rising tides, when $1.0 < H_{BP} < 1.5$ m, the flow is southwestward towards the boat harbour throughout the whole rising phase of the tide but the current speeds show the same pattern of variation as during mild conditions. The maximum current speed approaches 0.4 m/s when $z_0 \approx$ 2m. With larger values of H_{BP} (> 2.5 m), current speeds towards the boat harbour are between 0.5 and 0.6 m/s during the whole rising phase of the tide, suppressing the tidal currents.

On falling tides seaward flow over the northern reef-rim is reversed by breaking waves under similar H_{BP} and R combinations as previously. Southwestward flow towards the boat harbour always occurs when H_{BP} exceeds 1.0 to 1.25 m. When $H_{BP} > 2$ m the southwestward wave-generated flow has speeds varying inconsistently between 0.45 to 0.75 m/s. However, when winds are southwesterly and/or offreef waves breaking on the southern side of the reef are comparable in size to those breaking on the northern side of the reef, the critical value of H_{BP} required to completely reverse the northeastward flow over the northern reef-rim is increased. The data available from this period of analysis is insufficient to quantify this effect.

7. REEF-TOP CURRENTS 3 – 17 March 1996 to 18 March 1997

7.1 Introduction

It had been necessary to divide the twelve months data into three periods for processing since the amount of data was too large to be processed simultaneously on a desk-top computer. Detailed analyses were undertaken for the first period, 17 March to 30 June 1996, and the results of those have been reported in Chapter 6. All the data for the two following periods, 1 July to 31 October 1996 and 1 November 1996 to 18 March 1997, were plotted in the same initial way as for the first period. Subsequent analyses included

(i) an investigation of mild conditions, *i.e.* those where waves have a negligible influence upon reef-top currents (see Gourlay and Hacker 2008b); and

(ii) the relationship between wave-generated current velocity and offreef wave height (see section 7.4).

In this chapter the overall current data for the three periods is compared, taking account of the particular wind, wave and tidal conditions occurring during each period.

7.2 Wind, wave and tidal conditions

7.2.1 Wind climate

The hourly wind data (10 minute average) for both the whole twelve months 17 March 1996 to 18 March 1997 and the three analysis periods has been plotted on Figures 58 and 59. The percentage occurrence for each 10° increment of direction is given, together with the percentage occurrence of each 5 m/s increment in wind speed.

Overall the wind climate is bimodal with dominant eastsoutheasterly to southeasterly winds and less frequent and lighter northwesterly to northnorthwesterly winds (Figure 58a). Wind speeds during this period were most often between 5 and 10 m/s (Table 6). Strong winds (W ≥ 15m/s) only occurred for *ca* 0.4% of the time during four events (Table 7). Wind directions during these events were all different and it is clear that strong winds can come from any direction. The strongest 10 minute average wind speed recorded during the overall twelve month period was 18 m/s from 130° at 22:00 h on 9 March 1997 (T.C. "*Justin*").

Table 6 % occurrence of various wind speeds during analysis periods

Wind speed range m/s	% occurrence during specified period			
	17 Mar 1996 to 18 Mar 1997	17 Mar 1996 to 30 June 1996	1 Jul 1996 to 31 Oct 1996	1 Nov 1996 to 18 Mar 1997
$W < 5$	28.6	33.2	32.6	21.4
$5 \leq W < 10$	52.5	43.4	50.9	60.9
$10 \leq W < 15$	11.6	11.6	10.4	12.7
$W \geq 15$	0.39	0.08	0.07	0.93
Missing observations	6.9	11.7	6.0	4.1

Table 7 Occurrence of strong winds (≥ 15 m/s) at Heron Island 17 March 1996 to 18 March 1997

Date	Maximum Wind Speed m/s	Wind Direction degrees
1 May 1996 (twice)	16.5	40
21 Sep 1996	16.0	270
30 Sep 1996	15.4	350
T.C. *"Justin"* 7-11 Mar 1997 (several occasions)	18.0	130

The wind climate shows a distinct seasonal pattern. During the period 17 March to 30 June 1996 (Figure 58b), the winds were dominantly eastsoutheasterly to southsoutheasterly ($110° \leq \theta_w < 170°$) for approximately 45% of the time with relatively low percentages from most other directions. Generally the stronger winds were southsoutheasterly ($150° \leq \theta_w < 170°$) but the strongest winds (W = 16.5 m/s) recorded during this period were associated with a northeasterly storm on 1 May (Table 7).

In contrast, winds during the period, 1 July to 31 October 1996 (Figure 59a), were much more uniformly distributed in direction and, while eastsoutheasterly to southsoutheasterly winds were still significant, so also were northwesterly to northnorthwesterly winds. The most significant storm occurred on 27 July with eastnortheasterly winds almost reaching 15 m/s.

During the last period, 1 November 1996 to 18 March 1997 (Figure 59b), the pattern changed to one of generally greater concentration with 96% of winds coming from the northnorthwesterly to southsouthwesterly sector ($320° \leq \theta_w < 170°$). The dominant winds came from the eastsoutheasterly to southeasterly direction with an increased frequency of slight to moderate winds from the northeasterly sector and a minor peak of northnorthwesterly winds. Southerly to northwesterly winds were almost completely absent. Strongest winds were 15 to 18 m/s southeasterly on 9 March 1997 when Tropical Cyclone "*Justin*" was in the northern Coral Sea.

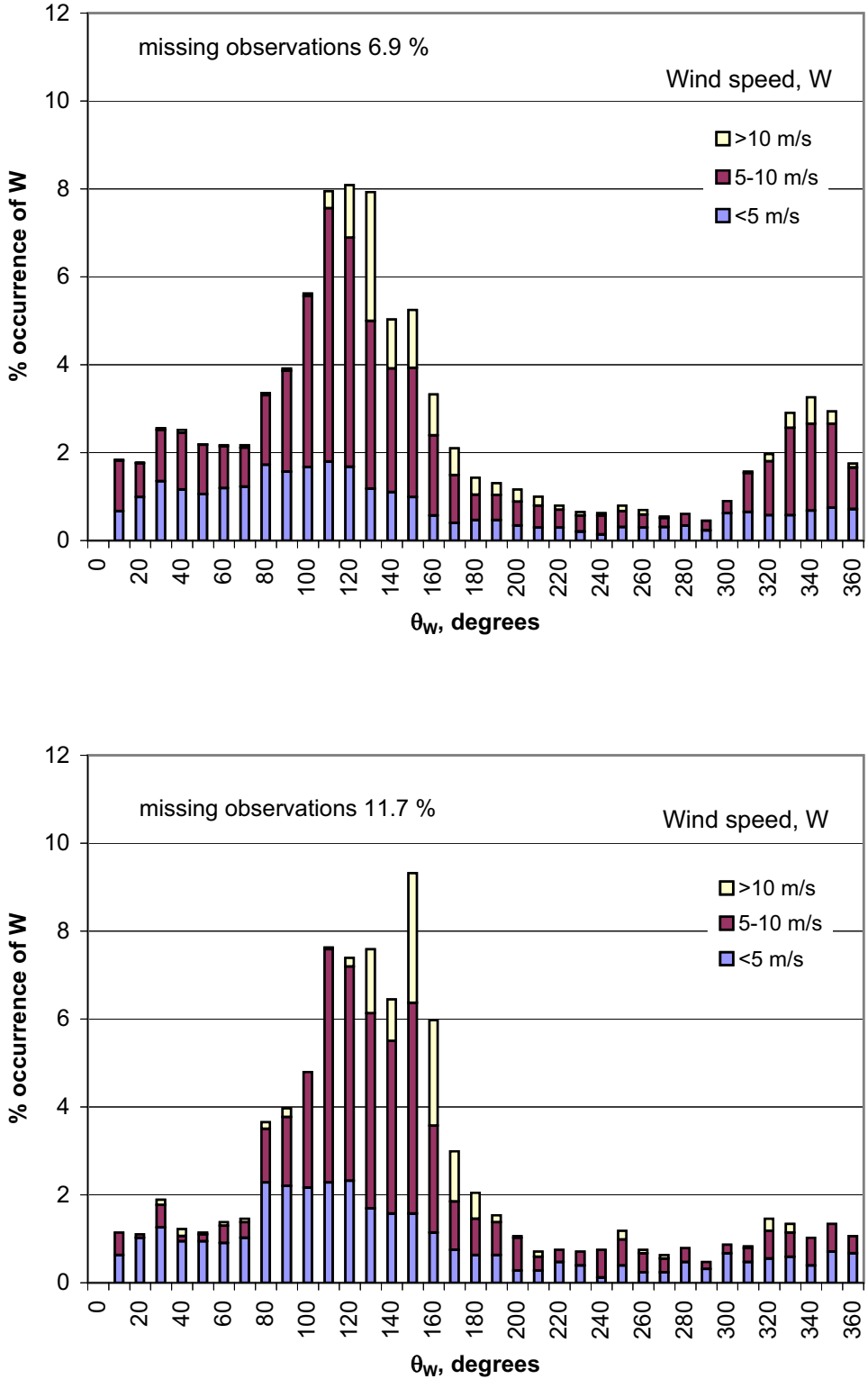

Figure 58. **Wind climate at Heron Island**
% occurrence of W for θ_W at Heron Island
Above 17 March 1996 to 18 March 1997
Below 17 March to 30 June 1996

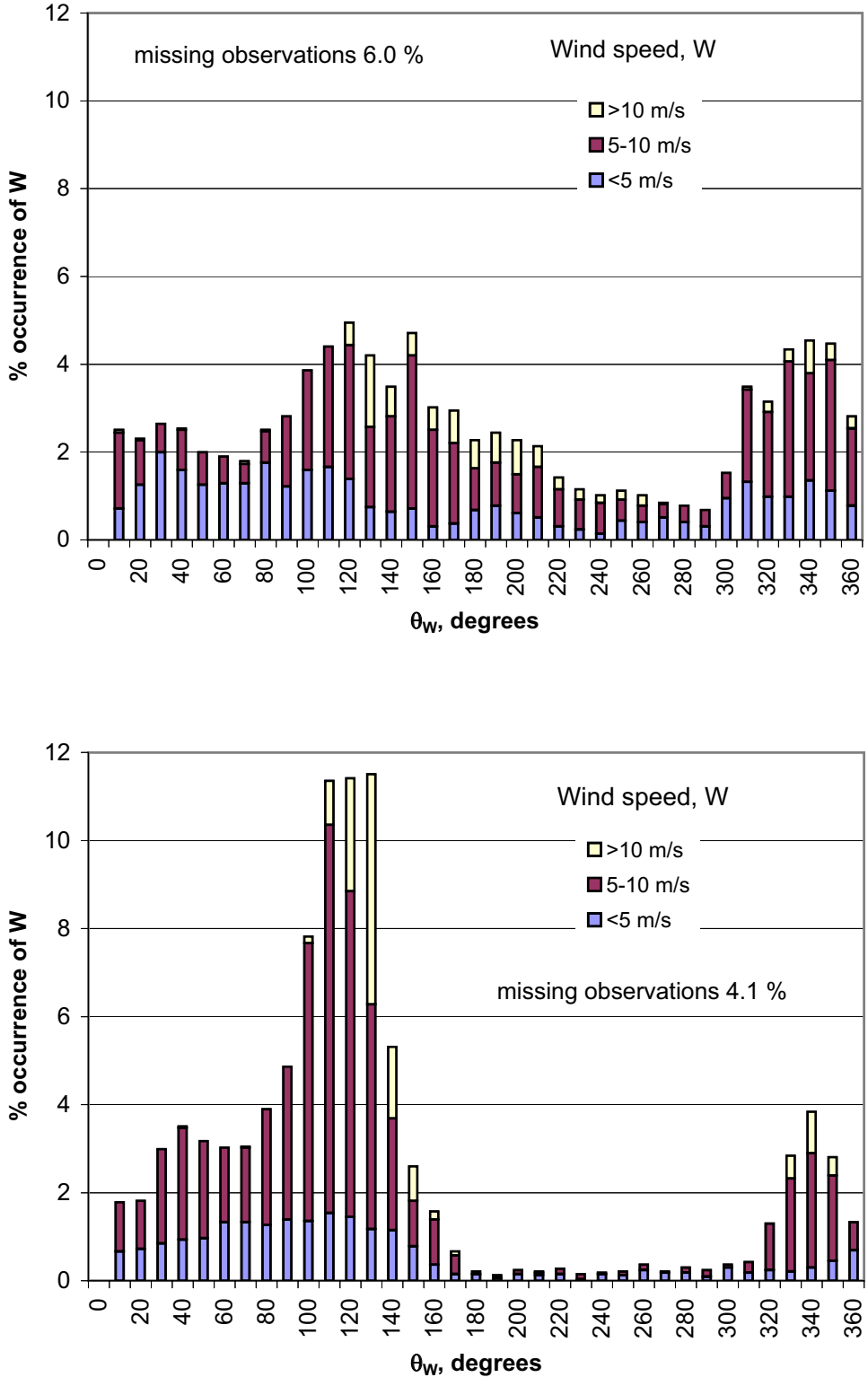

Figure 59. **Wind climate at Heron Island**
% occurrence of W for θ_W at Heron Island
Above **1 July to 31 October 1996**
Below **1 November 1996 to 18 March 1997**

7.2.2 Wave climate

The variations in wave conditions are most conveniently represented by scatter diagrams in which wave height H_s is plotted against wave period T_p for each recording site for a particular period (Figures 60 to 63). The $H_s - T_p$ diagrams show a common pattern with two different populations of waves, equivalent to sea and swell conditions. Seas are waves generated directly by the local winds seaward of the recording site. In deep water, seas are limited in height by the maximum stable wave steepness, *i.e.* ratio of wave height to wave length. Since the deep water wave length is proportional to the square of the wave period, H_s is proportional to T_p^2. This can be seen to be true for the sea populations in Figures 60 to 63.

T_p represents the wave period within the sea which has the most energy. The energy density spectrum provides a more complete representation of recorded wave conditions. Typical spectra for sea have a single relatively broad peak. The swell population shown on the scatter diagrams is represented by a band of waves generally with a relatively low wave heights (< 1 m) and variable periods ($5 < T_p < 18$ s). Swell represents waves which were generated by winds occurring further seaward (often much further seaward) and which have travelled freely across the ocean beyond the zone of generation to the recording site. During this propagation phase, long waves travel faster than short waves and so the spectra of swell are narrower and their T_p values are larger than those of sea. In some cases the local wind generates a sea on top of a swell. This gives rise to double peaked spectra with two values of T_p. Such waves generally appear on the scatter diagrams between the other two populations, with T_p values larger than those for sea and H_s values larger than those for normal swells.

Offreef waves recorded on the southern side of the reef by the Wistari wave rider buoy, show distinctive sea and swell conditions with some mixed sea and swell conditions Figure 60a. The largest significant sea waves recorded are just under 3 m and the longest swell waves just under 15.5 s. Generally the upper bound for seas is $H_{Wis} \approx T_p^2/20$.

During the period 17 March to 30 June 1996 (Figure 61a), the largest seas recorded at Wistari were 2.2 m high and the longest swells were about 13.5 s with heights less than 0.8 m, although the majority of swells were less than 0.5 m. Under calm conditions swells were less than 0.2 m in height. There were some mixed sea/swell conditions with $H_{Wis} \leq 2$ m and $T_p \leq 10.8$ s.

The period between 1 July to 31 October had a greater proportion of swell conditions with lower and longer swell waves and fewer mixed sea/swell conditions (Figure 62a). The following period,

1 November 1996 to 18 March 1997, was much more energetic. Maximum sea waves (H_s) almost reached 3 m and mixed sea/swell conditions were more prevalent (Figure 63a).

In contrast to Wistari on the southern side of Heron Reef, the Blue Pools wave rider buoy on the northern side of the reef recorded fewer seas and more mixed sea/swell conditions (Figure 60b). This is particularly the case for the first and last periods (Figures 61b and 63b). However, the largest waves during the twelve month period of observations were recorded at the Blue Pools site with $H_{BP} \geq 3$ m occurring in both the first and second periods. These are mostly mixed sea/swell situations with with $T_p \approx 10$ s. The longest swells, $T_p \approx 18$ s, also occurred at Blue Pools, generally between 1 July and 31 October 1996. (Figure 62b).

The wave climate conditions at the two sites during the three periods are consistent with both the wind climate and their geographical locations. The Wistari recording site is on the windward side of the reef exposed to the dominant eastsoutheasterly to southeasterly winds. Hence seas are relatively frequent. However, during the second period, 1 July to 31 October 1996, (Figure 62a) long low swells occurred often, which is consistent with the decreased frequency and strength of winds from the southeasterly sector and the increased frequency of opposing winds from the northwesterly sector during that time of year (Figure 59a). The Blue Pools recorder site is on the leeward side of the reef and therefore waves generated by the dominant southeasterly conditions reach this site after refraction and diffraction around the northeastern corner of Heron Reef. During this process, the longer period spectral components are refracted and diffracted to a greater degree than the shorter components, giving longer wavelengths, as well as reduced wave heights, off the northern side of the reef. So by the time the waves reach the recorder site they have the characteristics of swell, although in many cases their heights are still quite large. During the first period, 17 March to 30 June 1996, (Figure 61b) few seas were recorded at Blue Pools and this is consistent with the low frequency of occurrence of winds from the westerly to northeasterly directions during this period. However, during the second period, 1 July to 31 October 1996 (Figure 62b), low seas and long low swells at Blue Pools were more frequent than during the overall period, consistent with greater frequency of occurrence of northwesterly winds.

Overall, the wave conditions reflect the dominant southeasterly wind conditions which result in seas breaking more frequently on the southern side of the reef and swells, being recorded more frequently on the northern side of the reef. Wave conditions during the period from 17 March to 30 June 1996 (Figure 61) are generally more representative of overall conditions at both sites (Figure 60) than the two subsequent periods (Figures 62 & 63).

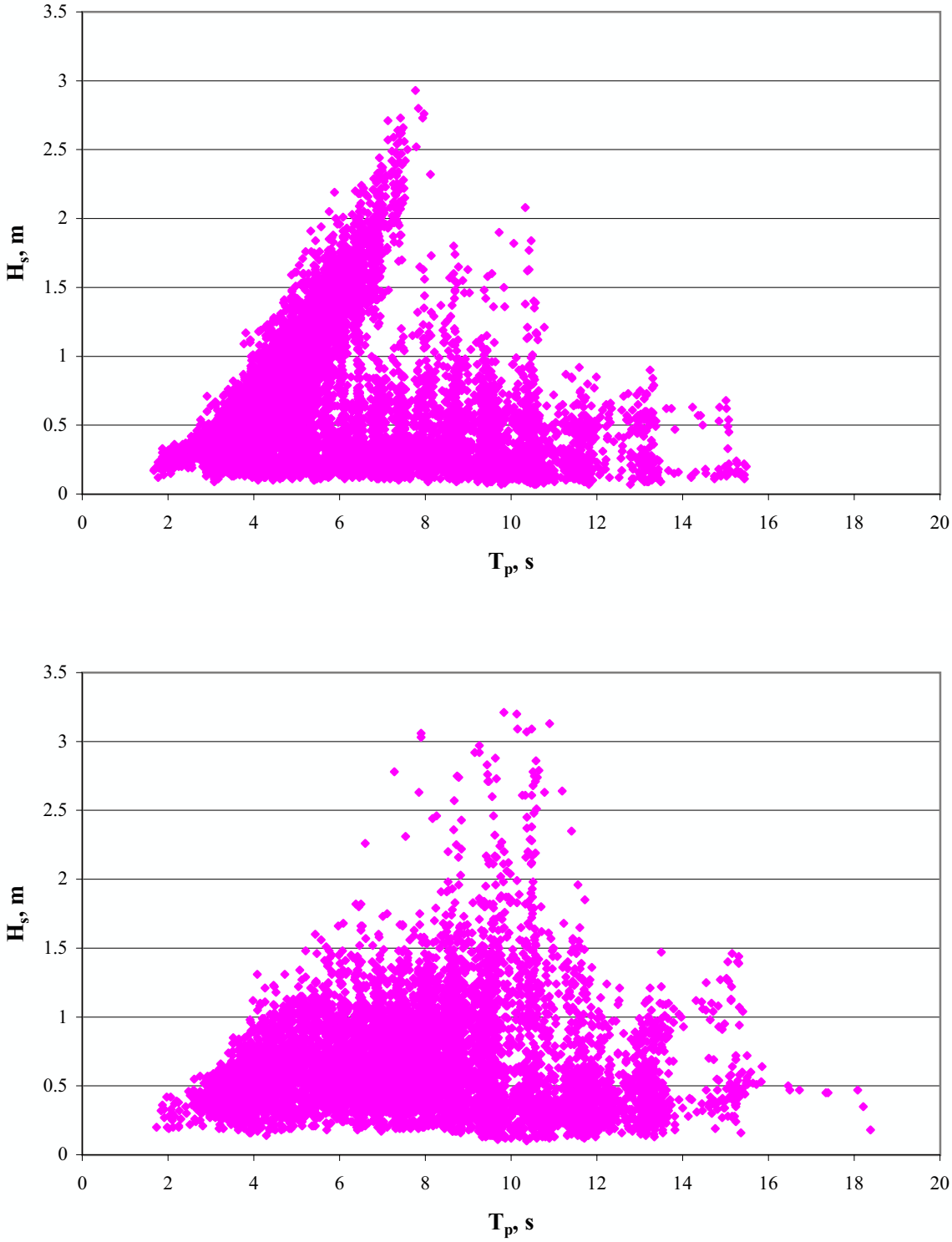

Figure 60. **Wave climate at Heron Island, H_s *vs* T_p**
17 March 1996 to 18 March 1997
Above **Wistari wave rider buoy**
Below **Blue Pools wave rider buoy**

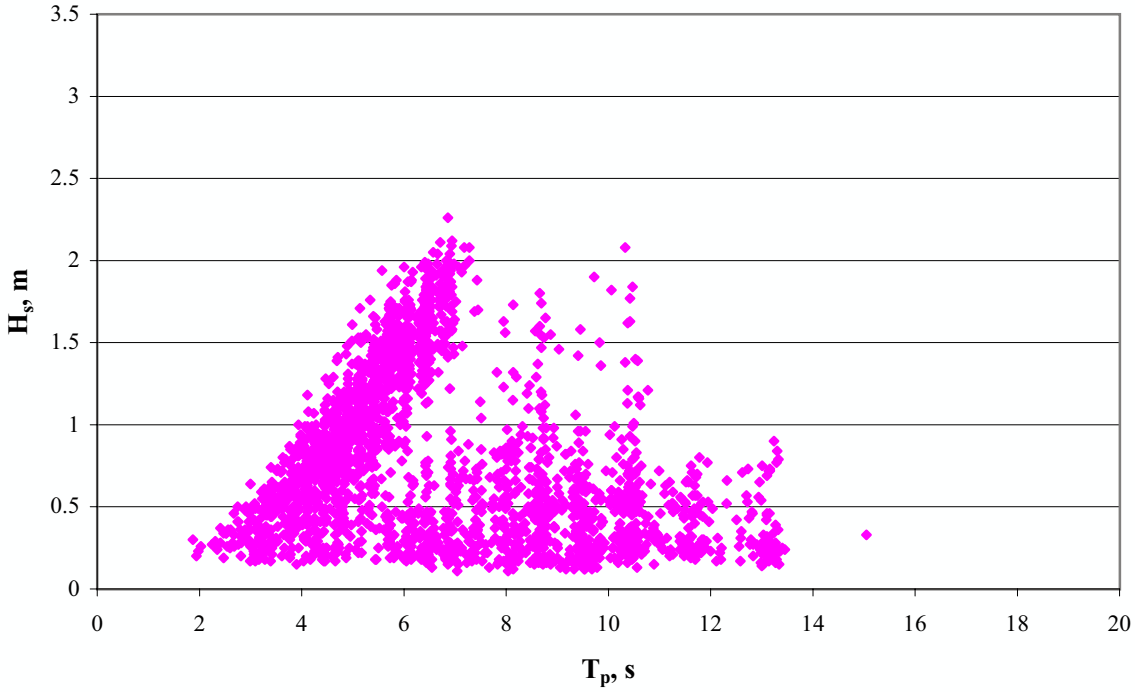

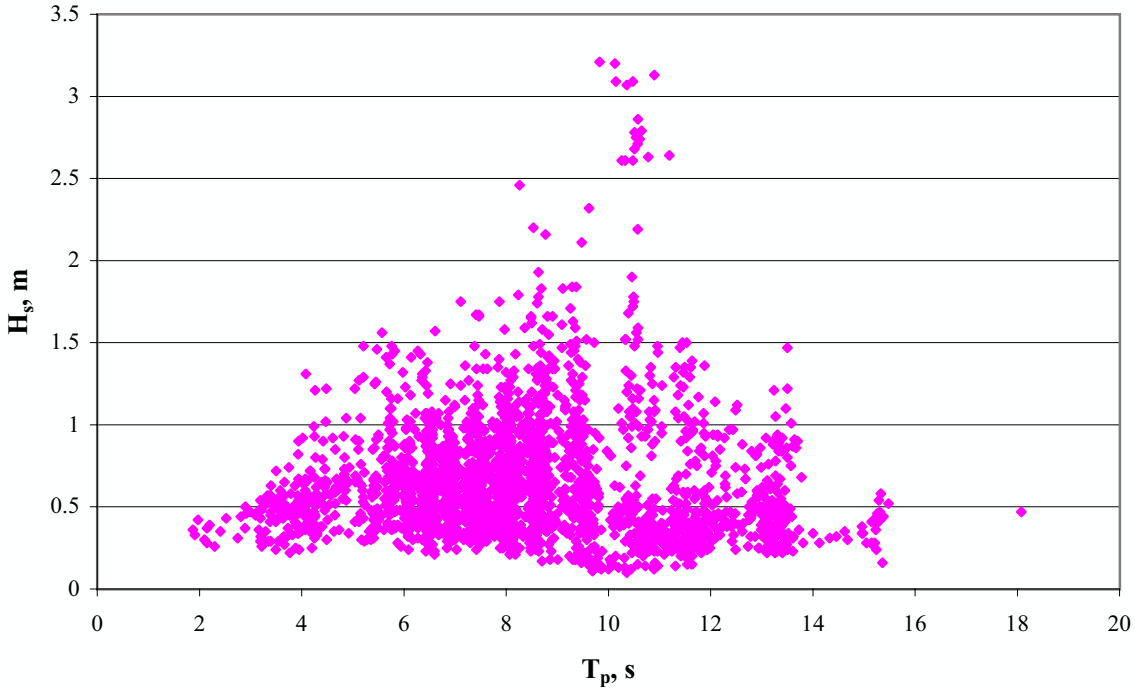

Figure 61. **Wave climate at Heron Island, H_s *vs* T_p**
17 March 1996 to 30 June 1996
Above **Wistari wave rider buoy**
Below **Blue Pools wave rider buoy**

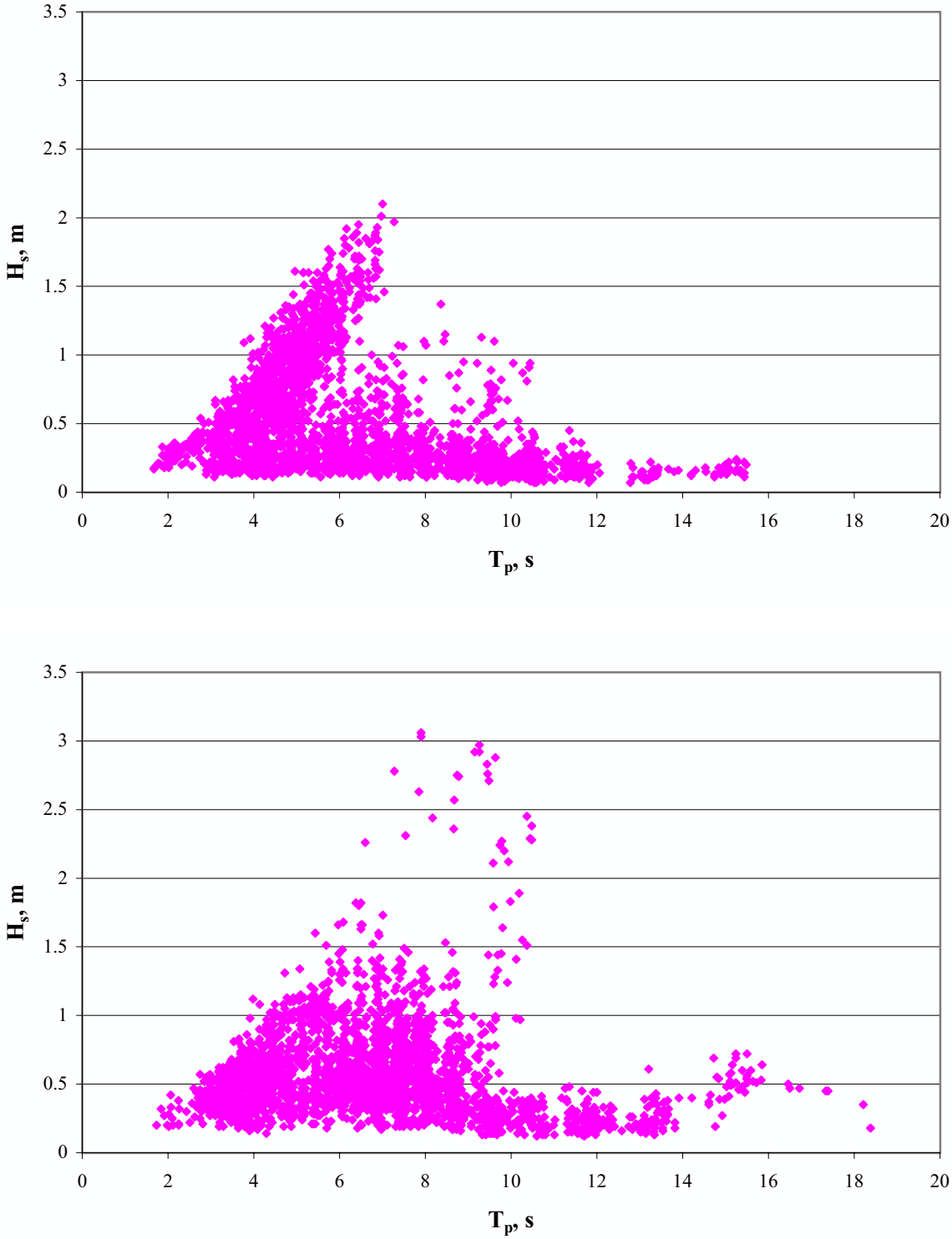

Figure 62. **Wave climate at Heron Island, H_s *vs* T_p**
1 July 1996 to 31 October 1996
Above **Wistari wave rider buoy**
Below **Blue Pools wave rider buoy**

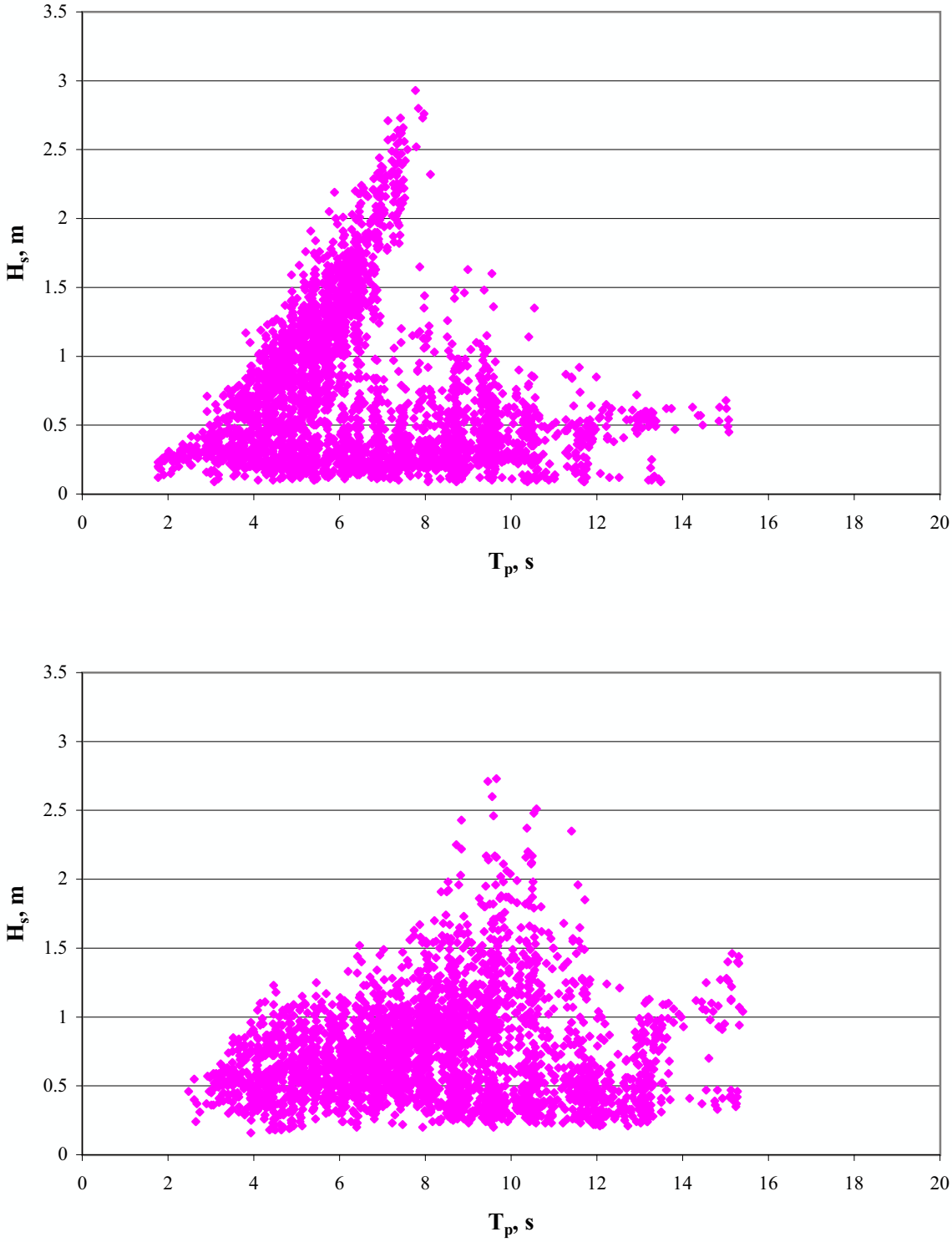

Figure 63. **Wave climate at Heron Island, H_s *vs* T_p**
1 November 1996 to 18 March 1997
Above **Wistari wave rider buoy**
Below **Blue Pools wave rider buoy**

7.2.3 Tidal range variation

The relative number of tides within a given 0.2 m increment of tidal range has been plotted in Figures 64 and 65. Rising and falling tides are indicated separately. There is considerable variation in the frequencies of occurrence of different tidal ranges during the three periods compared with their overall frequencies.

Overall; during the twelve month period, the most frequently occurring rising tides had ranges between 1.5 and 1.7 m (Figure 64a). Falling tides had a more uneven distribution with the most frequently occurring range being 2.1 to 2.3 m. For both rising and falling tides the largest ranges were < 3.3 m and the smallest > 0.5 m.

During the first period, 17 March to 30 June 1996 (Figure 64b), the most frequently occurring rising tides were between 1.9 and 2.1 m, *i.e.* larger than during the overall period, and the most frequently occurring falling tides were between 2.1 and 2.3 m. There were no tides between 3.1 and 3.3 m and the number of tides larger than 2.7 m was less than the overall proportion. During the second period, 1 July to 31 October 1996 (Figure 65a), the distribution of tidal ranges was more uniform with the proportion of both rising and falling tides in each increment between $1.3 < R < 2.3$ m being on average about 11 to 12% of the total number of tides. Tides above 2.7 m were generally more frequent during this period compared with the overall proportion.

Tidal range frequencies of occurrence during the third period, 1 November 1996 to 18 March 1997 (Figure 65b), were generally closer to the overall pattern than those during the two earlier periods. The most frequent rising tides had ranges between 1.5 and 1.7 m and the most frequent falling tides were between 2.1 and 2.3 m. There was greater variability between the frequencies of occurrence of tides in each tidal range increment compared with the overall distribution. The lowest rising tides were > 0.7 m.

During the three periods studied, there were variations in the proportion of tides occurring within each of the tidal range groups used in the analyses described in Chapter 6 (Table 8).

It can be seen that overall 26% of tides fell within the small tidal range group ($R < 1.4$ m). These tides generally are unlikely to expose the bund wall for significant periods of time. The remaining 64% of the tides were almost equally divided into the medium ($1.4 \leq R < 2.0$ m) and large ($R \geq 2.0$ m) tidal range groups. Considering the three periods, small tides only varied by a maximum of *ca* ± 1% from the overall percentage. Medium tides varied up to *ca* ± 2 to 3% and large ones

up to *ca* ± 3 to 4%. The first period had more medium rising tides, less medium falling tides, and more large falling tides; the second period had fewer medium rising tides and more large rising tides, while its falling tides generally were close to the overall percentage; and the third period had more small and medium tides and fewer large tides than overall.

The question of tidal asymmetry and its influence upon the tidal currents on Heron Reef is considered in the second report (Gourlay and Hacker 2008b, section 2.3).

Table 8 Change in percentage of tides within each tidal range group during each analysis period (Total number of tides is 706)

Period	Phase of tide	Tidal range group		
		R < 1.4m	**1.4 ≤ R < 2.0**	**R ≥ 2.0**
Overall 17 Mar 1996 to 18 Mar1997	Rising	25.9%	37.0%	37.1%
	Falling	25.5%	36.3%	38.2%
17 Mar 1996 to 30 Jun 1996	Rising	-0.3%	+1.4%	-1.1%
	Falling	-0.4%	-1.8%	+2.2%
1 Jul 1996 to 31 Oct 1996	Rising	-1.1%	-3.4%	+4.5%
	Falling	-1.1%	+0.3%	+0.9%
1 Nov 1996 to 18 Mar 1997	Rising	+1.3%	+1.9%	-3.1%
	Falling	+1.3%	+1.1%	-2.4%

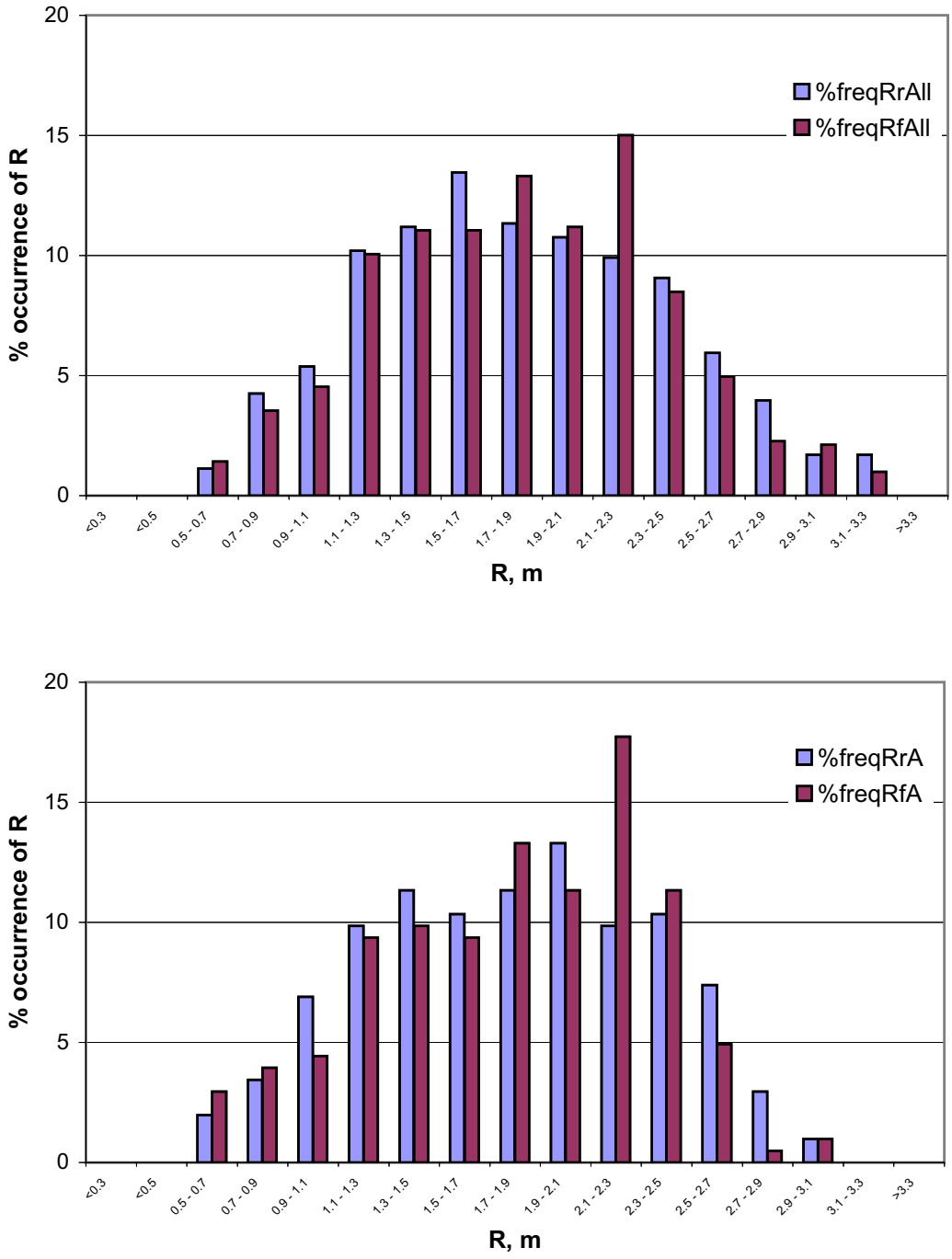

Figure 64. **Predicted tidal ranges at Heron Island**
% occurrence of R_r and R_f at Heron Island
Above 17 March 1996 to 18 March 1997
Below 17 March to 30 June 1996

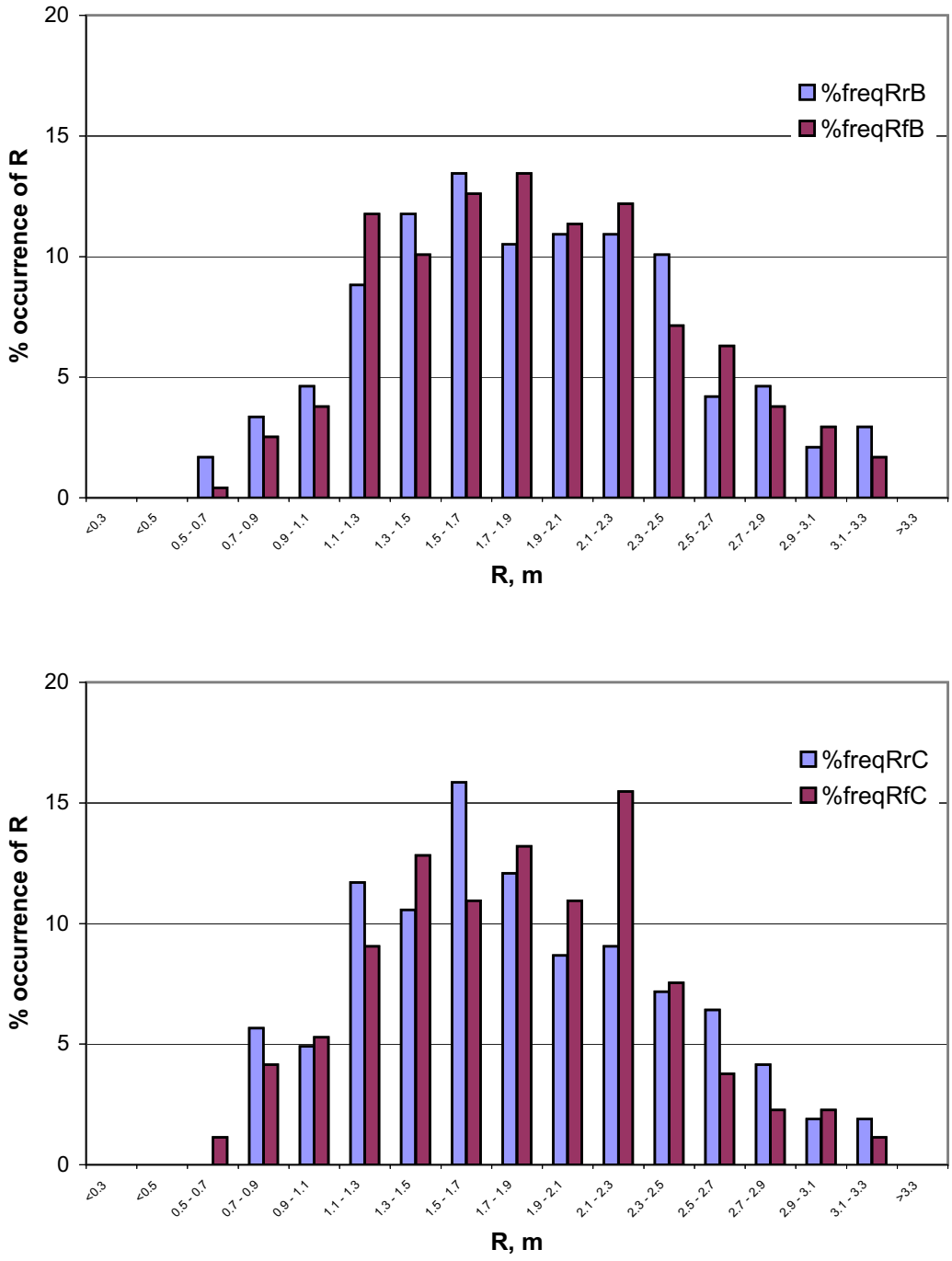

Figure 65. **Predicted tidal ranges at Heron Island**
% occurrence of R_r and R_f at Heron Island
Above **1 July to 31 October 1996**
Below **1 November 1996 to 18 March 1997**

7.2.4 Overall conditions

During the twelve month period of observations winds varied seasonally giving a characteristic bimodal distribution. Southeasterly winds dominated between 17 March to 30 June 1996 (*ca* 45%), and also between 1 November 1996 to 18 March 1997. During the latter period there were few occurrences of southerly to northwesterly winds. During the period 1 July to 31 October 1996 southeasterly winds were less frequent than during the other two periods and there were significantly more northwesterly winds.

The greater proportion of winds (52.5%) were between 5 and 10 m/s. Strong winds (>15 m/s) occurred during four events, totalling *ca* 0.4% of the time. These storm events were not always from the dominant southeasterly direction.

The wave climate included sea and swell as well as mixed sea and swell conditions. Offreef waves on the southern side of the reef (H_{Wis}) generally were dominated by seas generated by the southeasterly winds. In contrast offreef waves on the northern side of the reef (H_{BP}) were generally swell dominant or mixed sea and swell. This is a consequence of this site being sheltered from the dominant southeasterly conditions. The increased occurrence of swells between 1 July and 31 October 1996 is associated with a greater frequency of northwesterly winds during this period. Wave conditions during the period 17 March to 30 June 1996 generally are closest to the overall conditions.

During the twelve month period the percentage of small tides ($R < 1.4$ m) was 26% and those of medium ($1.4 \text{ m} \leq R < 2.0$ m) and large ($R \geq 2.0$ m) tides were both about 37%. During each of the three analysis periods the tidal range groups varied from their overall percentages by ± 1% for small tides; ± 2 to 3% for medium tides and ± 3 to 4% for large tides. The tides in each range group varied least between 17 March and 30 June 1996.

Hence, while there are significant seasonal variations in wind, wave and tidal conditions, the period 17 March to 30 June 1996 for which the detailed analyses were made is generally closer to overall conditions than the following two periods.

7.3 Reef-top currents

7.3.1 Southern current meter, rising tide

The plots of current directions θ_c and current speed v verses z_o for all data in each of the three tidal range groups have been compared for the three analysis periods. Similar data has been previously presented for the period 17 March to 30 June 1996 in Figures 7, 10 and 13 and is shown in Figures 66, 67 and 68 for the period 1 July to 31 October 1996 and in Figures 69, 70 and 71 for the period 1 November 1996 to 18 March 1997. The percentages of positive and negative currents in each tidal range group during each analysis period are given in Table 9.

Considering the large tides ($R \geq 2.0$ m), fewer negative currents and lower current speeds ($v \leq 0.25$ m/s) occurred between 17 March and 31 October 1996 (Figures 7 and 66) than between 1 November 1996 and 18 March 1997 (Figure 69) (see also Table 9). During the latter period stronger negative currents $v \leq 0.4$ m/s were recorded and there were more anticlockwise current reversals. These differences are consistent with the larger waves recorded on the southern side of the reef during the period between 1 November 1996 and 18 March 1997 (Figures 61a, 62a and 63a). These differences are not so clear with medium tides ($1.4 \text{ m} \leq R < 2.0$ m). For the total period, there was a greater proportion of negative velocities for small tides ($R < 1.4$ m) (Table 9) which is consistent with the relatively larger influence of waves in reversing the direction of flow of small tides. For small tides, the largest negative velocities during the period 17 March to 30 June 1996 were ≤ 0.35 m/s (Figure 13); during the period 1 November 1996 to 18 March 1997 they were ≤ 0.3m/s (Figure 71) and between 1 July and 30 November 1996 they were ≤ 0.25 m/s (Figure 68). These maximum velocities apparently increase with an increasing frequency of occurrence of southeasterly winds or conversely decrease with an increasing frequency of northwesterly winds.

Table 9 % positive and % negative currents in each tidal range group during each analysis period - southern current meter – rising tide – all data

Period	Direction θ_c *	Tidal range group			
		Large R ≥ 2.0 m	Medium 2.0 > R ≥ 1.4 m	Small R < 1.4 m	All
Overall 17 Mar. 1996 to 18 Mar. 1997	+ve	72.8	63.5	51.5	63.1
	-ve	27.2	36.5	48.5	36.9
1 17 Mar. 1996 to 30 Jun. 1996	+ve	79.7	51.5	39.4	56.6
	-ve	20.3	48.5	60.6	43.4
2 1 Jul. 1996 to 31 Oct. 1996	+ve	82.8	74.0	60.7	73.3
	-ve	17.2	26.0	39.3	26.7
3 1 Nov. 1996 to 18 Mar. 1997	+ve	58.8	64.9	53.2	59.5
	-ve	41.2	35.1	46.8	40.5

* $\theta_c < 225°$ is +ve ; $\theta_c \geq 225°$ is –ve.

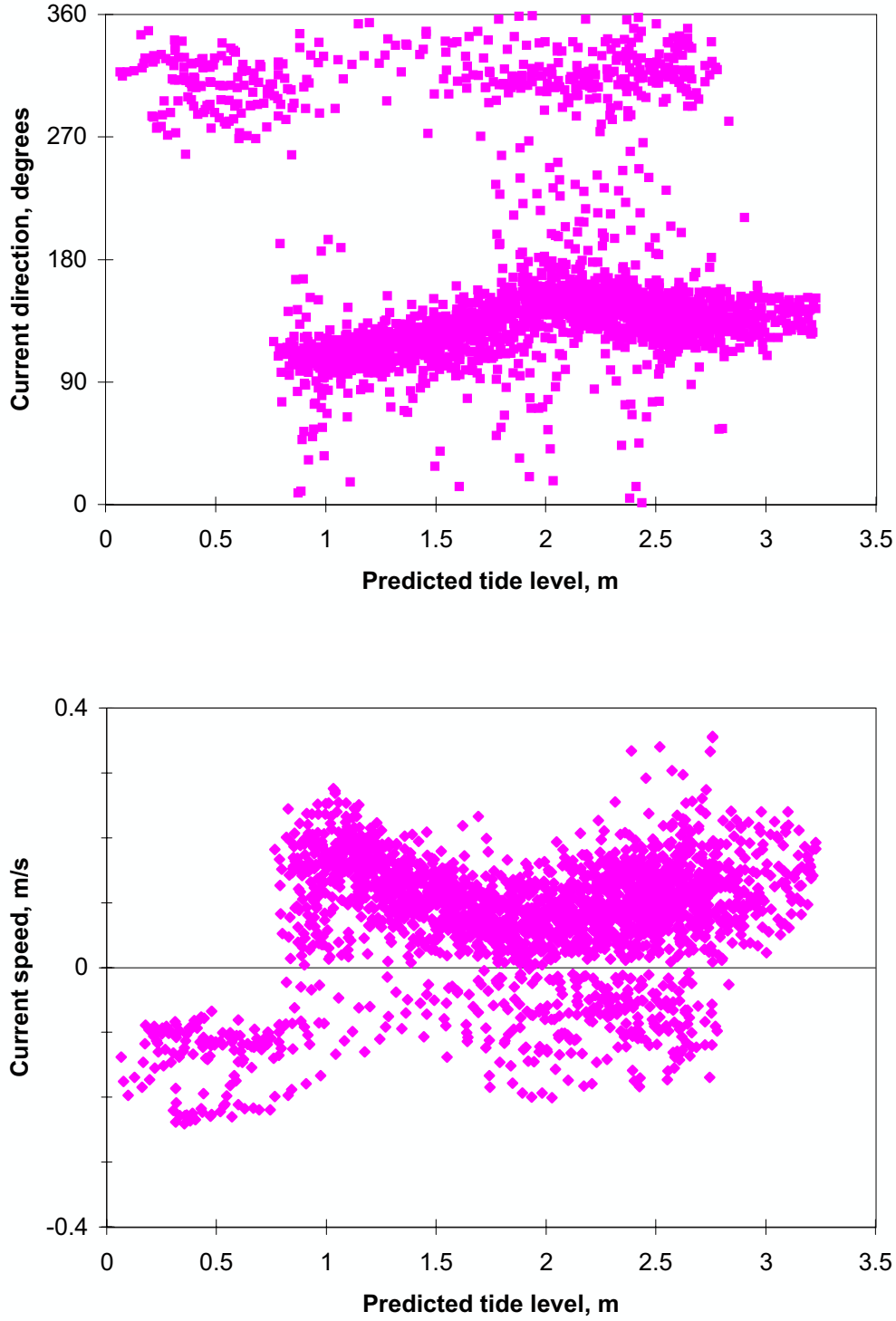

Figure 66. Southern current meter, rising tide, R >= 2.0 m
1 July 1996 to 31 October 1996

Above: **Current direction *vs* predicted tide level; all data**

Below: **Current speed *vs* predicted tide level; all data**

θ_c < 225°, positive θ_c >= 225°, negative

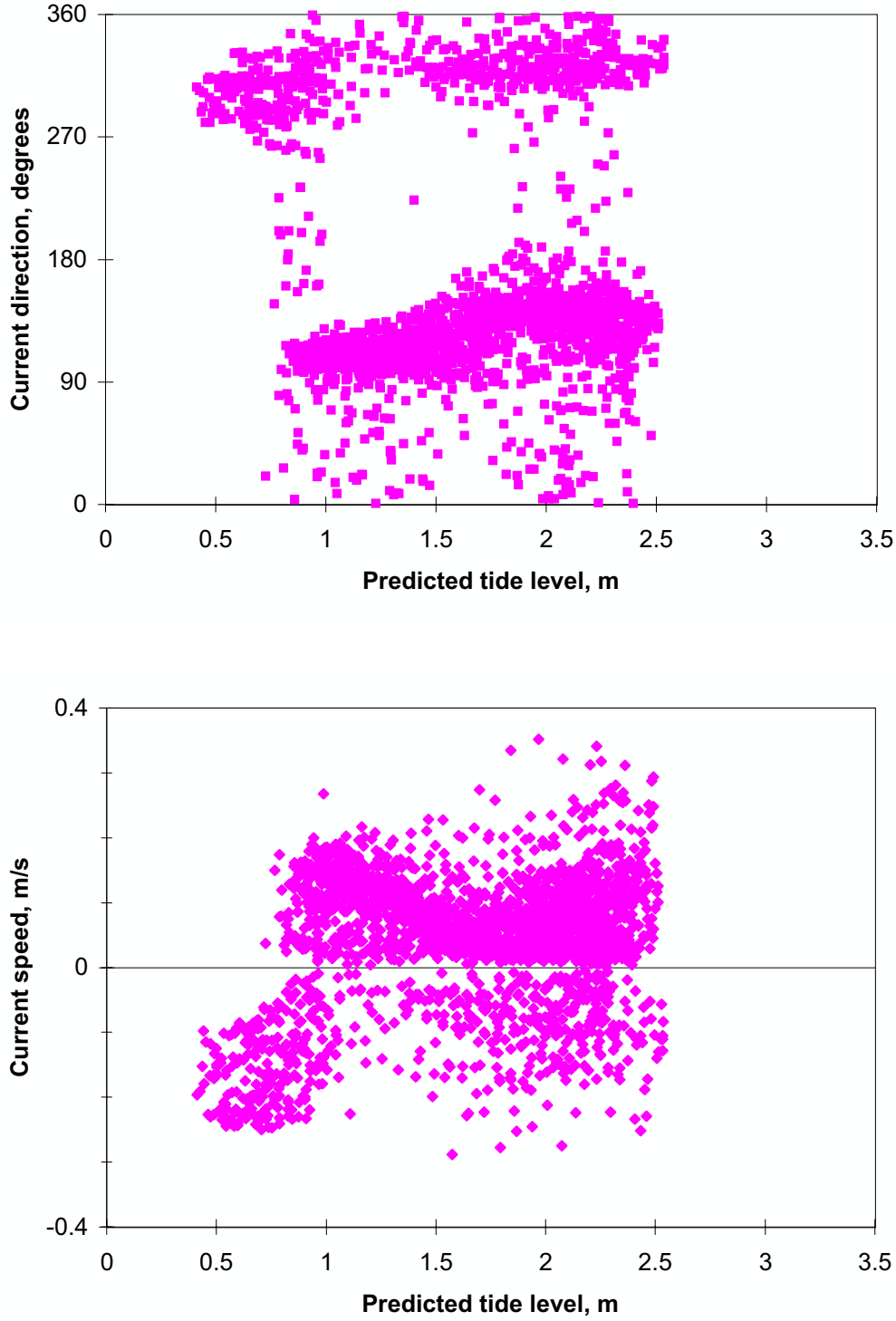

Figure 67. Southern current meter, rising tide, 1.4 m <= R < 2.0 m 1 July 1996 to 31 October 1996

Above: **Current direction *vs* predicted tide level; all data**

Below: **Current speed *vs* predicted tide level; all data**

$\theta_c < 225^o$, positive $\theta_c >= 225^o$, negative

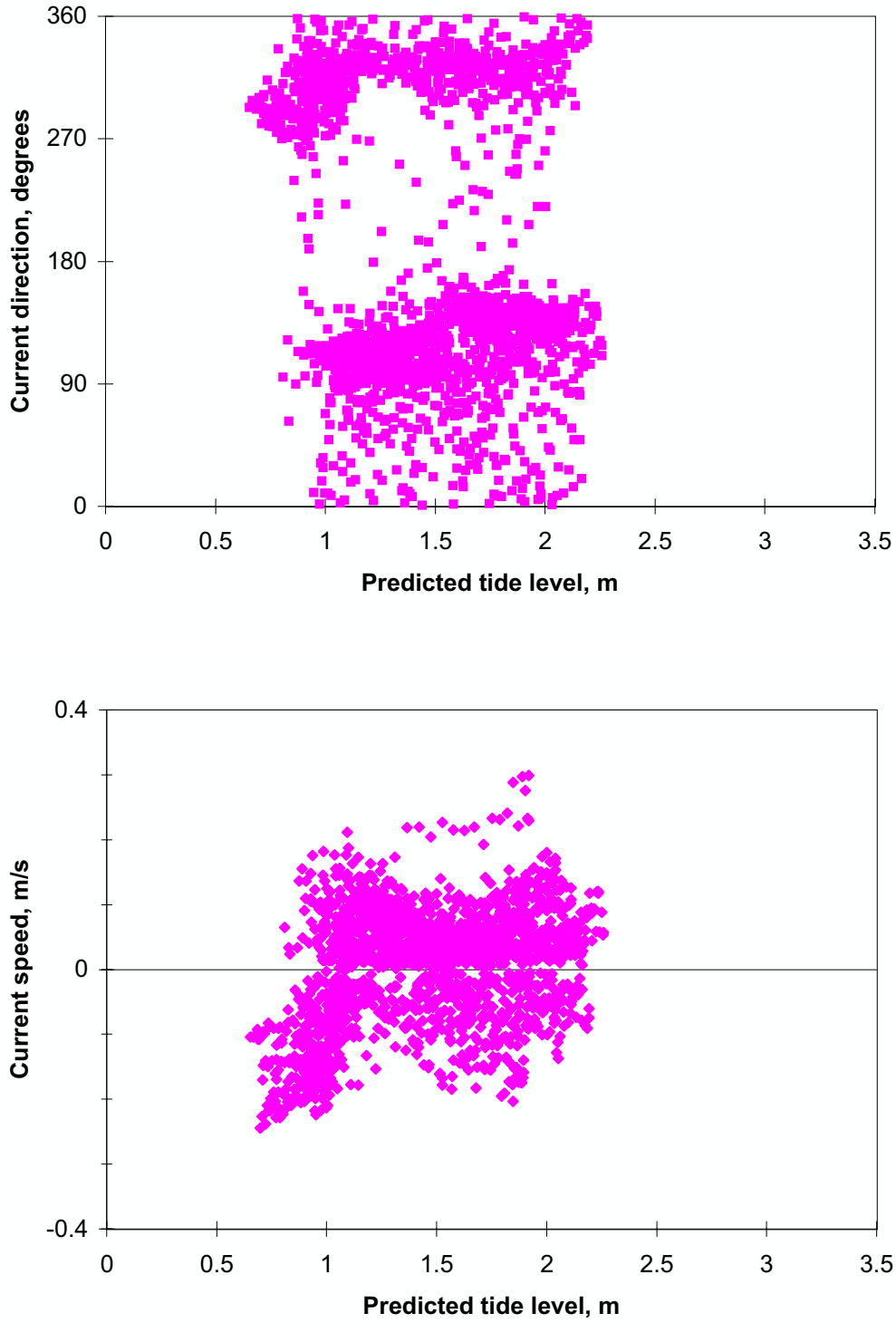

Figure 68. Southern current meter, rising tide, R < 1.4 m
1 July 1996 to 31 October 1996

Above: Current direction *vs* predicted tide level; all data

Below: Current speed *vs* predicted tide level; all data

$\theta_c < 225^o$, positive $\theta_c >= 225^o$, negative

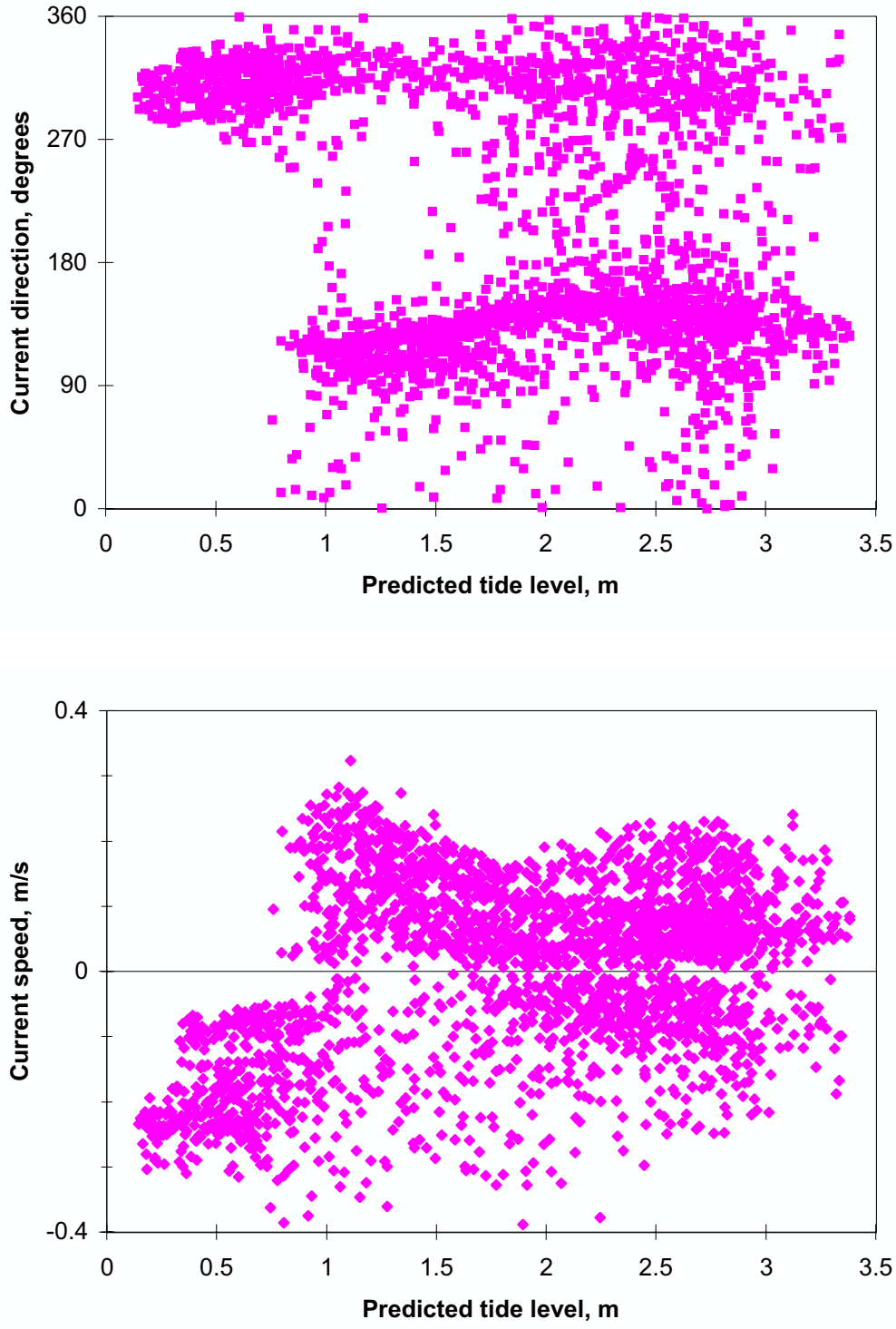

Figure 69. Southern current meter, rising tide, R >= 2.0 m
1 November 1996 to 18 March 1997

Above: **Current direction *vs* predicted tide level; all data**

Below: **Current speed *vs* predicted tide level; all data**

$\theta_c < 225^o$, positive $\theta_c >= 225^o$, negative

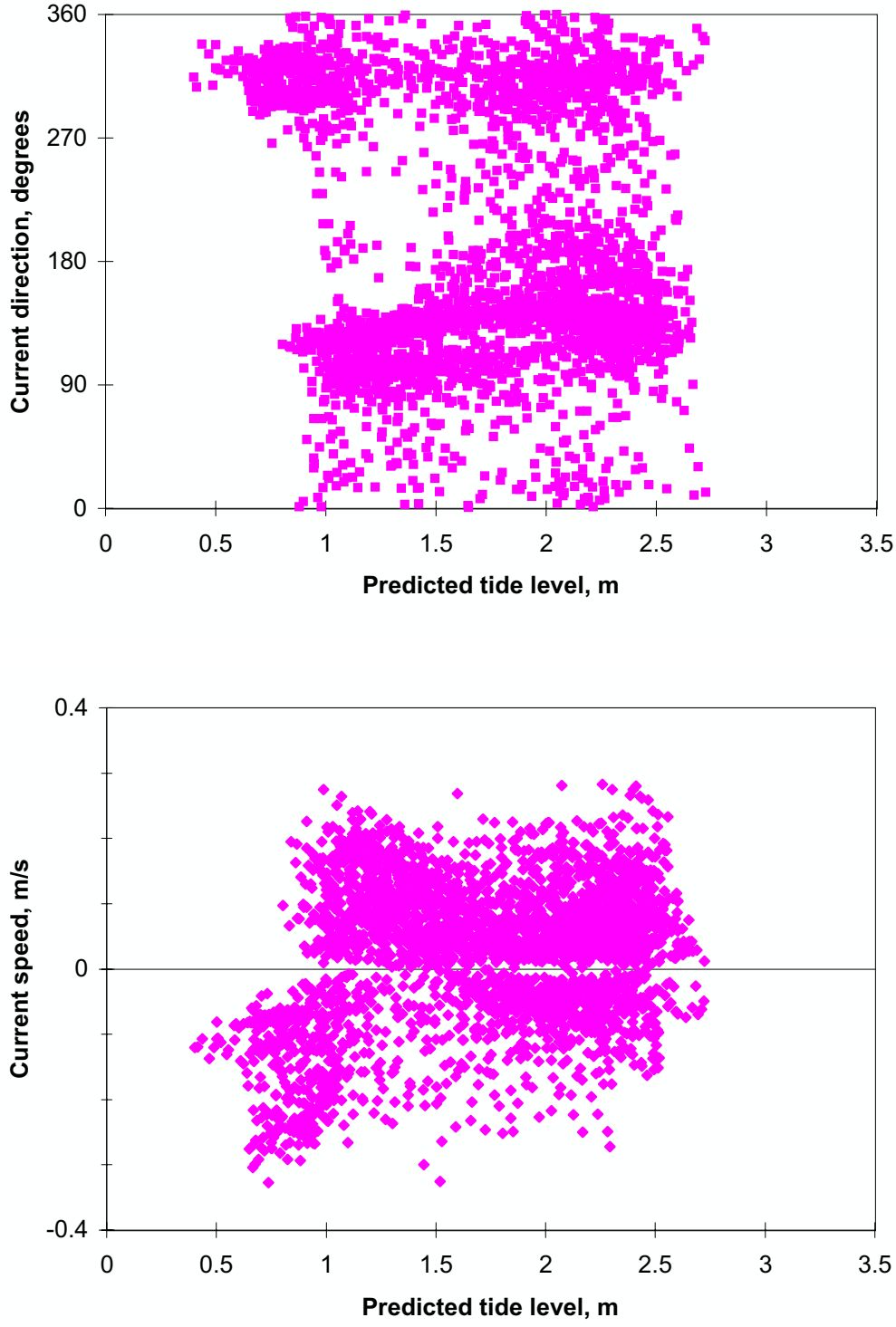

Figure 70. Southern current meter, rising tide, 1.4 m <= R < 2.0 m
1 November 1996 to 18 March 1997

Above: Current direction *vs* predicted tide level; all data

Below: Current speed *vs* predicted tide level; all data

θ_c < 225°, positive θ_c >= 225°, negative

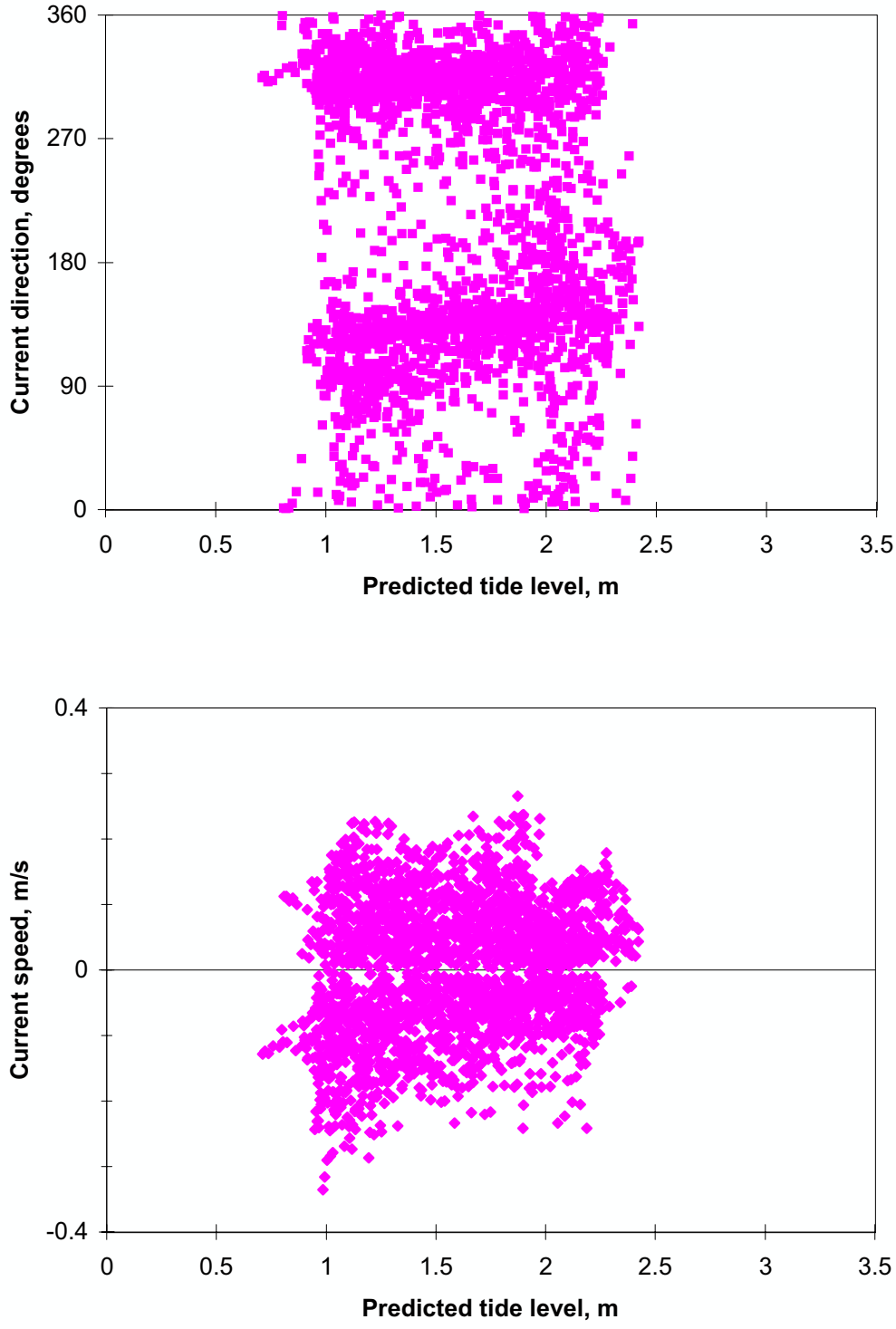

Figure 71. Southern current meter, rising tide, R < 1.4 m
1 November 1996 to 18 March 1997

Above: Current direction *vs* predicted tide level; all data

Below: Current speed *vs* predicted tide level; all data

θ_c < 225°, positive θ_c >= 225°, negative

7.3.2 Southern current meter, falling tide

The falling tidal velocities measured at the southern current meter during the period 17 March to 30 June 1996 have been presented previously in Figures 18, 21 and 24. Similar data for the period 1 July to 31 October 1996 is presented in Figures 72, 73 and 74 and for the period 1 November 1996 to 18 March 1997 in Figures 75, 76 and 77. The percentages of positive to negative currents in each tidal range group during each analysis period are given in Table 10.

Table 10 % positive and % negative currents in each tidal range group during each analysis period - southern current meter – falling tide – all data

Period	Direction θ_c *	Tidal range group			
		Large R ≥ 2.0 m	Medium 2.0 > R ≥ 1.4 m	Small R < 1.4 m	All
Overall 17 Mar. 1996 to 18 Mar. 1997	+ve	49.2	38.8	37.3	42.3
	-ve	50.8	61.2	62.7	57.7
1 17 Mar. 1996 to 30 Jun. 1996	+ve	47.8	28.0	23.9	35.1
	-ve	52.2	72.0	76.1	64.9
2 1 Jul. 1996 to 31 Oct. 1996	+ve	53.7	46.8	45.3	49.0
	-ve	46.3	53.2	54.7	51.0
3 1 Nov. 1996 to 18 Mar. 1997	+ve	46.6	39.9	40.1	42.3
	-ve	53.4	60.1	59.9	57.7

* $\theta_c < 225°$ is +ve ; $\theta_c \geq 225°$ is –ve.

For large tides (Figures 18, 72 and 75) the positive phase of the falling tidal current was generally the same during all three analysis periods. For tidally dominated conditions, current reversal occurred in a clockwise direction when 1.5 m > z_0 > 1.35 to 1.3 m. The maximum positive velocity was *ca* 0.3 m/s with some higher values > 0.4 m/s between 1 July and 31 October 1996. At higher tide levels the wave-dominated current reversal tended to occur in an anticlockwise direction, particularly during the period 1 July to 31 October 1996 (Figure 72). During the first

two analysis periods wave-induced current reversal only occurred when $z_0 \leq 2.9$ m (Figures 18 and 72) but during the last period some waves were large enough to reverse the flow at the highest tide levels (Figure 75).

Negative currents dominated during the period 17 March to 30 June 1996 and to a lesser extent between 1 November 1996 and 18 March 1997, whereas, between 1 July and 31 October 1996, positive and negative behaviour is consistent with the wind climates during these three periods (Figures 58 and 59). Southeasterly winds dominated between 17 March and 30 June 1996 and between 1 November and 1996 and 18 March 1997, although there was some northwesterly weather during the latter period. Both southeasterly and northeasterly conditions occurred between 1 July and 31 October 1996.

At low tide levels, *i.e.* when $z_o < 1$ m, the bund wall acts as a broad crested weir. Under such conditions water is ponded on the reef-flat. The flow over the bund wall is unaffected by the ocean tide level as the latter continues to fall below the bund wall crest, but depends only on the elevation of the ponded water above the bund wall crest.

During the period 17 March to 30 June 1996, the outflowing current attained a maximum speed generally between 0.15 m/s and 0.3 m/s but sometimes as large as 0.4 m/s when $z_0 \approx 1.1$ m (Figure 18). This maximum speed coincides with the onset of weir control by the southern bund wall. The current speed then reduced asymptotically to a value between 0.07 and 0.2 m/s as water drained off the reef-top independently of the predicted ocean tide level z_0.

During the two later analysis periods, the flow during weir control by the bund wall was bivalued, the graphs on Figures 72 and 75 having the appearance of a "crab's claw." Under some conditions the current attained a maximum of *ca* –0.45 m/s. This implies that the flow and hence the reef-top water level were greater for the latter conditions (Figure 78a). Alternatively, there had been a change in the lateral distribution of flow on the reef flat between the coral zone and the shoreline.[1] Bund wall control of reef-top currents during the latter stages of the falling tide and the relevance of the lateral distribution of flow is discussed more fully in the second report (Gourlay and Hacker 2008b).

These changes in water level and/or lateral velocity distribution must be a consequence of changes in the wind and wave climates. During the period 17 March to 30 June 1996 the winds were

[1] See also comments on possible effects of current meter calibration changes (Section 3.4).

dominantly from the eastsoutheasterly to southsoutheasterly directions. The frequency of northeasterly to northwesterly winds was low (Figure 58b). By contrast during the period 1 July to 31 October 1996 there were significantly fewer occurrences of winds from the southeasterly quarter and more northeasterlies and particularly northwesterlies than previously (Figure 59a).

The data for large tides (R ≥ 2 m) during the latter period (Figure 72) were separated into a number of subgroups based upon wind direction (Figures 79 to 84). The velocities during the weir control period for the various wind sectors are summarised in Table 11. The relationships between the wind direction sectors and Heron and Wistari Reefs is shown on Figure 78b.

Table 11 Influence of winds and waves upon current velocities at southern current meter when flow is controlled by bund wall crest for large tides.[1] - 1 July to 31 October 1996

Wind direction	Wave/Tide conditions	v, m/s		
		z_o, m		
		1.0	0.5	0
$0^o \leq \theta_w < 80°$	$H_{BP} > H_{Wis}$	0.25 – 0.35	0.18 – 0.31	0.20 – 0.24
$80° \leq \theta_w < 105°$	$H_{BP} > H_{Wis}$	0.15 – 0.25	0.08 – 0.13	-
$105° \leq \theta_w < 165°$	R or H_{Wis} small	0.18 – 0.35	0.09 – 0.17	0.05 – 0.11
	R or H_{Wis} large		0.18 – 0.25	-
$165° \leq \theta_w < 240°$	$H_{BP} >< H_{Wis}$	0.20 – 0.30	0.12 – 0.30	-
$240° \leq \theta_w < 315°$	$H_{BP} > H_{Wis}$	0.18 – 0.28	0.22 – 0.30	-
$315° \leq \theta_w < 360°$	$H_{BP} > H_{Wis}$ some large R	0.12 – 0.32	0.20 – 0.31	*ca* 0.20

The conditions, under which the flow of ponded water from the southern reef-flat into the boat harbour varied in magnitude, can now be deduced from Table 11 and Figure 78b. Flow and hence velocities are low when offreef waves are small and/or break on distant reef-rims or tidal ranges are smaller (*i.e.* R ≈ 2 m). For example, when θ_w lies between 80° and 105° (Figure 80) waves will break on the eastern section of Heron Reef's rim. This is about 8 km east of the boat harbour and much of the flow generated by these waves will flow either over the northern reef-rim or along the northern side of the island. Hence velocities at the southern current meter can be expected to be lower than for more exposed locations (Table 11). When θ_w lies between 105° and 165° (Figure 81) and offreef wave heights H_{Wis} are small and/or tidal ranges are smaller (*i.e.*

R ≈ 2 m), there is negligible wave-generated flow and the flow over the southern bund wall is essentially only caused by water ponded on the reef-top by the tide. However, if H_{Wis} is sufficiently large to reverse the tidal flow when $z_0 > 1.5$ m, there will be an additional inflow of water over the southern reef-rim, increasing the amount of water ponded on the reef-flat. Hence water levels behind the bund wall will be greater and outflow over the wall and current velocities approaching it will be larger. Velocities were even larger (≤ 0.5 m/s) between 1 November 1996 and 8 March 1997 (Figure 75) when H_{Wis} almost reached 3 m.

When θ_w lies between 165° and 240° (Figure 82) waves will break either on the southwestern or southern reef rims of both Wistari and Heron Reefs. During the period of observation wind frequencies and intensities from these directions were low and no significant wave-generated currents would have occurred. Variations in the tidal range may have been responsible for the variations of the current velocities under these conditions. However, even if large waves were generated from this sector during the passage of a tropical cyclone, it is unlikely that currents over the southern bund wall would be increased significantly because of the sheltering effect of Wistari Reef.

A different situation occurs when θ_w lies between 240° and 360° (Figures 83 and 84) and 0° and 80° (Figure 79). Under these conditions the flow over the southern bund wall is greater than for southeasterly conditions. The reason for this paradoxical behaviour becomes apparent when the geographical position of Heron Island is considered (Figure 78b). Considering initially the clockwise sector from 315° to 80°, it is clear that waves generated by winds from this sector will break along a 4 km length of reef-rim on the northern side of the island. Some of the flow generated by these breaking waves will be directed around the western side of the island and, as $z_0 \rightarrow 1$ m will flow over the northern bund wall into the boat harbour. However, a greater proportion of this flow initially will be directed southwards across the reef-flat and, as reef-top water levels drop below the southern reef-rim (z_0 = *ca* 1.1 m), clockwise around the island and over the southern bund wall into the boat harbour. Hence flow over the southern bund wall and reef-top current velocities on the southern side of the island are significantly increased when waves break on the northern reef-rim. Larger velocities also occur for the relatively infrequent westerly winds (240° ≤ θ_w < 315°), possibly for a similar reason, *i.e.* a clockwise circulation is generated on the reef-top. Low velocities also occur with some northwesterly winds (Figure 84), which possibly generate an anticlockwise circulation. Preliminary analysis suggests that larger velocities are associated with larger tides (R→ 3 m) and hence smaller velocities may be associated with smaller tides (R→ 2 m).

The same type of current velocity variation under bund wall control occurs for medium tides (Figures 21, 73 and 76) but not for small tides (Figures 24, 74 and 77). In the latter case the majority of tides do not fall below the bund wall and so the number of occasions where bund wall control of ponded water occurs is small and their duration limited. However, velocities into the boat harbour vary significantly as the height of waves breaking on the southern reef-rim varies. This is particularly noticeable during the period 1 November 1996 to 18 March 1997 (Figure 77) when H_{Wis} almost reached 3 m.

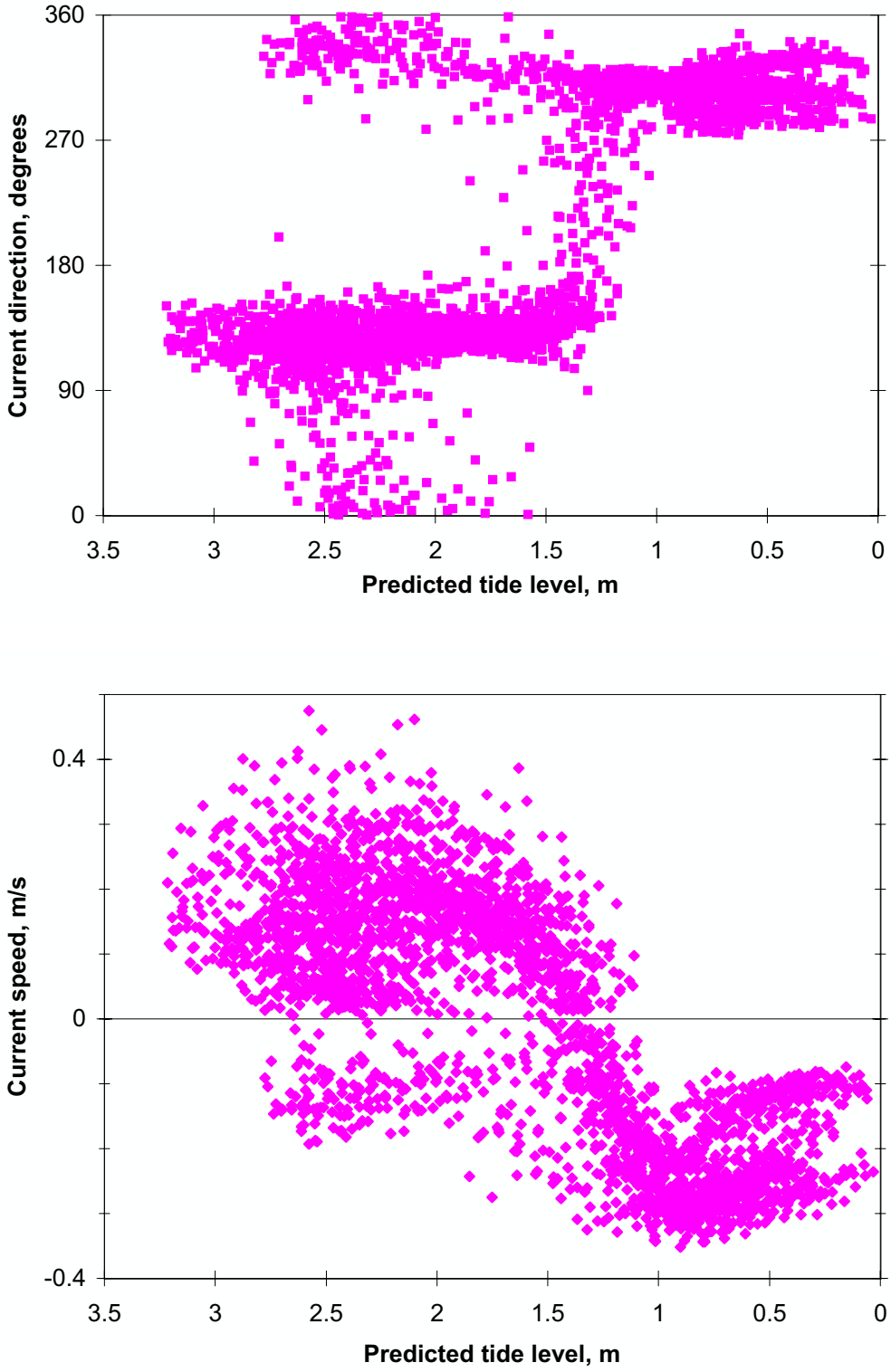

Figure 72. Southern current meter, falling tide, R >= 2.0 m
1 July 1996 to 31 October 1996

Above: **Current direction *vs* predicted tide level; all data**

Below: **Current speed *vs* predicted tide level; all data**

θ_c < 225°, positive θ_c >= 225°, negative

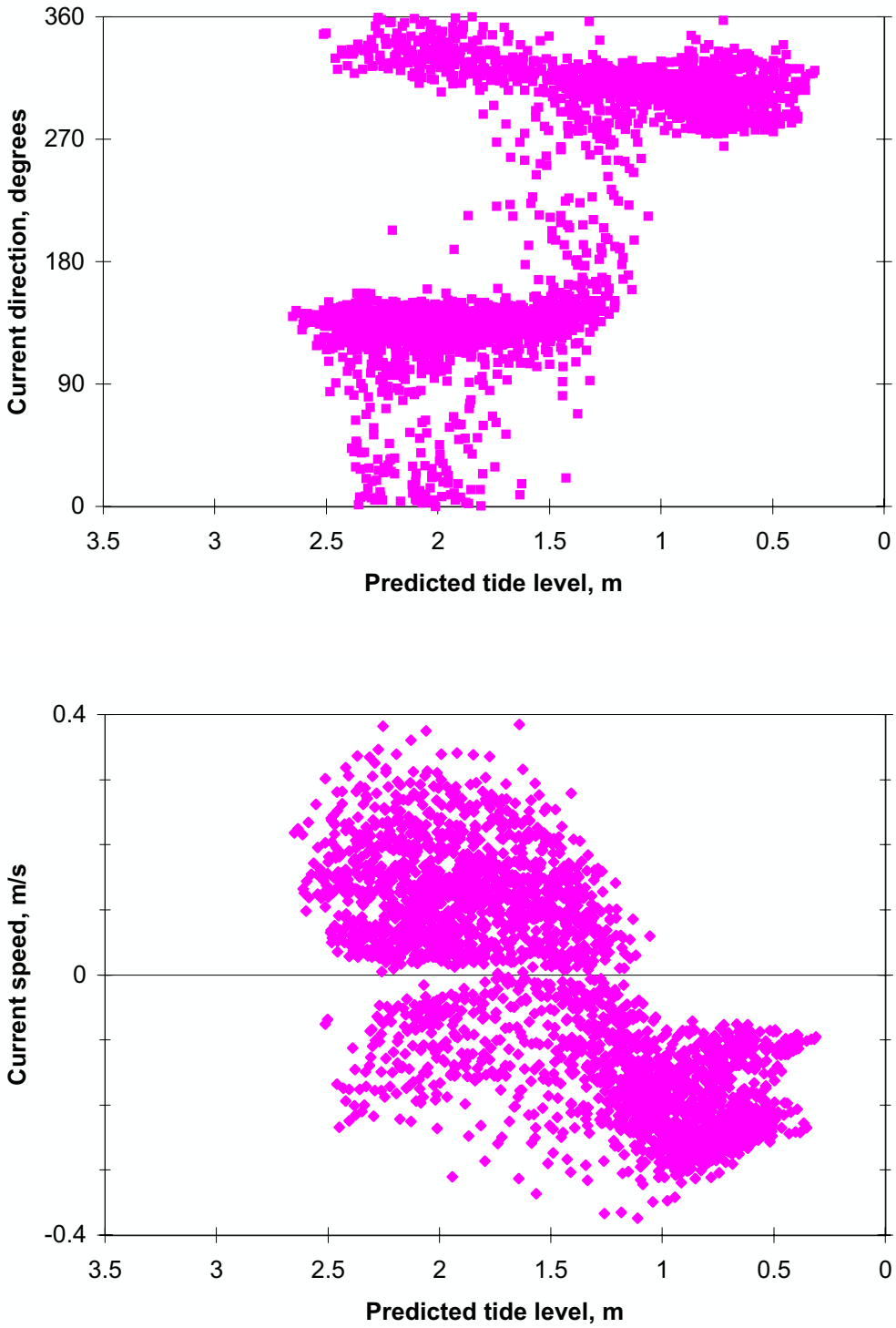

Figure 73. Southern current meter, falling tide, 1.4 m <= R < 2.0 m
1 July 1996 to 31 October 1996

Above: **Current direction *vs* predicted tide level; all data**

Below: **Current speed *vs* predicted tide level; all data**

θ_c < 225°, positive θ_c >= 225°, negative

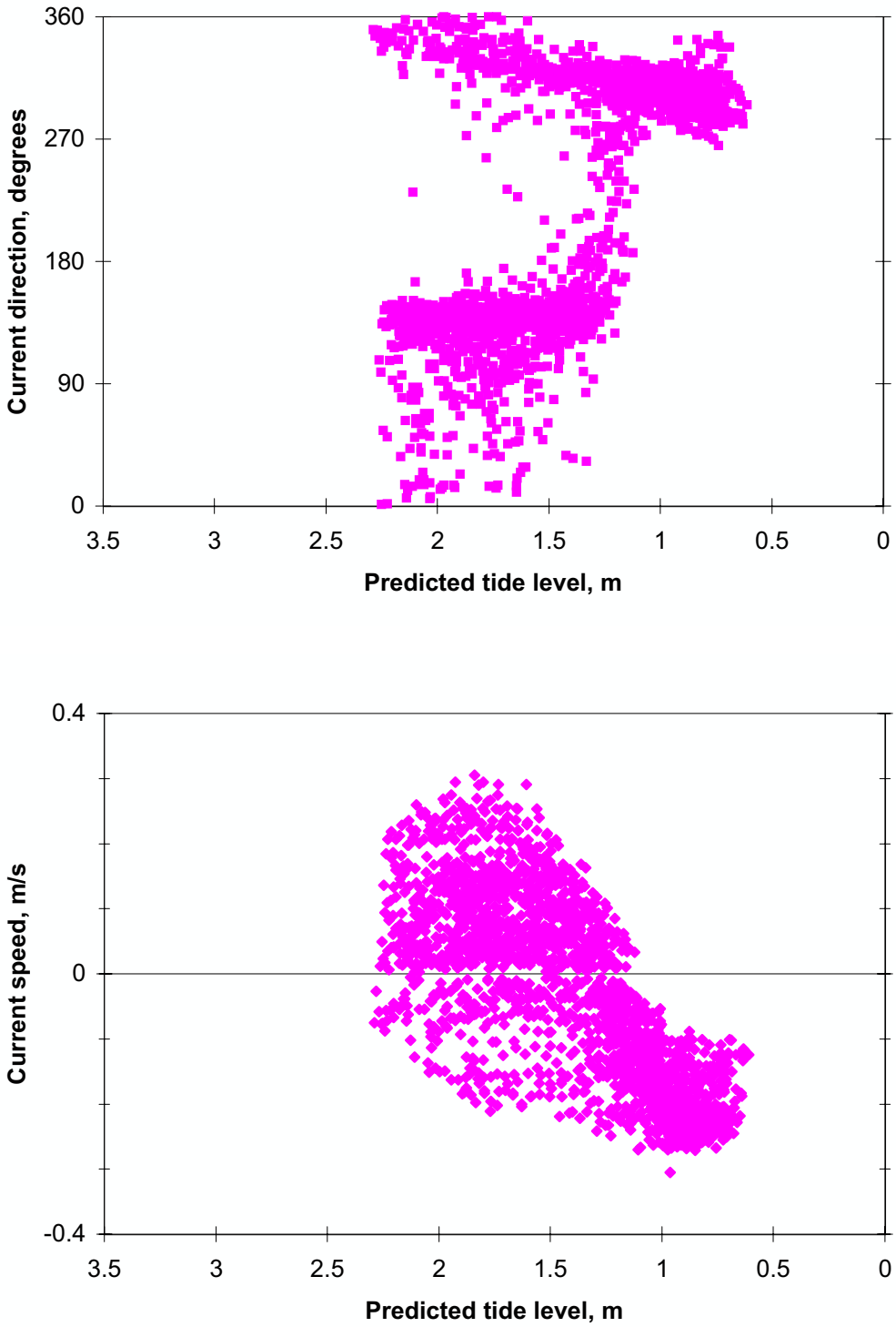

Figure 74. Southern current meter, falling tide, R < 1.4 m
1 July 1996 to 31 October 1996

Above: Current direction *vs* predicted tide level; all data

Below: Current speed *vs* predicted tide level; all data

θ_c < 225°, positive θ_c >= 225°, negative

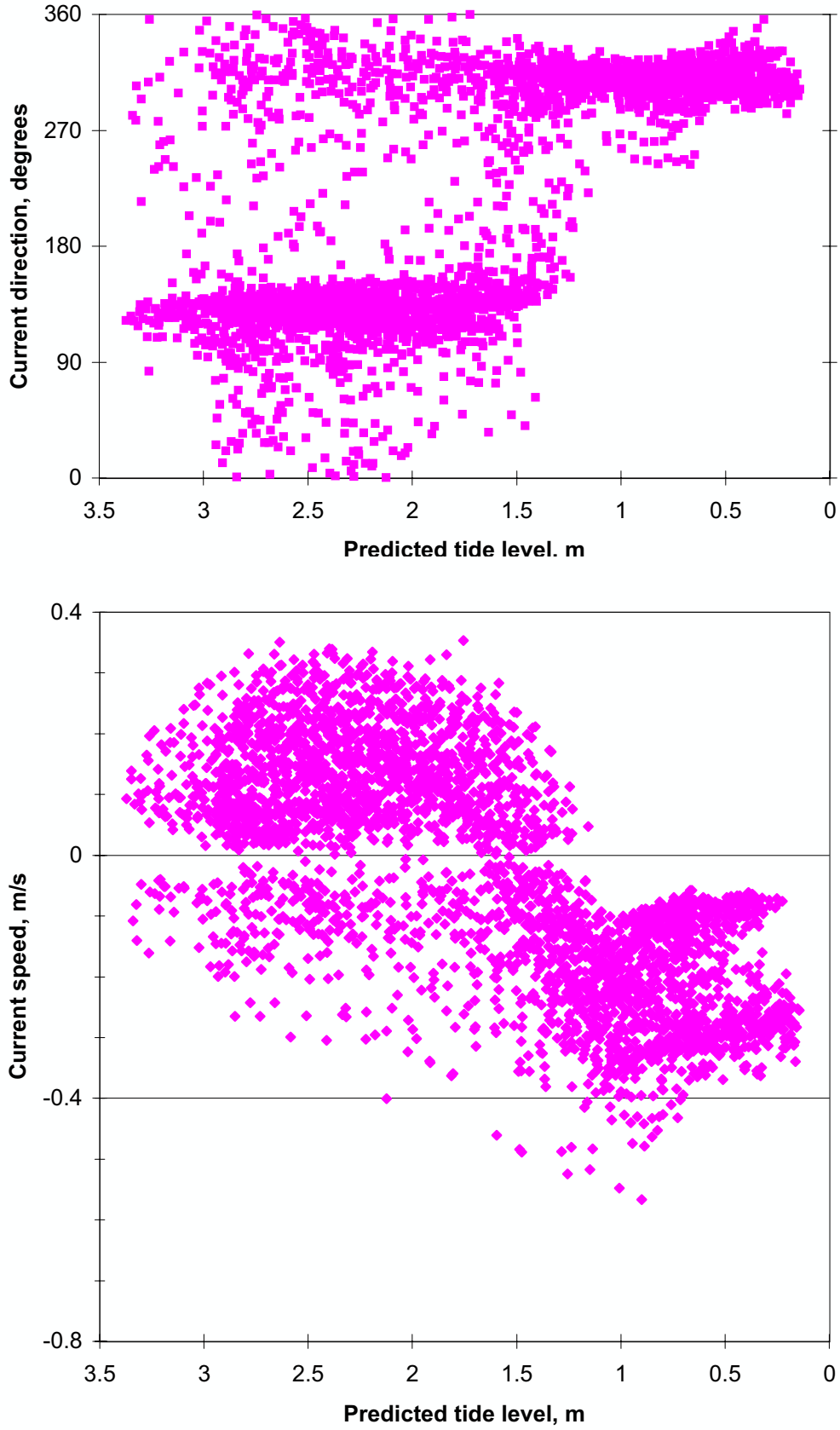

Figure 75. Southern current meter, falling tide, R >= 2.0 m
1 November 1996 to 18 March 1997

Above: Current direction *vs* predicted tide level; all data

Below: Current speed *vs* predicted tide level; all data

θ_c < 225°, positive θ_c >= 225°, negative

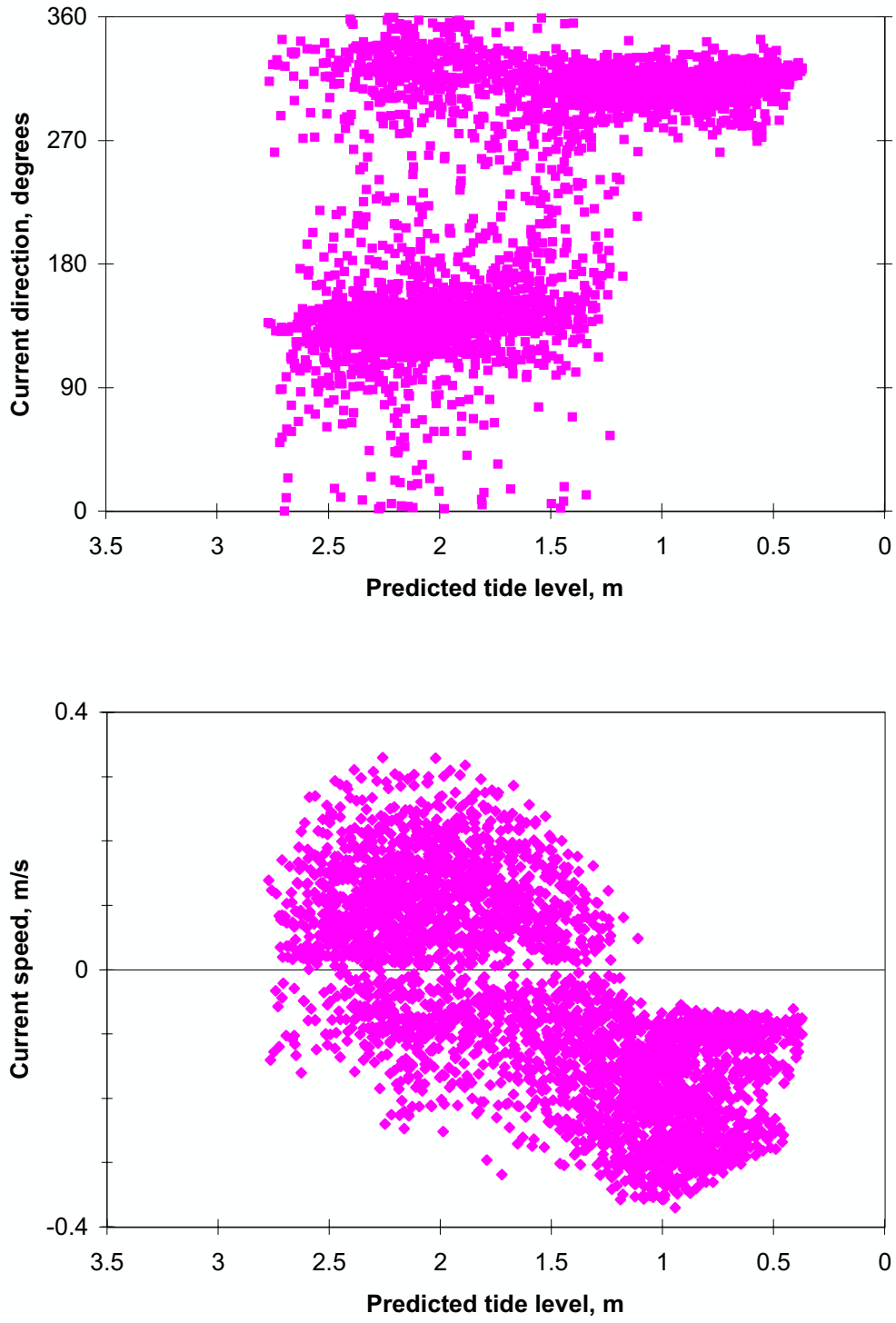

Figure 76. Southern current meter, falling tide, 1.4 m <= R < 2.0 m
1 November 1996 to 18 March 1997

Above: Current direction *vs* predicted tide level; all data

Below: Current speed *vs* predicted tide level; all data

$\theta_c < 225^o$, positive $\theta_c >= 225^o$, negative

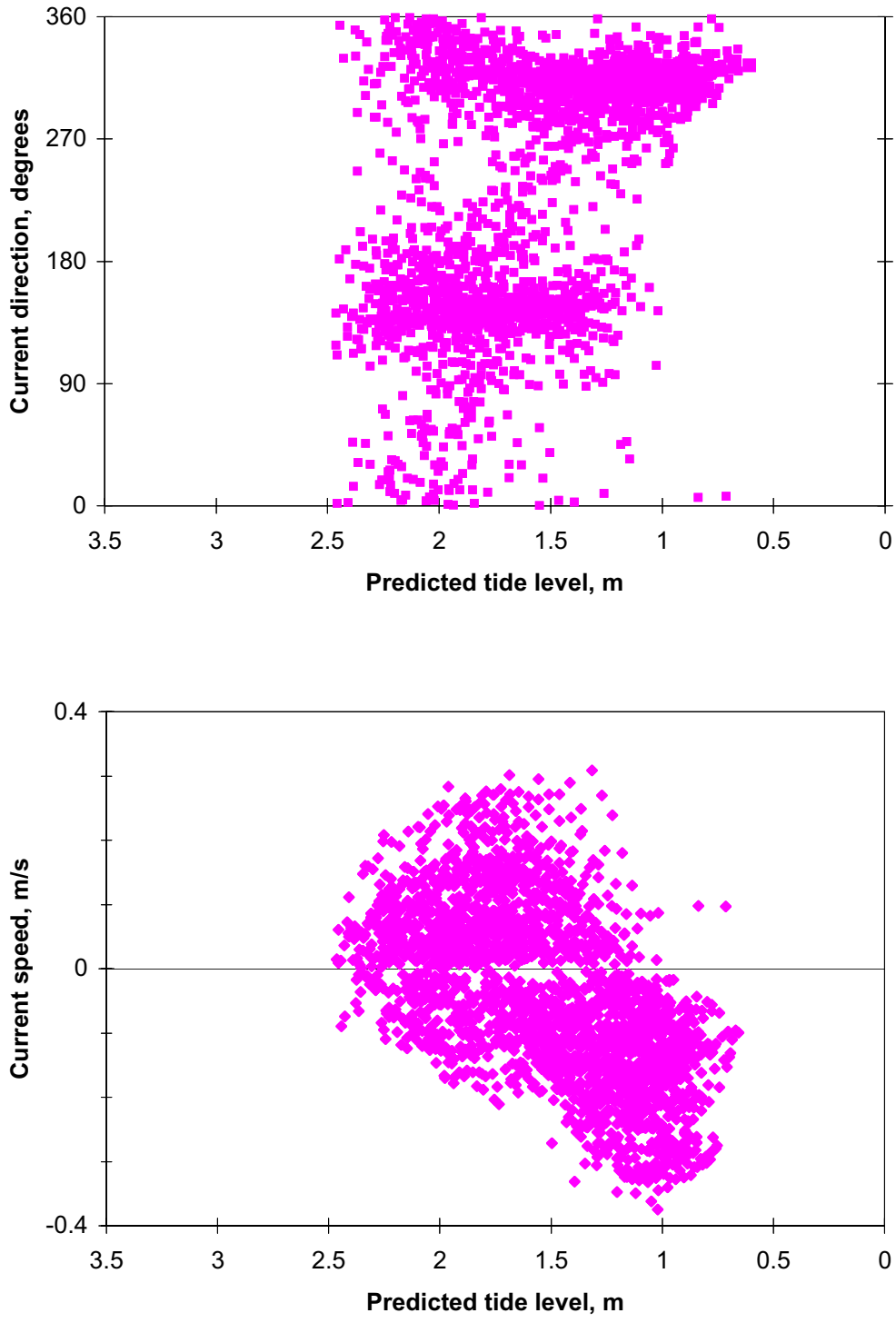

Figure 77. Southern current meter, falling tide, R < 1.4 m
1 November 1996 to 18 March 1997

Above: Current direction *vs* predicted tide level; all data

Below: Current speed *vs* predicted tide level; all data

θ_c < 225°, positive θ_c >= 225°, negative

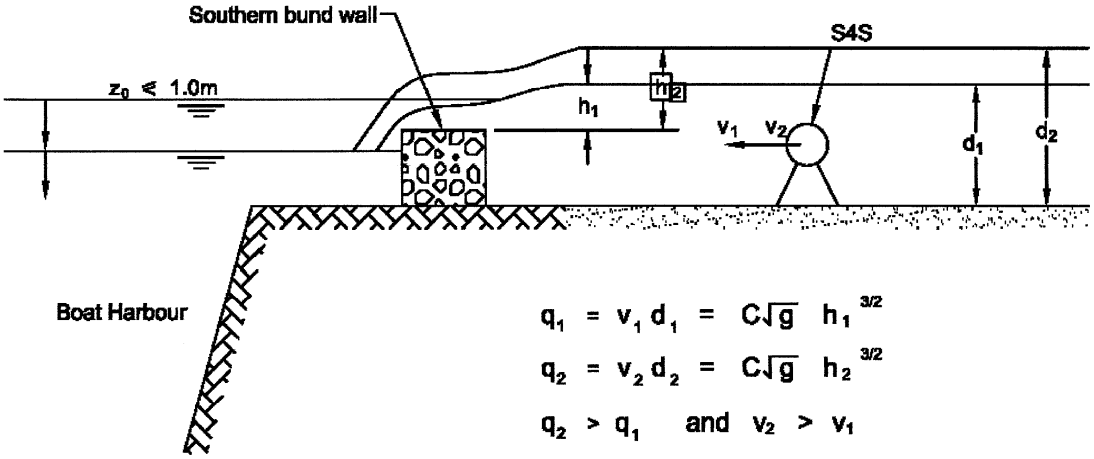

See Appendix B for definitions of symbols

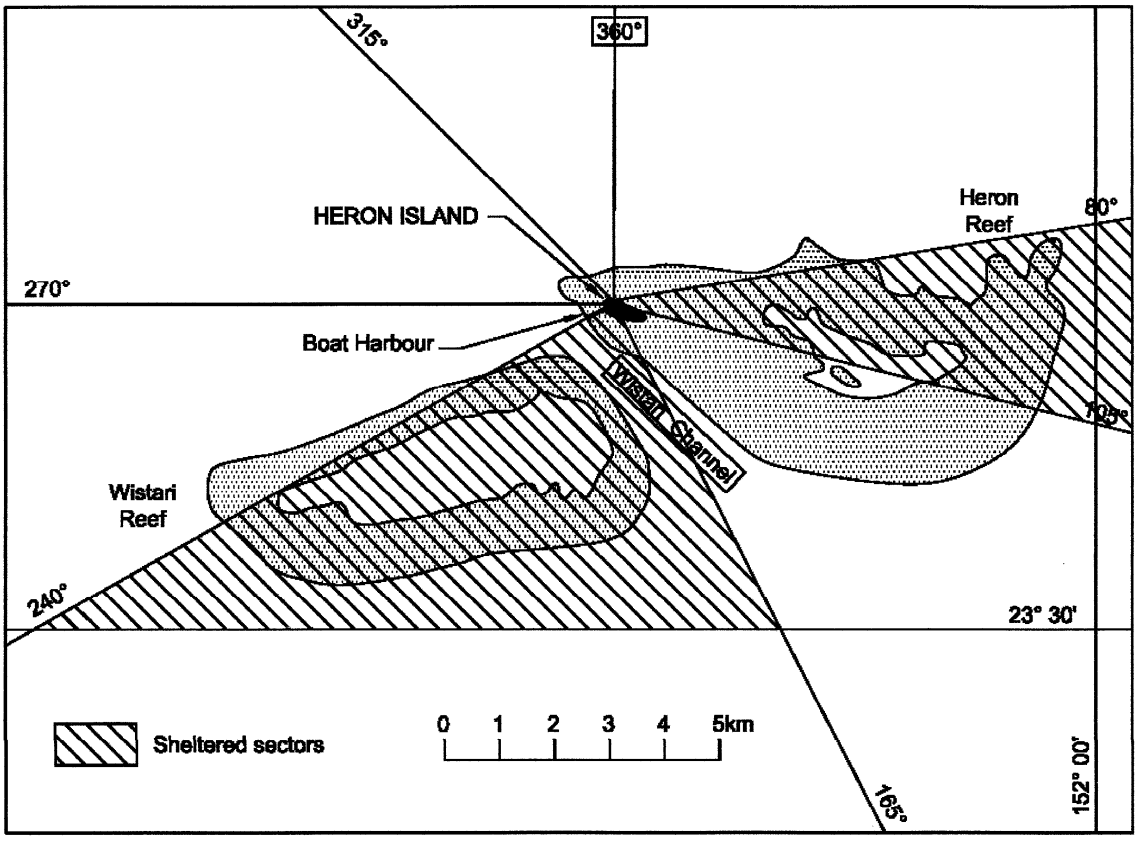

Figure 78. (a) Weir flow over bund wall
(b) Reef sheltering at Heron Island

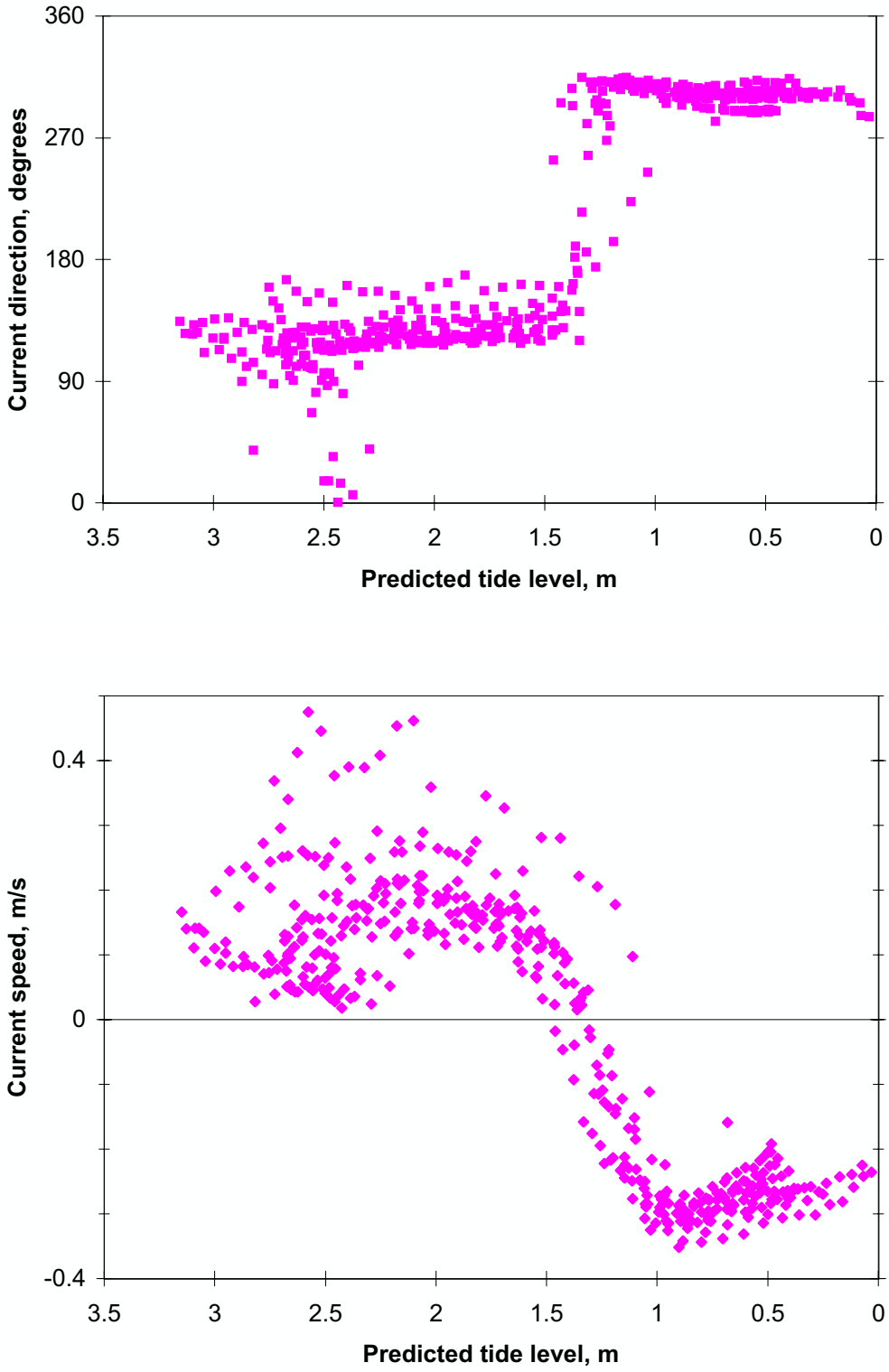

Figure 79. Southern current meter, falling tide, R >= 2.0 m
1 July 1996 to 31 October 1996

Above: **Current direction *vs* predicted tide level; $0^o <= \theta_w < 80^o$**
Below: **Current speed *vs* predicted tide level; $0^o <= \theta_w < 80^o$**
$\theta_c < 225^o$, positive $\theta_c >= 225^o$, negative

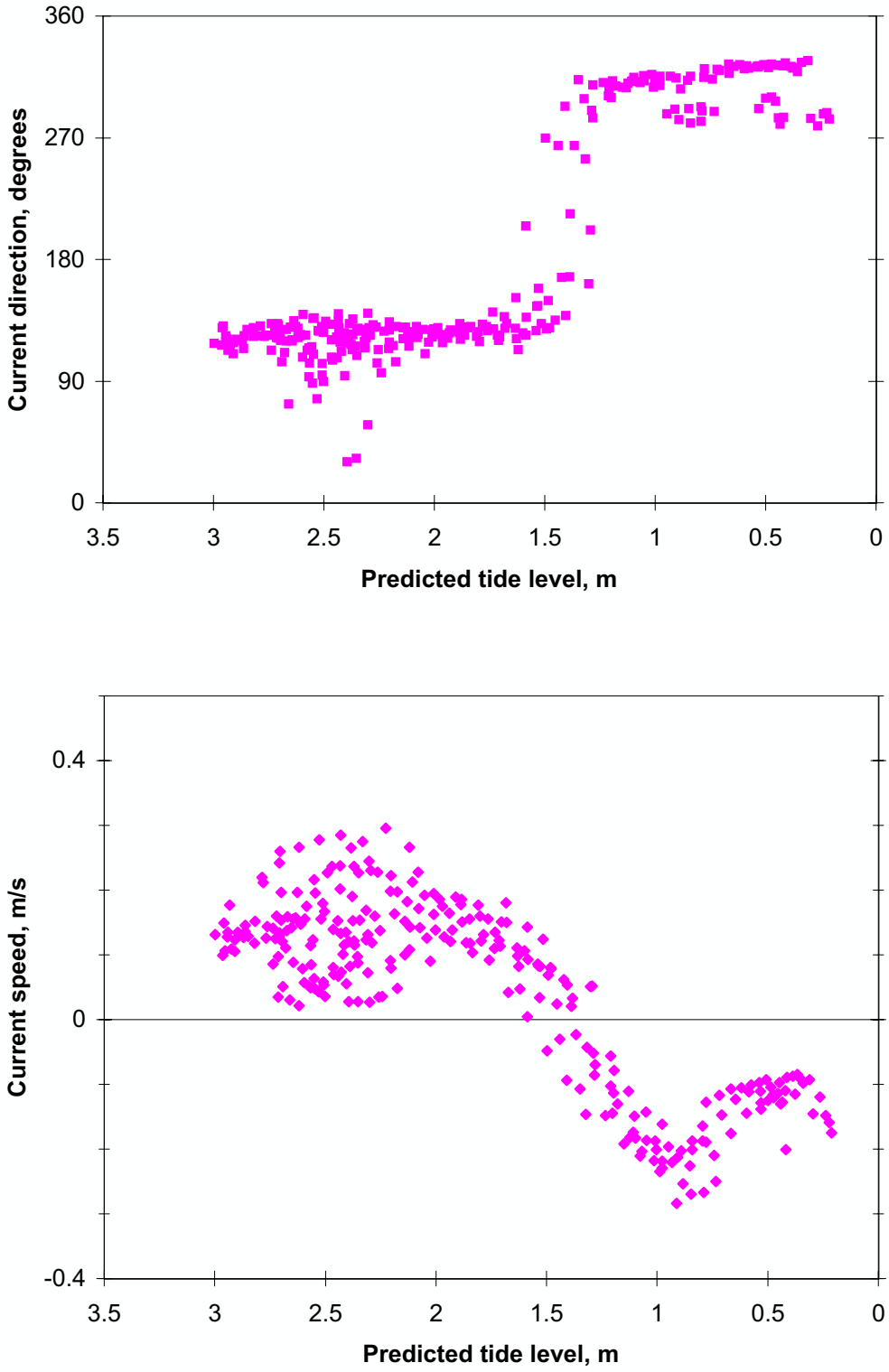

Figure 80. Southern current meter, falling tide, R >= 2.0 m
1 July 1996 to 31 October 1996

Above: **Current direction *vs* predicted tide level; $80^o <= \theta_w < 105^o$**
Below: **Current speed *vs* predicted tide level; $80^o <= \theta_w < 105^o$**
$\theta_c < 225^o$, positive $\theta_c >= 225^o$, negative

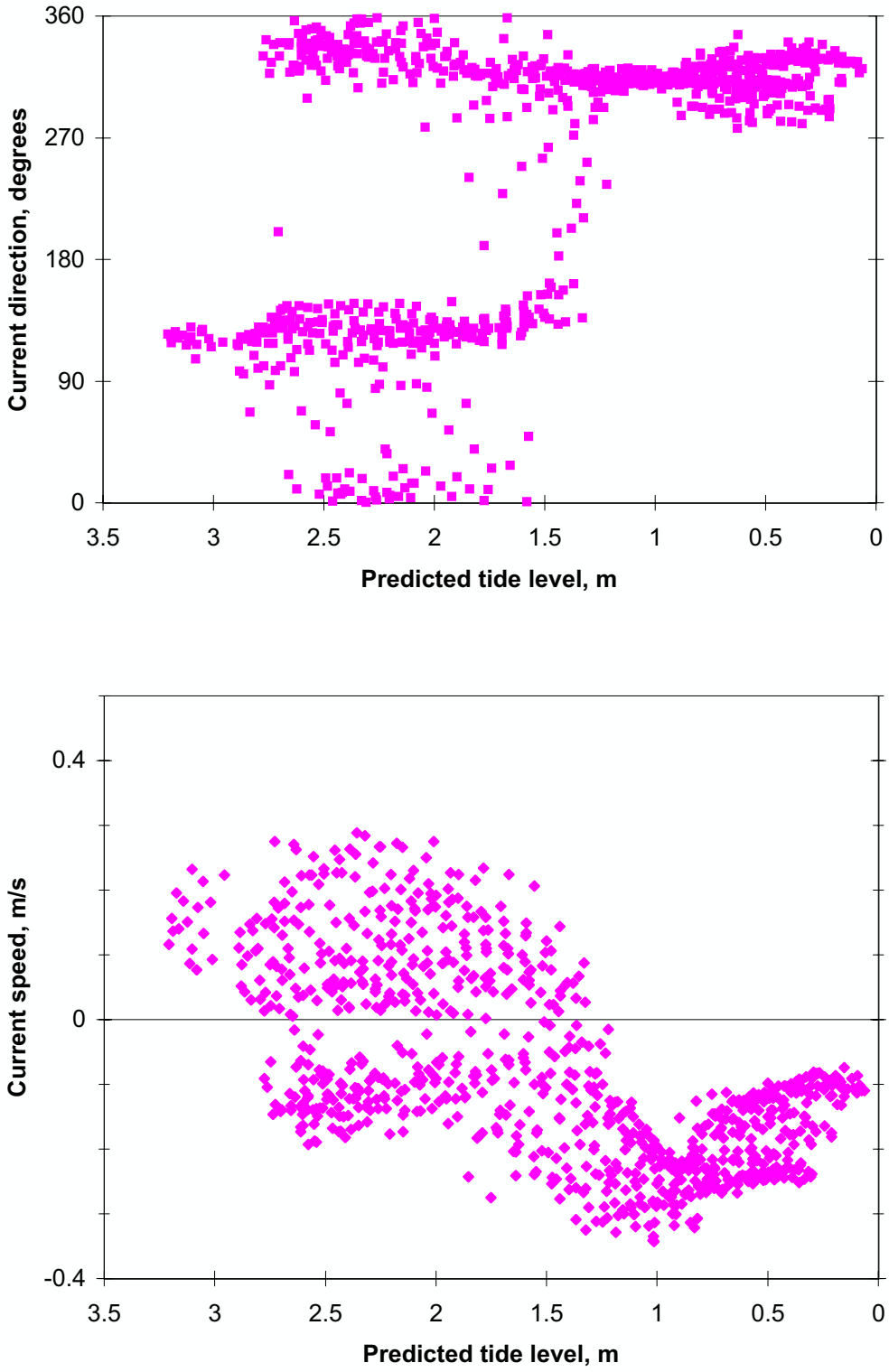

Figure 81. Southern current meter, falling tide, R >= 2.0 m
1 July 1996 to 31 October 1996

Above: **Current direction *vs* predicted tide level; $105^{o} <= \theta_{w} < 165^{o}$**
Below: **Current speed *vs* predicted tide level; $105^{o} <= \theta_{w} < 165^{o}$**
$\theta_{c} < 225^{o}$, positive $\theta_{c} >= 225^{o}$, negative

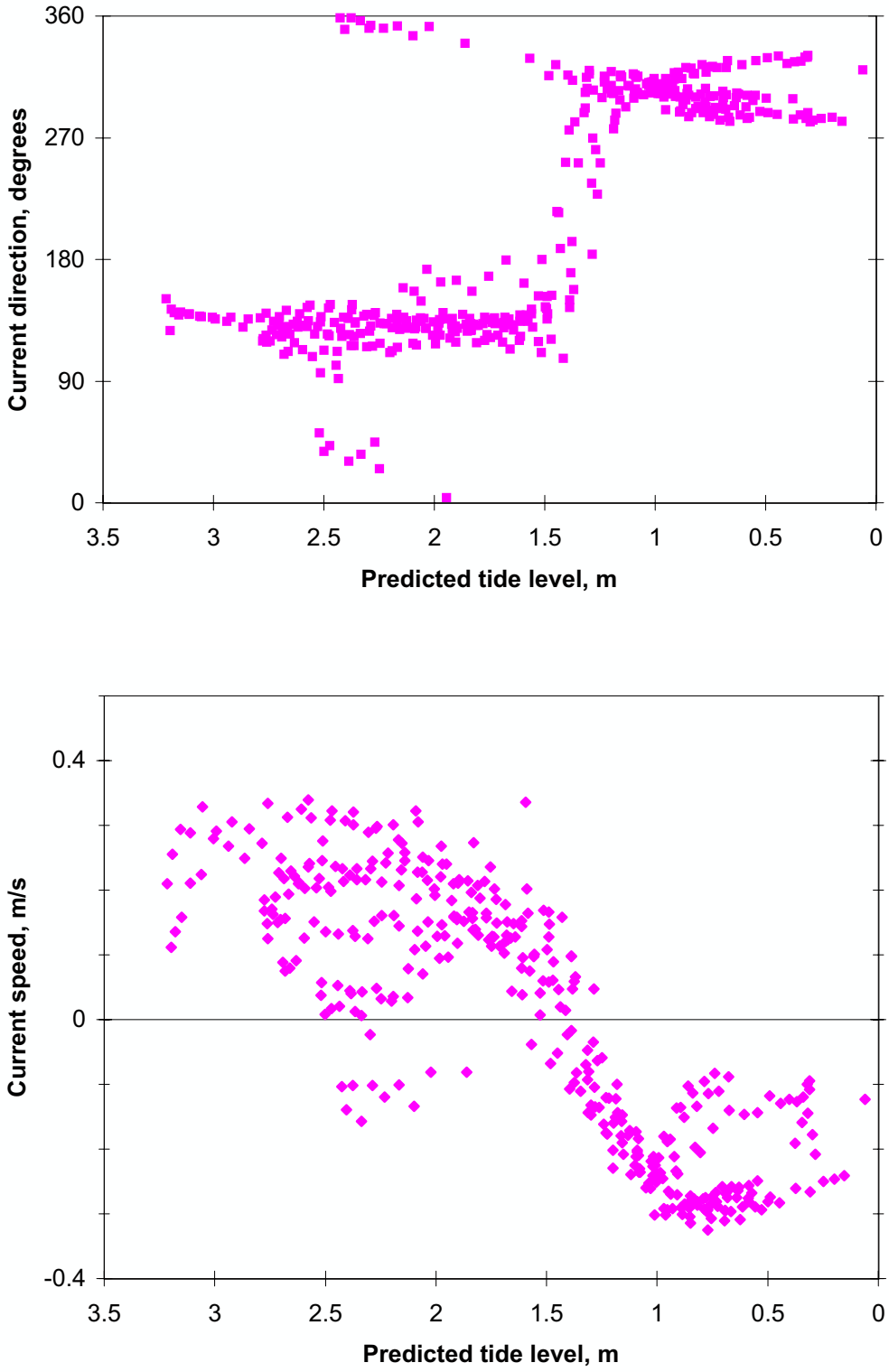

Figure 82. Southern current meter, falling tide, R >= 2.0 m
1 July 1996 to 31 October 1996

Above: **Current direction *vs* predicted tide level; $165^o <= \theta_w < 240^o$**
Below: **Current speed *vs* predicted tide level; $165^o <= \theta_w < 240^o$**
$\theta_c < 225^o$, positive $\theta_c >= 225^o$, negative

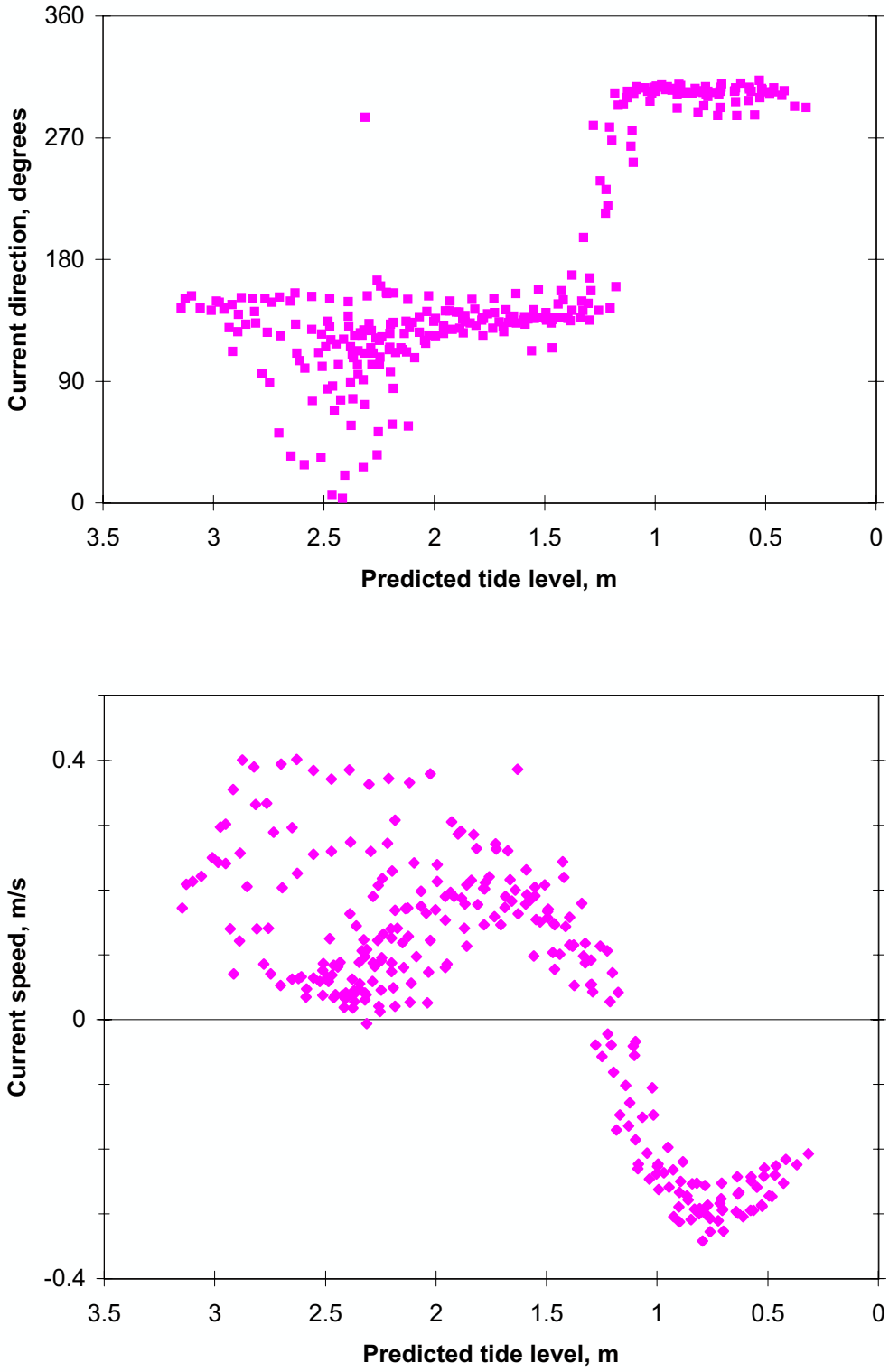

Figure 83. Southern current meter, falling tide, R >= 2.0 m
1 July 1996 to 31 October 1996

Above: **Current direction *vs* predicted tide level; $240^o <= \theta_w < 315^o$**
Below: **Current speed *vs* predicted tide level; $240^o <= \theta_w < 315^o$**
$\theta_c < 225^o$, positive $\theta_c >= 225^o$, negative

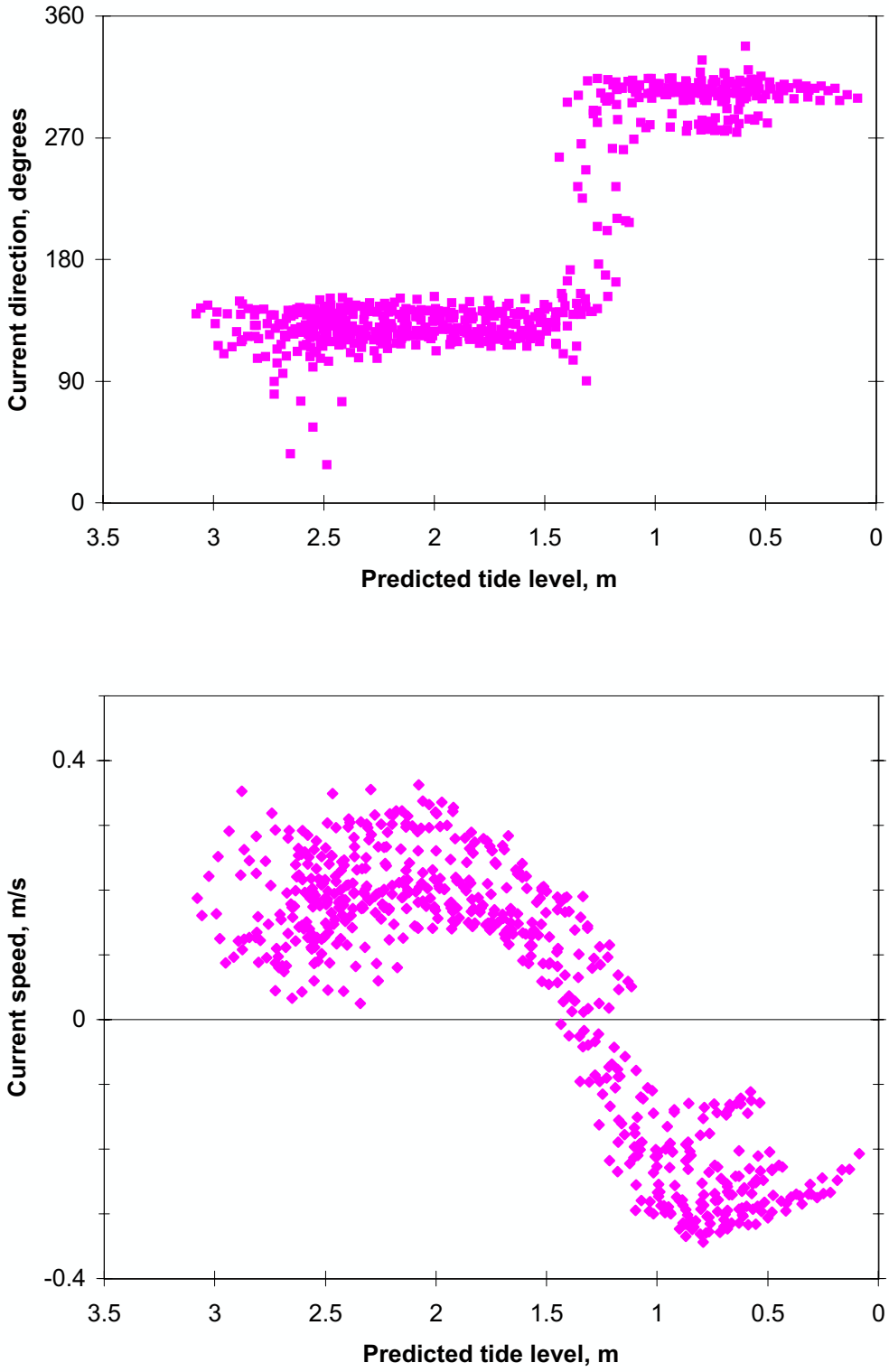

Figure 84. Southern current meter, falling tide, R >= 2.0 m
1 July 1996 to 31 October 1996

Above: **Current direction *vs* predicted tide level; $315^{o} <= \theta_w < 360^{o}$**
Below: **Current speed *vs* predicted tide level; $315^{o} <= \theta_w < 360^{o}$**
$\theta_c < 225^{o}$, positive $\theta_c >= 225^{o}$, negative

7.3.3 Northern current meter, rising tide

The rising tide velocities measured at the northern current meter during the period 17 March to 30 June 1996 have been presented previously in Figures 29, 33 and 37. Similar data for the period 1 July to 31 October 1996 is presented in Figures 85, 86 and 87 and for the period 1 November 1996 to 18 March 1997 in Figures 88, 89 and 90. The percentages of positive and negative currents in each tidal range group during each analysis period are given in Table 12.

For large tides (Figures 29, 85 and 88) the general pattern of variation for both θ_c and v was similar for tidally dominated conditions during all three periods. The first two periods show significant negative velocities, with maximum values exceeding 0.6 m/s, and continuous outflow over the bund wall during the whole rising phase of the tide. These conditions were associated with the two northeasterly storm events which occurred in early May and late July. No such events occurred during the third period of analysis.

In contrast during the period 1 November 1996 to 18 March 1997 (Figure 88) there were many more occasions with negative velocities occurring before the ocean tide level z_0 rose above the bund wall crest ($z_0 \leq 0.86$ m). However, the maximum negative velocity never exceeded 0.4 m/s. Moreover, there were more anticlockwise current reversals at high tide during this period compared with the two earlier ones.

This different behaviour during the last period was associated with the stronger eastsoutheasterly to southeasterly winds accompanying tropical cyclone *"Justin"* during early March 1997. Anticlockwise current reversals at high tide levels are more likely to occur during these wind conditions. However, the extended period of tidal outflow into the boat harbour before the ocean tide rises above the bund wall crest is caused by a different mechanism. This will be considered during the discussion of the falling tidal currents (section 7.3.4).

The current behaviour for medium tides during the three analysis periods (Figures 33, 86 and 89) was similar to that for the large tides.

With small tides (Figures 37, 87 and 90) there were more negative velocities during the first and third periods than during the second period (Table 12). This behaviour is probably a consequence of increased westward flow induced by the more frequent southeasterly winds during periods 17 March to 30 June 1996 and 1 November 1996 to 18 March 1997.

Table 12 % positive and % negative currents in each tidal range group during each analysis period - northern current meter – rising tide – all data

Period	Direction θ_c *	Tidal range group			
		Large R ≥ 2.0 m	Medium 2.0 > R ≥ 1.4 m	Small R < 1.4 m	All
Overall 17 Mar. 1996 to 18 Mar. 1997	+ve	32.5	36.6	28.4	32.8
	-ve	67.5	63.4	71.6	67.2
1 17 Mar. 1996 to 30 Jun. 1996	+ve	34.9	36.2	27.5	33.2
	-ve	65.1	63.8	72.5	66.8
2 1 Jul. 1996 to 31 Oct. 1996	+ve	35.9	43.0	42.8	40.3
	-ve	64.1	57.0	57.2	59.7
3 1 Nov. 1996 to 18 Mar. 1997	+ve	27.4	32.1	18.2	26.2
	-ve	72.6	67.9	81.8	73.8

* $\theta_c < 125°$ is +ve ; $\theta_c \geq 125°$ is –ve.

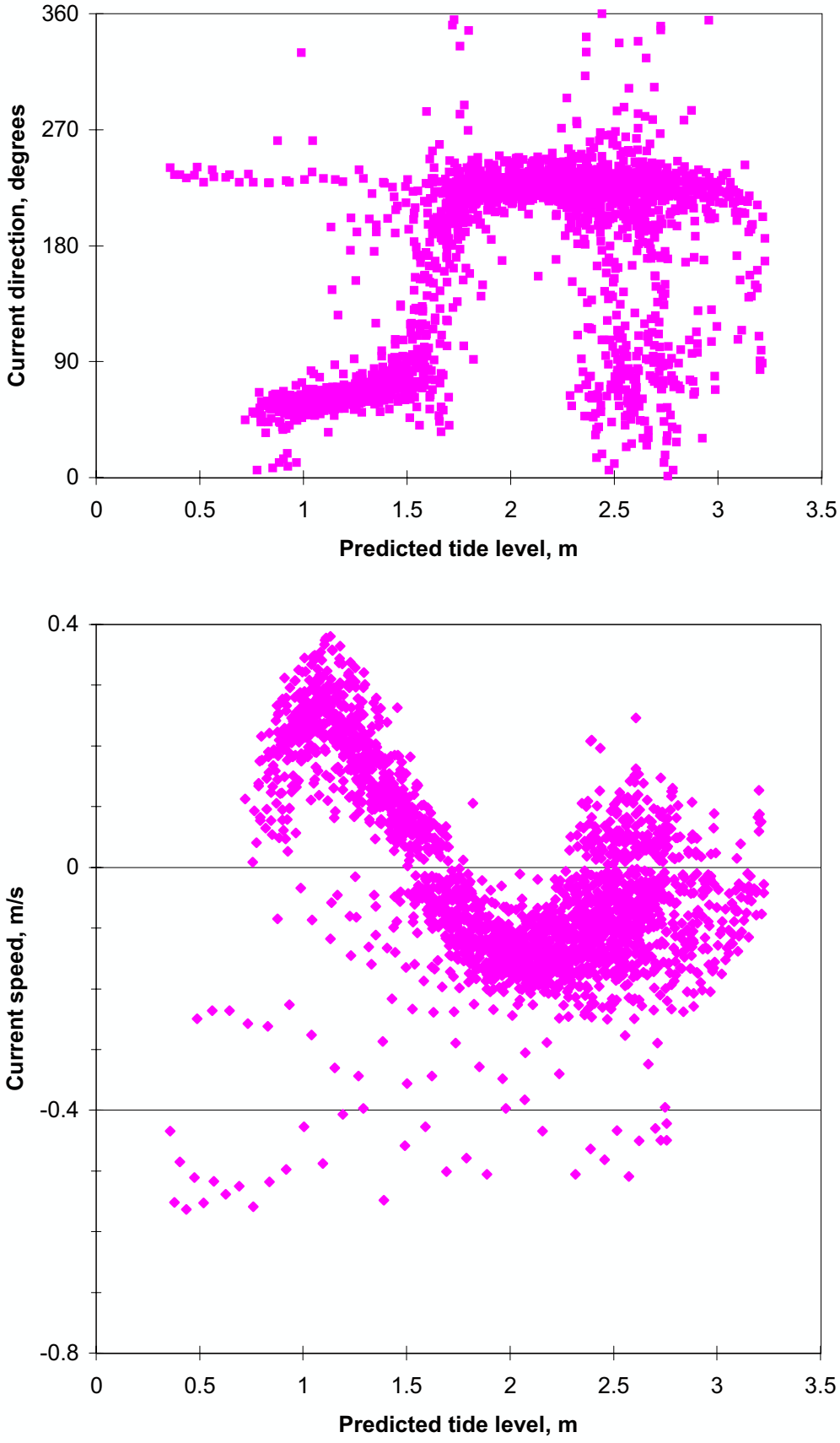

Figure 85. Northern current meter, rising tide, R >= 2.0 m
1 July 1996 to 31 October 1996

Above: **Current direction *vs* predicted tide level; all data**

Below: **Current speed *vs* predicted tide level; all data**

θ_c < 125°, positive θ_c >= 125°, negative

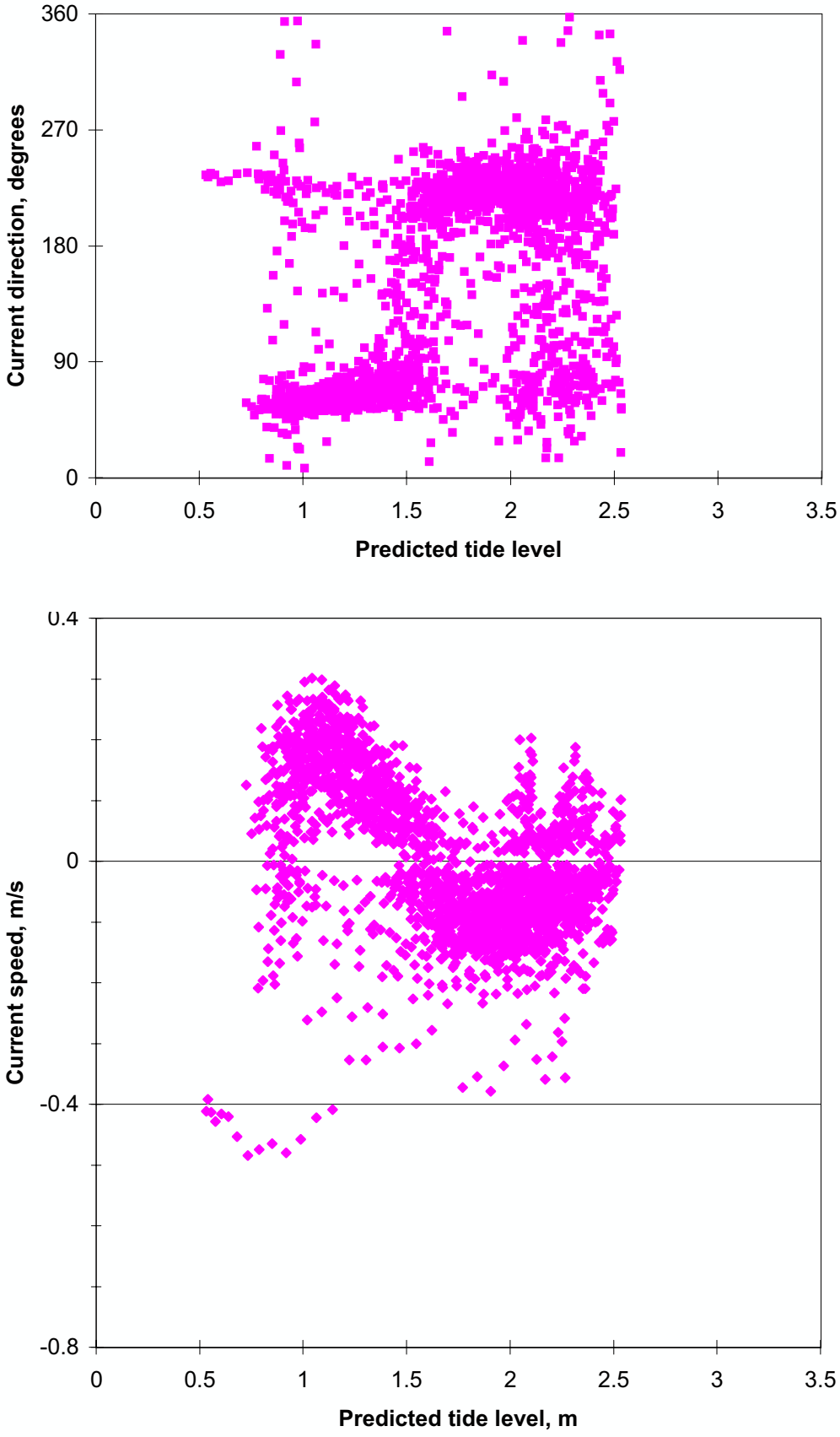

Figure 86. Northern current meter, rising tide, 1.4 m <= R < 2.0 m 1 July 1996 to 31 October 1996

Above: Current direction *vs* predicted tide level; all data

Below: Current speed *vs* predicted tide level; all data

θ_c < 125°, positive θ_c >= 125°, negative

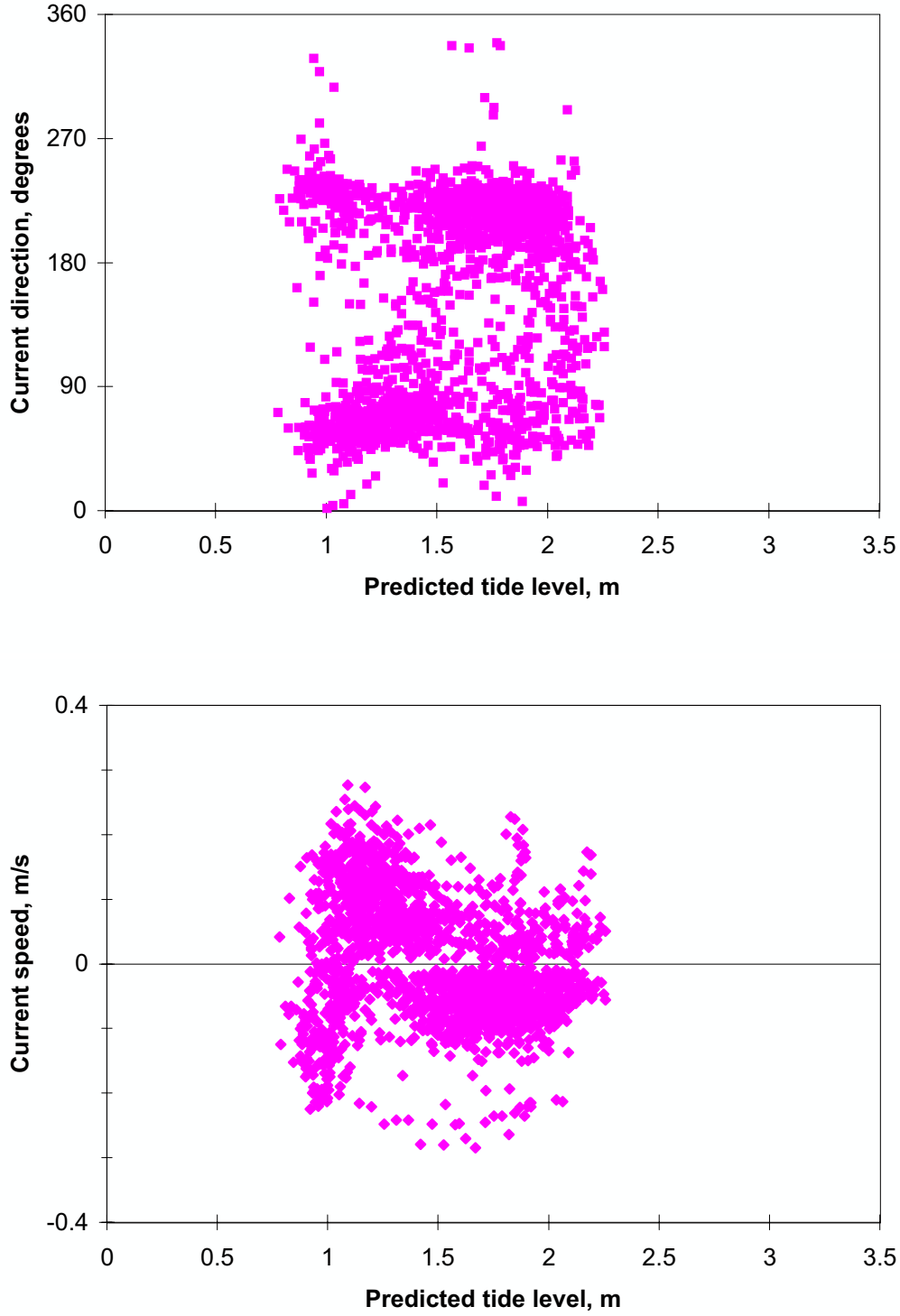

Figure 87. Northern current meter, rising tide, R < 1.4 m
1 July 1996 to 31 October 1996

Above: Current direction *vs* predicted tide level; all data

Below: Current speed *vs* predicted tide level; all data

θ_c < 125°, positive θ_c >= 125°, negative

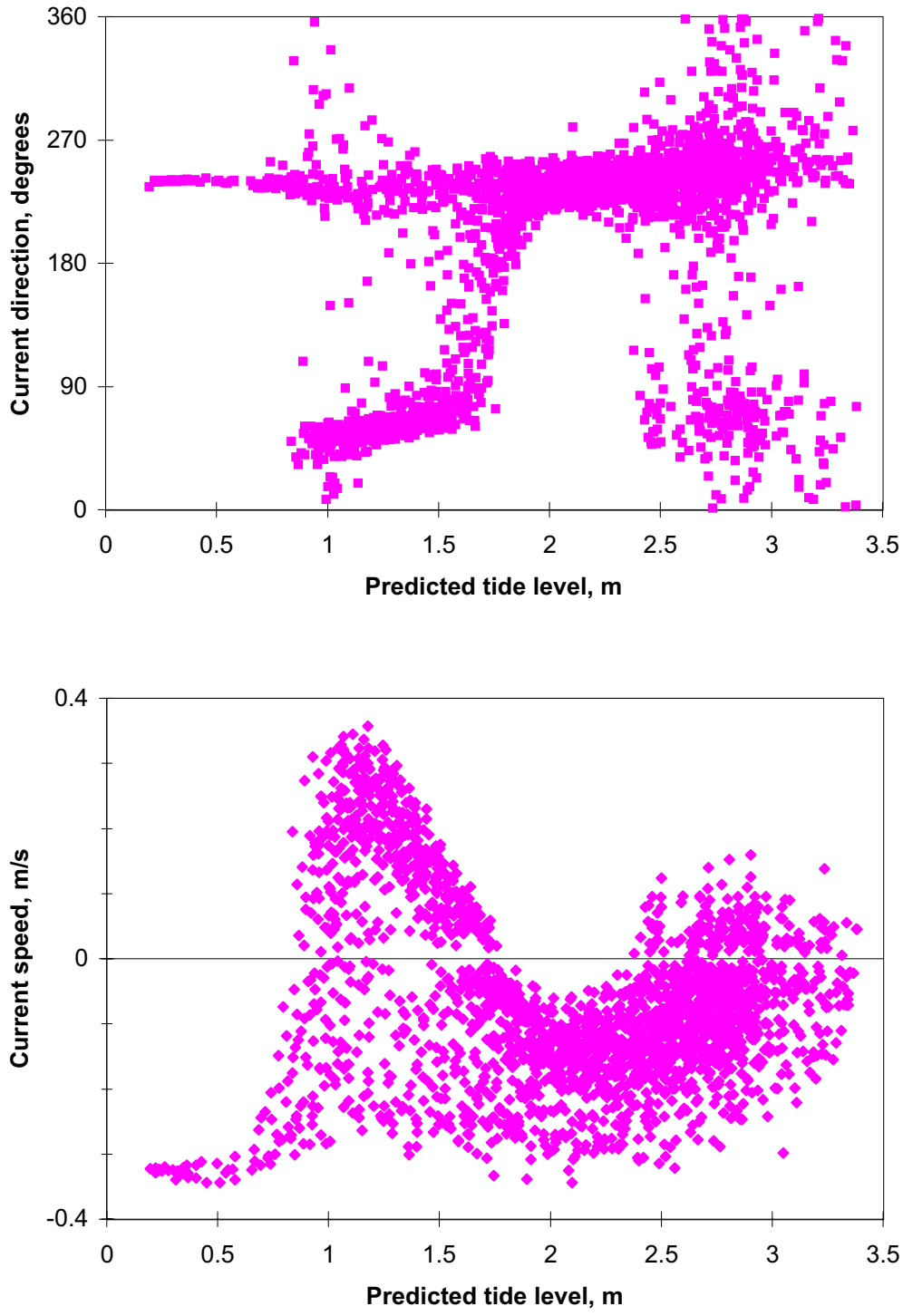

Figure 88. Northern current meter, rising tide, R >= 2.0 m
1 November 1996 to 18 March 1997

Above: Current direction *vs* predicted tide level; all data

Below: Current speed *vs* predicted tide level; all data

θ_c < 125°, positive θ_c >= 125°, negative

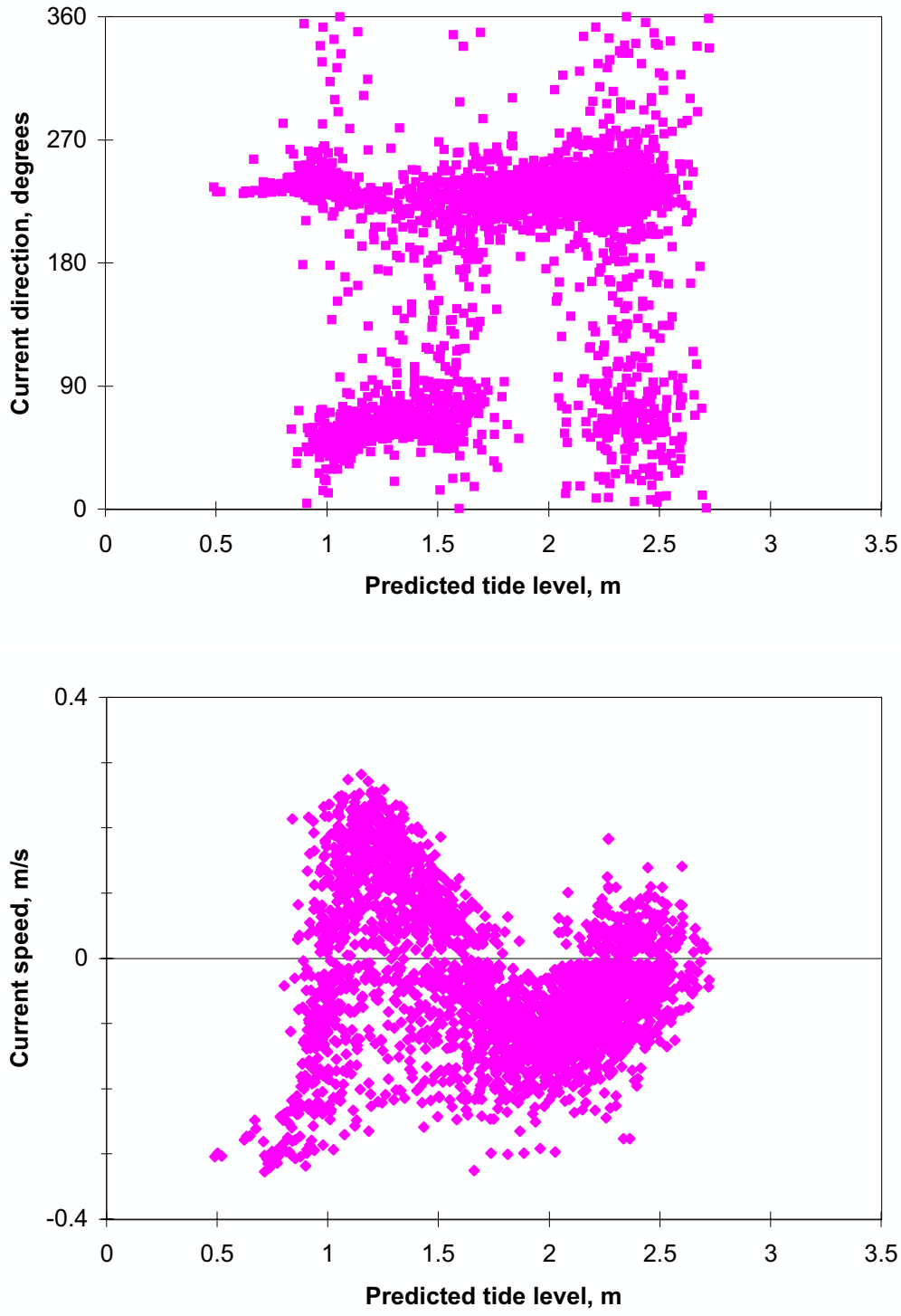

Figure 89. Northern current meter, rising tide, 1.4 m <= R < 2.0 m
1 November 1996 to 18 March 1997

Above: Current direction *vs* predicted tide level; all data

Below: Current speed *vs* predicted tide level; all data

θ_c < 125°, positive θ_c >= 125°, negative

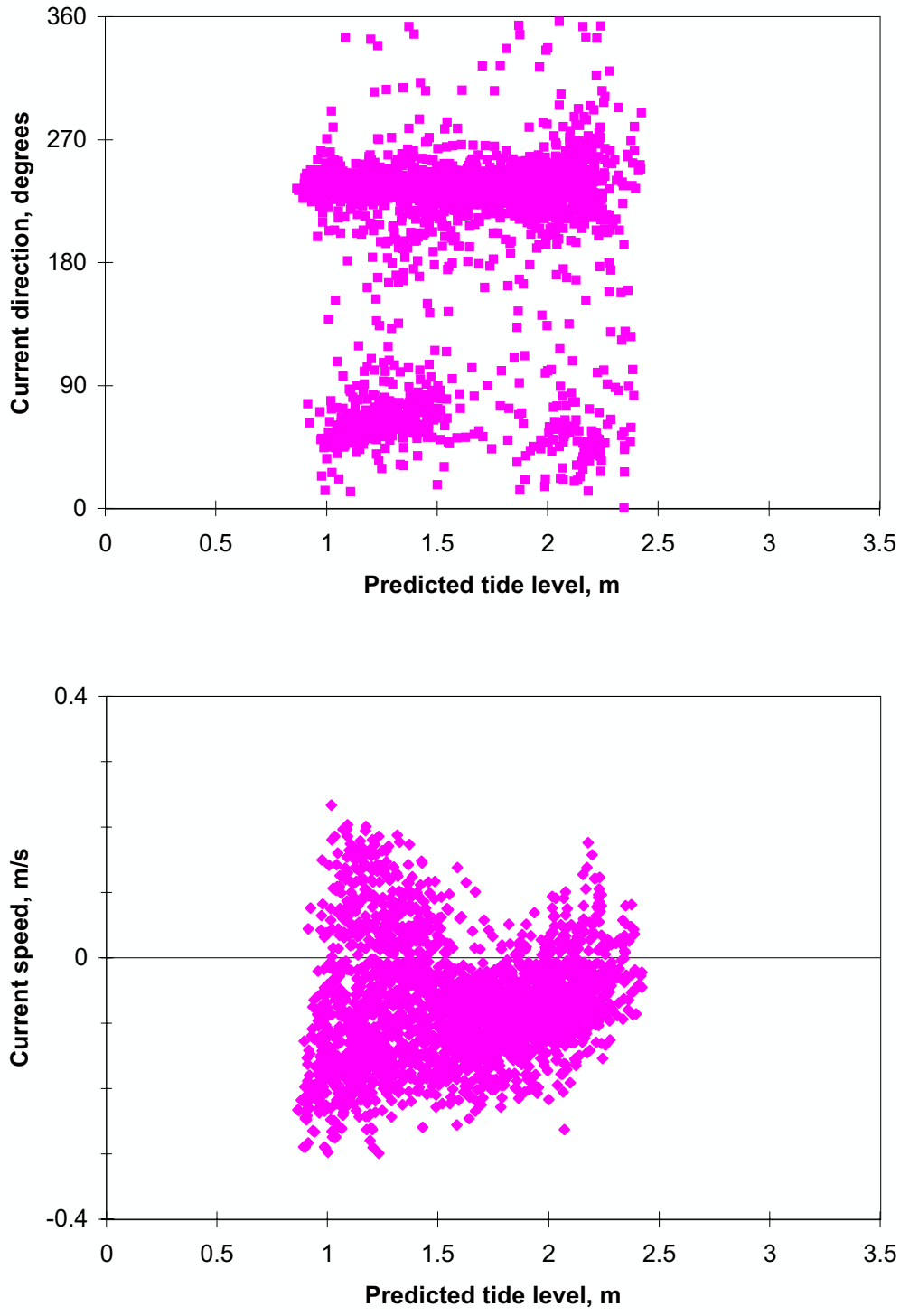

Figure 90. Northern current meter, rising tide, R < 1.4 m
1 November 1996 to 18 March 1997

Above: Current direction *vs* predicted tide level; all data

Below: Current speed *vs* predicted tide level; all data

θ_c < 125°, positive θ_c >= 125°, negative

7.3.4 Northern current meter, falling tide

The falling tidal velocities measured at the northern current meter during the period 17 March to 30 June 1996 have been presented previously in Figures 43, 47 and 51. Similar data for the period 1 July to 31 October 1996 is presented in Figures 91, 92 and 93 and for the period 1 November 1996 to 18 March 1997 in Figures 94, 95 and 96. The percentages of positive and negative currents in each tidal range group during each analysis period are given in Table 13.

Table 13 % positive and % negative currents in each tidal range group during each analysis period - northern current meter – falling tide – all data

Period	Direction θ_c *	Tidal range group			
		Large R ≥ 2.0 m	Medium 2.0 > R ≥ 1.4 m	Small R < 1.4 m	All
Overall 17 Mar. 1996 to 18 Mar. 1997	+ve	49.7	36.1	19.5	36.4
	-ve	50.3	63.9	80.5	63.6
1 17 Mar. 1996 to 30 Jun. 1996	+ve	53.3	42.2	18.4	39.8
	-ve	46.7	57.8	81.6	60.2
2 1 Jul. 1996 to 31 Oct. 1996	+ve	54.2	39.9	26.2	41.3
	-ve	45.8	60.1	73.8	58.7
3 1 Nov. 1996 to 18 Mar. 1997	+ve	43.1	29.1	15.2	30.0
	-ve	56.9	70.9	84.8	70.0

* $\theta_c < 125°$ is +ve ; $\theta_c \geq 125°$ is –ve.

For large tides (Figures 43, 91 and 94) the general pattern of variation of both θ_c and v was similar for tidally dominated conditions during all three periods. As for the rising tide (Figures 29 and 88) the two northeasterly storm events in early May and late July caused significant continuous outflow into the boat harbour with maximum negative velocities exceeding 0.7 m/s.

Again, during the period 1 November 1996 to 18 March 1997 (Figure 94), the more intense southeasterly winds caused more anticlockwise current reversals and fewer clockwise ones at high tide levels. Also during this period there were more negative outflows over the bund wall when low tides fell below its crest level than during the earlier two periods. Moreover, the maximum constant velocity under bund wall control (0.3 ± 0.05 m/s) was attained earlier during the first and third periods, when $z_0 \approx 1.1$ to 1.2 m, than during the second period, when $z_0 \approx 1.0$ m.

The occurrence of extended durations of outflow over the bund wall at low tides during the period 1 November 1996 to 18 March 1997 (Figure 94) is associated with the extended eastsoutheasterly to southeasterly event caused by tropical cyclone "*Justin*" in early March. For several days the offreef wave height H_{BP} varied in cyclical manner with the changing tidal conditions. H_{BP} was about 1.0 m during the initial phase of the rising tide when $z_0 < z_{msl} = 1.52$ m. It then increased to a maximum value of 2 to 2.5 m when the falling tide approached z_{msl} again. As discussed in sections 6.4.4 and 6.5.4, wave heights > 1.25 m are generally sufficient to completely reverse the current flow at the northern current meter during the complete tidal cycle. Hence the larger waves breaking on the northern reef-rim during the falling tide pump more water onto the northern reef-flat and cause continuous runoff over the northern bund wall and into the boat harbour during the falling tide, including the period when $z_0 < z_b$.

The current behaviour for medium tides during the three analysis periods (Figures 47, 92 and 95) was similar to that during large tides.

With small tides there were more anticlockwise current reversals during the first and third periods of analysis (Figures 51 and 96) when southeasterly winds were more frequent and fewer anticlockwise current reversals during the second period (Figure 93) when northwesterly winds were more significant than in the other two periods. Negative velocities dominated during all three periods but the proportion of positive velocities was greatest during the second period (Table 13).

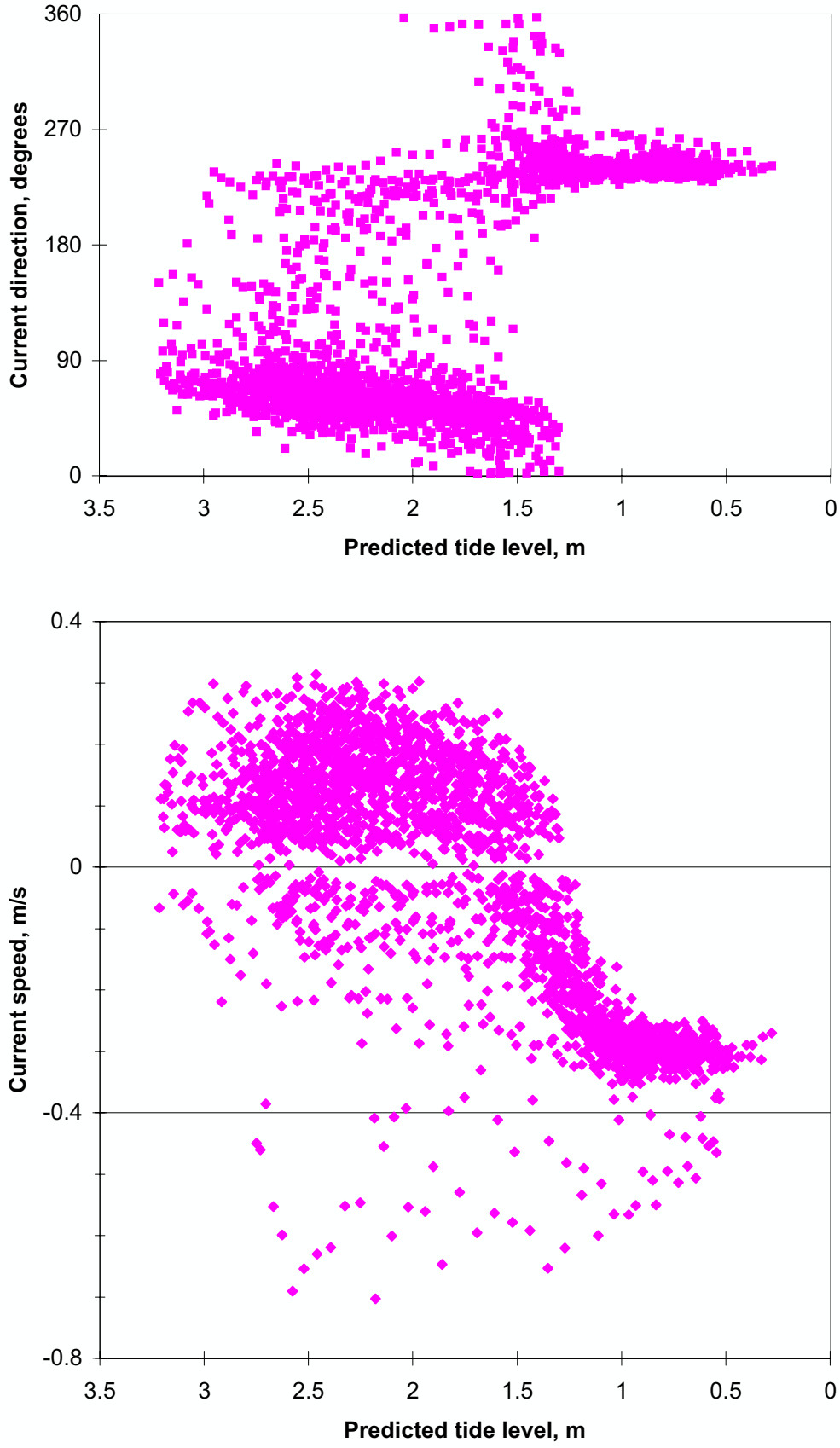

Figure 91. Northern current meter, falling tide, R >= 2.0 m
1 July 1996 to 31 October 1996

Above: Current direction *vs* predicted tide level; all data

Below: Current speed *vs* predicted tide level; all data

θ_c < 125°, positive θ_c >= 125°, negative

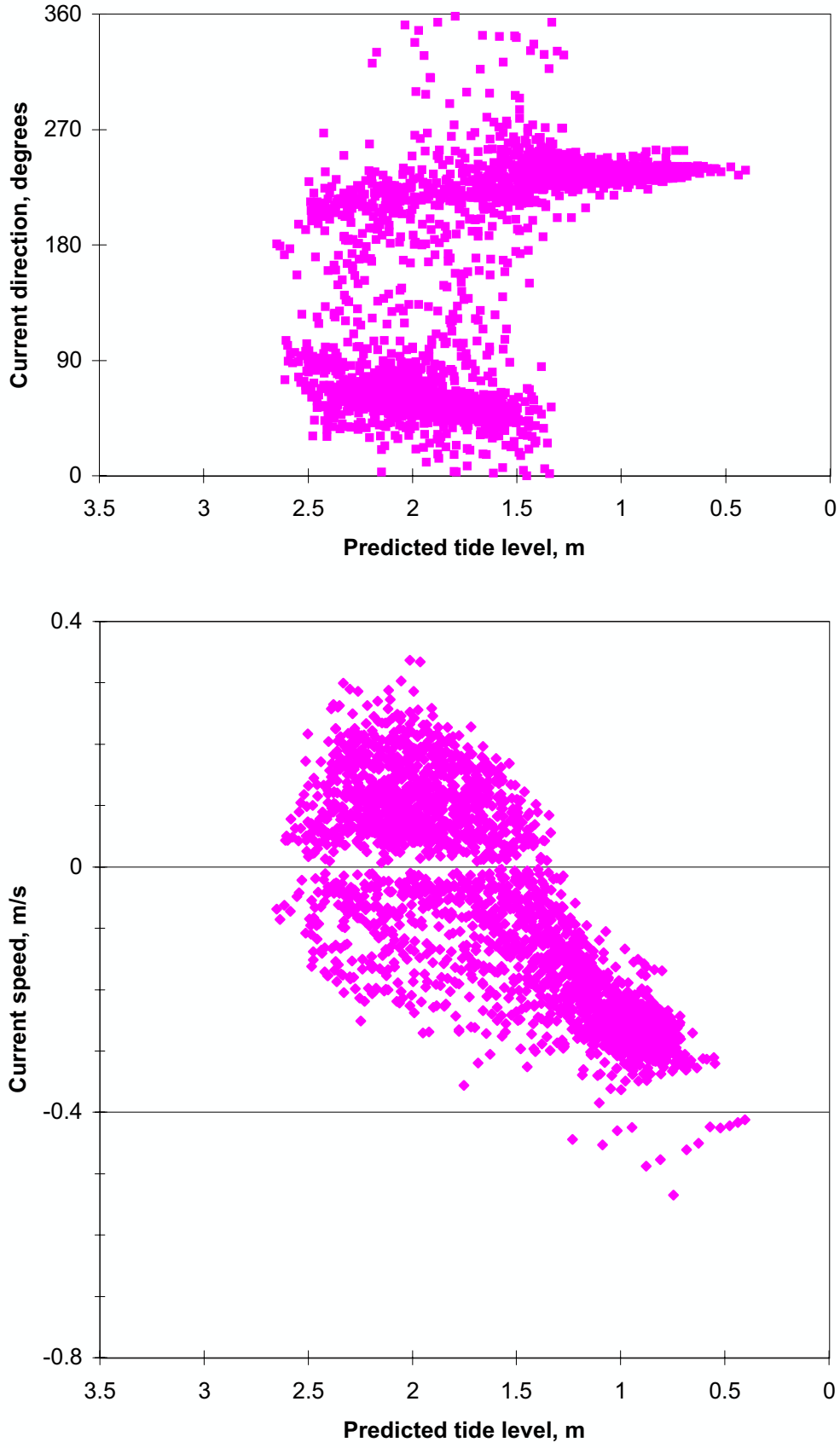

Figure 92. Northern current meter, falling tide, 1.4 m <= R < 2.0 m 1 July 1996 to 31 October 1996

Above: Current direction *vs* predicted tide level; all data

Below: Current speed *vs* predicted tide level; all data

θ_c < 125°, positive θ_c >= 125°, negative

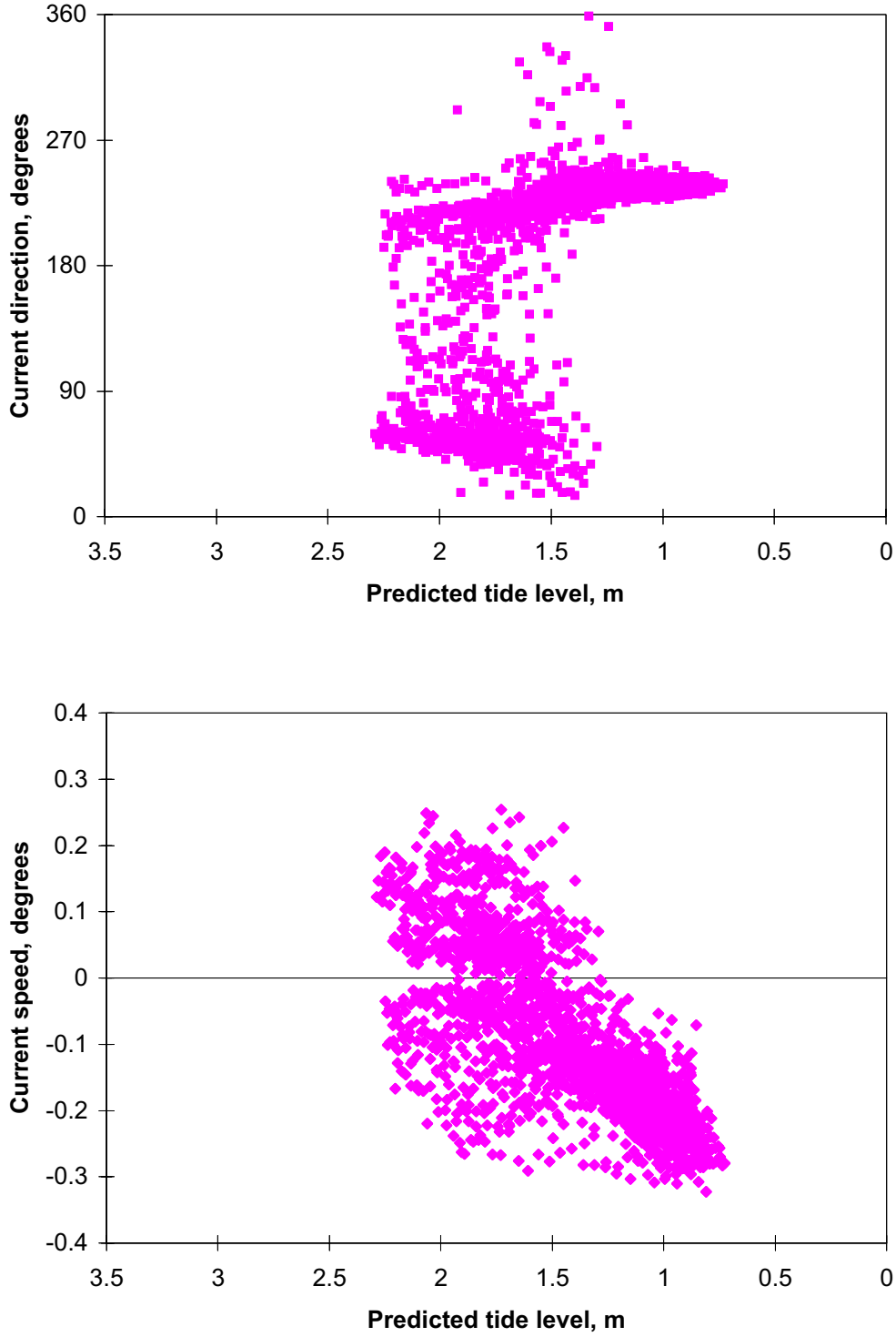

Figure 93. Northern current meter, falling tide, R < 1.4 m
1 July 1996 to 31 October 1996

Above: Current direction *vs* predicted tide level; all data

Below: Current speed *vs* predicted tide level; all data

θ_c < 125°, positive θ_c >= 125°, negative

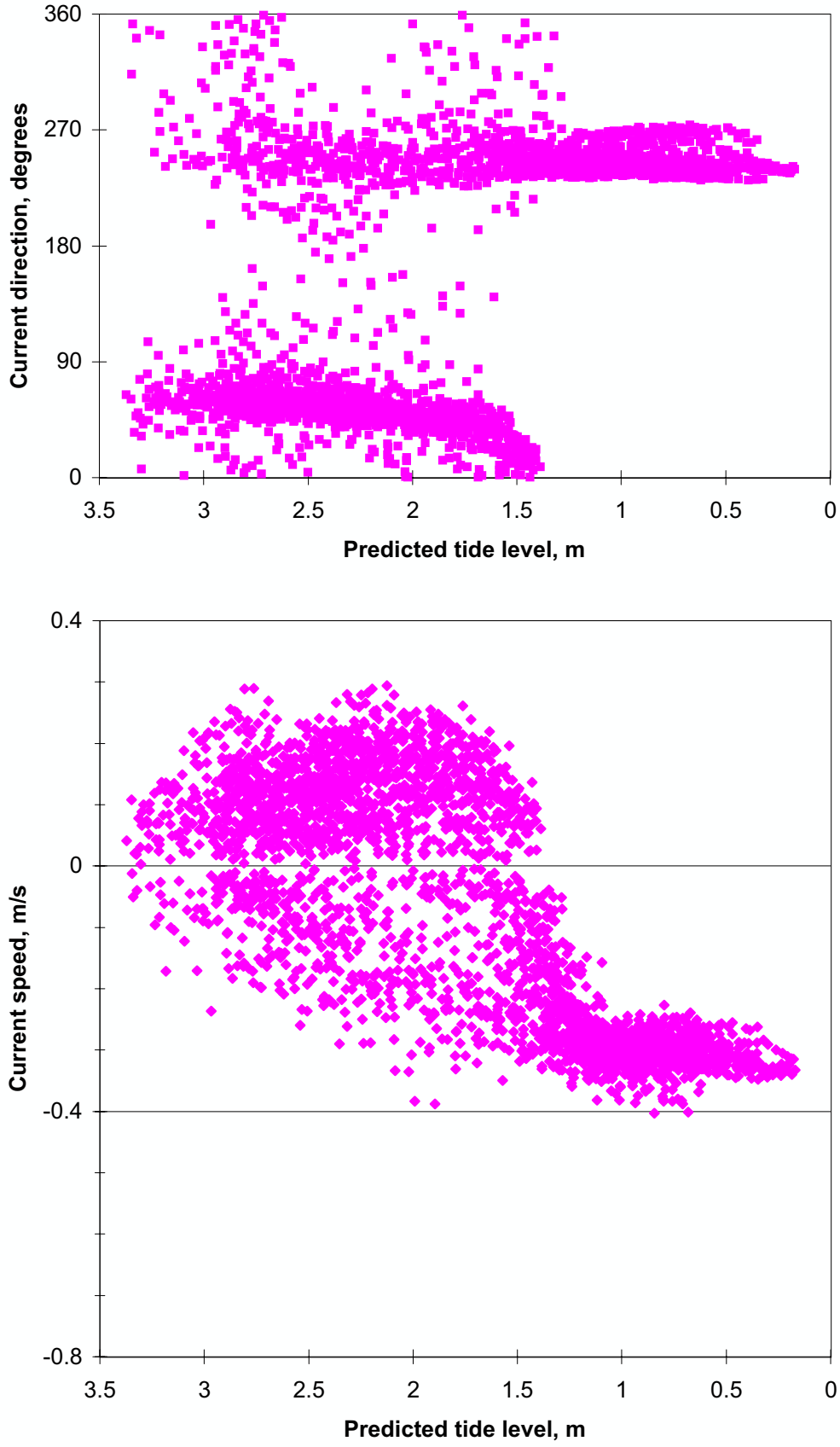

Figure 94. Northern current meter, falling tide, R >= 2.0 m
1 November 1996 to 18 March 1997

Above: Current direction *vs* predicted tide level; all data

Below: Current speed *vs* predicted tide level; all data

θ_c < 125°, positive θ_c >= 125°, negative

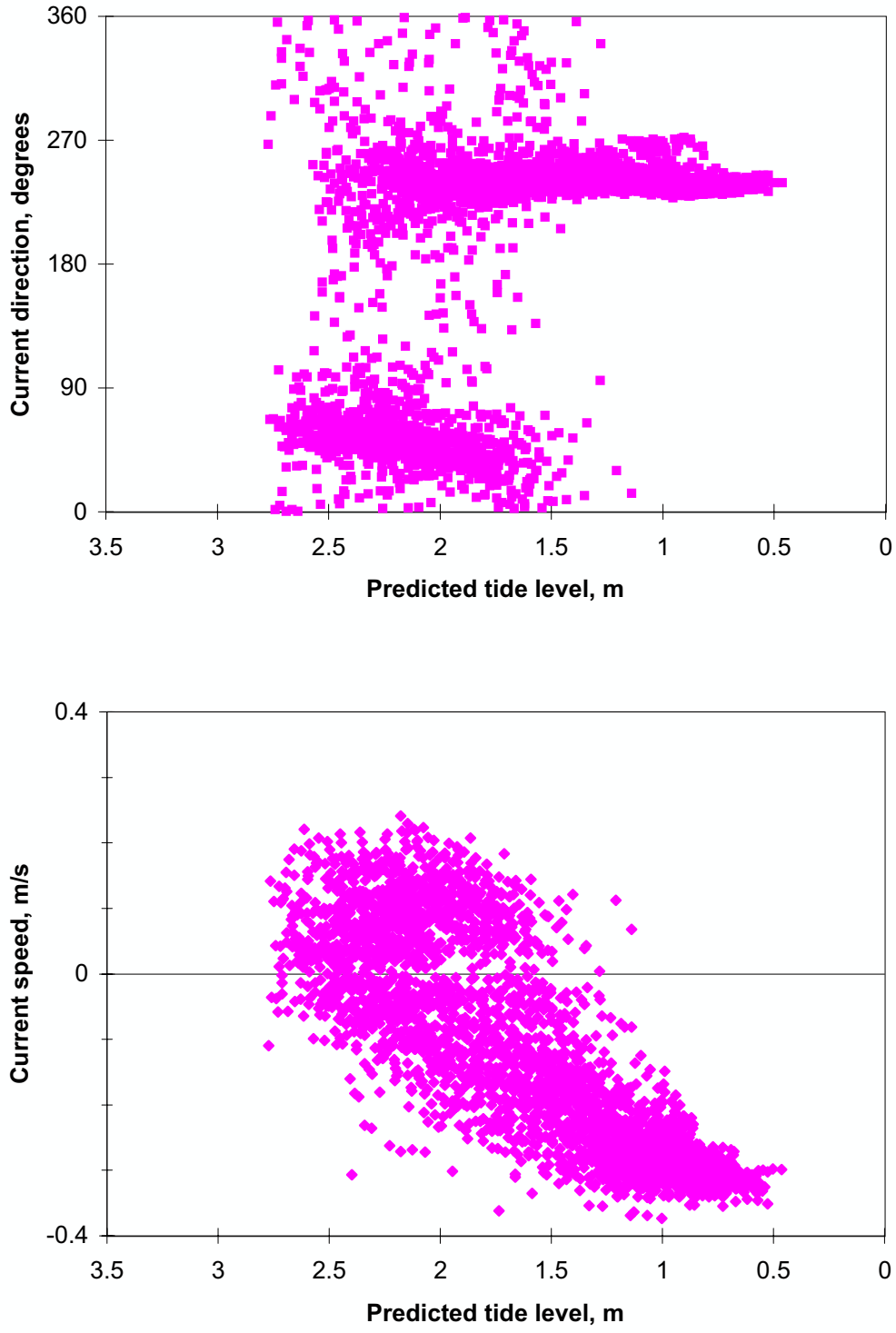

Figure 95. Northern current meter, falling tide, 1.4 m <= R < 2.0 m
1 November 1996 to 18 March 1997

Above: Current direction *vs* predicted tide level; all data

Below: Current speed *vs* predicted tide level; all data

θ_c < 125°, positive θ_c >= 125°, negative

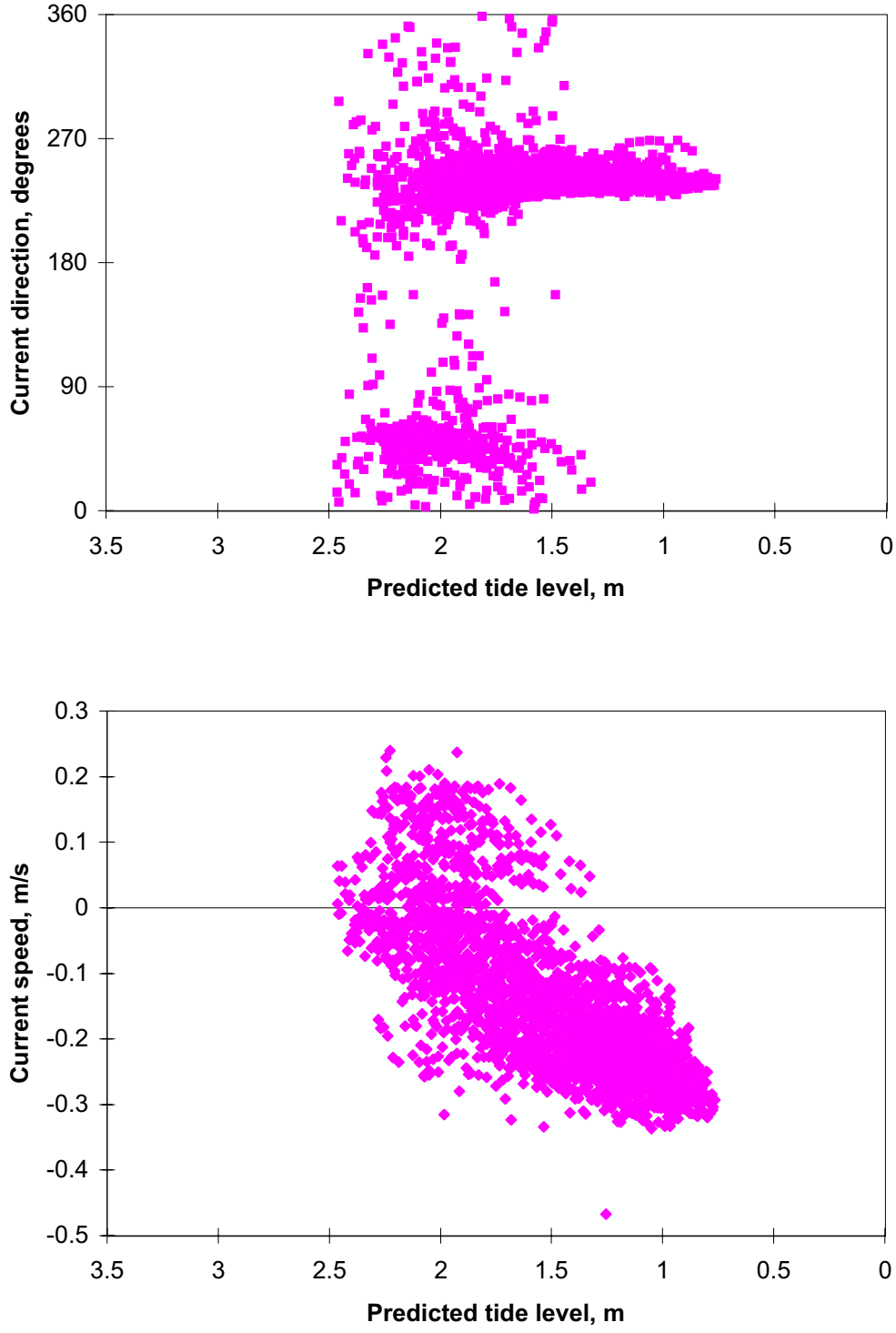

Figure 96. Northern current meter, falling tide, R < 1.4 m
1 November 1996 to 18 March 1997

Above: Current direction *vs* predicted tide level; all data

Below: Current speed *vs* predicted tide level; all data

θ_c < 125°, positive θ_c >= 125°, negative

7.4 Reef-top currents and offreef wave height

7.4.1 Introduction

The results of previous analyses in Chapter 6 and 7 clearly show that the magnitudes of the reef-top currents increase with increasing offreef wave heights. To investigate this relationship more specifically, the data from all three measurement periods were combined and a new analysis made in which current velocity is plotted against offreef wave height. As in previous analyses this new analysis, for both rising and falling tides at each current meter, involves the same three tidal range groups: -

Small tides	$R < 1.4$ m
Average tides	$1.4 \text{ m} \leq R < 2.0$ m
Large tides	$2.0 \text{ m} \leq R$

Since the amount of data in each file was very large, data for offreef wave heights less than 0.5 m was removed from each data set.[2] The deleted data corresponds to mild conditions when tidal currents dominate and the influence of waves upon the reef-top currents is small. In this analysis the trend lines and correlation coefficients have been calculated from second order polynomials.

7.4.2 Southern current meter, rising tide

Current speed is plotted as a function of offreef wave height H_{Wis} for the three tidal range groups in Figures 97, 98 and 99. Following the analysis of the effect of wind direction in section 7.3.2, each graph shows data from two groups:

(i) wind direction the same as the wave-generated current ($105^o \leq \theta_w < 165^o$); and
(ii) other wind directions ($165^o \leq \theta_w < 105^o$).

The data with winds in the same general direction as the wave-generated current has a much better correlation coefficient than that with opposing winds (Figures 97, 98 and 99). It also indicates an approximate linear relationship between velocity and wave height for each tidal group. In most cases, its correlation coefficient is slightly better than that for the overall data set comprising winds from all directions.

[2] In one case, average rising tides at the southern current meter, data for $H_{Wis} < 0.55$ m had to be removed to reduce the file to a manageable size (Figure 98).

7.4.3 Southern current meter, falling tide

In this case only data with winds from the sector $105^o \leq \theta_w < 165^o$ is shown (Figures 100, 101 and 102), since opposing winds are likely to reduce or deflect wave-generated currents on the reef-top. However, the data has been split into two groups, one for tide levels $z_o \geq 1.5$ m when tidal flows are generally eastward and a second one for $z_o < 1.5$ m when all flows are westward towards the boat harbour.

When $z_o \geq 1.5$ m the current velocity has an approximately linear relationship with wave height for large and average tides (Figures 100 and 101) but this tends to a non-linear relationship for small tides (Figure 102). It is noted that Figure 102 has no data points for wave heights greater than 2 m.

When $z_o < 1.5$ m there is a nonlinear relationship with a similar form for all tidal ranges (Figures 100, 101 and 102). At low wave heights (< 1 m) the current velocity tends to a constant average value of about 0.15 m/s but, as the wave height increases above 1 m, the velocity also increases. However, the correlation coefficient between velocity and wave height is significantly lower when $z_o < 1.5$ m ($R^2 \leq 0.32$) than when $z_o \geq 1.5$ m ($R^2 > 0.40$).

7.4.4 Northern current meter, rising tide

Current speed is plotted as a function of offreef wave height H_{BP} for the three tidal range groups in Figures 103, 104 and 105. Only data with wind directions from the sector $320^o \leq \theta_w < 180^o$ are shown so as to exclude winds opposing the wave-generated currents. However, the data has been split into two groups: one for tide levels $z_o < 1.7$ m, when tidal flows are generally northeastward opposing the wave-generated flow, and a second group for $z_o \geq 1.7$ m, when tidal flows are southwestward in the same direction as the wave-generated flow.

There is less data for wave heights larger than 1.5 m for the northern current meter than for the southern current meter. Hence the relationship between current velocity and wave height is not so well defined. Nevertheless, the larger wave heights clearly generate stronger currents than the smaller waves.

When $z_o < 1.7$ m and the tidal currents are opposing the wave-generated currents, the velocity–wave height relationship is concave upwards, reaching a maximum positive value when $H_{BP} \approx$ 0.5 m. These maximum values decrease with decreasing tidal range as indicated by curves A in

Figures 32, 36 and 39.[3] It is also clear that larger wave heights are necessary to reverse the currents from the larger tidal ranges, with average reversals occurring at wave heights of 1.0 m, 0.8 m and 0.6 m for large, average and small tides respectively.

When $z_o \geq 1.7$ m, generally the currents at this site are always negative (southwestward) and this behaviour results in the velocity–wave height relationship being convex upwards with a non-zero limiting average tidal current velocity of less than – 0.1 m/s when the wave height becomes negligible.

7.4.5 Northern current meter, falling tide

As for the rising tide at the northern current meter, only data with wind directions from the sector $320^o \leq \theta_w < 180^o$ are shown (Figures 106, 107 and 108). The data are split into two groups as for the southern current meter data, one for the early phase of the falling tide, when $z_o \geq 1.5$ m, and one for the later phase, when $z_o < 1.5$ m.

For large and average tides, the highest wave heights recorded are larger than those on the southern side of the reef, attaining values greater than 3 m. However, for small tides the largest wave heights recorded were only about 1.5 m compared with 2 m on the southern side of the reef.

When $z_o \geq 1.5$ m, the relationship between current velocity and wave height is linear for small and average tides but appears to be nonlinear (convex upwards) for large tides. The wave height large enough to reverse the tidal currents increases from 0.5 m for small tides to more than 1 m for large tides.

When $z_o < 1.5$m, only large tides show a nonlinear relationship between current velocity and wave height similar to that found at the southern current meter site. At the northern current meter site the average and small tides show an almost linear relationship on the falling tide when $z_o < 1.5$ m.

As the wave height decreases below 1.5 m, the maximum negative velocity tends to a constant value of about 0.35 m/s under all tidal conditions.

[3] The relationship between tidal currents during mild conditions and wave generated currents is discussed further in Section 4.6 of Gourlay and Hacker 2008b.

7.5 Summary

The wind, wave and tidal conditions during each of the three analysis periods have been reviewed and it appears that the first period, 17 March to 30 June 1996, for which the detailed analyses described in Chapter 6 were made, is generally the most similar to the conditions for the whole period during which data was collected.

The reef-top current conditions are generally similar during the three periods of analysis but there were some significant differences associated with both seasonal variations in wind and wave climates and the occurrence of storm events.

The direction of current reversals, either clockwise or anticlockwise, is affected by wind direction particularly at higher tide levels. The strength and duration of flow over the bund walls, when ocean low tides fall below the bund wall crests and water is ponded on the reef-flat by weir action, is affected significantly by changes in wind and wave direction and probably also by variations in tidal range. Paradoxically, outflow over the southern bund wall on the falling tide increases when winds/waves are larger on the northern side of the reef and reduces when easterly waves break on distant reef-rims. Outflow over the northern bund wall on the falling tide increases for eastsoutheasterly to southeasterly conditions because tide modulated refraction increases wave heights breaking on the northern side of the reef.

The wave-generated currents on the reef-top generally increase in magnitude with increasing offreef wave height. When the influence of tidal currents is negligible the relationship is approximately linear (see Gourlay and Hacker 2008b, Chapter 4, for detailed analysis and discussion of this relationship).

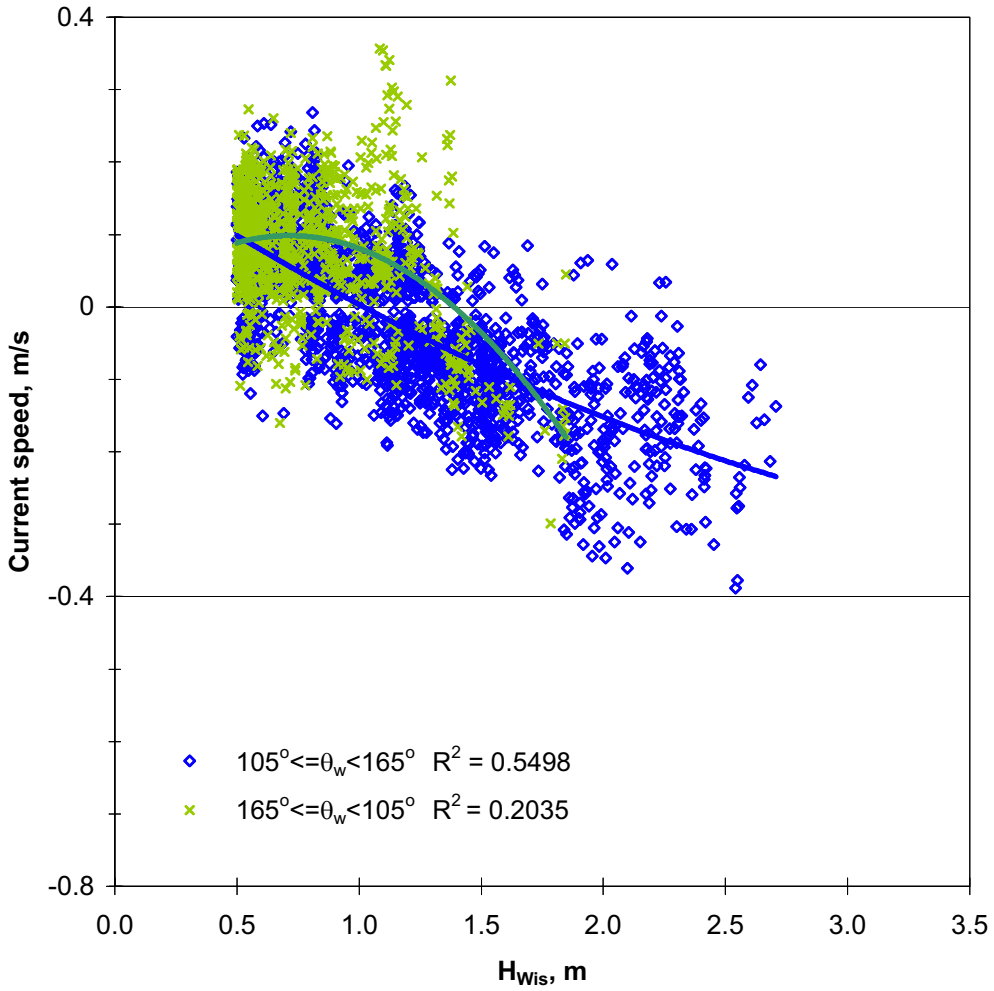

Figure 97. Southern current meter, rising tide, R >= 2.0 m
17 March 1996 to 18 March 1997
Current speed vs wave height in Wistari Channel, H

Only data with H_{Wis} >= 0.5 m and H_{BP} < H_{Wis}

θ_c < 125°, positive θ_c >= 125°, negative
Trendlines 2nd order polynomials

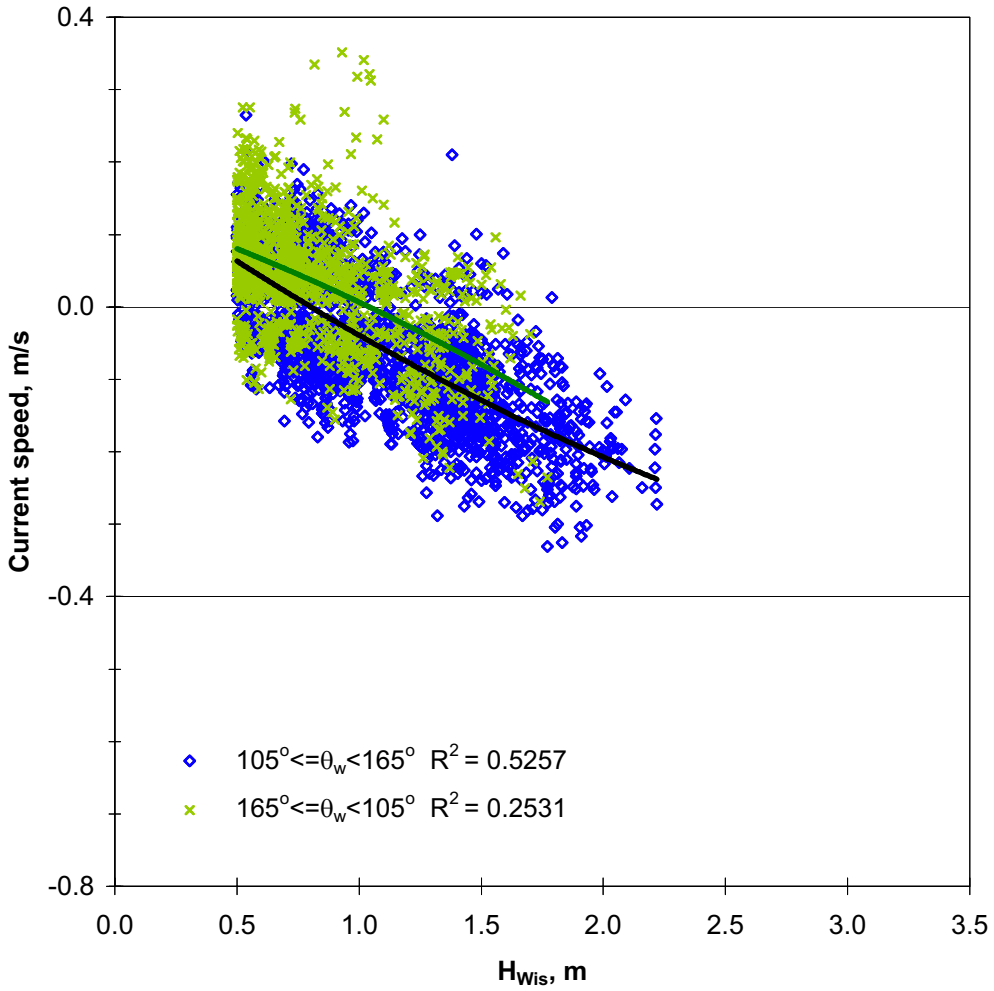

Figure 98. Southern current meter, rising tide, 1.4 m<= R < 2.0 m
17 March 1996 to 18 March 1997
Current speed vs wave height in Wistari Channel, H

Only data with H_{Wis} >= 0.55 m

θ_c < 125°, positive θ_c >= 125°, negative
Trendlines 2nd order polynomials

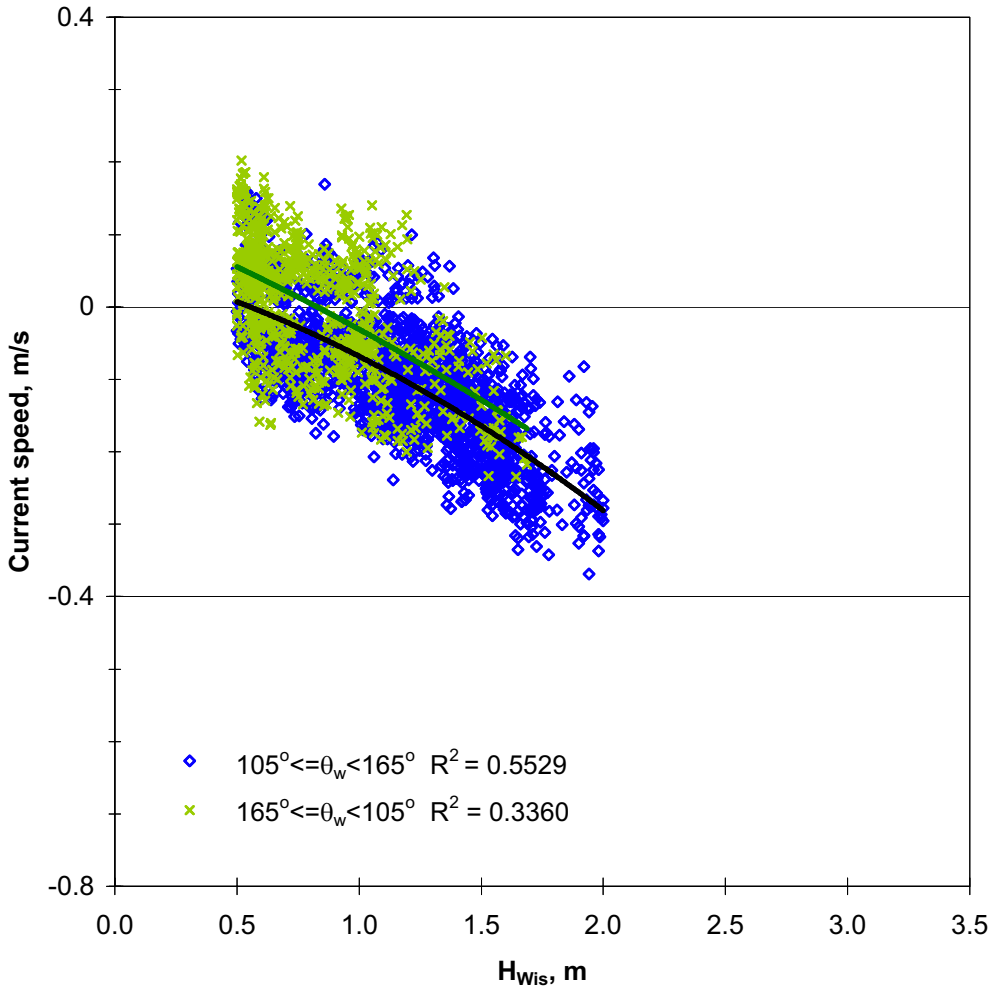

Figure 99. Southern current meter, rising tide, R < 1.4 m
17 March 1996 to 18 March 1997
Current speed vs wave height in Wistari Channel, H

Only data with H_{Wis} >= 0.5 m

θ_c < 125°, positive θ_c >= 125°, negative
Trendlines 2nd order polynomials

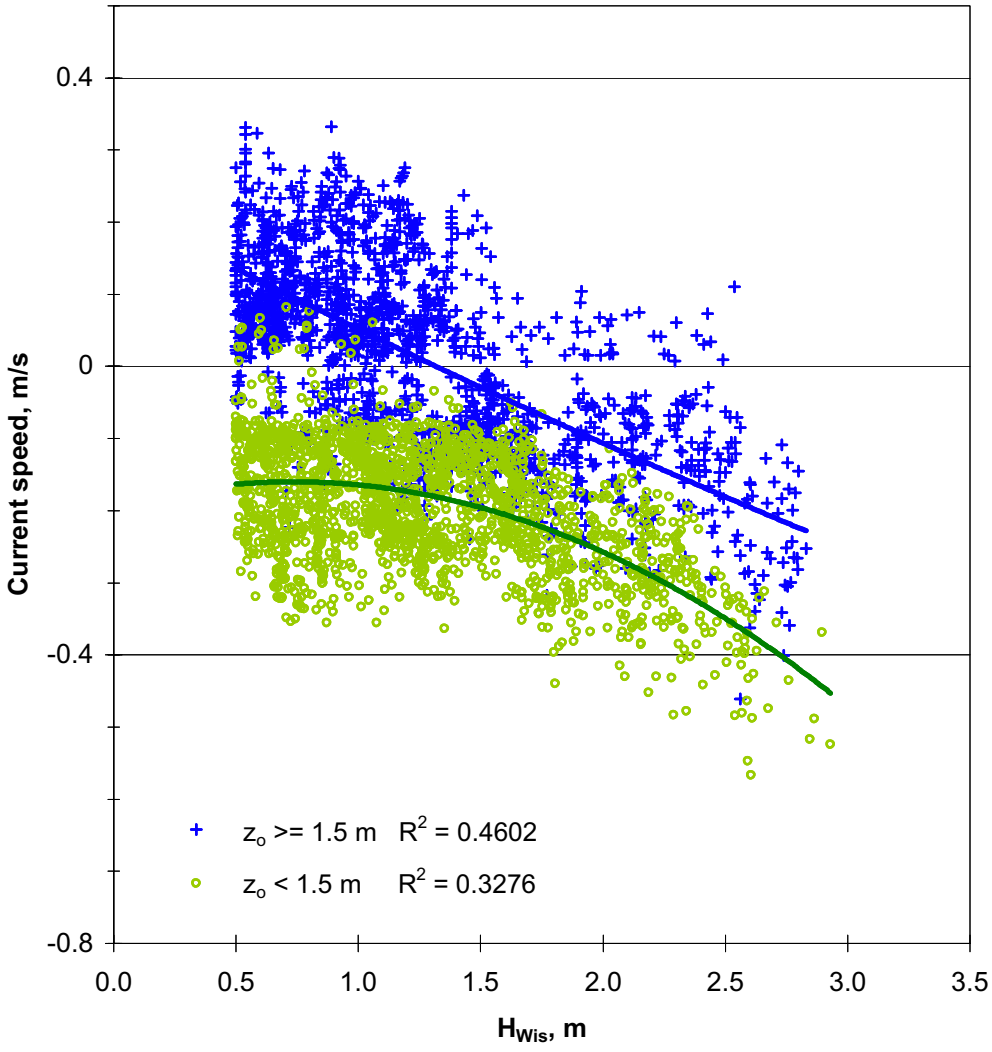

Figure 100. Southern current meter, falling tide, R >= 2.0 m
17 March 1996 to 18 March 1997
Current speed vs wave height in Wistari Channel, H

Only data with H_{Wis} >= 0.5 m

Only data with $105^{o} <= \theta_{w} < 165^{o}$

$\theta_c < 125^{o}$, positive $\theta_c >= 125^{o}$, negative

Trendlines 2nd order polynomials

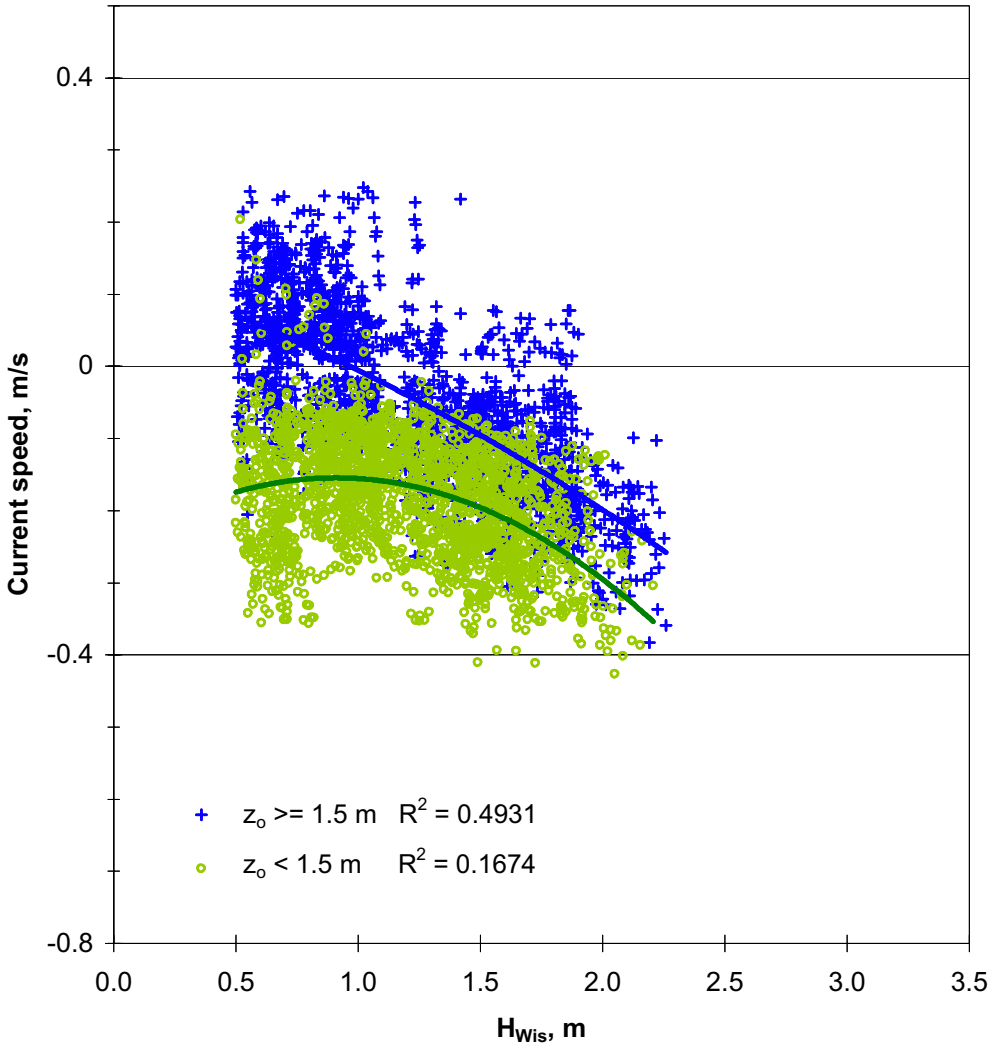

Figure 101. Southern current meter, falling tide, 1.4 m <= R < 2.0 m
17 March 1996 to 18 March 1997
Current speed vs wave height in Wistari Channel, H

Only data with H_{Wis} >= 0.5 m

Only data with $105^{o} <= \theta_{w} < 165^{o}$

$\theta_c < 125^{o}$, positive $\theta_c >= 125^{o}$, negative

Trendlines 2nd order polynomials

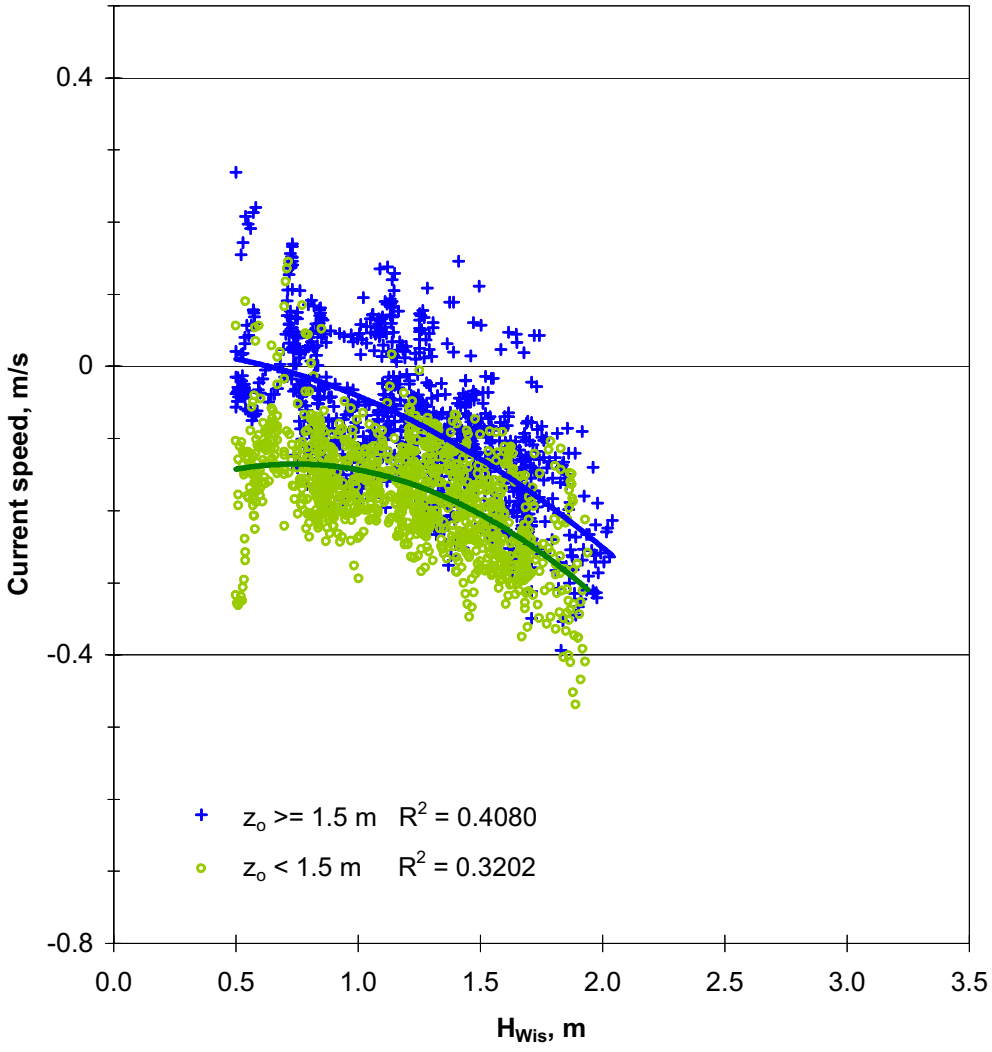

Figure 102. Southern current meter, falling tide, R < 1.4 m
17 March 1996 to 18 March 1997
Current speed vs wave height in Wistari Channel, H

Only data with H_{Wis} >= 0.5 m

Only data with 105^{o} <= θ_w < 165^{o}

θ_c < 125^{o}, positive θ_c >= 125^{o}, negative

Trendlines 2nd order polynomials

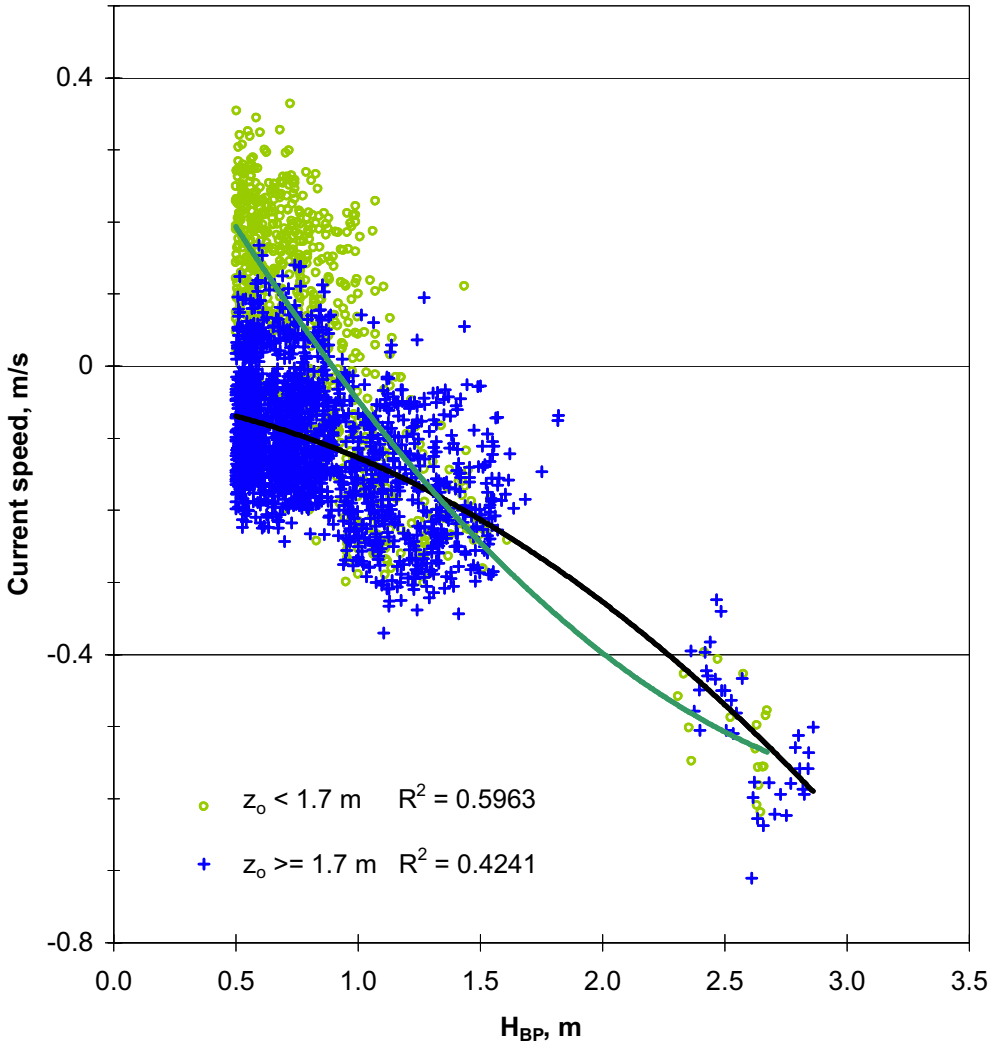

Figure 103. Northern current meter, rising tide, R >= 2.0 m
17 March 1996 to 18 March 1997
Current speed vs wave height offreef from Blue Pools, H_{BP}

Only data with H_{BP} >= 0.5 m

Only data with 320^o <= θ_w <180^o

θ_c < 125^o, positive θ_c >= 125^o, negative

Trendlines 2nd order polynomials

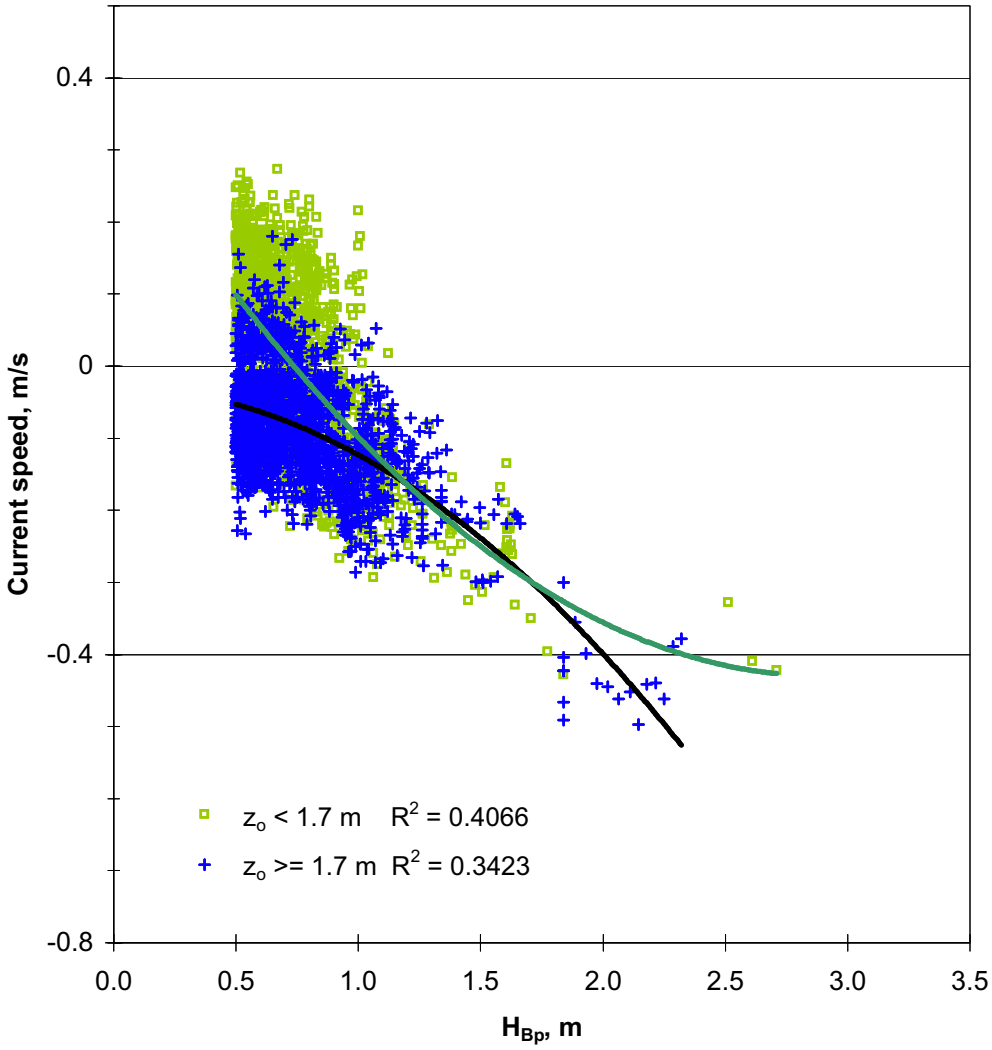

Figure 104. Northern current meter, rising tide, 1.4 m <= R < 2.0 m
17 March 1996 to 18 March 1997
Current speed vs wave height offreef from Blue Pools, H_{Bp}

Only data with H_{BP} >= 0.5 m

Only data with 320^o <= θ_w <180^o

θ_c < 125^o, positive θ_c >= 125^o, negative

Trendlines 2nd order polynomials

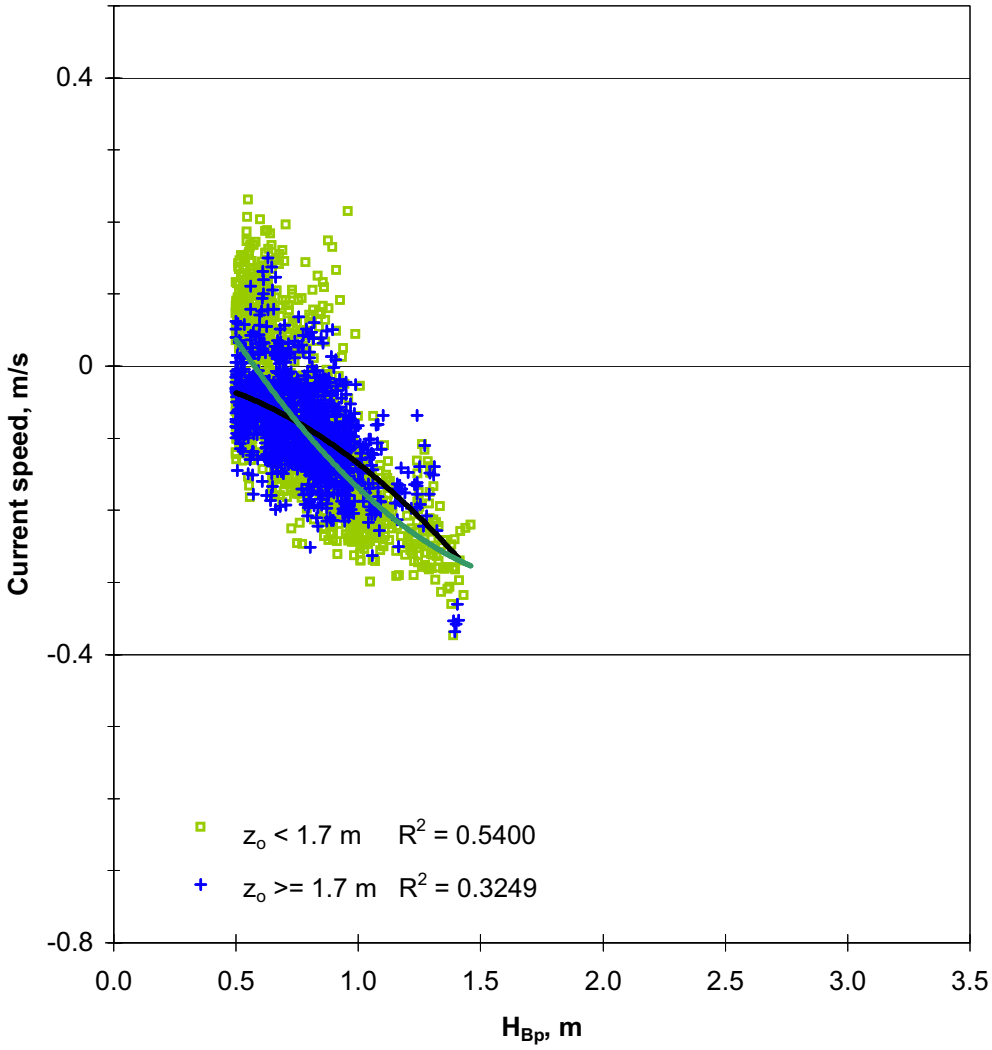

Figure 105. Northern current meter, rising tide, R < 1.4 m
17 March 1996 to 18 March 1997
Current speed vs wave height offreef from Blue Pools, H_{Bp}

Only data with H_{BP} >= 0.5 m

Only data with 320^o <= θ_w <180^o

θ_c < 125^o, positive θ_c >= 125^o, negative

Trendlines 2nd order polynomials

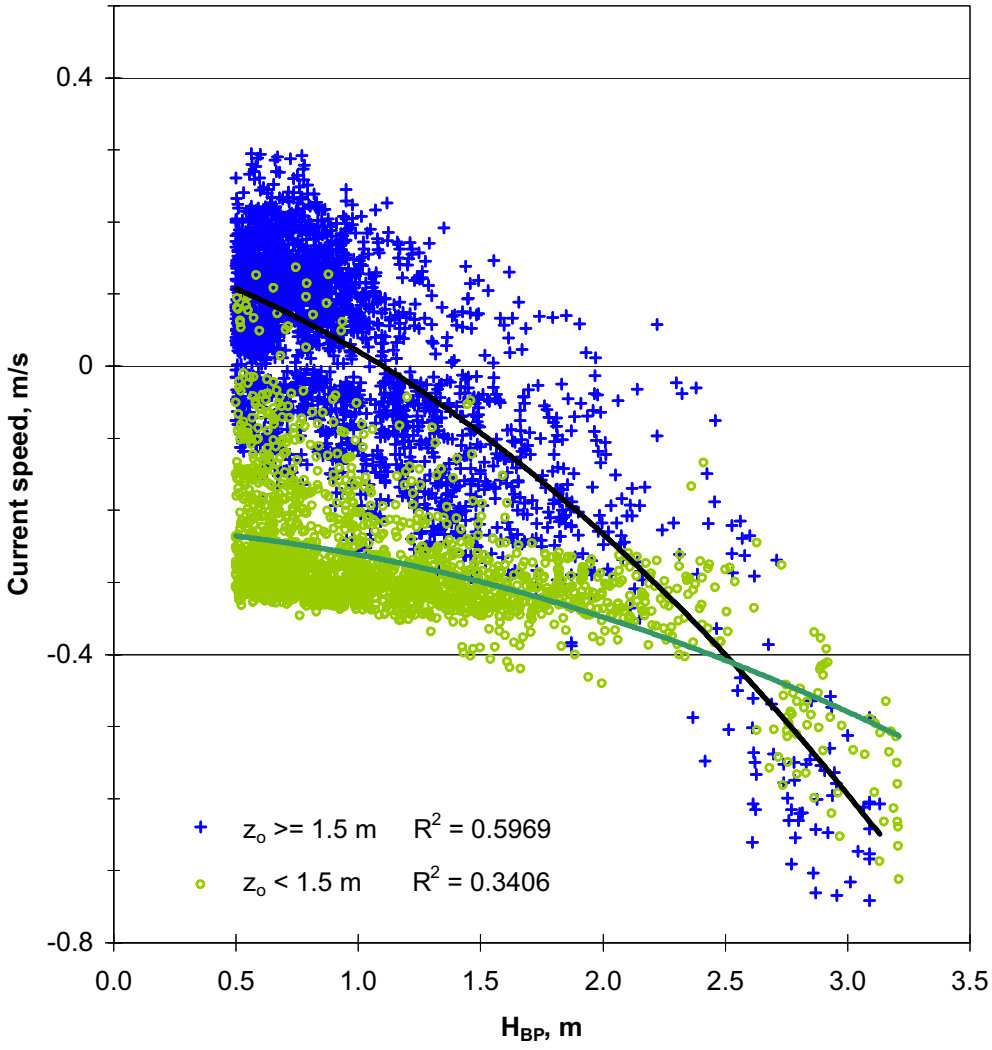

Figure 106. Northern current meter, falling tide, R >= 2.0 m
17 March 1996 to 18 March 1997
Current speed vs wave height offreef from Blue Pools, H_{BP}

Only data with H_{BP} >= 0.5 m

Only data with $320^o <= \theta_w < 180^o$

$\theta_c < 125^o$, positive $\theta_c >= 125^o$, negative

Trendlines 2nd order polynomials

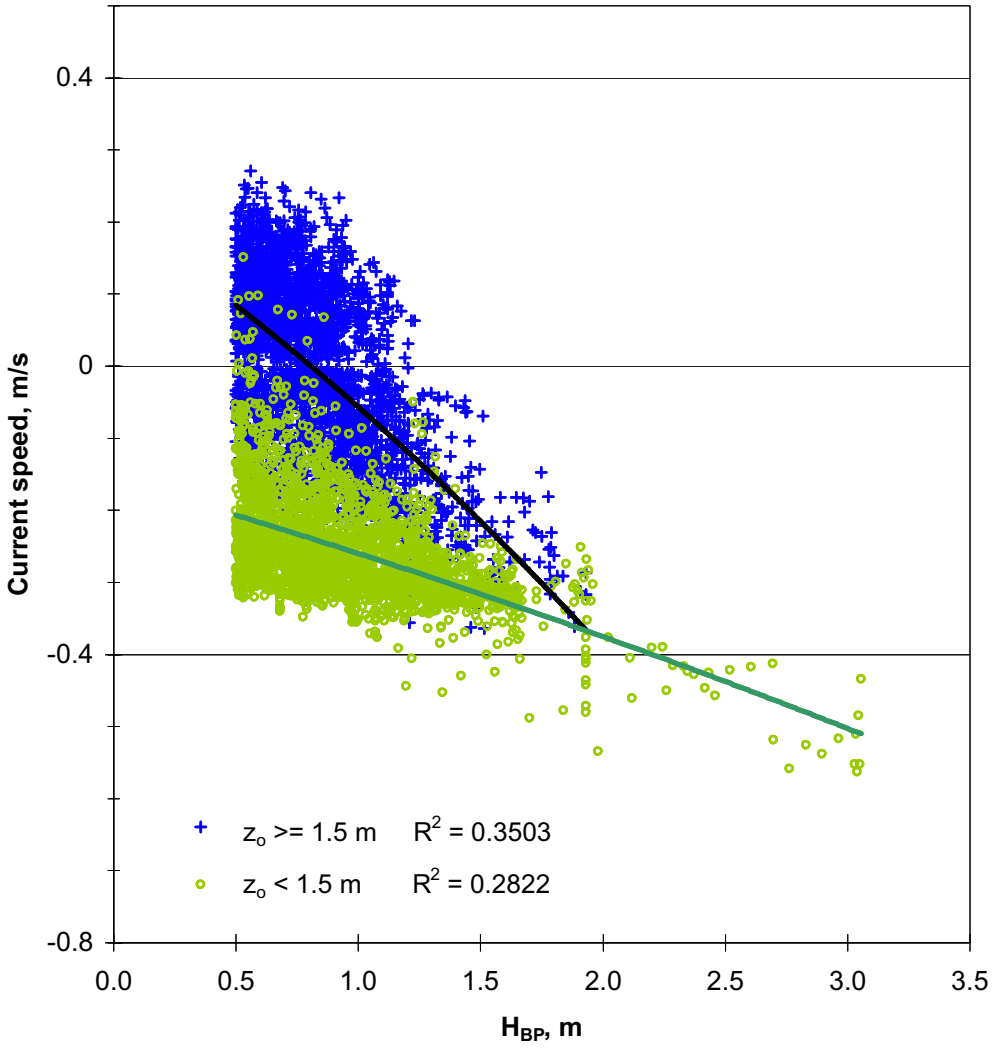

Figure 107. Northern current meter, falling tide, 1.4 m <= R < 2.0 m
17 March 1996 to 18 March 1997
Current speed vs wave height offreef from Blue Pools, H_{BP}

Only data with H_{BP} >= 0.5 m

Only data with 320^{o} <= θ_w <180^{o}

θ_c < 125^{o}, positive θ_c >= 125^{o}, negative

Trendlines 2nd order polynomials

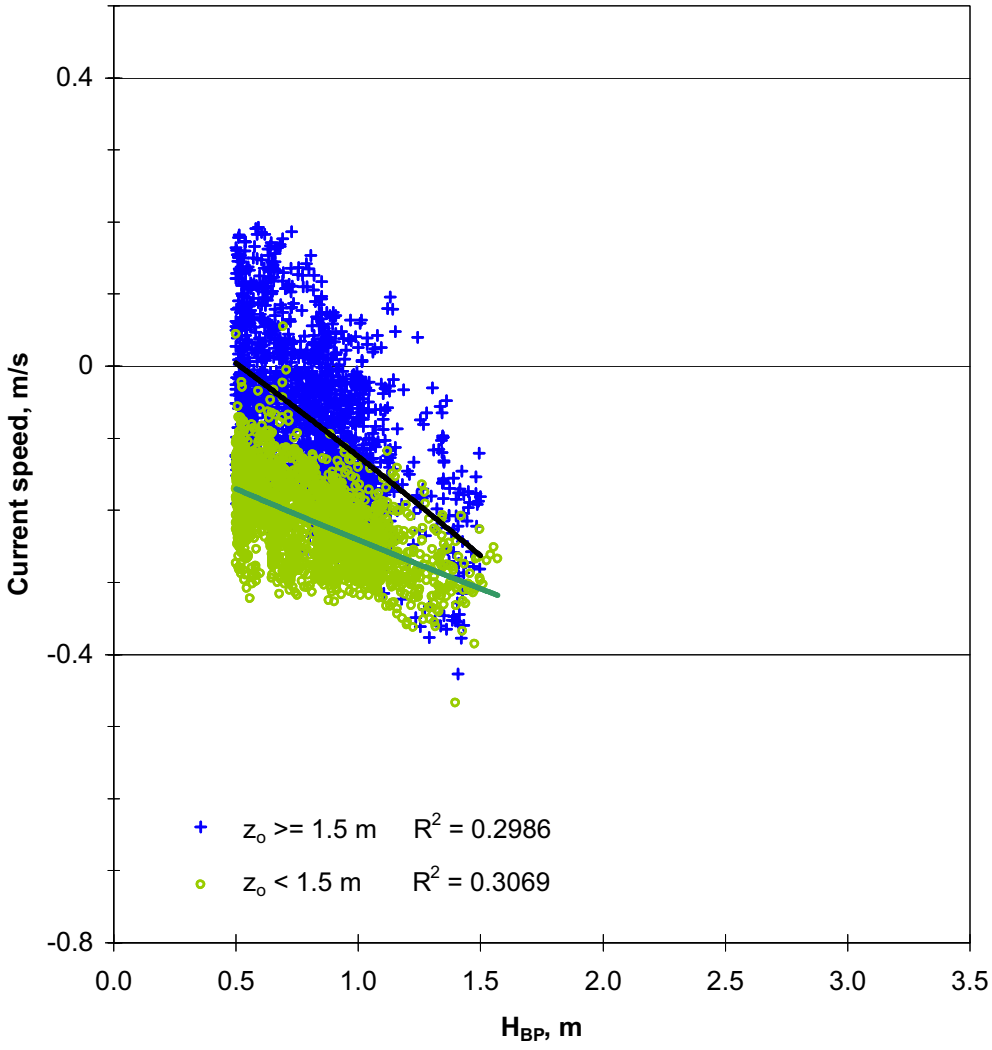

Figure 108. Northern current meter, falling tide, R < 1.4 m
17 March 1996 to 18 March 1997
Current speed vs wave height offreef from Blue Pools, H_{BP}

Only data with H_{BP} >= 0.5 m

Only data with 320^{o} <= θ_w <180^{o}

θ_c < 125^{o}, positive θ_c >= 125^{o}, negative

Trendlines 2nd order polynomials

8. REVIEW AND CONCLUSIONS

(i) Offreef waves and reef-top currents at the western end of Heron Reef were measured over a fourteen month period during 1996-1997. The purpose of these measurements was to explain the processes which cause sediment to be transported from the reef-flat and the island's beaches into the boat harbour, out though its entrance channel and thus ultimately off the reef platform.

(ii) Analyses have been made of the interactions between waves, currents, local winds, reef-top and ocean tide levels, and reef-top topography to establish both the relationships between the forcing functions, winds, waves and tides, and the resultant currents and the variation of these relationships with changing seasonal conditions.

(iii) Under mild conditions, when wind speed, $W < 5$ m/s, and wave height, $H_s < 0.5$ m, and with average spring tides, tidal range, $R = 2.1$ to 2.2 m, tidal flow conditions dominate with the maximum current velocities $v \leq 0.3$ m/s during the last stage of the falling tide when flow off the reef platform is controlled by weir action of the boat harbour bund walls. On the southern side of the island there are two current reversals during a tidal cycle, whereas on the northern side of the island differences in reef topography elevations result in four current reversals during a tidal cycle. In the latter case the rising tide initially flows over the low western reef-rim and in through the boat harbour onto the northern reef-flat. Subsequently this flow is reversed as the tide flows inwards over the whole northern reef-rim onto the reef-flat. On the falling tide outflow is initially radially over the northern reef-rim but later, as the tide falls below mean sea level, flows towards the boat harbour.

(iv) During storm events with offreef significant wave heights of about 3m breaking on the reef-rim the tidal flow pattern is suppressed and unidirectional wave-generated flow occurs from the reef-rim surf zones to the boat harbour and lower western reef-rim. For example, during a northeasterly storm in late July 1996 which occurred during a period of medium to large range tides ($1.4 < R < 2.4$ m), there was a wave set-up of about 0.2 m on the northern reef-flat and a quasi constant unidirectional flow with velocities ≤ 0.6 m/s towards the boat harbour. Later in March 1997 during tropical cyclone "*Justin*" southeasterly winds and waves generated a unidirectional flow towards the boat harbour on the southern reef-flat. Wave set-up at the current meter site was at least 0.2 m. However, tidal ranges were larger ($R \leq 3$ m) and the

unidirectional flow fluctuated in magnitude with the rising and falling offreef tide and attained a maximum value of only about 0.4 m/s.

(v) A filter analysis, using the velocities measured every ten minutes, has been used for a detailed analysis of the current data. The latter was divided into rising and falling tides at the two current meter sites and separated into three tidal range groups; small, medium and large. Because of the large amount of data the analysis was undertaken in three parts, *i.e.* for 17 March to 30 June 1996; for 1 July to 31 October 1996; and for 1 November 1996 to 18 March 1997.

(vi) Analysis of mild conditions ($W < 5$ m/s; $H_s < 0.5$ m) indicated that the variation of current velocity during the tidal cycle could be represented by the dimensionless parameters vT/R and $Z = (z_0 - z_b) / (z_H - z_b)$. This is generally valid for large and medium tides ($R \geq 1.4$ m), although it is not always valid for falling tides. Small tides ($R < 1.4$ m), which generally do not fall below the bund wall crest, are not affected to the same extent by the presence of the bund wall or by reef topography. Consequently Z, which is based upon the bund wall crest elevation z_b, does not represent their behaviour adequately.

(vii) Increasing offreef wave action reverses and eventually suppresses the tidal flow on the western reef-top around Heron Island. Current reversal over the complete tidal cycle occurs under the following conditions at both current meter sites

Small tides $R < 1.4$ m	$H_{Wis} > 0.75$ m	southern reef-flat
	$H_{BP} > 0.75$ m	northern reef-flat
Medium tides $1.4 \leq R < 2.0$ m	$H_{Wis} > 1.0$ m	southern reef-flat
	$H_{BP} > 1.0$ m	northern reef-flat
Large tides $R \geq 2.0$ m	$H_{Wis} > 1.25$ m	southern reef-flat
	$H_{BP} > 1.25$ m	northern reef-flat

As H_{Wis} or H_{BP} increase above these threshold values the current velocity becomes increasingly independent of the variation of ocean tide levels. Under some conditions, for example, southwesterly winds or $H_{Wis} \approx H_{BP}$, the threshold value of H_{BP} which causes unidirectional flow on the northern reef-flat is greater than those given above.

(viii) During the twelve month period, 17 March 1996 to 18 March 1997, the wind climate varied seasonally with the dominant eastsoutheasterly to southeasterly winds occurring more frequently during the summer and autumn months and northwesterly winds occurring during the spring months. Storm events with W > 15 m/s occurred at various times and from different directions during the year.

Both sea and swell waves occurred with sea conditions being more frequent at the more exposed Wistari recording site on the southern side of the reef and swell waves more frequent at the more sheltered Blue Pools site on the northern side of the reef. Combined sea and swell conditions also occurred at both sites.

The period 17 March to 30 June 1996, for which the detailed analysis of tidal currents was made, is generally more representative of the conditions during the whole period than the later two periods.

(ix) Variations in wind directions and resulting waves during the second and third analysis periods (1 July to 31 October 1996 and 1 November 1996 to 18 March 1997) influenced current velocities, particularly during the latter stages of the falling tide when reef-top current velocities are controlled by weir action of the bund wall crest. Paradoxically, in some situations the velocities of these latter currents increase when waves are breaking on the opposite side of the reef and island.

(x) When the influence of tidal currents is negligible the reef-top wave-generated currents increase approximately linearly with increasing offreef wave heights.

(xi) Further analyses of the wave and current data measured at Heron Island are presented in a second report (Gourlay and Hacker 2008b) which examines the following:

- tidally dominated flows during mild conditions, including the effects of tidal asymmetry and the spatial flow pattern around the island;
- bund wall control of reef-top currents during the latter stages of the falling tide;
- the characteristics of wind and/or storm events and their effects upon the reef-top current system;
- theoretical approaches to the prediction of wave-generated currents on coral reefs;
- the relationship between reef-top current velocities and offreef wave heights;
- reef-top sediment transport and boat harbour sedimentation during tropical cyclones.

REFERENCES

Berkelmans, R., Oliver, J., Byron, G. & Olds, J. 1998. 'Heron Island: the history of the bund wall and an impact assessment of its 1993 redevelopment on nearby coral communities'. *In*: Greenwood, J.G. & Hall, N.J. eds (1998), *Proceedings of the Australian Coral Reef Society 75th Anniversary Conference, Heron Island October 1997*. School of Marine Science, The University of Queensland, Brisbane, pp. 11-28.

Gourlay, M.R. 1995. 'Impact of Heron Island boat harbour upon its adjoining reef and cay', *Preprints: 12th Australasian Conference on Coastal Engineering and 5th Australasian Port and Harbour Conference. 28 May – 2 June, 1995, Melbourne*, *Australia*. Instn Engrs, Aust., Nat. Conf. Publ. No. 95/5, pp 31-36.

Gourlay, M.R. & Hacker, J.L.F. 1997. 'Reef-top hydrodynamics at Heron Island', *Great Barrier Reef, Science, Use and Management: a national conference: proceedings. Townsville, 25-29 Nov. 1996*, Vol. 2, pp 49-54.

Gourlay, M.R. & Hacker, J.L.F. 1999. 'Influence of waves and winds on reef-top currents at Heron Island, Southern Great Barrier Reef', *Coasts & Ports '99: Proceedings: 14th Australasian Coastal and Ocean Engineering Conference and 7th Australasian Port and Harbour Conference, 14-16 April, 1999, Perth, WA.* Instn. Engrs, Aust. Publ No. 1/99, vol. 1, pp. 222-227.

Gourlay, M.R. & Hacker, J.L.F. 2008b. Reef-top Currents in Vicinity of Heron Island Boat Harbour - 2. Detailed analyses of effects of tides, winds and waves on currents. University of Queensland. Civil Engineering Research Report CH73/08 ISBN 9781864999 365

Hacker, J.L.F. & Gourlay, M.R. 1997. 'Harbour bund wall construction at Heron Island: coral response', *Great Barrier Reef, Science, Use and Management: a national conference: proceedings. Townsville, 25-29 Nov. 1996.* Vol. 2, pp 55-60.

Queensland Department of Transport, 1997. *The Official Tide Tables & Boating Safety Guide 1998,* Queensland Department of Transport, Brisbane.

APPENDIX A – Tidal Planes at Heron Island

Tidal Planes at Heron Island
based on Standard Port Gladstone

Tidal Plane	Elevation above LAT, m	Elevation above low water datum, m
HAT	3.20	3.28
MHWS	2.65	2.73
MHWN	2.08	2.16
ML	1.44	1.52
MLWN	0.98	1.06
MLWS	0.39	0.47
LAT	0.00	0.08
Av. time difference. Ratio = 0.70	HW = -43 min	LW = -38 min

Source Queensland Department of Transport (1997)

APPENDIX B – Definitions of Symbols

Definitions of Symbols

C	dimensionless constant in broad crested weir equation (-)
d	water depth (m)
g	gravitational acceleration (m/s^2)
h	head (water surface height) above bund wall crest (m)
H_{BP}	offreef significant wave height at Blue Pools site (m)
H_{Wis}	offreef significant wave height at Wistari Channel site (m)
H_{rms}	root mean square wave height (m)
H_s	significant wave height (m)
q	flow per unit length of bund wall crest (m^2/s)
R	tidal range (= $z_H - z_L$) (m)
T	half-tidal period, i.e. time interval between z_{L1} and z_H or z_H and z_{L2} (s)
T_{Hs}	significant wave period (s)
T_p	period corresponding to peak of an ocean wave energy density spectrum (s)
v	current velocity or speed (m/s)
v_E, v_N	current velocity components in eastward and northward directions respectively (m/s)
W	wind speed (m/s)
z	elevation relative to tidal datum (LWD) (m)
z_b	elevation of bund wall crest (= 0.86m)
z_H	elevation of high tide (m)
z_L	elevation of low tide (m)
z_{L1}, z_{L2}	elevations of low tides preceding and following high tide (m)
z_{msl}	elevation of mean sea level (= 1.52m)
z_0	elevation of ocean tide (m)
Z	dimensionless tidal level parameter (= $(z_0 - z_b)/(z_H - z_b)$) (-)
θ_c	direction towards which current flows
θ_w	direction from which wind blows
σ	standard deviation

See also Figures 6a, 6b and 78a

BIBLIOGRAPHIC REFERENCE OF THE REPORT CH72/08

The Hydraulic Model research report series CH is a refereed publication published by the Division of Civil Engineering at the University of Queensland, Brisbane, Australia.

The bibliographic reference of the present report is :

GOURLAY, M.R., and HACKER, J.L.F. (2008). "Reef-top currents in Vicinity of Heron Island Boat Harbour, Great Barrier Reef, Australia: 1 Overall Influence of Tides, Winds and Waves." *Report No. CH72/08*, Div. of Civil Engineering, The University of Queensland, Brisbane, Australia, October, 184 pages (ISBN 9781864999 358).

The Report CH72/08 is available, in the present form, as a PDF file on the Internet at UQeSpace :

http://espace.library.uq.edu.au/

HYDRAULIC MODEL RESEARCH REPORT CH

The Hydraulic Model Report CH series is published by the Division of Civil Engineering at the University of Queensland. Orders of any of the Hydraulic Model Reports should be addressed to the Departmental Secretary.

Departmental Secretary, Div. of Civil Engineering, The University of Queensland
Brisbane 4072, Australia - Tel.: (61 7) 3365 3619 - Fax : (61 7) 3365 4599
Url: http://www.eng.uq.edu.au/civil/ Email: hodciveng@uq.edu.au

Report CH	**Unit price**	Quantity	**Total price**
FURUYAMA, S., and CHANSON, H. (2008). "A Numerical Study of Open Channel Flow Hydrodynamics and Turbulence of the Tidal Bore and Dam-Break Flows." *Report No. CH66/08*, Div. of Civil Engineering, The University of Queensland, Brisbane, Australia, February, 56 pages (ISBN 9781864999068).	AUD$60.00		
TREVETHAN, M., CHANSON, H., and BROWN, R.J. (2007). "Turbulence and Turbulent Flux Events in a Small Subtropical Estuary." *Report No. CH65/07*, Hydraulic Model Report series, Div. of Civil Engineering, The University of Queensland, Brisbane, Australia, November, 67 pages (ISBN 9781864998993).	AUD$60.00		
FELDER, S., and CHANSON, H. (2008). "Turbulence and Turbulent Length and Time Scales in Skimming Flows on a Stepped Spillway. Dynamic Similarity, Physical Modelling and Scale Effects." *Report No. CH64/07*, Div. of Civil Engineering, The University of Queensland, Brisbane, Australia, March, 217 pages (ISBN 9781864998870).	AUD$60.00		
MURZYN, F., and CHANSON, H. (2007). "Free Surface, Bubbly flow and Turbulence Measurements in Hydraulic Jumps." *Report CH63/07*, Div. of Civil Engineering, The University of Queensland, Brisbane, Australia, August, 113 pages (ISBN 9781864998917).	AUD$60.00		
KUCUKALI, S., and CHANSON, H. (2007). "Turbulence in Hydraulic Jumps: Experimental Measurements." *Report No. CH62/07*, Div. of Civil Engineering, The University of Queensland, Brisbane, Australia, July, 96 pages (ISBN 9781864998825).	AUD$60.00		
CHANSON, H., TAKEUCHI, M, and TREVETHAN, M. (2006). "Using Turbidity and Acoustic Backscatter Intensity as Surrogate Measures of Suspended Sediment Concentration. Application to a Sub-Tropical Estuary (Eprapah Creek)." *Report No. CH60/06*, Div. of Civil Engineering, The University of Queensland, Brisbane, Australia, July, 142 pages (ISBN 1864998628).	AUD$60.00		
CAROSI, G., and CHANSON, H. (2006). "Air-Water Time and Length Scales in Skimming Flows on a Stepped Spillway. Application to the Spray Characterisation." *Report No. CH59/06*, Div. of Civil Engineering, The University of Queensland, Brisbane, Australia, July (ISBN 1864998601).	AUD$60.00		
TREVETHAN, M., CHANSON, H., and BROWN, R. (2006). "Two Series of Detailed Turbulence Measurements in a Small Sub-Tropical Estuarine System." *Report No. CH58/06*, Div. of Civil Engineering, The University of Queensland, Brisbane, Australia, Mar. (ISBN 1864998520).	AUD$60.00		
KOCH, C., and CHANSON, H. (2005). "An Experimental Study of Tidal Bores and Positive Surges: Hydrodynamics and Turbulence of the Bore Front." *Report No. CH56/05*, Dept. of Civil Engineering, The University of Queensland, Brisbane, Australia, July (ISBN 1864998245).	AUD$60.00		

CHANSON, H. (2005). "Applications of the Saint-Venant Equations and Method of Characteristics to the Dam Break Wave Problem." *Report No. CH55/05*, Dept. of Civil Engineering, The University of Queensland, Brisbane, Australia, May (ISBN 1864997966).	AUD$60.00		
CHANSON, H., COUSSOT, P., JARNY, S., and TOQUER, L. (2004). "A Study of Dam Break Wave of Thixotropic Fluid: Bentonite Surges down an Inclined plane." *Report No. CH54/04*, Dept. of Civil Engineering, The University of Queensland, Brisbane, Australia, June, 90 pages (ISBN 1864997710).	AUD$60.00		
CHANSON, H. (2003). "A Hydraulic, Environmental and Ecological Assessment of a Sub-tropical Stream in Eastern Australia: Eprapah Creek, Victoria Point QLD on 4 April 2003." *Report No. CH52/03*, Dept. of Civil Engineering, The University of Queensland, Brisbane, Australia, June, 189 pages (ISBN 1864997044).	AUD$90.00		
CHANSON, H. (2003). "Sudden Flood Release down a Stepped Cascade. Unsteady Air-Water Flow Measurements. Applications to Wave Run-up, Flash Flood and Dam Break Wave." *Report CH51/03*, Dept of Civil Eng., Univ. of Queensland, Brisbane, Australia, 142 pages (ISBN 1864996552).	AUD$60.00		
CHANSON, H,. (2002). "An Experimental Study of Roman Dropshaft Operation : Hydraulics, Two-Phase Flow, Acoustics." *Report CH50/02*, Dept of Civil Eng., Univ. of Queensland, Brisbane, Australia, 99 pages (ISBN 1864996544).	AUD$60.00		
CHANSON, H., and BRATTBERG, T. (1997). "Experimental Investigations of Air Bubble Entrainment in Developing Shear Layers." *Report CH48/97*, Dept. of Civil Engineering, University of Queensland, Australia, Oct., 309 pages (ISBN 0 86776 748 0).	AUD$90.00		
CHANSON, H. (1996). "Some Hydraulic Aspects during Overflow above Inflatable Flexible Membrane Dam." *Report CH47/96*, Dept. of Civil Engineering, University of Queensland, Australia, May, 60 pages (ISBN 0 86776 644 1).	AUD$60.00		
CHANSON, H. (1995). "Flow Characteristics of Undular Hydraulic Jumps. Comparison with Near-Critical Flows." *Report CH45/95*, Dept. of Civil Engineering, University of Queensland, Australia, June, 202 pages (ISBN 0 86776 612 3).	AUD$60.00		
CHANSON, H. (1995). "Air Bubble Entrainment in Free-surface Turbulent Flows. Experimental Investigations." *Report CH46/95*, Dept. of Civil Engineering, University of Queensland, Australia, June, 368 pages (ISBN 0 86776 611 5).	AUD$80.00		
CHANSON, H. (1994). "Hydraulic Design of Stepped Channels and Spillways." *Report CH43/94*, Dept. of Civil Engineering, University of Queensland, Australia, Feb., 169 pages (ISBN 0 86776 560 7).	AUD$60.00		
POSTAGE & HANDLING (per report)	AUD$10.00		
GRAND TOTAL			

OTHER HYDRAULIC RESEARCH REPORTS

Reports/Theses	Unit price	Quantity	Total price
TREVETHAN, M. (2008). "A Fundamental Study of Turbulence and Turbulent Mixing in a Small Subtropical Estuary." *Ph.D. thesis*, Div. of Civil Engineering, The University of Queensland, 342 pages.	AUD$120.00		
GONZALEZ, C.A. (2005). "An Experimental Study of Free-Surface Aeration on Embankment Stepped Chutes." *Ph.D. thesis*, Dept of Civil Engineering, The University of Queensland, Brisbane, Australia, 240 pages.	AUD$80.00		

TOOMBES, L. (2002). "Experimental Study of Air-Water Flow Properties on Low-Gradient Stepped Cascades." *Ph.D. thesis*, Dept of Civil Engineering, The University of Queensland, Brisbane, Australia.	AUD$120.00		
CHANSON, H. (1988). "A Study of Air Entrainment and Aeration Devices on a Spillway Model." *Ph.D. thesis*, University of Canterbury, New Zealand.	AUD$60.00		
POSTAGE & HANDLING (per report)	AUD$10.00		
GRAND TOTAL			

CIVIL ENGINEERING RESEARCH REPORT CE

The Civil Engineering Research Report CE series is published by the Division of Civil Engineering at the University of Queensland. Orders of any of the Civil Engineering Research Report CE should be addressed to the Departmental Secretary.

Departmental Secretary, Dept. of Civil Engineering, The University of Queensland

Brisbane 4072, Australia

Tel.: (61 7) 3365 3619 Fax : (61 7) 3365 4599

Url: http://www.eng.uq.edu.au/civil/ Email: hodciveng@uq.edu.au

Recent Research Report CE	Unit price	Quantity	Total price
CALLAGHAN, D.P., NIELSEN, P., and CARTWRIGHT, N. (2006). "Data and Analysis Report: Manihiki and Rakahanga, Northern Cook Islands - For February and October/November 2004 Research Trips." *Research Report CE161*, Division of Civil Engineering, The University of Queensland.	AUD$10.00		
GONZALEZ, C.A., TAKAHASHI, M., and CHANSON, H. (2005). "Effects of Step Roughness in Skimming Flows: an Experimental Study." *Research Report No. CE160*, Dept. of Civil Engineering, The University of Queensland, Brisbane, Australia, July (ISBN 1864998105).	AUD$10.00		
CHANSON, H., and TOOMBES, L. (2001). "Experimental Investigations of Air Entrainment in Transition and Skimming Flows down a Stepped Chute. Application to Embankment Overflow Stepped Spillways." *Research Report No. CE158*, Dept. of Civil Engineering, The University of Queensland, Brisbane, Australia, July, 74 pages (ISBN 1 864995297).	AUD$10.00		
HANDLING (per order)	AUD$10.00		
GRAND TOTAL			

Note: Prices include postages and processing.

PAYMENT INFORMATION

1- VISA Card

Name on the card :	
Visa card number :	
Expiry date :	
Amount :	AUD$ .....

2- Cheque/remittance payable to : THE UNIVERSITY OF QUEENSLAND and crossed "Not Negotiable".

N.B. For overseas buyers, cheque payable in Australian Dollars drawn on an office in Australia of a bank operating in Australia, payable to: THE UNIVERSITY OF QUEENSLAND and crossed "Not Negotiable".

Orders of any Research Report should be addressed to the Departmental Secretary.

Departmental Secretary, Div. of Civil Engineering, The University of Queensland
Brisbane 4072, Australia - Tel.: (61 7) 3365 3619 - Fax : (61 7) 3365 4599
Url: http://www.eng.uq.edu.au/civil/ Email: hodciveng@uq.edu.au